Secretion of neurotoxic vesicles by muscle cells of ALS patients

Laura Le Gall

Sorbonne Université
Complexité du Vivant – ED515
Center for Research in Myology
&
Ulster University
Northern Ireland Center for Stratified Medecine

Thèse de doctorat en Sciences du Vivant

Secretion of neurotoxic vesicles by muscle cells of ALS patients

Laura Le Gall

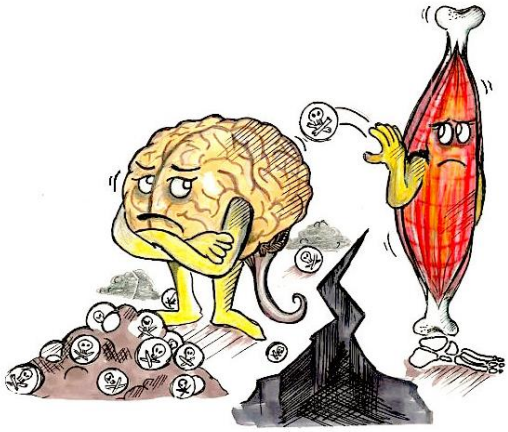

Présentée et soutenue publiquement le 6 Septembre 2019

Devant un jury composé de :

Ludo Van Den Bosh (VIB-KU Leuven Center for Brain & Disease Research - Belgique)	Rapporterur
Nicolas Charlet-Berguerand (IGBMC - France)	Rapporteur
Séverine Boillée (ICM - Paris - France)	Examinatrice (SU)
Paul Thompson (Biomedical Sciences Research Institute - Coleraine - UK)	Examinateur (UU)
Cécile Martinat (ISTEM - Evry - France)	Examinatrice
Hélène Blasco (INSERM U930 Imagerie et Cerveau - Tours - France)	Examinatrice
Stéphanie Duguez (Ulster University)	Directrice de thèse
Gillian Butler-Browne (Sorbonne Université)	Directrice de thèse

Dedicated to

My parents Xavier and Jacinta

And to my brother, Erwan

Acknowledgements

I would like to express my deepest gratitude to my supervisor Stéphanie Duguez. You've made this PhD journey so much better by always being patient and supportive, no matter the circumstances. I can't thank you enough for sharing your passion about science and research, but above all to trust me to complete this project. I could not have asked for anything else during all this time, and for that I'll be forever grateful. Alors Stéphanie, merci infiniment pour tout ce que tu as fait pour moi depuis le début de cette aventure en 2015. Merci de m'avoir transmis toutes ces connaissances, et merci pour tout le reste ! Hvala ! (Slovénie, 2017).

Next I would like to thank my second supervisor Gillian Butler-Browne and the members of my jury starting with my two assessors Dr Ludo Van Den Bosh and Dr Nicolas Charlet-Berguerand, Dr Séverine Boillée to represent Sorbonne Université and Paul Thompson to represent Ulster University, and finally Dr Cécile Martinat and Dr Hélène Blasco.
I would like to thank my two thesis committee assessors Dr Luc Dupuis and Dr Hélène Blasco for their constructive discussion and help during this PhD.

To the entire "Egripe 4" team in C-Tric, Bill, Christina, Ekene, Owen, Stephen and Vanessa, a massive thank you to all of you. Thank you for the good time and memories shared with you during my time in Derry, a second family like Vanessa would say.
Bill, thank you for welcoming me in beautiful Northern Ireland on my first day and thank you for making me run my first marathon (who would have thought)! Christinaki, I would never forget all the time you've spend with me to help me focus and finish writing my thesis. Thank you for being such an amazing friend. Ekene, thanks for sharing your addiction to cookies during those few weeks spend confined in the teaching lab. Owen, thank you for all the good time spend in C-Tric and outside, from sitting in the sun to enjoy Derry's summer to our secret meeting in tissue culture. Stephen, I hope someday you'll speak French without swearing but until that thanks for always lighten the mood in the office when the rest of the team is losing hope. And finally Vanessa, thanks for bringing us all together in massive laughing fit with your french accent and most of all thank you for all the good moment we've spend together!
My dear Jessica, thank you for helping me create the most fabulous drawing ever for my 3MT competition slide. To the rest of the PhD and placement students from C-Tric, thank you all for making the lab a brighter place!

Melody, je n'ai pas les mots pour te dire à quel point ta rencontre à tout changé pour moi à Derry. Ensemble nous avons partagé tellement d'aventures en commençant par mon déménagement à deux portes de chez toi jusqu'à ton départ pour Boston. Merci pour toutes ces belles aventures et souvenirs lors de nos nombreuses sorties à vélo. Tant de kilomètres parcouru avec toi et Juha et autant de souvenirs et de photos pour me rappeler chaque jour à quel point ton soutien a été important. To the best Chou-Sef ever … a Huge (Jackman) thank you!

A mes deux super volailles Cécile et Abi, merci pour votre amitié et votre soutien au cours de ces 4 dernières années. Chaque jour est un souvenir de notre temps passé à étudier et à faire nos schémas bilans sur le tableau des amphithéâtres de la fac. C'est grâce à vous que j'ai choisis cette voie, grâce à votre volonté à toute épreuve et surtout à votre passion pour les Sciences. Cécile, je ne te remercierai jamais assez pour ton réconfort dans les moments les plus difficiles, mais aussi pour les heures de

discussion au téléphone afin de rattraper le temps perdu. Abi, merci d'avoir été toujours là pour moi et d'avoir commencé cette aventure avec moi !

Fanny, nous avons commencé cette aventure toute les deux à Paris et voilà que nous sommes déjà sur le point de la terminer ensemble. Malgré la distance tu auras toujours été d'un soutien important pendant cette période et pour cela je te remercie infiniment. Merci d'avoir toujours été à l'écoute et d'avoir partagé tant de bons souvenirs à Paris, surtout les mardis soir lorsqu'il était temps pour nous de prendre la direction du cinéma. Merci de m'avoir fait découvrir ta belle Ecosse et de m'avoir permis de m'évader l'espace d'un instant. J'ai hâte de découvrir ce que le prochain chapitre nous réservera.

Emma, merci d'avoir partagé avec moi autant de bons moments et d'avoir été d'un énorme soutien lors de ces derniers mois. Je suis ravie que nos chemins se soit croisé à Derry et j'espère te retrouver très vite après la fin de notre chapitre à Derry !

To Ryan, I can't thank you enough for your constant support, affection and love during the last months of my PhD. Thank you a million time for making me discover hidden paradise in Ireland and making me escape reality for a moment. I love you!

Et pour finir, à mes deux parents et à mon frère, merci pour votre soutien et votre amour depuis le début. Merci d'avoir partagé avec moi les bons comme les mauvais moments, mais surtout de m'avoir permis d'atteindre mes objectifs. L'Irlande ne nous aura finalement pas séparés puisque vous étiez tous les trois avec moi jours après jours. Paps et Mams, merci d'avoir eu confiance en moi et de m'avoir toujours supporté dans mes études, sans vous je n'aurai pas pu parcourir tout ce chemin ! Erwan même si la chanson dit I've got you brother, les rôles auront largement été inversés alors merci d'être un petit frère aussi formidable. Love you all !

List of Abbreviations

Ach	Acetylcholine
AD	Alzheimer's disease
ALS	Amyotrophic lateral sclerosis
ALS-bi	ALS with behaviour impairment
ALS-ci	ALS with cognitive impairment
ALSFRS	Amyotrophic lateral sclerosis functional rating scale
AMPA	Alpha-amino-3-hydroxy-5-methyl-4-isoxazolepropionic acid
ARE	Antioxidant response element
bv-FTD	Behavioural variant frontotemporal dementia
CME	Clathrin mediated endocytosis
DC-SIGN	Dendritic Cell-Specific Intercellular adhesion molecule-3-Grabbing Non-integrin C type lectin receptor
DPR	Dipeptide repeat protein
EEAT2	Excitatory amino acid transporter 2
EM	Electron microscopy
ERAD	Endoplasmic reticulum-associated protein degradation
ERK	Extracellular signal-regulated kinase
ESCRT	Endosomal sorting complex required for transport
EVs	Extracellular vesicles
fALS	Familial ALS
FGFBP1	Fibroblast growth factor binding protein 1
FTD	Frontotemporal dementia
HREM	Hexanucleotide repeat expansion mutation
HRS	Heptocyte growth factor-regulated tyrosine kinase substrate
ICAM	InterCellular Adhesion Molecule
ILVs	Intraluminal vesicles
LFA-1	Lymphocyte Function-associated Antigen 1
LMN	Lower motor neuron
MCT1	Monocarboxylate transporter 1
MFG-E8	Milk Fat Globule-EGF factor 8
MND	Motor neuron disease
MVB	Multivesicular bodies
NLS	Nuclear localisation signal

NMDA	N-methyl-D-aspartate
NMJ	Neuromuscular junction
NRF2	Nuclear erthroid 2-related factor
nSMase	Neutral sphingomyelinase
NTA	Nanoparticle tracking analysis
PA	Phosphatidic acid
PD	Parkinson's disease
PI3P	Phosphoatidylinositol 3-phosphate
PLD2	Phospholipase D2
PLS	Primary lateral sclerosis
PM	Plasma membrane
PMA	Progressive muscular atrophy
PS	Phosphatidylserine
PTM	Post translational modifications
RBP	RNA binding protein
ROS	Reactive oxygen species
sALS	Sporadic ALS
SIRPα	SIgnal Regulatory Protein α
SLA	Sclérose latérale amyotrophique
SNAP	Soluble NSF attachment protein
SNARE	SNAP-attachment protein receptor
SOD1	Superoxide dismutase 1
SRSF1	Serrin/arginine-rich splicing factor
STAM	Signal transducing adaptator molecule
TfR	Transferrin receptor
UMN	Upper motor neuron
UPR	Unfolded-protein response
UPS	Ubiquitin-proteasome system
VABP	Vesicle-associated membrane protein B
VCP	Valosin containing protein
VSV	Vesicular stomatitis virus

List of tables and figures

Table 1: ALS age of onset variability and their clinical features. 9
Table 2: Clinical features for behavioural variant FTD (bvFTD) diagnosis. 12
Table 3: Diagnostic criteria table for ALS-bi and ALS-ci variant. 13
Table 4 : El Escorial criteria and revisions for ALS diagnosis. 15
Table 5 : Amyotrophic lateral sclerosis functional rating scale, revised ALSFRS-R. 17
Table 6 : Cell types releasing exosomes 36
Table 7: Exosomes heterogeneity explained by size and buoyant densities variability in extracted vesicles population. 40
Table 8 : Summary ligand – receptor interaction in exosomes/cell communication. 51
Table 9 : Table of antibodies and their dilutions used in immunocytochemestry, immunohistochemistry or in western blotting. 91
Table 10 : Housekeeping gene primer sequences. 96
Table 11 : Exosomal marker and FUS primer sequences. 97
Table 12 : Table summarizing experimental conditions and analysis performed on MN cultures treatment. 107
Table 13 : Table summarizing experimental conditions and analysis performed on muscles cells treatment with exosomes. 107
Table 14 : Table summarizing samples characteristics. 112
Table 15 : Number of cells extracted per biopsy and proportion of muscle cells. 113

Figure 1 : Upper and lower motor neuron involvement in ALS. 5
Figure 2 : Upper and lower motor neurons role in different "ALS variants. 10
Figure 3 : Clinical features of ALS and role in prognosis. 18
Figure 4: Hypothesis for GGGGCC repeat expansion in C9orf72 gene-mediated pathology. 20
Figure 5 : Molecular and cellular mechanisms involved in ALS pathogenesis. 23
Figure 6 : Protein homeostasis dysregulation. 24
Figure 7 : RNA and miRNA biogenesis defects in ALS. 26
Figure 8 : Biogenesis and secretion of exosomes. 44
Figure 9: Exosome and recipient cell communication 47
Figure 10 : The neuromuscular junction and muscle contraction. 60
Figure 11 : Housekeeping gene expression level measurement. 96
Figure 12 : Similar myotubes differentiation after ALS and control exosomes treatment. 115
Figure 13 : Primary motor neuron survival after ALS or healthy exosomes treatment 116
Figure 14 : TDP43 granulation in ALS and healthy muscle cells. 118
Figure 15 : ALS muscle cells secrete neurotoxic exosomes. 172
Figure 16 : Graphical abstract. Speculation on how muscle exosomes can have a role in the propagation of the disease. 174

Table of content

ABSTRACT **1**

RESUME **2**

LITTERATURE REVIEW **3**

CHAPTER 1: ALS **4**

I. ALS DESCRIPTION AND DEFINITION 5
1. Epidemiology *6*
2. Pathological definition of ALS: clinical features and phenotype variability *6*
- Clinical symptoms of ALS patients 7
- Site of onset variability 7
- Age of onset variability 8
- Motor neuron involvement in "ALS variants" 9
- Non motor involvement in ALS and overlap with FTD 11
- Diagnostic tools 13
- ALSFRS 15

3. Genetic and sporadic forms of ALS *18*
- Most common ALS associated gene mutations 18
- Other gene mutations associated with ALS 21

II. MOLECULAR AND CELLULAR PATHOGENESIS MECHANISMS IN ALS 22
1. Impaired protein homeostasis *23*
- Ubiquitin – proteasome system (UPS) dysregulation 24
- Autophagy defects 25
- Protein aggregation 25

2. Aberrant RNA metabolism *25*
- Transcription defects: 26
- Alternate splicing impairment: 27
- miRNA biogenesis dysfunction: 27
- Stress granules formation: 27

3. Mitochondrial dysfunction *28*
4. Nucleoplasmic transport defects *28*
5. Endosomal and vesicular transport impairment *29*
6. Axonal transport dysregulation *29*
7. Glutamate excitotoxicity *29*
8. Oxidative stress *30*
9. ER stress *30*
10. Motor neuron vulnerability *31*

CHAPTER 2: EXOSOMES BIOLOGY **32**

INTRODUCTION **33**

I. EXOSOMES DISCOVERY 33
II. PHYSICAL CHARACTERISTICS OF EXOSOMES 36
1. Exosomes isolation methods *36*
2. Secretion of exosomes subpopulations *37*
III. EXOSOMES BIOGENESIS AND SECRETION 40
1. Molecular content of exosomes *40*
2. Exosomes cargo sorting *40*
3. Intraluminal vesicles biogenesis *41*

- *ESCRT-dependent mechanism* 42
- ESCRT-independent mechanisms 43
- Exosome secretion: MVB and PM fusion 44

IV. EXOSOMES INTERACTIONS WITH RECIPIENT CELLS 47

1. Evidence for exosomes uptake 49

- Functional exosomal content transfer 49
- Exosomes tracking in recipient cells 49

2. Indirect communication: soluble ligand mediated signalling 49

3. Exosomes uptake by target cells 50

- Ligand – receptor interaction 50
- Fusion of exosomes with PM 51
- Endocytosis 52
- Lipid raft-mediated endocytosis 53

4. Recycling or degradation: fate of exosomes inside the targeted cells 53

5. How exosomes deliver functional content to the targeted cells 54

6. Exosomes function in intercellular communication 54

- Role in development biology and cancer 55
- Exosomes-induced signalling and role in the central nervous system 55
- Role in protein recycling and intercellular communication 56

CHAPTER 3: NEUROTOXIC COMMUNICATION IN ALS 57

I. INTERCELLULAR COMMUNICATION IN ALS 58

1. Evidence for non-neuronal cell toxicity 58

2. Non-cell autonomous toxic mechanisms 58

II. AXONOPATHY MECHANISMS AND MUSCLE INVOLVEMENT 59

1. The neuromuscular junction 59

2. Distal axon degeneration 60

3. The role of skeletal muscle in ALS patients 61

4. Secreted vesicles and role in pathogenesis 61

5. Conclusion 62

OBJECTIVES 63

MATERIAL AND METHODS 64

MUSCLE STEM CELLS EXTRACTION AND CULTURE (1) - MUSCLE BIOPSY DISSECTION: MICRO- EXPLANT CULTURE 65

MUSCLE STEM CELLS EXTRACTION AND CULTURE (2) - MYOBLASTS PROLIFERATION, SORTING AND DIFFERENTIATION 67

HUMAN IPSCS MOTOR NEURONS CULTURE 71

MYCOPLASMA SCREENING 74

EXOSOMES EXTRACTION FROM CULTURE MEDIUM 77

EXOSOMES PKH26 LABELLING 78

PROTEIN EXTRACTION AND QUANTIFICATION FROM CELL PELLETS SAMPLE 79

PROTEIN EXTRACTION AND QUANTIFICATION FROM EXOSOMAL SAMPLES 81

WESTERN BLOTTING – CELL LYSATE SAMPLES 82

EXOSOMES SAMPLES PREPARATION FOR IMMUNOBLOTTING 87

IMMUNOCYTOCHEMISTRY (ICC) 89

RT-QPCR AND RELATIVE GENE EXPRESSION ANALYSIS 92

SIRNA-BASED FUS SILENCING 98

EXOSOMES TREATMENT 101

RESULTS 109

I. EXOSOMAL PATHWAY DISRUPTION IN ALS PATIENTS. 109

II. MUSCLE EXOSOMES CHARACTERIZATION AND TOXICITY STUDY 112

DISCUSSION 172

CONCLUSION 176

PUBLICATIONS 177

POSTER COMMUNICATIONS 191

1. *European Alliance for Personalized Medicine (EAPM) Congress – Belfast / UK: 191*
2. *28th International Symposium on ALS/MND – Boston, MA 194*
3. *29th International Symposium on ALS/MND – Glasgow – UK 197*

ORAL COMMUNICATIONS 200

1. *2ème Journées de la recherche sur la SLA et les maladies du neurone moteur – Paris – France 200*
2. *3ème Journées de la recherche sur la SLA et les maladies du neurone moteur – Paris – France 200*
3. *3MT Competition – Ulster University, Derry/Londonderry – UK 200*

REFERENCES 202

Abstract

To date, amyotrophic lateral sclerosis (ALS) remain incurable and the causes for motor neuron death are unknown. The primary involvement of skeletal muscle in ALS pathogenesis is still controversial. Several studies suggested that a distal axon degeneration occurs prior to the onset of ALS clinical symptoms. Moreover, there are growing evidences for a disruption of exosomes biogenesis and secretion pathways in genetic forms of ALS. Knowing that the skeletal muscle can be a source of exosomes, we hypothesised that ALS skeletal muscle could contribute to the toxic environment of motor neurons and thus participate in ALS pathogenesis through their secretion of exosomes. During my PhD, I investigated the secretion of exosomes by muscle cells from sporadic ALS patients and their role in motor neuron death. First, we show that muscle cells present a consistent signature across ALS patients with an accumulation and over-secretion of exosomes. Second, ALS muscle exosomes are toxic toward healthy human iPSCs motor neurons by inducing shorter, reduced branching neurites and cell death. Third, we observed that ALS muscle exosomes contain FUS protein and are enriched in proteins involved in RNA maturation and transport. Fourth, ALS muscle exosomes induced a disruption in RNA transport in healthy human motor neuron. Fifth, the exosome toxicity is dependent on FUS expression level in the recipient cells, as an over-expression of FUS in the recipient cells exacerbated the ALS exosome toxicity while an inhibition of FUS expression decreased their toxic effect. The greater sensitivity of motor neurons to ALS muscle exosomes might thus be explained by their higher expression level of FUS compare to healthy muscle cells. Altogether, these results suggest that ALS muscle exosomes could contribute to the degeneration of motor neuron in ALS patients.

Key words: ALS, muscle exosomes, RNA, muscle stem cells, intercellular communication, neurotoxic vesicles

Résumé

A ce jour, les causes de la sclérose latérale amyotrophique (SLA) ne sont pas connues et il n'existe aucun remède. L'implication du muscle dans la pathogénèse de la SLA est toujours controversée, néanmoins il a été démontré qu'il existe une atteinte axonale distale primaire à l'apparition des premiers symptômes de la SLA. De plus, plusieurs données de la littérature suggèrent une perturbation de la voie de biogénèse et de sécrétion des exosomes chez certains patients atteints de forme mono-génique de la SLA. Sachant que le muscle squelettique peut être une source d'exosomes, nous émettons l'hypothèse que le muscle pourrait contribuer à la toxicité de l'environnement des motoneurones, à leur dégénérescence et donc à la pathogénèse de la SLA. J'ai donc étudié au cours de ma thèse la sécrétion d'exosomes par les cellules musculaires de patients sporadiques SLA et leurs rôles dans la SLA. Dans un premier temps, nous avons observé l'existence d'une signature associée à la SLA dans l'ensemble des cellules musculaires analysées, avec une accumulation et sursécrétion d'exosomes. Ces exosomes musculaires de patients SLA étaient toxiques pour les motoneurones dérivés d'iPSCs, induisant une réduction du nombre de branchements, une diminution de la longueur des neurites et une mort des motoneurones. Nous avons ensuite observé que les exosomes ALS contenaient la protéine FUS et d'autres protéines impliquées dans le transport et la maturation des RNAs. Or, le traitement des motoneurones avec des exosomes musculaire SLA induisait une accumulation de RNA dans leurs noyaux. Enfin, nous avons observé que la toxicité des exosomes SLA était dépendante du niveau d'expression de FUS de la cellule réceptrice. En effet, la toxicité des exosomes SLA était exacerbée lorsque FUS était surexprimé dans la cellule réceptrice et était diminuée lorsque l'expression de FUS était éteinte. Or les motoneurones présentent un niveau d'expression de FUS supérieur aux cellules musculaires, suggérant leur sensibilité accrue aux exosomes musculaires SLA. Ensemble ces données suggèrent une implication du muscle dans la dégénérescence des neurones moteurs de patients SLA.

Mots clés : SLA, exosomes musculaires, RNA, cellules souches musculaires, communication intercellulaire, vésicules neurotoxiques.

Litterature review

Chapter 1: ALS

I. ALS description and definition

Motor neuron diseases or MND is a group of disorders characterised by a progressive and fatal degeneration of upper and/or lower motor neurons (UMN and LMN respectively) resulting in muscle weakness and wasting. Motor neurons are responsible for movement initiation. LMN directly innervates skeletal muscle fibres and their cell bodies are located either in the spinal cord (their axons stimulate upper and/or lower limb muscles) or in the brainstem (axons stimulating bulbar muscles including throat and tongue muscles). Descending pathways from the motor cortex comprise the UMN whose cell bodies are located in the cortex and their descending axons synapse with LMN cell bodies in the brainstem or the spinal cord (Figure 1). UMN from the motor cortex are responsible for initiation and transmission of voluntary movements.

ALS or amyotrophic lateral sclerosis is the most common form of MND[1] and specifically associated with the deterioration of both UMN and LMN[2]. Despite the long-established concept of ALS described as a neurodegenerative disease they are growing evidence for a cognitive impairment in some ALS patients[3]. So far, no diagnostic tools have been developed for ALS, however diagnostic criteria (El Escorial[4] and revisions[5], and Awaji-shima criteria[6]) help stratifying ALS patients according the severity, fast or slow progressors, and sites of onset.

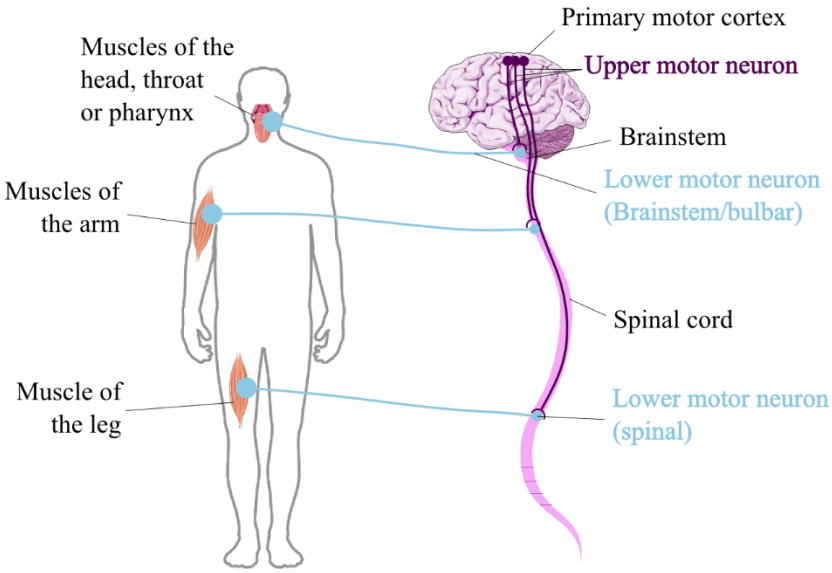

Figure 1 : Upper and lower motor neuron involvement in ALS
ALS is diagnosed based on combinatorial degeneration of upper and lower motor neurons The upper motor neuron (UMN) cell bodies are located in the motor cortex and the brainstem, and project down to establish synaptic communication directly with the lower motor neuron (LMN) or through interneurons. UMN thus modulate LMN activities. LMN cell bodies reside in the spinal cord and in the brainstem. Their axons project out towards skeletal muscles fibres to make contact at the neuromuscular junction to transmit movement information. UMN and LMN originating from the brainstem are responsible for activating bulbar-innervated muscle (pharyngeal muscles and tongue involved in speech and swallowing). UMN and LMN originating from the spinal cord are responsible for upper and lower limb movement.

1. Epidemiology

ALS global incidence varies between 1 to 2.6 cases per 100,000 people every year[7]. In Europe, the incidence is ~ 2.6/100,000 person per year[8], ranging from 0.5/100,000 persons in Serbia to 3.6/100,000 persons in the Faroe Islands annually[9]. Thus the number of newly diagnosed ALS cases reaches about 15,400 every year[10]. In Asia, the incidence varies dramatically country to country with an extremely low number of new cases in China, ~0.3/100,000 to a higher rate in Japan, with 2.5/100,000 new cases/year[9]. Following the Gulf War, the number of veterans diagnosed with ALS was reported to be 20 out of 690,000 [7], thus a ratio of 2.8 cases per 100,000 while the ALS incidence was ~ 1.7-1.8/100,000 in the US population between 1993-1994[9].

Because of the short life expectancy – 3 to 5 years after the onset -, the number of ALS patients living at a given time can be quite low compare to other rare diseases. Worldwide ALS prevalence is about 6 cases per 100,000 persons with some variation region to region. In Europe, the average prevalence is ~ 8 patients per 100,000 persons, with ~ 40,000 persons affected by ALS in 1995/2011[9]. It varies from 1.1/100,000 in Yugoslavia to 8-8.2/100,000 in the Netherlands, in some Italian regions and in the Faroe Islands respectively[7]. In the US, the prevalence was estimated at ~ 5 /100,000 population in 1994[11]. in Asia, the prevalence ranged from 1.0/100,000 in China to 11.3/100,000 in Japan[9]. ALS affects particularly elderly people and its prevalence increases with ageing, reaching a ratio of 20/100.000 in a population aged between 70-79 years old[11]. Consequently, as the population is ageing, it is expected that the total number of cases observed worldwide in 2005 -number ~ 222,801 - will increase by 69% in 35 years and reached 376,674 in 2040[12].

Disease onset age for ALS ranges from 54 to 67 years old, with a mean age of 61.8 ± 3.8 years[9] and mean ALS diagnostic age is 64.4 ± 2.9 years[9]. There is an average diagnostic delay of 11-12 months[13] before reaching a definite diagnosis. The age of onset between sporadic and familial cases of ALS slightly differs with peak of age onset at 58-63 years for sporadic cases and 47-52 for familial cases[14] (Table 1). Three categories of onset can be observed in the total ALS population, with extremely rare juvenile cases where the onset occurs before 25 years old, cases with a young-onset from 25 to 45 years old[15,16], and cases with old-onset where ALS patients are diagnosed in their seventh decade[17]. Worldwide men are diagnosed with ALS at 1.3 to 1.56 times the rate of women[7], with an exception in China where male:female ratio ranges from 1.45 to 1.98[18].

2. Pathological definition of ALS: clinical features and phenotype variability

ALS is a fatal neurodegenerative disorder with an adult onset, characterized by the degeneration of upper and lower motor neurons responsible for muscle denervation, leading to muscle weakness and wasting in ALS patients. Muscles controlling the speech, swallowing and other motor functions are dramatically

affecetd[2]. ALS symptoms unceasingly spread and progress quickly causing paralysis and disability as patients lose their ability to control their muscles. With inexorable progression of symptoms appears intercostal and diaphragm muscles weakness following thoracic and cervical spinal cord involvement, responsible for common death due to respiratory failure of ALS patients within 3 years of first symptomatic features onset[2,19]. Despite these generic features observed across ALS patients, ALS phenotypes vary patient to patient as patients can present different site of onset and a variability in clinical features. For example, some patients can develop pure motor dysfunction ALS phenotype while others will present a mixed phenotype associated with extra-motor involvement such as behavioural changes and language difficulties typifying frontotemporal dementia (FTD) disease[3] (see I. 2. 4. Non-motor involvement in ALS: overlap with FTD).

- **Clinical symptoms of ALS patients**

El Escorial criteria characterises ALS by a progressive and relentless degeneration of both UMN and LMN[4]. UMN and LMN dysfunction are associated with several clinical features in order to assess the certainty of the disease. UMN dysfunction includes pathological spread of reflexes and hyperreflexia. Various reflexes can be tested for UMN impairment, such as 1) the jaw jerk reflex, 2) Hoffmann's sign, and 3) Babinski reflex[20]. A positive jaw jerk reflex is identified when a sudden and upward jaw contraction is observed due to brisk contraction of the masseter muscles. The Hoffmann's reflex test is based on flexion and adduction of thumb after flicking the finger nail of the middle finger. Finally a positive Babinski reflex is seen when upward movement (or movement towards the top the foot) of the big toe after stroking the sole of the foot occurs. Additionally, patients can present spasticity causing stiffness and tightness in the muscle and involuntary muscle contraction, or clonus. Concerning bulbar-innervated muscles impairment, UMN dysfunction are defined as spastic dysarthria or difficult and laboured speech. LMN signs are characterized by muscle weakness and certain wasting accompanied by fasciculations of wasted limbs. Similarly, tongue wasting often with dysarthria and dysphagia, or difficulty to swallow, are typical features of bulbar LMN dysfunction[20].

- **Site of onset variability**

Site of onset varies among ALS patients. In a majority of ALS cases (70%), symptoms initially begins in one limb[20]. Usually muscle weakness is focal and patients will present a foot drop or a clumsy hand[13]. The affected body region progressively become more and more weaken, and finally fasciculate and waste. UMN dysfunction might precede muscle atrophy such as spasms and cramps, and ultimately symptoms spread into the whole body affecting all the limbs. In 25% of ALS cases however, symptoms develop initially in the bulbar-innervated muscles[20], also referred as bulbar palsy[21]. Usually bulbar-onset ALS is affecting less men than women[13], especially after 70 years (M:F ratio 1:1,6[17]). Dysarthria and dysphagia are frequently

associated with bulbar-onset ALS and cognitive impairment are often present[21]. For approximatively 3% and 5%[1] of ALS cases, respiratory or cognitive onset presentation respectively occurs[14]. Initial trunk or respiratory onset ALS is associated with poor prognosis, the mean survival time is 1.4 years with fast progressing disease only[22,23]. Cognitive onset ALS patients usually present characteristic FTD symptoms, such as a changes in behaviour, personality and cognition suggesting frontal impairment[24].

- **Age of onset variability**

Although ALS occurs in patients in their sixth decade, ALS symptoms onset happens at almost all age (Table 1). Extremely rarely, <1/1,000,000 cases, juvenile ALS occurs in patients younger than 25 years old[15]. Juvenile ALS is usually associated with a slower symptoms progression, hence a longer survival time and better prognosis[23]. Some mutations are now described to be specifically related to juvenile ALS such as mutations in FUS, ALS2 or SETX genes[15]. UMN features dysfunction are predominantly represented among juvenile ALS cases. Young-onset ALS includes patients ranging from 25 to 45 years old[15] and upper motor neuron predominant is mainly observed in those patients (60%)[15]. Contrary to "classic ALS phenotype", bulbar-onset is more rare in young-onset ALS and represent ~15% of the cases[23]. In addition, a greater proportion of male are affected with a male : female ratio at 3:1[15]. These young-onset cases are also associated with a better prognosis than older ALS patients. For most patients, ALS symptoms onset peaks approximatively at 61 years old. A last ALS patient subgroup has been identified with an onset after 80 years old[17]. A likelihood of developing UMN predominant phenotype increases ~20% in old-onset ALS patients, as well as initial development of symptoms in bulbar muscles. Moreover, elderly bulbar-onset ALS cases present a greater proportion of females patients (M:F ratio 1-1.6)[15,17]. Symptoms onset after 80 years old is associated with a more aggressive disease and poor prognosis with mean survival time of less than 20 months[17].

		Juvenile ALS	Young-onset ALS	Classic ALS	Late-age onset ALS
Disease onset		≤25 years old	>25 to ≤45 years old	>45 to ≤70 years old 58-63 yo sALS 47-52 yo fALS	>70 years old
M:F ratio		_	3-3.6 : 1	1.3-1.56 : 1	1 : 1.25
Genetics		Mostly familial cases (FUS, SETX, ALS2 mutations)	Mostly familial	~90% sALS ~10% fALS	_
Site of onset	*Limb onset*	_	_	~70%	~40%
	Bulbar onset		~16%	~25%	~50% (M:F = 1:1.6)
	Respiratory/cognitive onset		_	~5%	_
Survival (from symptoms onset)		Generally longer survival >10 years		Variable: 50% : <30 months 5-10% : 5-10 years	~20 months
Clinical features	*Classic ALS (UMN+LMN)*	_	~40%	~80%	~72%
	UMN-predominant	Predominant	~60%	~17%	_
	LMN-predominant	_	_	~13%	~19%

Table 1: ALS age of onset variability and their clinical features.
Summary of classic clinical features for "Classic ALS" and age variants from Chio et al[25], Forbes et al[17], Swinnen et al[23], Turner at al[15], Sabetelli et al[16], and Kiernan et al[14]. In addition to the classical ALS phenotype with age onset ranging from 45 to 70 years old (mean age ~ 61 years old), 3 additional ALS-variants (columns) are characterised depending on age of onset. Male to female ratios, genetic characteristics, site of onset, estimated survival time, and clinical features are further displayed in the following rows if applicable. sALS: sporadic ALS. fALS: familial ALS. UMN: upper motor neurons. LMN: lower motor neurons.

- **<u>Motor neuron involvement in "ALS variants"</u>**

ALS patients can also present with either a LMN or UMN predominance (Figure 5). Signs of pure LMN dysfunction are considered as progressive muscular atrophy (PMA) cases whereas predominant UMN signs are associated with primary lateral sclerosis (PLS)[20]. PMA and PLS patients both are rare diseases and represent 5% of MND patients[23].

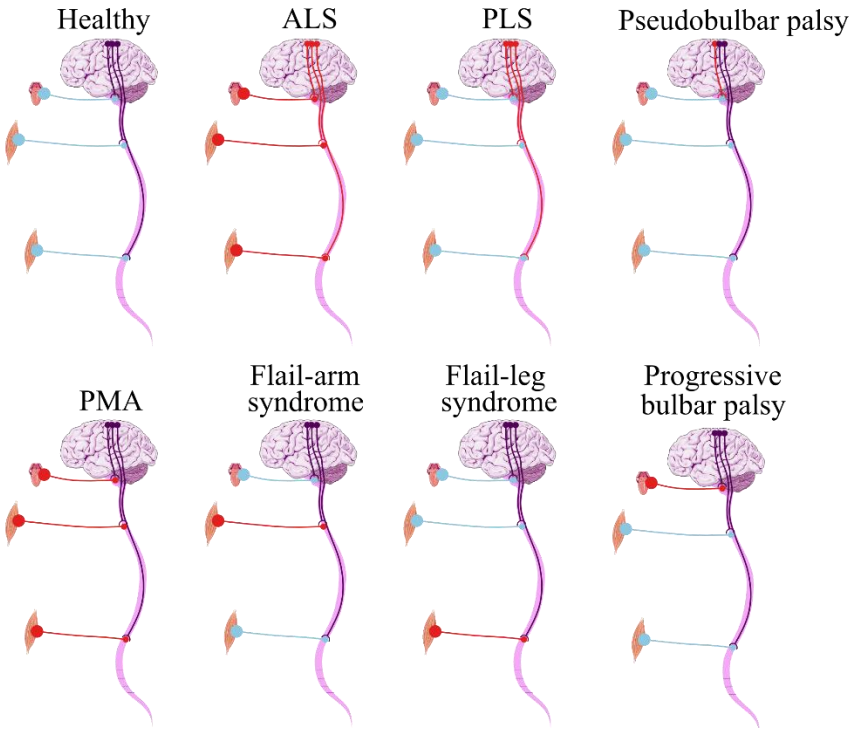

Figure 2 : Upper and lower motor neurons role in different "ALS variants.
ALS is a disease with high clinical phenotype variability. "Classic ALS" patients will present with signs of both UMN and LMN degeneration. However patients with progressive muscular atrophy (PMA) and primary lateral sclerosis (PLS) ALS variants present with LMN-predominant or UMN-predominant signs respectively. LMN-predominant patients also includes flail-arm syndrome and flail-leg syndrome ALS variants where LMN signs are present in upper or lower limbs respectively. ALS patients might present symptoms in bulbar-innervated muscles, if LMN are predominantly affected the term progressive bulbar palsy is used. However if UMN signs are predominant, patients are diagnosed with pseudobulbar-palsy. Blue colour indicate non-affected neurons. Red colour indicate the UMN/LMN signs associated with each ALS variants. ALS: Amyotrophic lateral sclerosis. PLS: Primary lateral sclerosis. PMA: Progressive muscular atrophy.

UMN-dominant ALS variants:

At first assessment patients can present a "UMN-predominant" dysfunction revealed by UMN signs (see I. 2. 1. Clinical symptoms of ALS) with LMN signs usually initiated in distal upper limb before affecting the proximal upper limbs and in later stage of the disease lower limbs and respiratory muscles[20]. Clinical features showing UMN predominant phenotype can progress to ALS, and represent nearly 40% of PLS cases[26]. However if UMN dysfunction are still observed 4 years after disease onset a pure PLS is diagnosed[20]. Patients diagnosed with PLS for not meeting the diagnostic criteria for ALS can still slowly develop signs of LMN dysfunction and therefore present both UMN and LMN signs[23]. Prognosis of PLS patients is better than classic ALS cases as symptoms progression is slow. Yet if UMN signs are predominant in bulbar-innervated muscles patients are diagnosed with pseudobulbar palsy[27].

²LMN-dominant ALS variants:

Conversely patients can also develop a LMN-dominant phenotype that includes PMA, flail-arm and flail-leg syndromes "ALS variants". PMA patients are similar to classic ALS patients without obvious signs of UMN. However 50 to 60% PMA patients develop degeneration of upper motor neurons during the progression of the disease[28]. In patients with flail-arm or flail-leg syndromes, LMN dysfunction can remain limited to either the upper or lower limbs for at least 12 months [23]. When pseudobulbar palsy is described as a predominant UMN dysregulation in bulbar muscles, patients with bulbar LMN signs predominantly are diagnosed with progressive bulbar palsy[27].

- **Non motor involvement in ALS and overlap with FTD**

For many years ALS was described as an exclusive neurodegenerative disorder with no extra-motor involvement, including cognitive defects. Today it is now accepted that other neurological components are impaired in ALS patients[3]. If early studies suggested low proportions of ALS patients experiencing non motor impairment (3% among sporadic cased and 15% among the familial cases[29]), studies nowadays propose that approximatively 35% of ALS patients present behavioural and/or cognitive changes (ALSci or ALSbi) and 15% of them meet the Neary criteria[30] for FTD diagnosis (ALS-FTD)[29]. ALS and FTD sometimes are described as part of one continuum with pure ALS patients (without any extra motor involvement) and pure FTD cases (for whom no motor dysfunction have been described) represent opposite sides of the spectrum.

FTD disease comprise 3 variants defined by the Neary criteria[30]: frontal variant FTD (also called behavioural variant FTD[31]), non-fluent progressive aphasia or semantic dementia. Usually ALS patients meet criteria for behavioural variant FTD characterized by defects in cognitive functions, personality traits and behaviour collapse. Among ALS cases experiencing extra motor dysfunction, language (particularly deficit in verbal fluency[31]) and cognition are mostly affected, and apathy is the most frequent personality feature impaired encountered[29] in patients.

Dementia in ALS patients – ALS-FTD variants:

ALS-FTD diagnosis is made upon the presence of ALS phenotype associated with behavioural or cognitive defects meeting FTD diagnosis:

- Progressive impairment of behavioural/cognitive functions and observation of at least 3 of behavioural symptoms defined by Rascvosky et al[32] (see Table 2)
- Or loss of insight and/or psychotic features associated with at least 2 of Rascvosky et al[32] symptoms.
- Or language impairment combined with semantic dementia (defined in Neary et al[30]).

Possible bvFTD	3 recurrent or persistent behavioural/cognition symptoms	Early behavioural disinhibition Apathy or inertia Loss of sympathy or empathy Perseverative, stereotypes or compulsive/ritualistic behaviour Hyperorality and dietary changed Neurophysiological profile: executive/generation deficits with relative sparing of memory and visuospatial functions
Probable bvFTD	Criteria for possible bvFTD and functional disability	Meets criteria for possible bvFTD Exhibits significant functional decline At least 1 Imaging results consistent with bvFTD: - Frontal/anterior temporal atrophy - Frontal/anterior hypofusion or hypermetabolism
Definite bvFTD	Criteria for possible or probable bvFTD associated with supplemented with one of the following criterion	Histopathological evidence of FTD on biopsy or at post-mortem Presence of a known pathogenic mutation

Table 2: Clinical features for behavioural variant FTD (bvFTD) diagnosis.

Cognitive changes in non-demented ALS patients – ALSci and ALSbi variants:

Non-demented ALS patients presenting with behavioural impairment are classified as ALSbi-variant, while ALS patients experiencing cognitive deterioration represented by language defects are considered to be ALSci-variant[29]. Based on the revised diagnostic criteria from Strong et al[33], ALS patients can be diagnosed as ALSci variant if either 1) executive impairment (social cognition) or 2) language dysfunction or 3) a combination of the two features are evident during diagnosis (see Table 3). Diagnostic criteria for ALSbi variant require 1) apathy with or without other behavioural symptoms, or 2) two or more behavioural changes, such as disinhibition, loss of sympathy/empathy, perseverative/stereotype/compulsive behaviour, hyper orality/dietary change, loss of insight and psychotic symptoms (see Table 3).

ALS-ci *Evidence of either executive or language dysfunction, or both*	**Executive impairment criteria**	Impaired verbal fluency (letter). Verbal fluency deficits must control for motor and/or speech impairments to be valid
		Or impairment on 2 other non-overlapping measures of executive functions: • Screening (ALS-CBS test ALS CBS is a brief measure of cognition and behaviour in patients with ALS) • Screening and assessment (ECAS test cognitive test) • Fluency (Verbal fluency test) • Concept formation • Divided attention • Attention inhibition
	Language impairment (2 non-overlapping tests):	• APACS test (Assessment of Pragmatic Abilities and Cognitive Substrates test) • Picture description • Naming tests • Naming test (verbs only) • Semantic/concepts (pyramid and palm trees test or kissing and dancing test) • Single word comprehension • Receptive grammar tests • Syntax production tests • Pragmatic/social language tests • Spoken language tests
ALS-bi		Identification of apathy with or without behaviour change
		OR presence of two or more of the following behavioural symptoms: • Disinhibition • Loss of sympathy and empathy • Perseverative, stereotypes or compulsive behaviour • Hyper orality/dietary change • Loss of insight • Psychotic symptoms (somatic delusions, hallucinations, irrational beliefs)

Table 3: Diagnostic criteria table for ALS-bi and ALS-ci variant.

- **<u>Diagnostic tools</u>**

In the absence of a diagnostic tool for ALS, evidence of progressive combination of UMN and LMN signs in patients is associated with positive diagnostic in the event of prior exclusion of ALS-mimic disease. Since diagnostic criteria have been developed in 1990 by the World Federation of Neurology[4] to establish different level of disease burden (Table 4). ALS diagnosis based on those criteria demand evidence of disease progression within regions of the body that includes: 1) bulbar regions (speech and swallowing function dysregulation), 2) cervical regions (upper limb weakness and deterioration), 3) thoracic regions (abdominal muscles), and 4) lumbar regions (lower limb defect), associated with UMN and LMN

involvement signs. The original diagnostic criteria ranged diagnostic certainty into 4 categories: suspected ALS, possible ALS, probable ALS, and definite ALS. In the Airlie House criteria (revised El Escorial criteria[5]) disease certainty is classified as clinically possible ALS to definite ALS, deleting the suspected ALS category from the diagnostic criteria and adding a new clinically probable ALS – laboratory supported. More recently the Awaji-shima criteria further increased the specificity of ALS diagnosis, allow an earlier detection of LMN loss and simplified ALS diagnosis criteria into 3 categories including clinically possible, probable and definite ALS[6,34].

The El Escorial diagnosis criteria[4] and its revisions[5,6] do not include cognitive and behavioural deficits in ALS patients. However independent stratification tools have been developed to classify ALS patients with extra-motor involvement such as the Edinburgh Cognitive and Behavioural ALS Screen (ECAS), a cognitive test designed for patients with motor function impairment designed to minimise the impact of motor dysfunction on the classification of the patient[35].

Differential diagnosis:

Among other motor neuron disease, spinal muscular atrophy type III and IV (SMAIII/IV) and spinal-bulbar muscular atrophy (SBMA or Kennedy's disease) are two motor neuron diseases mimicking early stages of ALS – with SBMA being one of the most frequently misdiagnosis with ALS[21]. Thus establishing a diagnosis at an early stage of ALS is challenging. The diagnosis is even more complexify by the existence of ALS variants with pure bulbar (pseudobulbar palsy and progressive bulbar palsy), pure UMN signs (PLS) or pure LMN dysfunctions (PMA and flail-arm/leg syndromes ALS variants) are part of ALS differential diagnosis[21]. However, ALS is defined as a motor neuron disease associated with progressive UMN and LMN dysfunction. Any symptoms that would not progress over months are signs of ALS mimic syndromes.

El Escorial criteria (1994)	*Revised El Escorial criteria (2000)*	*Awaji-shima criteria (2008)*
Suspected ALS: - LMN signs only in 2 or more regions	–	–
Possible ALS: - UMN + LMN signs in 1 region - UMN signs alone present in ≥2 region - LMN signs rostral to UMN signs	**Clinically possible ALS:** - UMN + LMN signs in 1 region - UMN signs alone present in ≥2 regions - LMN signs rostral to UMN signs	**Clinically possible ALS:** Clinically and electrophysiological indication of : - UMN + LMN signs in 1 region - UMN signs alone present ≥ 2 regions LMN signs rostral on UMN signs
–	**Clinically probable ALS - laboratory supported**: - UMN + LMN signs in 1 region only - UM signs in 1 region and LMN signs defined by EMG criteria present in ≥2 regions	–
Probable ALS: UMN + LMN signs ≥ 2 regions	**Clinically probable ALS:** UMN + LMN signs ≥ 2 regions	**Clinically probable ALS**: Clinically and electrophysiological indication of UMN + LMN signs ≥ 2 regions with some UMN signs necessarily rostral to the LMN signs
Definite ALS: - UMN + LMN signs in bulbar regions and ≥ 2 spinal regions - UMN + LMN signs in 3 spinal regions	**Clinically definite ALS**: - UMN + LMN signs in bulbar region and ≥2 spinal regions UMN + LMN signs in 3 spinal regions	**Clinically definite ALS:** Clinical and electrophysiological indication of - UMN + LMN signs in bulbar region and ≥ 2 spinal regions UMN + LMN signs in 3 spinal regions

Table 4 : El Escorial criteria and revisions for ALS diagnosis.
El Escorial diagnosis criteria created in 1990 and revised in 2000 to help with diagnosis of ALS patients. In the original El Escorial criteria patients were classified into 4 categories (suspected ALS, possible ALS, probable ALS or definite ALS). In 2000, the revised criteria or Airlie House criteria disease burden ranges clinically possible to clinically definite ALS. The Awaji-shima criteria further simplified the revised El Escorial criteria into 3 subgroups: clinically possible, clinically probable and clinically definite. UMN: upper motor neuron. LMN: lower motor neuron.

- **ALSFRS**

Without specific biomarkers for ALS, it is still challenging to study the rate of progression of ALS patients. Today, the Amyotrophic Lateral Sclerosis Functional Rating Scale (ALSFRS) is the most commonly tool used by clinicians and in clinical trials. The ALSFRS is a questionnaire-based tool establishing the level of impairment in physical function carried out during activities of daily living in ALS patients[36]. However the ALSFRS was lacking establishment of respiratory dysfunction progression. Hence development of revised ALSFRS to equally weight respiratory function disability to limb and bulbar function[37]. Additional questions regarding evaluation of respiratory defects progression have been developed and added to the questionnaire. The new ALSFRS-R questionnaire is composed of 10 questions scale (Table evaluating

gross motor task, fine motor task, bulbar function and respiratory function, including dyspnea, orthopnea and the need for ventilator support, see Table 5). Shortly after establishment of the revised scale, ALSFRS-R was validated in 2 studies[38] as ALSFRS scores powerfully correlated with level of muscle weakness and survival. Lower ALSFRS scores were assigned to ALS patients who died during the course of the study.

	Speech		**Turning in bed**
4	Normal	***4***	Normal
3	Detectable disturbance	***3***	Slow and clumsy, no help required
2	Intelligible with repeating	***2***	Can turn alone and adjust sheets but with great difficulty
1	Combined with non-vocal communication	***1***	Can initiate, but unable to turn and adjust sheets alone
0	Loss of speech	***0***	Helpless
	Salivation		**Walking**
4	Normal	***4***	Normal
3	Slight, but definite excess of saliva	***3***	Early ambulation difficulties
2	Moderate excessive saliva	***2***	Walks with assistance
1	Marked excess of saliva, and drooling	***1***	Non-ambulatory functional movement
0	Marked drooling	***0***	No purposeful leg movement
	Swallowing		**Climbing stairs**
4	Normal	***4***	Normal
3	Early eating problems	***3***	Slow
2	Dietary consistency changes	***2***	Mild unsteadiness or fatigue
1	Supplemental tube feeding needed	***1***	Needs assistance
0	Exclusively parental or enteral feeding	***0***	Cannot do
	Handwriting		**Dyspnoea***
4	Normal	***4***	None
3	Slow and legible	***3***	Occurs when walking
2	Not all words are legible	***2***	Occurs with 1 or more of the following: eating, bathing, dressing
1	Able to grip a pen but, unable to write	***1***	Occurs at rest, difficulty breathing when either sitting or lying
0	Unable to grip a pen	***0***	Significant difficulty, considering using mechanical respiratory support
	Cutting food and handling utensils		**Orthopnoea***
4	Normal	***4***	None
3	Slow and clumsy, no help required	***3***	Some difficulty sleeping sur to shortness of breath
2	Can cut foods, but clumsy and needs some help		Not more than 2 pillows routinely required
1	Food must be cut by someone else	***2***	Extra pillows needed to be able to sleep (>2)
0	Needs to be fed	***1***	Sleeping only in sitting up position
		0	Unable to sleep
	Dressing and hygiene		**Respiratory insufficiency***
4	Normal	***4***	None
3	Independent, although decreased efficiency for self-care	***3***	Intermittent use of BiPAP
2	Intermittent assistance or substitute methods	***2***	Continuous use of BiPAP at night
1	Needs attendant for self-care	***1***	Continuous use of BiPAP all day
0	Total dependence	***0***	Invasive mechanical ventilation by intubation or tracheostomy

Table 5 : Amyotrophic lateral sclerosis functional rating scale, revised ALSFRS-R.
In 1996, a simple questionnaire measuring physical function carried out daily by ALS patients was validated. A revision of the ALSFRS aimed to better assess respiratory function of ALS patients (added questions are marked by an *) resulting in the above improved 10 questions questionnaire. The ALSFRS is used by clinicians in practice and in clinical trials, the ALSFRS allows to establish a rate of decline in ALS patients based on 4 domains: gross and fine motor tasks, bulbar function and respiratory function. BiPAP: bi-level intermittent positive air pressure (non-invasive ventilator assistance for ALS patients).

In summary, ALS is a clinically heterogeneous disease with variable phenotypes that makes difficult to predict the progression speed of the symptoms as well as survival time. However multiples features of ALS have been associated with a poor prognosis (Figure 3). Classically disease onset in ALS patients is around 61 years old. Young age-associated ALS include juvenile-ALS and young-ALS with disease onset before 25 and 45 years old respectively and are usually associated with slower progression and better survival than "Classic-ALS"[15]. On the contrary, old-onset ALS is characterized by development of ALS symptoms later (after 70 years old) and is associated with poor prognosis, especially among elderly female with bulbar-onset phenotype[17]. Initial site of symptoms onset varies among ALS patients from classic limb-onset to rare cognitive-onset phenotypes. Poor prognosis is often associated with bulbar and respiratory onset[14]. Finally, shorter predicted survival of time is also related with disease progression speed. The fastest the symptoms progress the more the survival time shortens. Disease progression can either be assessed depending on diagnostic delay or using ALS rating score (ALSFRS). Poor prognosis is associated with patients whose ALS diagnostic has been given under 8 months after symptoms onset or losing more than 1.4 points on the ALSFRS scale[27].

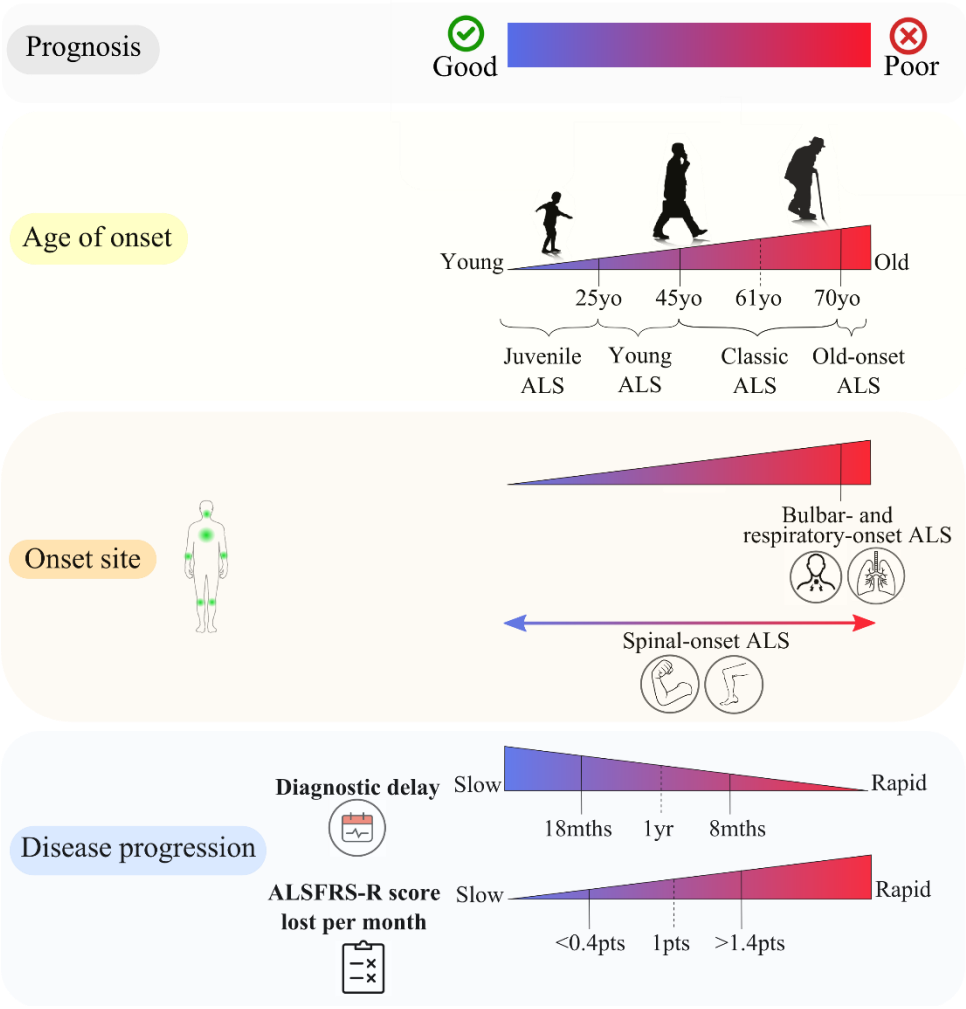

Figure 3 : Clinical features of ALS and role in prognosis.
Diagram displaying ALS features associates with typical good or bad prognosis. ALSFRS: Amyotrophic lateral sclerosis functional rating scale.

3. Genetic and sporadic forms of ALS

ALS is mainly sporadic with 90% of ALS cases (sALS) arising at random and approximatively 10% of ALS cases are familial (fALS)[7]. Today more than 30 genes mutations have been related to some sALS (10%)[39] patients as well as fALS cases (70%)[39,40]. The hexanucleotide expansion repeat in C9orf72 gene is the most common genetic cause in fALS (~25%) and sALS (~5%) patients, followed by SOD1 (~20% in fALS and ~2% in sALS cases), TARDBP/TDP43 (~5% in sfALS and ~1% in sALS patients), and FUS (~3% in fALS and 0.5% in sALS cases)[41].

- **<u>Most common ALS associated gene mutations</u>**

<u>Superoxide dismutase1, *SOD1*:</u>

The first identified gene to be linked with ALS was *SOD1* in 1993[42]. SOD1 is ubiquitously expressed in human cells, and is localized in the nucleus, mitochondria, and cytoplasm cell compartments. SOD1 protects cells from ROS (Reactive Oxygen Species) by catalysing the reduction of superoxide anion to oxygen and hydrogen peroxidase. Mutated form of SOD1 present a toxic gain of function responsible for neurotoxicity through ER stress, misfolded protein aggregates, and oxidative stress[40].

C9orf72:

In 2011, the GGGGCC (G4C2) hexanucleotide repeat expansion mutation (HREM) within C9orf72 gene has been observed in patients with ALS and FTD[43,44]. The HREM is located in intron 1 of *C9orf72* and induces pathological repeat in ALS patients. In healthy subjects, G4C2 repeat length ranges from 2 to 23 units[43]. Even if a pathological number of hexanucleotide units clear cut-off has not been established yet, large G4C2 expansion ranges from 30 and above have been observed in ALS patients[43,45]. Considering the localization of the repeat expansion on *C9orf72* gene, several hypothesis of loss of function- or gain of function-mediated toxicity from the HREM in *C9orf72* have been proposed (Figure 4). The first one is based on reduction of *C9orf72* mRNA levels due to G4C2 repeats-mediated inhibition of transcription or haploinsufficiency hypothesis[40]. Sense and antisense RNA generated from the bidirectional transcription of G4C2 repeats have been proposed to induce a toxic gain of function in ALS patients' cells. Thus the G4C2 repeats may become toxic by sequestering RNA binding proteins, and forming RNA foci that will disrupt the RNA metabolism processing in cells[45]. A third hypothesis involves repeat-associated non-AUG translation (RAN) of G4C2 (or G2C4) repeats in dipeptide repeat proteins (DPR). RAN occurs in both sense and antisense reading frame[46] resulting in the production of 5 different DPRs: glycine-alanine (GA), glycine-arginine (GR), proline-arginine (PR), proline-alanine (PA), and glycine-proline (GP)[47]. And finally HREM in C9orf72 is associated with impaired nucleoplasmic transport mediated through repeat-RNA or DPRs[40]. Epidemiologic analysis allowed to establish an age-related penetrance of the pathogenic expansion in *C9orf72* gene ranging from non-penetrant in carriers younger than 35 years, to 50% penetrant by mean age of ALS disease onset, and fully penetrant by 80 years.[48]

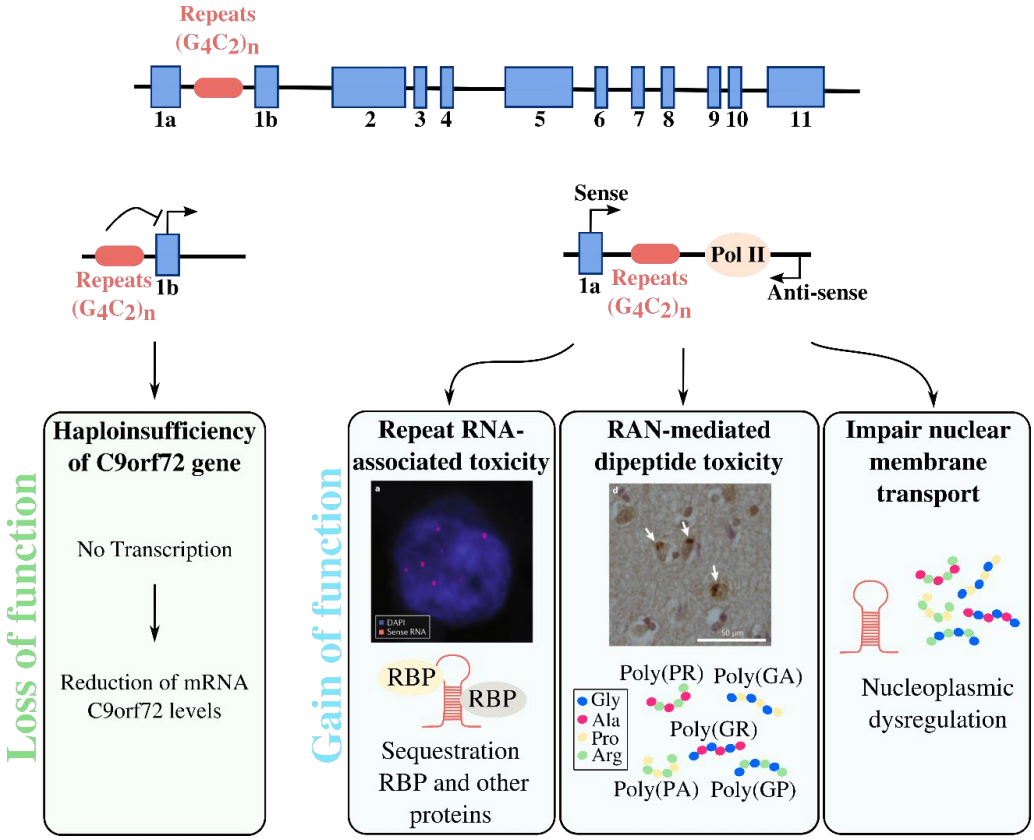

Figure 4: Hypothesis for GGGGCC repeat expansion in C9orf72 gene-mediated pathology.
The most pathogenic mutation represented among both sALS and fALS is the hexanucleotide repeat expansion in the *C9orf72* gene. 1) Inhibition of *C9orf72* transcription by repeat expansion induce a toxic reduction of *C9orf72* mRNA levels in ALS patients. 2) Generation of toxic repeat-containing RNA assembling in RNA foci. 3) Repeat-associated non-AUG translation mediated DPR toxic effects. 4) Finally both repeat-RNA and DPR products interact with the nucleus-cytoplasm machinery, inducing a toxic nucleoplasmic dysregulation. RBP: RNA-binding protein. RNA foci and DPR accumulation pictures from Balendra et al[45].

TARDBP/TDP43:

A common pathological features in ALS histology is the cytoplasmic localization and accumulation of TDP43 proteins in ALS and FTD patients[21]. *TARDBP* gene encodes for TDP43 protein, a ribonucleoprotein that is ubiquitously expressed and described with a range of functions from gene transcription to mRNA biogenesis regulation[40]. In ALS patients, mutations of *TARDP* gene[49] leads to a mislocalisation of TDP43 from the nucleus to the cytoplasm where it accumulates in pathological inclusions. Both overexpression of mutated TDP43 forming toxic aggregates in the cytosol[50] and knock down inducing a nuclear depletion of TDP43[50–52] lead to an ALS-like phenotype. These studies imply that both toxic gain and loss of function of mutant TDP43 hypothesis play a role in neurodegeneration occuring in ALS[46].

FUS/TLS:

FUS mutations in ALS cases have been described in 2009[53,54] and induce variable phenotype in patients with a high frequency in juvenile-onset ALS[15]. Similarly to TDP43, FUS is nuclear RNA-binding protein

possessing multiple functions in RNA and miRNA metabolism. It also may play a key role in neuronal integrity and plasticty[40]. Mutations in *FUS*, and more particularly in its nuclear localization signal (NLS) domain, causes a dominant cytoplasmic mislocalisation probably associated with both toxic loss- and gain-function[55].

- **Other gene mutations associated with ALS**

VAPB: Vesicle associated membrane protein-associated protein B or *VAPB* mutations are first observed in ALS patients in 1960's[40]. VAPA and VAPB are part of the VAP protein family which are well known components of vesicular regulation and trafficking. VAPB plays a role in degradation of misfolded proteins in the ER through activation of the ubiquitin-proteasome system (UPS)[56].

VCP: Valosin-containing protein (VCP) is an ubiquitous protein belonging to the AAA+ ATPases protein family[57]. VCP is involved in various functions regarding protein homeostasis such as protein degradation, among others including a role in the UPS pathway[58].

ANG: *ANG* encodes for angiogenin involved in the maintenance of a normal vascularisation by activating angiogenesis mechanisms in many tissues including the central nervous system[59].

SETX: Similarly to some *FUS* mutations, *SETX* gene is linked to juvenile-onset forms of ALS with slow progression of the symptoms and a longer life expectancy compared to classic ALS. Patients exhibiting *SETX* mutations, usually develop a classic ALS phenotypes, however an absence of bulbar and respiratory symptoms have been reported[60]. *SETX* gene encodes for a ubiquitously expressed protein involved in a various cellular function among them the RNA metabolism regulation.

SQSTM1: *SQSTM1* gene encodes for sequestrosome 1 proteins also referred as to ubiquitin-binding protein p62. P62 protein is involved in a range of different function including proteasome-mediated protein degradation, and autophagy through its binding with LC3 autophagosome protein[61]. Mutations in *SQSTM1* observed in rare ALS cases and in FTD patients[62] lead to p62 protein inclusions in motor neurons of both patients[63]. *SQSTM1* ALS patients present a longer survival compare to most ALS patients.

ALS2 (Alsin): Like *FUS* and *SETX*, *ALS2* gene mutations is associated with juvenile-onset ALS variant patients. So far, no known *ALS2* mutations have been recorded in adult-onset ALS cases[64]. Similarly to *VABP*, alsin protein is involved in vesicle trafficking and axonal growth maintenance[64].

OPTN: *OPTN* mutations mediated ALS cases reveal a high variability in clinical features phenotypes with an age of onset ranging from young- to old-onset ALS patients, and a disease progression varying from aggressive to up to 10 years disease duration[62]. Optineurin protein is an ubiquitous protein required in a

variety of cellular functions such as autophagy maintenance where optineurin acts as a autophagy receptor, vesicle trafficking and Golgi homeostasis[65].

TBK1: *TBK1* mutations have been recently identified in ALS and FTD patients[40]. TBK1 is a multifunctional kinase associated with multiple signalling pathway such as autophagy through the phosphorylation and activation of autophagy adaptors such as optineurin and p62 proteins[66].

UBQLN2: *UBQLN2* mutations have been identified to participate in various ALS phenotypes variants (including familial juvenile- and adult-onset ALS and FTD patients)[67]. It was shown that both fALS and sALS can develop ubiquilin-positive inclusions[68]. Its function in UPS regulation, ER stress associated-ERAD pathway and autophagy suggest a role of ubiquilin in protein homeostasis[67].

II. Molecular and cellular pathogenesis mechanisms in ALS

Numerous pathological mechanisms have been proposed to explain the neurodegeneration occurring in ALS. However the process is still not fully understood and appears to be multifactorial (Figure 5). The most studied pathological hypotheses in ALS includes mitochondrial dysfunction, glutamate-mediated excitotoxicity, axonal and vesicular trafficking dysregulation, RNA metabolism alteration and ROS-associated oxidative stress[69–80]. Numerous pathways dysregulation involving RNA processing have been studied in ALS patients such as RNA metabolism[78], splicing defects[80] or impaired nucleoplasmic transport[46,81]. Impairment in protein homeostasis is also characteristic of ALS patients, including proteins aggregates toxicity[49], DPR toxicity[82], autophagy and lysosomal activity defects[83] and impaired ubiquitin proteasome system[84]. Moreover, neighbouring cells also participate in the toxic environment of motor neurons in ALS. Astrocytes and microglia cells are both involved in the release of inflammatory mediators contributing to neuroinflammation.

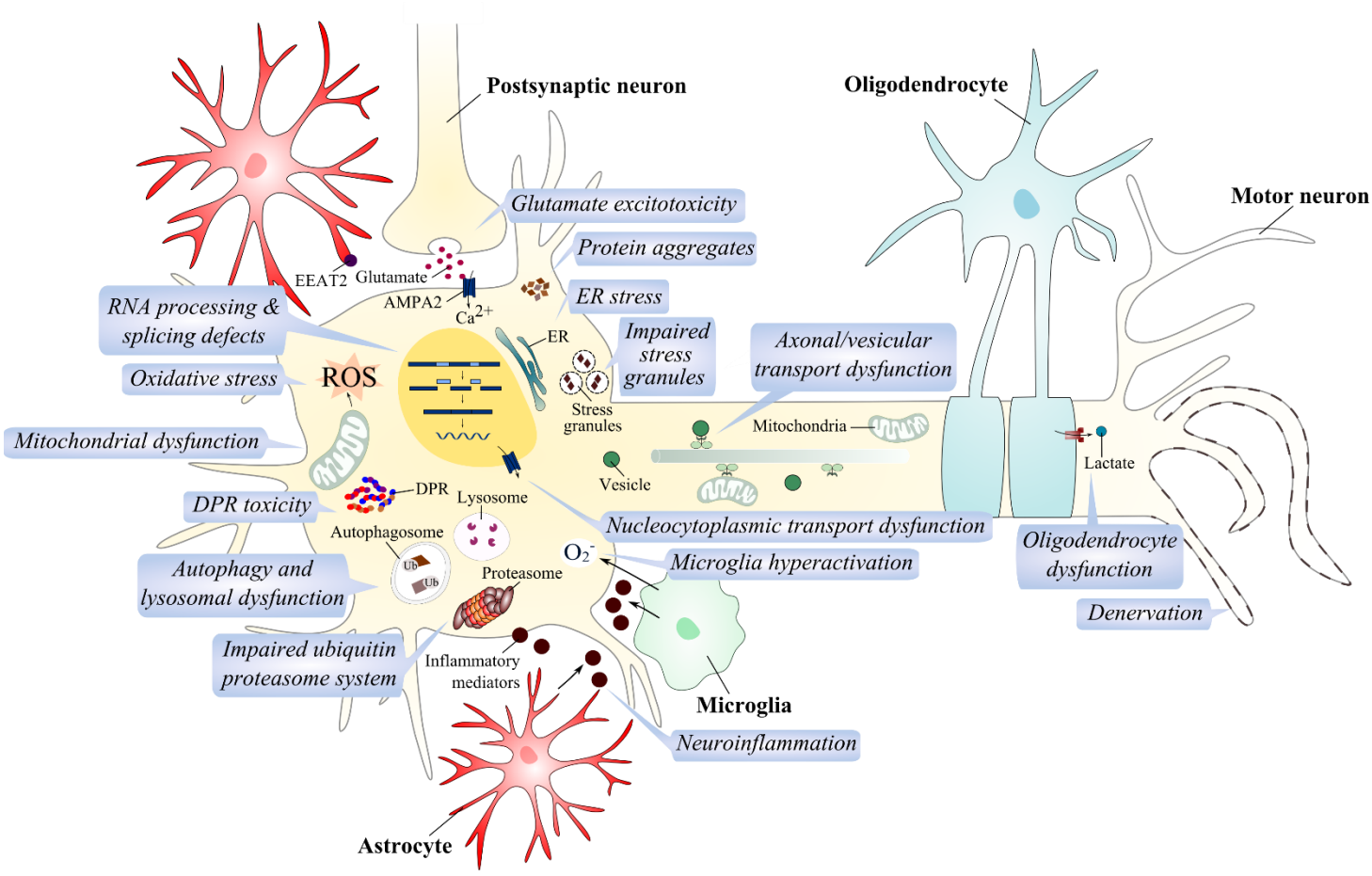

Figure 5 : Molecular and cellular mechanisms involved in ALS pathogenesis.
Multiple pathological mechanisms have been proposed to be involve in ALS pathogenesis. Among the most studied and well known dysregulated pathways are: RNA metabolism, autophagy and protein homeostasis, neuroinflammation and glutamate excitotoxity.

1. Impaired protein homeostasis

Several gene mutations involve aggregations of misfolded proteins in abnormal cellular compartments accompanied by a failure of the proteasome-based and autophagic-degradation pathways[85,86] (Figure 6), both ubiquitin-proteasome system and autophagy protein degradation pathways being key actors in ALS pathogenesis[82].

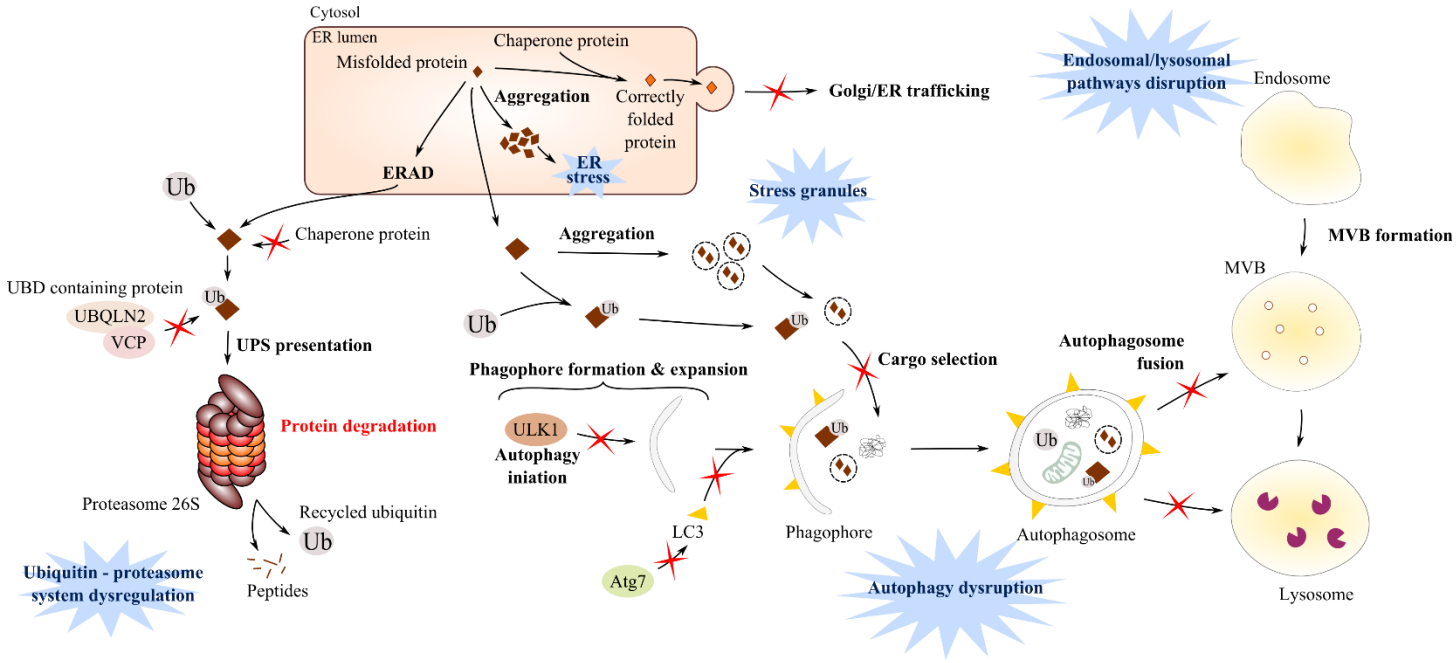

Figure 6 : Protein homeostasis dysregulation.
Protein homeostasis dysregulation is mediated by multiple pathways including defects in autophagy, dysregulation of ubiquitin-proteasome system (UPS) or endoplasmic reticulum stress. In the event of misfolded protein, activation of ERAD lead to a proteasome-mediated degradation to avoid accumulation of misfolded protein in the ER lumen and thus resulting in ER stress. Several ALS-associated gene mutations are reported to inhibit the proteasome-mediated toxicity via sequestration of the UPS pathway components such as ubiquilin and chaperone proteins. Proteolytic activity of the proteasome has also been demonstrated to be targeted by gene mutations in ALS. Once initiated, the autophagy pathway involves the formation and maturation of phagophores that will engulf selected transported-cargo and form autophagosome. Fusion with lysosome enables the degradation of the autophagosome content. Autophagy initiation and expansion via dysregulation of phagophore formation or impaired cargo transport are observed in ALS patients. ER: endoplasmic reticulum. ERAD: endoplasmic reticulum-associated protein degradation.

- **<u>Ubiquitin – proteasome system (UPS) dysregulation</u>**

Evidence for UPS dysregulation in ALS patients started with the identification of mutations of genes encoding proteins such as ubiquilin 2 or VCP[87], two proteins involved in protein clearance via the ubiquitin-proteasome pathway. In addition, SOD1[85], VABP[56], HREM in C9orf72[70,88], and p62[89] mutants are reported to reduce UPS activation. Further studies illustrate the dysregulation of the proteasomal pathway, as ubiquitin-positive inclusions were observed in motor neurons of fALS and sALS[84] patients as well in post-mortem neuronal and muscular tissue of *C9orf72*-associated ALS patients[90]. Concordantly, the sequestration of proteasome component in mutated SOD1 aggregates[91] , and chaperone proteins in ubiquilin 2 mutations[92] confirm the protein homeostasis impairment in ALS patients (Figure 6).

- **Autophagy defects**

A neuroprotective effect was observed on primary and human iPSC-derived neurons with *TDP43* mutations when the autophagy was stimulated and led to a greater clearance of TDP43 proteins[93]. *C9orf72*-ALS patients bear signs of *C9orf72* loss of function such as hypersensitivity to autophagy defects and decrease in autophagy function supporting the implication of autophagy dysregulation in ALS patients. Concordantly, *C9orf72* knockdown efficiently inhibits the autophagy and generates ubiquitin-, p62-, and TDP43-positive inclusions in cytoplasm[45,83], suggesting a significant role of autophagy in protein aggregation feature observed in ALS and the neurodegeneration process. Multiple pathological processes might be involved in autophagy dysregulation. Degradation of ubiquitinated protein through autophagy pathway includes 1) initiation and extension of bilayer vacuole into phagophore, 2) transport of selective cargoes (including ubiquitinated protein, dysregulated mitochondria or protein aggregates), 3) maturation into autophagosome, and 4) fusion with lysosome, forming autolysosome inducing degradation of content. Several ALS associated genes encode for protein involved in early steps of autophagy regulation such as optineurin[94], p62[89], and ubiquilin[67]. Impairment of TBK1[95] and p62[96] functions inhibit the autophagic cargo delivery towards the autophagosome. Finally, the autophagosomes maturation is impaired in ALS cells carrying FUS[97], VCP[21], and CHMP2B[98] mutations. Altogether, these studies illustrate numerous autophagic steps impaired in ALS patients (illustrated in Figure 6).

- **Protein aggregation**

In most cases, TDP43 inclusions[99,100] and neurofilament-positive aggregation[46] are a hallmark of ALS pathology and observed in the cytoplasm of both sALS and fALS. In accordance with UPS defects, ubiquitin-positive protein aggregation are observed in neurons[88] and sometimes in skeletal muscles[43] of ALS patients. These ubiquitin-positive inclusions can also contain/"trap" non-mutated forms of SOD1[101], TDP43[102], optineurin[77], and ubiquilin 2[68], proteins associated with ALS. In addition, SOD1[103], FUS[53], and C9orf72-derived dipeptides repeat protein[104] can generate toxic aggregates. Overall, protein aggregation is a common feature in ALS and underline a defect in protein clearance.

2. Aberrant RNA metabolism

FUS and TDP43 are RNA-binding proteins involved in multiples steps of RNA metabolism. In ALS patients, both mutant proteins are mislocalised in the cytoplasm resulting in the loss of function and affecting the RNA processing. RNA metabolism is a key feature of ALS pathogenesis and includes transcription defects, alternate splicing changes, miRNA biogenesis, and stress granules formation (Figure 7). In addition, FUS and TDP43 proteins interact with numerous targets expanding the risk of RNA processing dysfunction even further. TDP43 binds to over 6,000 targets in the brain[80], similarly FUS interacts with numerous binding targets in the brain[105].

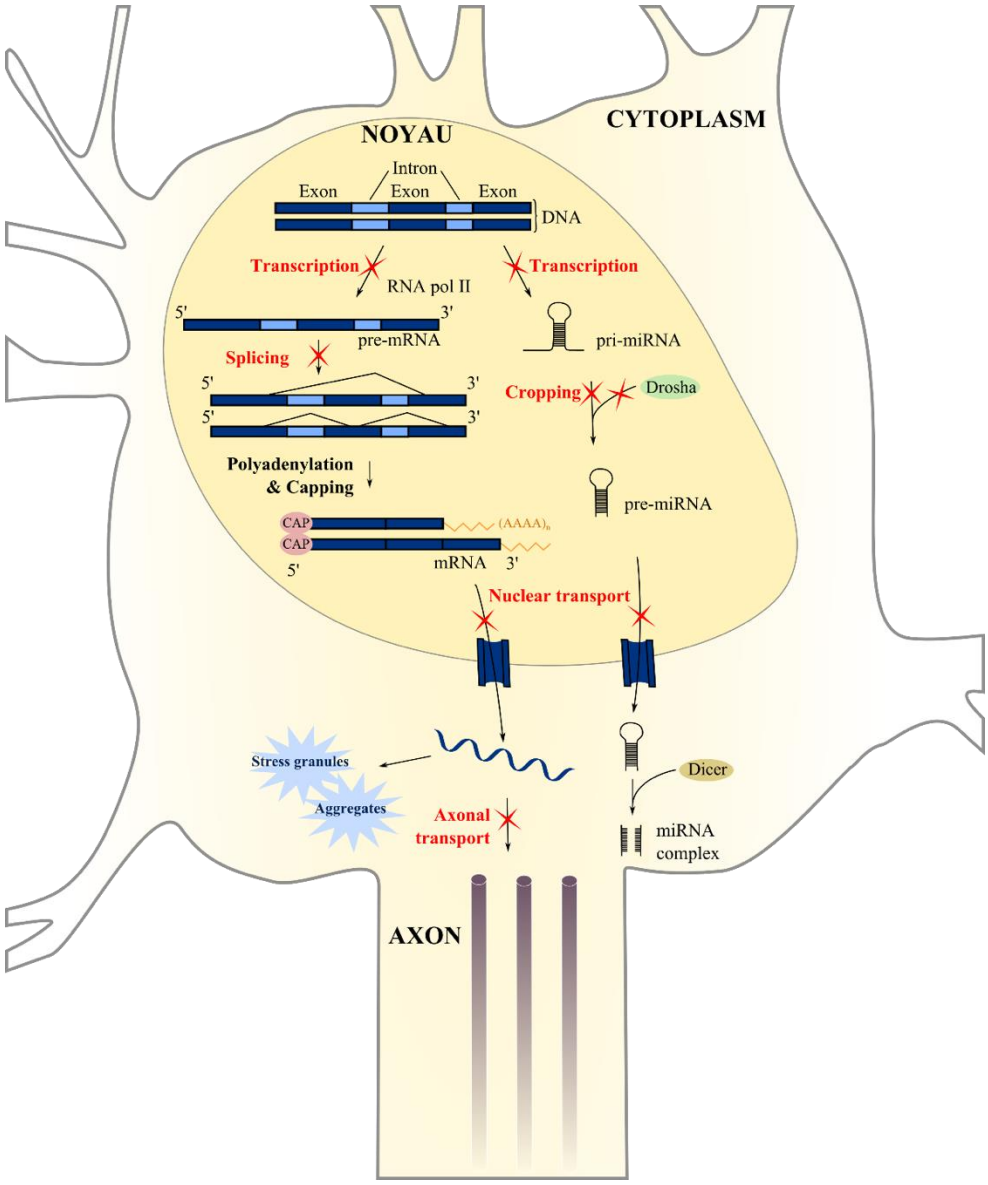

Figure 7 : RNA and miRNA biogenesis defects in ALS.
Many processes in RNA and miRNA pathways are disrupted in ALS patients, including transcription defects, alternate splicing events, miRNA biogenesis and nucleus-cytosol transport impairment. RNA metabolism defects are particularly relevant in ALS pathogenesis since TDP43 and FUS are both well-known ALS-associated genes involved in RNA processing. Both FUS and TDP43 mutated proteins miss-localize to the cytoplasm of ALS motor neurons, leading to a probable loss and toxic gain of function of these proteins.

- **<u>Transcription defects:</u>**

Given the large number of possible protein-protein interaction between FUS or TDP43 and their partners, it is easy to expect important RNA processing defects in ALS patients[21]. Among the differentially expressed binding targets of FUS and TDP43 in ALS, multiple proteins are involved in neuronal physiology such as components of the synaptic plasticity pathways[78,79,106] and dendritic branching process[79,107,108]. In addition,

HREM in *C9orf72* generate repeat-RNA, and RNA foci, repressing gene expression of RNA metabolism regulator (such as hnRNPA3)[109] or sequester TDP43[109,110] and FUS[109] proteins, indirectly inhibiting transcription of RNA-metabolism associated gene. Similarly to C9orf72-mediated RNA processing defects, *FUS* mutant has been associated with major transcriptional defects due to its function in transcription with RNA polymerase II[111].

- **Alternate splicing impairment:**

TDP43 knock down in murine tissues results in alternate splicing changes in 965 mRNA transcripts[52,80] and loss of function of FUS induce splicing defects in more than 300 genes[78], suggesting important alternate splicing event in ALS patients. It is not surprising regarding the ability of FUS to sequester numerous component of the splicing process such as key splicing factors[112], U1 snRNP and U11/U12 snRNPs[108,113] involved in minor introns splicing. Alternative splicing changes have been identified in neuronal genes involved in cytoskeleton organization, axonal growth and guidance in *FUS*-mutated ALS patients[114,115], and interestingly axonopathy or axon retraction are early stages of ALS[116].

- **miRNA biogenesis dysfunction:**

Evidence for miRNA processing defects have been obtained from studies reporting differential expression of several miRNA in TDP43 (miRNA9, miRNA132, miRNA143 and miRNA558)[117] and FUS (miRNA125 and miRNA192)[118] patients. It has been demonstrated that both TDP43 and FUS, as well as C9orf72-mediated DPRs interacts with Drosha [117,119,120]. Additionally TDP43 protein associates with the DICER enzyme[117], results that are all consistent with a defective miRNA processing in ALS patients.

- **Stress granules formation:**

In response to stressful conditions, RNA granules also known as stress granules are generated. Under those conditions, FUS and TDP43 can be recruited to stress granules[46,121]. However in ALS patients, mutations in those RNA binding proteins disrupt stress granules dynamics. Mutants *FUS* and *TDP43* have been shown to increase the persistence of stress granules in the cytoplasm resulting in a possible toxic gain of function[86] by inhibiting translation and thus contributing to ALS pathological progression. In mutants *C9orf72* ALS patients, stress granules also involves sequestration of other proteins such as RAN GAP[122], a protein required for functional nucleoplasmic transport.

3. Mitochondrial dysfunction

Mitochondria is the power house of the cell and source of intracellular energy or ATP and are required in cellular respiration, calcium buffering and regulation of apoptosis. Functional mitochondrial defects[69] such as altered morphology and swelling have been identified in neuronal and muscular tissues of ALS patients carrier of *SOD1*[21] and *C9orf72* mutations[21,70]. Several mechanisms can trigger mitochondrial dysfunction in the cell. SOD1 mutant deposition in mitochondria[123] induce the formation of vacuoles in the mitochondrial inter-membrane space as well on the cytoplasmic face of the outer membrane[124]. Consequently, mitochondrial respiration and energy production are defective and lead to oxidative stress generation. Oxidated proteins and lipids in the mitochondria then exacerbate the respiratory chain dysregulation and the oxidative stress[125]. To maintain axonal integrity and survival, neurons transport all components to their distal sites, including mitochondria. Defective mitochondrial transport is mediated through *SOD1* mutants in ALS[74] and is responsible for a decrease in ATP production, calcium mishandling[69] at the neuromuscular junction contributing to distal axonopathy. Defective axonal transport induce an accumulation of impaired mitochondria and a decrease in recycling of dysfunctional mitochondria in distal sites[124]. Pro-apoptotic signalling activation through impaired mitochondria dysfunction[124] such as the caspase-dependent[126] or bcl-2-dependant pathways[124] might be responsible for motor neuron degeneration. Not only the mitochondria are impaired in SOD1 mutated cells, but also the calcium homeostasis[127]. Calcium level dysregulation will then affect many metabolic pathway in motor neurons, as well as the synaptic communication. For instance, a decrease in calcium homeostasis is associated with higher risk of motor neuron damage, and a greater sensitivity to glutamate excitotoxicity[127].

4. Nucleoplasmic transport defects

Cells actively transport proteins and RNA from the cytoplasm to the nucleus and vice-versa via numerous protein transporters. An impaired nucleoplasmic transport of molecules have been identified in *C9orf72* ALS patients[21]. Like *FUS* and *TDP43*, *C9orf72* mutations can generate stress granules and sequester proteins required for effective nucleoplasmic transport such as RAN GAP[122] or importins and exportins proteins[81]. Generation of repeat-RNA *C9orf72* is one of the mechanisms associated with *C9orf72* toxicity in ALS patients. By sequestering the nuclear export adaptator serine/arginine-rich splicing factor (SRSF1), the repeat-RNA *C9orf72* are efficiently transported in the cytoplasm were translation of DPR can occur[128]. Newly formed DPR like poly PR, in turn binds to nuclear pores transporters impairing the import and export of molecules and thus taking part in impairing nucleoplasmic transport[46,81].

5. Endosomal and vesicular transport impairment

Trafficking of endosome and vesicles in cells is mediated through proteins of the large Rab family. *C9orf72* has been proposed to activate Rab proteins because of its structural similarities with the DENN guanine nucleotide exchange factor involved in vesicular trafficking[45]. A reduced endocytosis and defective endosomal/lysosomal trafficking have been described in *C9orf72* mice models, and ALS patients[45]. Genetic evidence also suggest impairment of endosomal and vesicular trafficking pathways through several mutations associated with ALS. Thus mutations occurring in the following genes are highly associated with endosomal defects: 1) alsin protein[64] a guanine nucleotide-exchange factor involved in endosomal pathway such as endosome motility and fusion with lysosome, 2) VCP[129] a ubiquitous AAA+ ATPase that interacts with clathrin protein during endocytosis, 3) VABP component of vesicular trafficking pathway, and 4) CHMP2B or charged multi vesicular protein 2B[98] and optineurin[77] two components of the endosomal sorting complex required for transport (ESCRT) involved in the cargo sorting into intraluminal vesicles.

6. Axonal transport dysregulation

Motor neurons have particularly long axons up to 1 meter, and their physiological function relies on the transport of organelles such as mitochondria and divers molecules (RNA, proteins and lipids). Protein translation at the neuromuscular junction requires the transport of translation components, including RNA and ribosomal proteins towards synaptic structures[130]. The anterograde transport in axons, or movement from cytoplasm towards distal sites, depend on microtubule-dependent kinesin and dynein motors[74]. In both sALS and fALS patients, neurofilament network disorganization have been reported[47]. In *SOD1* mutant models, both anterograde and retrograde transport are impaired[74]. The high level of tumor necrosis factors in mutated *SOD1* motor neurons leads to a disruption of the motor-kinesin dependent axonal transport [131], results in an axonal accumulation of defective mitochondria and autophagosomes, a decrease in mitochondria-dependent energy production[74], and ultimately leads to motor neurons death.

7. Glutamate excitotoxicity

In healthy motor neurons, glutamate, which is the most common neurotransmitter, is released from the presynaptic neurons into the synaptic cleft activating NMDA and AMPA receptors that will mediate an influx of calcium and sodium in the postsynaptic neurons – influx necessary to generate an action potential. Glutamate is then removed from the synaptic cleft by glutamate transporters or excitatory amino acid transporter 2 (EEAT2) located at the membrane of the surrounding astrocytes and postsynaptic neuron. Glutamate excitotoxicity refers to an excessive release of glutamate resulting in abnormal activation of glutamate receptors and thus excessive influx of calcium in the postsynaptic neuron causing an extreme firing of neurons[132]. Glutamate excitotoxicity is thought to be mediated through disruption of intracellular

calcium levels and generation of ROS that will impair normal mitochondrial function. In ALS patients the function of EEAT2 glutamate transporter is disrupted in surrounding astrocytes which contribute to the accumulation of glutamate in synaptic clefts[21], and higher levels of glutamate in the CSF of patients have been measured[132]. Today Riluzole is the only drug validated to slow disease progression, and is believed to target glutamate excitotoxicity damage through its anti-glutamatergic properties[2].

8. Oxidative stress

Oxidative stress results from an imbalance between production and elimination of ROS, and the ability to repair ROS-mediated toxicity. Oxidative stress has been of particular interest in ALS pathogenesis as SOD1 is a major antioxidant proteins. An increase in oxidative damage in ALS patients was among the first hypothesis of how SOD1 mutations could drive toxicity. In fact several body fluids from sporadic ALS patients, including CSF, serum and urine show an elevation of oxidative stress biomarkers[71]. Likewise, *TDP43* mutants also induces an increase in free radical damage[133]. At the cellular level, accumulation of ROS has been linked with oxidative damage to protein, RNA, DNA, and lipids in post-mortem tissue from both sporadic ALS and *SOD1* mutation-related familial ALS cases[72,134,135]. In healthy cells under oxidative stress, the transcription factor NRF2 (Nuclear erythroid 2-Related Factor) will activate the expression of antioxidant response element (ARE) genes that encode for anti-oxidant responsible for ROS removal[136]. In ALS patients the NRF2-ARE signalling pathway is impaired [137], the oxidative stress is out of control and will induce damages that interact with other pathological mechanisms such as mitochondrial dysfunction, ER stress and impaired protein homeostasis, potentially exacerbating their damage to cells and ultimately contributing to the neuronal loss.

9. ER stress

During the formation of misfolded protein, unfolded-protein response (UPR) initiate the recognition of these proteins and transport to the ER where ER-resident protein chaperones will properly fold the protein[138]. Accumulation of misfolded proteins in the ER activates the ER stress response pathway or endoplasmic reticulum-associated protein degradation (ERAD) and consists in the translocation of misfolded protein from the ER lumen to the cytosol[138]. Misfolded protein will undergo ubiquitination and degradation through the proteasome machinery[138]. In ALS patient cells, signs of ER stress have been demonstrated through activation of UPR markers and their co-localisation with mutated SOD1 inclusions[139]. Increase in toxic inclusions number through inhibition of UPR marker suggest protective role of UPR component. Additionally, CSF of ALS patients also displayed an accumulation of ER stress markers[139] and exposing healthy neurons to ALS patients' CSF induce ER stress with ER fragmentation and caspase-dependent apoptosis activation[140]. ER dysregulation have been associated with *C9orf72*-

derived DPRs (such as poly-GA) and mutated *SOD1*[85] through binding to cytoplasmic face of ER surface and leading to an inhibition of ERAD response.

10. Motor neuron vulnerability

The primary feature of ALS is the selective loss of motor neurons, however why this neuronal group is more vulnerable than other is not fully understood. A major characteristic of motor neuron includes their large size and long axons with a cell body of 50-60µm and axons length up to 1 meter[141]. Functional motor neurons have high demands in metabolic support and efficient axonal transport to support their demands in energy. Optimal mitochondrial function to supply sufficient energy is thus essential for motor neurons. However, mitochondria are also responsible for ROS generation, and an increase in mitochondrial demand results in a higher risks of ROS production[141]. Mitochondria in ALS spinal motor neurons are more sensitive to toxicity and cell damage[142] therefore causing a motor-neuron-specific mitochondrial dysfunction risk. SOD1 mutant-mediated toxicity include numerous mechanisms (mitochondrial function[74,123,124], oxidative stress[72,143], ER stress[85], reduced proteasomal activity[91]) and a higher physiological expression of *SOD1* in motor neurons[144] involves a greater susceptibility to mutant SOD-mediated toxicity. Finally, motor neurons are highly sensitive to glutamate excitotoxicity especially through an increase in intracellular calcium concentration as motor neuron possess a reduced calcium buffering activity and more calcium permeable AMPA receptors[145].

Chapter 2: Exosomes biology

Introduction

Intercellular communication occurs in many physiological and pathological situations, and has first been characterized by a direct cell-to-cell interaction or secretion of soluble factors. Extracellular vesicles (EVs) are also now considered as mediators of cell-cell communication[146–150]. Based on their physical properties and biogenesis, EVs can be categorized into 3 groups: 1) exosomes, 2) ectosomes or shedding microvesicles and 3) apoptotic bodies (Reviewed in [151]). They share common features such as a lipid bilayer delimiting a round structure containing a cargo of proteins, genetic materials (RNA, miRNA, DNA), lipids and metabolites. However, their origin (endosomal or from the plasma membrane), biogenesis and buoyant densities differ significantly[151].

Exosomes are 50-100nm vesicles formed by inward budding of endosomal compartment membranes[152]. Intraluminal vesicles (ILVs) or exosomes progressively accumulate inside multivesicular structures (called multivesicular bodies, MVBs) that can either fuse with lysosomes for degradation or with the plasma membrane (PM) to release the exosomes into the extracellular space. Once extracted, exosomes present a characteristic cup shape morphology by electron microscopy. Ectosomes (also described as shedding microvesicles or microparticles) are larger vesicles 100-1000nm, and are formed and secreted at the plasma membrane of cell through outward budding. Apoptotic bodies just like ectosomes are a heterogeneous population of 50-500nm vesicles secreted from cells subjected to apoptotic cell clearance. Contrary to the cup-shape appearance of exosomes observed by electron microscopy, microparticles and apoptotic bodies appear as light vesicles presenting heterogeneous sizes[153,154].

In the 1990's, exosomes secreted by B cells were recurrently observed enriched in MHC class I molecule and consequently suggested to act as antigen-presenter vesicles[148]. Since then, their content has been increasingly investigated (more than 11,000 publications since 1996). It is know that they vehicle functional proteins including diverse signalling proteins and metabolic enzymes, modifying the phenotype of recipient cells[155–157]. Nowadays, exosomes are suggested to be important mediators of intercellular communication and organ crosstalk.

I. Exosomes discovery

The secretion of exosomes by cells was first characterized by two studies published in the 1980s[158,159] describing the release in the extracellular space of the transferrin receptor (TfR) by reticulocyte during their maturation process into erythrocytes. The iron transport receptor was secreted in ~50nm vesicles originating from multivesicular organelles that fused with the plasma membrane (PM) of the cell. Using electron microscopy, Harding et al managed to follow the TfR stained with gold particles in the reticulocytes. They

speculated that the decrease in TfR staining was due to TfR degradation via lysosomes during the maturation of reticulocytes into erythrocytes. However, only rare lysosomes were positive for TfR. Instead, they observed that small 50nm vesicles enclosed inside multivesicular bodies were positive for TfR. These multivesicular bodies fused with the PM, and the vesicles positive for TfR were released in the extracellular space. These vesicles could be then isolated from cell culture supernatant by ultracentrifugation at 100,000g for 90mn. The term exosomes was used for the first time to define the secreted vesicles originating from the invagination of the multivesicular bodies membrane and released by fusion with the plasma membrane of the reticulocytes[160].

Since 1980's, research on exosome biogenesis and understanding their functions grown exponentially. Today, many different cell types are known to release exosomes into the extracellular space and found them in biological fluids (Table 1).

Exosomes origin				**Alix**	**CD9**	**CD63**	**CD81**	**Flotillin**	**Hsp70**	**Tsg101**	**General morphology**	**References**
Non cancerous cells	***Neuronal cells***	*Rat primary cortical neurons*		x				x		x	x	161
		Neuroglial cells	*Microglial cell*		x	x					x	162
			Murine neuroglial cells					x		x		163
			Murine oligodendrocytes	x						x	x	147
			Rat schwann cells			x		x	x	x		164
			Rat astrocytes	x						x		165
		Rat hippocampal neurons		x						x		166
	Muscle cells	*Cardiac muscle cells*	*Cardiomyocytes progenitors cells*					x			x	167
		Skeletal muscle cells	*Human satellite cells derived muscle cells*		x	x	x		x		x	168
		Smooth muscle cells	*Human aortic vascular smooth muscle cell*		x	x				x	x	169
	Hematopoietic cells	*B-cells*									x	148
		Dendritic cells (DC)				x				x		170
		Mast cells	*mouse bone marrow-derived mast cells*								x	171
		Natural killer cells				x						172
		Platelets				x						173

	T-cells				x					x	174
Stem cells	*Mesenchymal stem cells*	*Human mesenchymal stem cells*								x	175
	Neural stem cells	*Human neural stem cells*								x	176
		Neural fetal stem cells		x		x				x	177
Epithelial cells	*Intestinal epithelial cells*				x						178
	Mammary epithelial cell		x						x	x	179
	Salivary gland epithelial cells									x	180
Other	*Adipocytes*							x		x	181
	Endothelial cells	*Human umbilical vein endothelial cells*	x	x						x	182
	Granulosa cells		x		x					x	183
	Hepatocytes								x	x	184
	Keratinocytes							x		x	185
	Macrophages	*Monocyte-derived macrophages*									186
	Monocyte		x		x	x				x	187
Cancerous cells	*Aortic adenocarcinoma*							x			188
	Basophilic leukemia cells									x	189
	Bladder cancer cells			x	x	x			x	x	190
	Brain cancer cells	*D54MG / SMA560 brain cancer cell line*						x		x	191
		Primary cell cultures from pediatric high grade gliomas		x		x				x	177
	Breast cancer		x						x	x	179
	Colon carcinoma	*Murine colon adenocarcinoma cells*								x	192
		HCT116 and COLO205 cells lines		x	x	x		x			193
		RKO and Caco-2 colon cell lines			x		x			x	194
	Glioblastoma multiforme			x	x					x	195
	Lung carcinoma			x	x	x		x			193
	Lymphoma				x	x			x	x	196
	Mammary adenocarcinoma cell									x	192
	Mastocytoma cell									x	192
	Myeloma				x		x				197
	Nasopharyngeal carcinoma			x	x						198
	Ovarian carcinoma			x							199
	Pancreatic adenocarcinoma										200
	Prostate cancer cell line				x						201

Biological fluids	*Amniotic Fluid*			x					x	202
	Aqueous humor			x				x	x	203
	Breast milk				x				x	204
	Bronchoalveolar lavage fluid								x	205
	Cerebrospinal fluid								x	206
	Follicular fluid (Ovarian)			x					x	207
	Plasma		x	x					x	208
	Saliva								x	209
	Seminal fluid								x	210
	Synovial fluid								x	211
	Urine	x	x					x	x	212

Table 6 : Cell types releasing exosomes
Non exhaustive list of different cell types secreting exosomes including (1) non-cancerous like cells neuronal cells (cortical neurons and neuroglial cells), muscle cells (skeletal muscle cells) and hematopoietic cells (B cells and dendritic cells) and (2) cancerous cells. Exosomes are also secreted *in-vivo* and isolated from various body fluids such as plasma, urine and saliva. Listed are the classic positive exosomal markers used to identify and characterize the extracted vesicles (Alix, CD9, CD63, CD81, Flotillin, Hsp70, and Tsg101). General morphology column indicate the analysis of physical properties of exosomes including shape (electron microscopy analysis) and size (nanoparticle tracking analysis method).

II. Physical characteristics of exosomes

1. Exosomes isolation methods

Exosomes have been isolated from conditioned cell culture supernatant and body fluids as plasma, serum or saliva (see Table 1). Yet there is no gold standard protocol for exosomes extraction and the best method must be determined depending on the biological question raised by the study. Exosomes are found in serum used for cell culture. It is therefore important to avoid contamination by serum-exosomes by either growing cells in the absence of foetal bovine serum to produce an exosomes-serum- free medium or deplete the serum from any exosomes by ultracentrifugation if cells do not survive in serum-free conditions[213].

The most commonly used method for exosomes isolation is ultracentrifugation[214], allowing small vesicles as exosomes to cluster at the bottom of the tube at 100,000g. Usually prior to exosomes sedimentation, several centrifugation steps are performed to remove larger vesicles and contaminants potentially sedimenting at 100,000g (300g to remove cells, 2000g to pellet dead cells and 10,000g for cell debris and 50,000g for ectosomes and apoptotic bodies)[213]. Various modification have been proposed over the last decade to improve the quality of extracted exosomes such as 1) higher speed ultracentrifugation (110,000g[198,215,216] or 140,000g[217,218]) and 2) additional purification steps by filtration of large debris and

vesicles using 0.1 to 0.22µm filters[213,219]. Ultracentrifugation doesn't allow the purification of exosomes as vesicles and proteins aggregates contaminants can be isolated from the 100,000g pellet as well[219].

Sucrose (or iodixanol) gradients allow the separation of exosomes from protein aggregates and non-specific associated exosome proteins based on their different capacity to float on sucrose gradient[213]. Due to their small size, exosomes have buoyant densities ranging from 1.13 to 1.19g/ml (See Table 2), while protein aggregates will sediment and pellet at the bottom of the gradient. Similarly to ultracentrifugation modified protocols, additional steps can be added to increase the purity of exosomes by combining floatation on sucrose gradients with filters, concentration columns and/or ultracentrifugation to remove diverse contaminants. Sucrose gradients have been shown to give the purest population of exosomes compare with other extraction protocols such as ultracentrifugation[220], but it requires more sample and time.

Immunoaffinity based protocols allow the isolation of exosomes depending on their membrane molecular composition. So far, multiple exosomal markers have been used in immunoaffinity protocols and relatively pure vesicle subpopulations have been obtained as no protein contaminants are isolated with the exosomes. This strategy requires the identification and detection of a membrane protein of interest that may not be expressed across all exosomes, and thus ignoring a portion of the exosome population. Moreover, once bound to affinity-beads, exosomes are not easily eluted, rendering difficult to test their effects on other cells[213].

Finally commercial kits (*eg* Total exosomes isolation from Life technologies or ExoQuick) based on polymers base preparations[221,222] allow a rapid and easy extraction of exosomes using short low-speed centrifugation. This rapid strategy decrease the risk of exosomal content degradation and allow to extract exosomes from large fluid volumes –as needed in cell culture condition. However ready-to-use kits are usually more costly than other isolation methods and are still considered as questionable methods despite their efficient extraction of exosomes from various cell culture supernatants[187,194,207].

2. Secretion of exosomes subpopulations

Cells secrete a heterogeneous population of exosomes, in terms of molecular composition, physical properties such as the buoyant densities and morphology. During the isolation of secreted vesicles, several subpopulations of exosomes are commonly mixed leading to a bulk analysis of EVs. Depending on the isolation strategy used, the exosome characterization may thus vary. Ultracentrifugation extraction method takes into consideration the size and density of the vesicles while the immunoprecipitation technique is based on the molecular composition of the exosomal membranes and the presence of the protein of interest. Below will be developed the typical vesicle features explaining the exosome heterogeneity.

Heterogeneity can easily be observed in term of size as exosomes usually range between 30 to 100nm as measured by Théry et al[223] (Table 7 summarizes studies reporting heterogeneous population of exosomes). Surprisingly, same cells, *eg* prostate epithelial cells, can produce two populations of exosomes, one fraction larger than the other[224]. Exosomes can be categorized in distinct subpopulation according to their morphological aspect observed by cryo-electron microscopy (cryo-EM) [210,225]. Contrary to EM, the cryo-EM technique does not require the sample to be stained or fixed, preserving the near-atomic resolution of the exosomes and allowing the visualization of both internal and surface features[226]. Different subgroups based on exosomal morphology have been identified: 1) multiple vesicles (corresponding to single/double/triple or more vesicles, i.e. vesicles containing secondary or tertiary vesicles), 2) elongated or oval-like structured vesicles (most of the vesicles have a round shape, but elongated, egg-shaped or even tubular vesicles have also been identified), 3) vesicles coated with external features such as protrusions and 4) electron dense vesicles[225].

Different exosome subpopulations have been identified using buoyant density properties[224,227,228]. Depending on their composition, exosomes float at different densities[227]. Moreover, exosome composition will affect the speed to reach the equilibrium buoyant density – with exosomes enriched in tetraspanins reaching slowly this equilibrium[224]. Not only the exosome composition will affect their migration speed across the sucrose gradient, but also their size. For example, small vesicles (approximatively 60nm) will reach their equilibrium density faster than large vesicles (100nm average vesicles)[224,228]. Consequently, a longer ultracentrifugation (62h) allow the isolation of exosomes having the same buoyant density.

The RNA and protein content varies from exosome to exosome even originating from the same cells, suggesting the existence of different exosomes subpopulation [178,224,225,227–231]. This is particularly true for polarized cells where two distinct groups of exosomes can be secreted at different cell membrane location (*eg* apical vs basolateral[178]). RNA occupancy varies from exosome to exosome, introducing the hypothesis that a subgroup of exosomes will have a high miRNA content while other will have a low concentration. To illustrate this, one copy of the miRNA (eg miR-126, miR-223 and miR-720) was observed in only one exosome out of hundred[229]. In addition, the pathway involved in the release of the MVB content in the extracellular space will influence the protein composition of the exosome membrane (see III. 3. 3. Exosomes secretions: MVB and PM fusion below), and lead to the secretion of specific exosome subpopulations[227]. Even if heterogeneous exosome populations are secreted by cells, most of the studies analyse exosomes as bulk isolates masking vesicle subpopulations. It is still challenging to specifically target a distinct group of exosomes, but solving this technical challenge would allow researchers to target the exosome subpopulation of interest whether it is for general exosome biogenesis and secretion understanding or for therapeutic purposes.

Exosome origin	Ref	Exosome marker	Density (g/ml)													
			1,07	1,08	1,09	1,1	1,11	1,12	1,13	1,14	1,15	1,16	1,17	1,18	1,19	1,2
Rat primary cortical neurons	161	Alix							100							
Murine oligodendrocytes	147							55								
Oligodendrocyte cell line	157					95										
Oligodendrocyte cell line	271										75					
Murine neuroglial cells	417	Tsg101							70							
Oligodendrocyte cell line	271										75					
Bladder cancer cells	190								65							
B-cells	148	MHC-II							70							
Dendritic cells	284									100						
Intestinal epithelial cells	178									60						
Murine neuroglial cells	417	Hsc70/ Hsp70							70							
Oligodendrocyte cell line	157									95						
Natural killer cells	172	Rab5b				70										
Murine neuroglial cells	147	Flotillin							70							
Oligodendrocyte cell line	271										75					
Cardiomyocytes progenitors cells	167					100										
Human satellite cells derived muscle cells	168	CD63					70									
Human satellite cells derived muscle cells	168	CD81	70				70									
Human satellite cells derived muscle cells	168	CD9					70									70

Table 7: Exosomes heterogeneity explained by size and buoyant densities variability in extracted vesicles population.
This table summarizes studies conducted on multiple exosomes including vesicles originating from cell culture supernatant from cancerous and non-cancerous cells or biological fluids. Exosomes are ranked depending on their buoyant flotations (in sucrose g/ml) and associated with the mean vesicle size in nm as measured by electron microscopy (EM) or nanoparticle tracking analysis (NTA) methods. Size ranges and density properties are reported in the table, including classic exosome markers used to identify exosome populations on density gradient separation (listed in third column).

III. Exosomes biogenesis and secretion

1. Molecular content of exosomes

Exosomal protein and lipid composition come from different cellular compartments (cytosol, PM or endocytic compartments) and will vary among different cell types. Lipid bilayer membrane delimited-exosomes are enriched in ceramide, cholesterol, phosphatidylserine andsphingolipids[232–236], as well as in tetraspanin membrane organisers (CD9, CD81, CD63 and CD82 for example)[223,235]. Membrane transport and fusion proteins (cytoskeletal, annexins or flotillin proteins), adhesion molecules (integrins and lactadherins) are also found at the exosome membrane. Transmembrane proteins will be incorporated during the invagination process of the endosomal membranes while cytosolic cargoes are incorporated within the ILVs. Most abundant proteins identified in the exosome lumen include proteins required for the biogenesis and function of exosomes such as ESCRT proteins machinery and the associated proteins ALIX and TSG101[223,235,237] – proteins shared across different exosome subpopulations. Depending on the donor cells, ILVs are loaded with numerous ubiquitous proteins and cell-type-specific proteins, suggesting variations in exosomes molecular composition between cell type and conditions. Additionally, the exosomal lumen contains nucleic acids such as mRNA, miRNA, long non-coding RNAs and t-RNA[149,238–240]. In summary, exosomes contain various intraluminal cargo including proteins, nucleic acid and lipids. However, most studies in the literature have performed exosomes molecular composition of bulk populations of secreted vesicles, masking the ILV-specific composition involved in the fate and function of exosomes (reference to paragraph 2.2).

2. Exosomes cargo sorting

Molecules are not randomly loaded in exosomes, protein cargo sorting inside EV is controlled by specific machineries. Proteins can undergo post-translational modifications (PTM) (including ubiquitination, sumoylation or phosphorylation) and can act as protein cargo sorting signal in exosomes[241]. Ubiquitination of protein is the most important modification involved in sorting of protein in exosomes and involves the endosomal sorting complex required for transport (ESCRT) protein machinery (see paragraph III. 3 Intraluminal vesicles biogenesis). During the ESCRT-dependent exosomes biogenesis, mono-ubiquitinated

proteins are recruited and clustered at the limiting membrane of MVB prior to inward budding and ILVs formation inside the large MVBs[242]. Likewise ESCRT-independent mechanisms involving other PTMs are involved in the sorting of protein cargo such as sumoylation[243] and phosphorylation, citrullination or oxidation [241]. It is noteworthy that not all exosomal protein cargo are modified and that not all modified proteins are sorted into exosomes, thus further studies are required to better understand the sorting of specific PTM proteins into the exosomes. There are other mechanisms that will influence the protein composition of exosomes such as the lipid-rafts or the tetraspanins which are proteins present at the exosomal membrane and that interact with cytosolic proteins[233,241,244,245]. To date it is not clear whether all these protein sorting machineries overlap or are completely independent and/or specific to a sub-type of ILVs. The composition of exosome membranes will also vary depending on the biogenesis pathway used to generate exosomes such as ESCRT-, tetraspanins-microdomain- or lipid raft-dependent[241], contributing to the generation of sub-populations of exosomes (See paragraph II. 2).

The exosomal RNA composition differs from the donor cell's cytoplasm content, and requires specific mechanism(s) for RNA sorting [240]. So far, four main mechanisms are described for exosomes RNA sorting: 1) RNA binding proteins (RBP)[246,247], such as hnRNA2B1[243], carry RNA to ILVs; 2) ceramide via its production by neutral sphingomyelinase 2 (nSMase 2)[241]; 3) RNA binds to the limiting membrane of MVB through raft-binding sequences named EXOmotifs (such as GCCG, UGAC, UCCG, and GGCC), and will be then included in exosome lumen after lipid rafts formation[239]; and 4) RNA modification such as exosomes-specific D-loop may trigger the RNA sorting toward exosomes[248].

3. Intraluminal vesicles biogenesis

During exosomes biogenesis, early endosomes will mature into late endosomes where ILVs are formed and accumulated in their lumen. The process of exosomes formation includes 1) the clustering of sorted cargo at the membrane of the multivesicular body (MVB) forming microdomains and 2) subsequent membrane curvature and fission of vesicles. Generally the fate of MVB is to fuse with lysosomes for degradation of their content, however MVBs can be targeted to the plasma membrane of the cell where ILVs (exosomes) are released in the extracellular space upon membrane fusion[249]. In breast cancer for example, cancer-associated fibroblasts-derived exosomes promote metastasis by stimulating protrusive activity of breast cancer cells. Indeed, once up-taken by breast cancer cells, these fibroblast-derived exosomes are loaded with Wnt11 and are secreted again into the extracellular space to stimulate cell protusions and motility and thus stimulate the invasion capacity of the breast cancer cells[249].

The paragraphs developed below will attempt to describe the heterogeneity of exosomes, harbouring diverse content and membrane composition, as various actors such as ESCRT family proteins, lipids and /or tetraspanins are involved in their biogenesis and secretion (Figure 1).

- *ESCRT-dependent mechanism*

The ESCRT proteins are a group of proteins involved in the sorting of ubiquitinated cargo into ILVs. ESCRT proteins are clustered into 4 complexes: ESCRT-0, I, II and III with associated proteins[242]. Investigations on the role of ESCRT proteins in the biogenesis of exosomes started when studies identified several members of the ESCRT family in secreted exosomes such as Alix and TSG101[250]. A targeted RNAi screen for 23 ESCRT proteins and associated proteins has further demonstrated the function of ESCRT proteins in exosomes formation[251] (Figure 1).

- ESCRT-0 complex binds and clusters ubiquitinated transmembrane proteins at the membrane of the endosomes
- ESCRT-I and –II complexes induce the deformation of the endosomal membrane into nascent ILVs containing sorted cargo
- ESCRT-III structure subsequently stimulate neck constriction contributing towards detachment of ILVs by vesicle membrane scission.

As a result, a set of cargo is sequestered in the inward budding vesicles within the lumen of the MVBs.

ESCRT-0: The ESCRT-0 complex is composed of HRS (Hepatocyte growth factor-regulated tyrosine kinase substrate) and STAM (Signal transducing adaptator molecule) proteins and is recruited to the endosomal membrane via ubiquitinated cargo and phosphatidylinositol 3-phosphate (PI3P). HRS will recognize ubiquitinated protein - ubiquitin acting as a targeting signal for specific incorporation of molecules in ILVs - and binds to PI3P[235,252]. The HRS/STAM complex will then recruit ESCRT-I via TSG101/VPS28 (two components of the ESCRT-I complex) to the endosomal membrane and form an ESCRT-0/ESCRT-I complex.

ESCRT-I: ESCRT-I complex contain one copy of each TSG101, VPS28, VS37 (one of four isotypes VPS37 A-D[252]) and MVB12. Its recruitment at the endosomal membrane is enhanced by ubiquitinated transmembrane cargo. Both ESCRT-0 and –I are involved in the clustering of selected ubiquitinated cargo into microdomain, and in mobilizing the ESCRT-II complex.

ESCRT-II: ESCRT-II complex is a heterodimer comprising one copy of VPS36 and VPS22 and two VPS25 subunits[253]. Together with ESCRT-I complex, ESCRT-II complex initiate the negative curvature of the emerging ILV at the MVB membrane and uptake of cytosolic cargo[235]. Finally, the association of ESCRT-I and –II will recruit the ESCRT-III complex at the ILV biogenesis site via either ALIX or through a direct interaction with VPS25 – VSP25 belonging to ESCRT-II.

ESCRT-III and ATPase VPS4: The components of the ESCRT-III complex polymerize into filaments after recruitment at the MVB membrane[253]. The interaction between the VPS25 dimer from ESCRT-II with VPS20 from ESCRT-III initiate the polymerization of SNF7, the most abundant protein in the ESCRT-III

complex. In turn, SNF7 recruits VPS2 and VPS24 that will form one subunit while SNF7 and VPS20 form another[252] resulting in formation of the last ESCRT component, ESCRT-III. These two substructures forming ESCRT-III inside the nascent neck of the ILV will lead to the closure and detachment of the vesicles containing a specific cargo inside the MVB lumen[235]. Another ESCRT-mediated exosome biogenesis involving the interaction of the ESCRT-III/ALIX with the transmembrane proteoglycan receptor syndecan and its binding partner syntenin has been recently identified[217]. The heparan sulfate proteoglycan syndecans first assemble together at the MVB membrane followed by the cleavage of syndecan auto-repulsive domain. Consequently, the syndecans remain clustered and syntenin can bind to the syndecans. Syntenin will then interact with ALIX, recruit the ECRT-III unit with VPS4 and subsequently lead to the endosomal membrane inward budding and abscission.

The dissociation and recycling of the ESCRT subunits requires the recruitment of the AAA-ATPase VPS4 functioning as a ring shaped oligomers to unfold and separate the ESCRT proteins complexes from the MVB membrane[223,254]. VPS4 protein is composed of 2 hexameric rings stacked on top of each other forming a central core where ESCRT complexes will be disassembled and recycled[223]. ALIX initiate the recruitment of de-ubiquitinating enzymes such as UBPY to remove the ubiquitin from cargoes[242], contributing to the maintenance of the ubiquitin level in the cells[252]. This de-ubiquitination step occurs before the incorporation of the proteins into the ILV and before the closure of the later[252].

- **ESCRT-independent mechanisms**

In addition to the ESCRT-mediated exosomes biogenesis, there is now evidence that ESCRT-independent pathways also promote the sorting of cargo and biogenesis of ILVs. Indeed, the depletion of components of the four ESCRT complexes does not totally abrogate the formation of exosomes[232,251,255] indicating other mechanisms supporting the exosome biogenesis.

Lipid-mediated biogenesis

Similarly to the cell plasma membrane lipid rafts, exosomes are enriched in cholesterol, sphingolipids and ceramide. The neutral sphingomyelinase[232] (nSMase) converting sphingomyelin into ceramide plays a key role in ESCRT machinery-independent ceramide-mediated exosome genesis (Figure 1), as nSMase inhibitor leads to a decrease in the amount of secreted exosome[232]. Phospholipase D2[218] (PLD2) converts phosphatidylcholine into phosphatidic acid (PA)[218] (Figure 1). Both ceramide and PA generated at the limiting membrane of the MVBs possess a cone-shaped structure that may contribute to the negative curvature of the endosomal membrane, leading to inward budding and ultimately the formation of ILVs[256].

Tetraspanins-mediated biogenesis

Proteins of the tetraspanins family have also been described as regulators of non-ESCRT dependent exosome biogenesis (Figure 1). Members of the tetraspanin family are very similar, strongly suggesting

that all tetraspanins proteins present the same configuration. They are transmembrane proteins composed of 4 transmembrane domains resulting in two extracellular domain and three intracellular regions[257]. The crystal structure of the tetraspanin CD81 analysis has recently uncovered an intramembrane pocket in between separated transmembrane regions through and where interaction with cholesterol is possible[258]. Tetraspanin proteins can be glycosylated at various degrees[257] and form homo- and hetero-oligomers with tetraspanins and/or other proteins leading to the formation of protein-enriched microdomain at the PM[259]. The functional role of tetraspanins glycosylation modifications is still unknown but is possibly contributing to tetraspanin complex formation[260] . Due to their cone-shaped conformation and their ability to cluster into microdomain, tetraspanins could induce the inward budding of the late endosomal membrane and exosomes formation[258].

- **Exosome secretion: MVB and PM fusion**

MVBs will be either directed to lysosomes for degradation or to the PM to release the exosomes in the extracellular space (Figure 1). The secretion requires several factors such as the cytoskeleton, associated molecular motors, small GTPases and the fusion machinery including SNARES and tethering proteins[261,262]. Small GTPase Rab and SNAREs protein families are particularly required in the transport of the MVB towards the periphery of the cell, their docking and fusion with the PM[236]. The exosome secretion will be mediated by different Rabs. For example, RAB27 B with its effector exophilin 5 will transport the MVB at the PM along the actin cytoskeleton[263]. The MVBs will then anchore and fuse with the limiting membrane of the cell via RAB27A and its effector synaptotagmin-like protein 4[264]. Different Rabs proteins can be preferably associated with early or late endosomes. For instance, Rab11[264] and Rab35[265] mediate preferably the fusion of early endosome with the PM while Rab27 is involved in the late endosome fusion. The subsequent fusion of the MVB limiting membrane with the PM requires soluble factors (NSF and SNAP), SNAP-attachment protein receptor (SNARE) protein complexes and protein from the synaptotagmin family[223,236]. The v-SNARE complex present at the vesicles membrane will interact with the t-SNARE complex located at the cell membrane. The SNAREs protein will then form bridges between the opposing membranes and bring them to a sufficient proximity to induce fusion of both lipid bilayers. Consequently, ILVs present in the MVBs will be released into the extracellular space.

Figure 8 : Biogenesis and secretion of exosomes.
Schematic representation of exosomes formation and release in the extracellular space. **(1)** Exosomes are produced as ILVs by inward budding of the endosomal membrane and accumulate in the lumen of the endosome. **(2)** Several mechanisms are involved in the biogenesis of exosomes such as ESCRT protein-, lipid-rafts- and tetraspanins microdomain-dependent pathways. Whether one or multiple pathways are required simultaneously on one population of MVB or if each pathway is specific to one population of MVB is still not clear. **ESCRT-dependent pathways: A)** the most described mechanism involve in the biogenesis of exosomes is the ESCRT-dependent pathway requiring protein of the ESCRT family. Specific transmembrane ubiquitinated cargo are recruited and clustered at the MVB membrane by ESCRT-0

complex, subsequently binding to ESCRT-I structure. ESCRT-II complex is activated and together with ESCRT-I will create and/or stabilize the vesicle neck. Finally, ESCRT-III and its associated proteins will drive the neck constriction. **B)** The second ESCRT-dependent biogenesis pathway is the syntenin/Alix pathway. The formation of syndecans enriched microdomains leads to the syndecans cleavage, and the formation of syntenin/syndecan complexes that interact with ALIX. The syntenin-syndecan-ALIX complex will then favour the recruitment of ESCRT-III complex to support the MVB membrane curvature and abscission. **ESCRT-independent pathways: C)** Ceramide- and phosphatidic acid-dependent pathways are based on the formation of lipid-rafts where sphingomyelin is converted to ceramide or phosphatidylcholine to phosphatidic acid. The ceramide- and phosphatidic acid-enriched rafts induce the inward curvature of the MVBs membrane. **D)** Similarly, tetraspanins enriched microdomains can induce a negative curvature in the MVB membrane. **(3)** MVBs will either fuse with lysosomes for degradation or with the PM which will consequently release exosomes in the extracellular space **(4)**. Several proteins have been identified in the transport and fusion of the MVB to the PM such as proteins from the Rab protein family and SNAREs complexes.

ESCRT: endosomal sorting complex required for transport, SNARE: SNAP (Soluble NSF Attachment Protein) receptor.

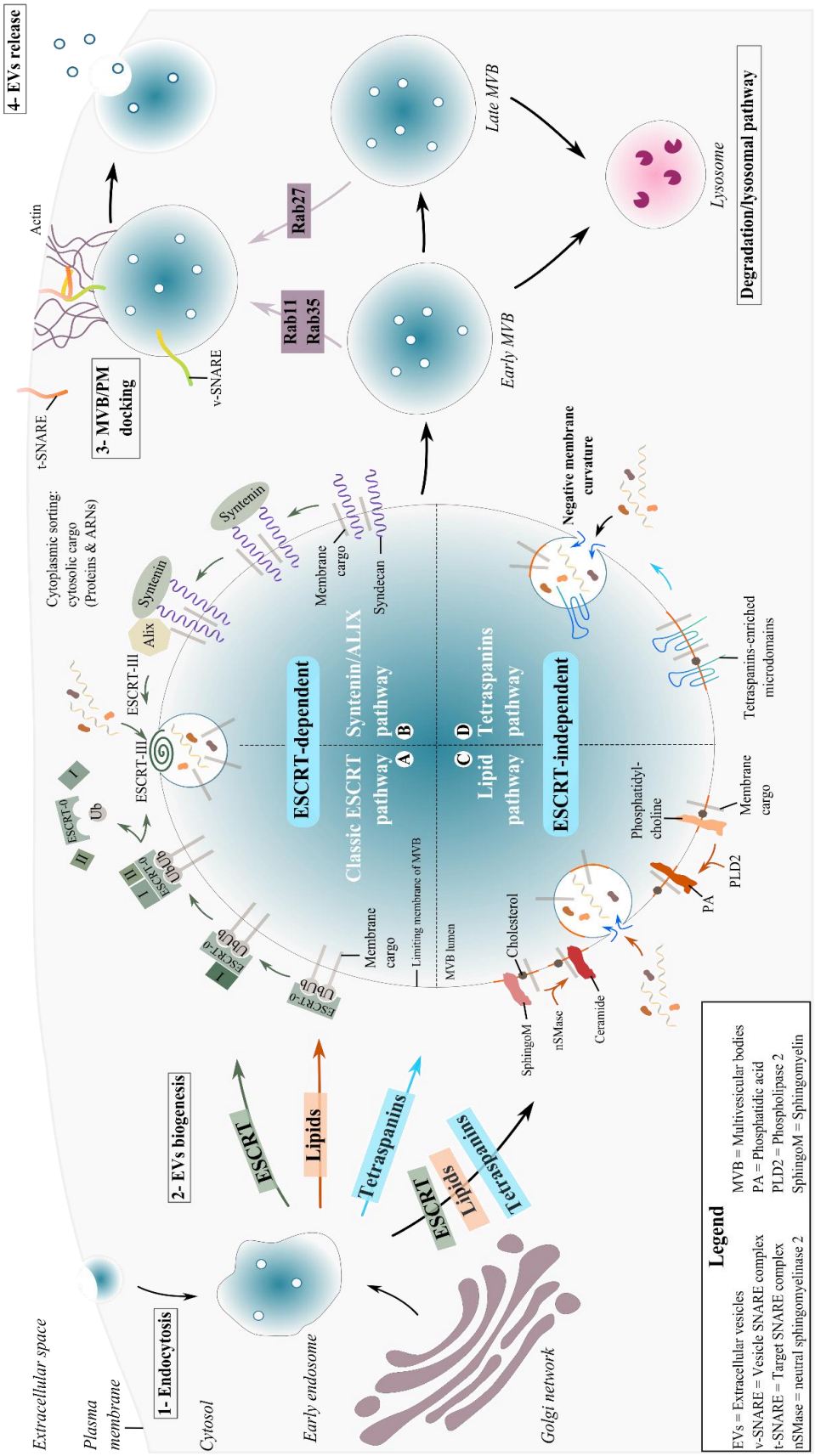
4- EVs release
Actin
t-SNARE
3- MVB/PM docking
v-SNARE
Rab11
Rab35
Rab27
Late MVB
Early MVB
Lysosome
Degradation/lysosomal pathway
Cytoplasmic sorting: cytosolic cargo (Proteins & ARNs)
Syntenin
Alix
ESCRT-III
Membrane cargo
Syndecan
Negative membrane curvature
ESCRT-dependent
Classic ESCRT pathway
Syntenin/ALIX pathway
A B
C D
Lipid Tetraspanins pathway
ESCRT-independent
Limiting membrane of MVB
MVB lumen
Cholesterol
SphingoM
nSMase
Ceramide
Phosphatidyl-choline
PA
PLD2
Membrane cargo
Tetraspanins-enriched microdomains
Ub
ESCRT-0
ESCRT-I
ESCRT-II
UbUb
1- Endocytosis
2- EVs biogenesis
ESCRT
Lipids
Tetraspanins
Extracellular space
Plasma membrane
Cytosol
Early endosome
Golgi network
Legend
EVs = Extracellular vesicles
v-SNARE = Vesicle SNARE complex
t-SNARE = Target SNARE complex
nSMase = neutral sphingomyelinase 2
MVB = Multivesicular bodies
PA = Phosphatidic acid
PLD2 = Phospholipase 2
SphingoM = Sphingomyelin

IV. Exosomes interactions with recipient cells

The most popular function in physiological or pathological condition of exosomes is to mediate cell-to-cell communication. The hypothesis of exosomes as intercellular messengers suggest that exosomes secreted by one cell communicate with another targeted cell and induce a cellular response. Exosomes are able to deliver biologically active molecules such as lipids, proteins or genetic materials[266] to recipient cells, and they can act as therapeutic vehicles as they potentially convey therapeutic molecules or drugs[267]. Consequently, it is important to unravel the mechanisms underlying the exosome interactions with its recipient cell. Intercellular communication mediated by secreted exosomes occur in different manners, via 1) indirect signalisation mediated by a soluble fragment cleaved from the vesicles acting as a ligand to cell surface receptor; 2) docking of the exosomes at the PM of the targeted cell; 3) activation of surface proteins by direct ligand-receptor interaction; or 4) internalization or fusion of the vesicle by/with the targeted cell that will release the exosomal content (Figure 2). It is noteworthy that the recipient cell can also uptake its self-produced exosomes in an autocrine mechanism.

Figure 9: Exosome and recipient cell communication
Schematic diagram summarizing exosomes-cell interactions. Once secreted into the extracellular space exosomes mediate cellular responses via distinct pathways. Exosomes are described as messenger of functional cargo altering the physiology of the targeted cell once internalized. However exosomes uptake and direct contact with the targeted cell to mediate cell-exosomes communication are not constantly required. Indirect interaction between secreted vesicles and cells is possible through soluble **ligand signalling**. Exosomes carry transmembrane protein on their surface, accessible for cleavage by proteases to produce soluble forms of proteins that interact with specific receptor on the PM. Once reaching the targeted recipient cell, exosomes will **dock** at the PM. Following the anchorage of the vesicles, activation of multiple distinct intercellular signalling pathways might occur via ligand/receptor interaction, also known as juxtacrine signalling. Most of the studies however describe an internalization of exosomes by the recipient cells. **Exosomes uptake** involved several mechanisms such as endocytosis of exosomes including: 1) clathrin dependent mechanism, 2) caveolin mediated endocytosis, 3) macropinocytosis, 4) phagocytosis and 5) lipid-raft dependent endocytosis. To release their content into the cytoplasm, secreted exosomes can directly fuse with the PM. The vesicle-cell interaction generate distinct **cellular responses.** Communication mediated by ligand signalling, Juxtacrine signalling or direct fusion with the PM possibly results in intercellular signalling pathway activation since the endocytosis-lysosomal pathways are not involved in the processing of exosomes molecular composition. On the other hand once endocytosed by the cells, exosomes content are systematically release to the endocytic compartments and are more likely to undergo degradation via fusion of endosomes with lysosomes. Some vesicles however have been described to escape degradation by back fusion of the exosomes-containing MVB with the PM of by transport of exosomes towards the golgi apparatus. MVB: Multivesicular bodies.

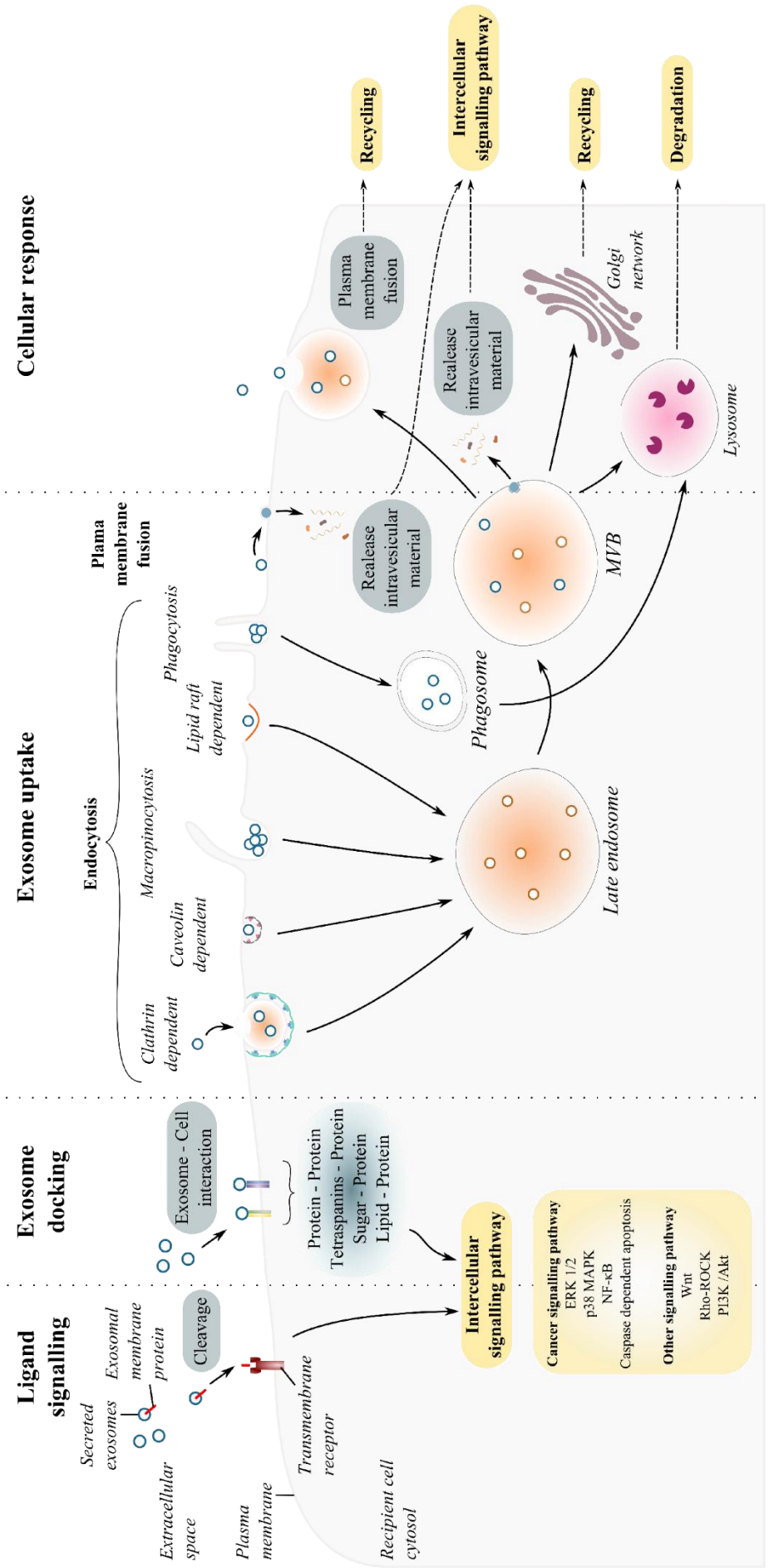
Ligand signalling
Exosome docking
Exosome uptake
Cellular response
Secreted exosomes
Exosomal membrane protein
Extracellular space
Plasma membrane
Cleavage
Transmembrane receptor
Recipient cell cytosol
Exosome - Cell interaction
Protein - Protein
Tetraspanins - Protein
Sugar - Protein
Lipid - Protein
Intercellular signalling pathway
Cancer signalling pathway
ERK 1/2
p38 MAPK
NF-κB
Caspase dependent apoptosis
Other signalling pathway
Wnt
Rho-ROCK
PI3K /Akt
Endocytosis
Clathrin dependent
Caveolin dependent
Macropinocytosis
Lipid raft dependent
Phagocytosis
Plama membrane fusion
Late endosome
Phagosome
MVB
Realease intravesicular material
Realease intravesicular material
Plasma membrane fusion
Recycling
Intercellular signalling pathway
Golgi network
Recycling
Lysosome
Degradation

1. Evidence for exosomes uptake

Direct (tracking of exosomes inside the recipient cell) and indirect (functional transfer of cargo) methods exists to assess the uptake of exosomes.

- **<u>Functional exosomal content transfer</u>**

Multiple studies have reported the transfer of exosomal cargo to recipient cells[149,230,267,268]. Interspecies transfer of exosomal cargo from mouse exosomes to human cells[149] demonstrated that both mRNA and miRNA are functionally transported from one cell to another, and was able to mediate a cellular response. Like genetic material, proteins such as enzymes, can also transmit an enzymatic activity to a recipient cell[154]. Finally, by using exosomes as a vehicle for short interfering RNA, it has been demonstrated that exosomes can carry exogenous molecules to specific cells. For instance, by using a tagged brain-targeted exosomes that is loaded with specific siRNA, BACE1 knockdown (protease involved in formation β-amyloid peptide aggregations in Alzheimer's disease pathogenesis) was efficiently achieved suggesting the potential use of exosomes in delivering tissue-specific drugs[267].

- **<u>Exosomes tracking in recipient cells</u>**

Direct visualisation of exosomes inside cytoplasm of recipient cells efficiently allows tracking of their uptake *in-vitro*. Organic dyes such as PKH lipophilic dyes (including PKH67 or PKH26[157,195,268–275]) or rhodamine molecules[172,188,276] are fluorescent labelling dyes easy to use to visualise lipid bilayered-structures such as exosomes. Because of the resolution limitation, researchers can't distinguish single exosomes however cluster of exosomes that are large enough allow the visualisation of fluorescence under a microscope. The use of fluorescent lipophilic dyes present some limitations as it allows the labelling of extracted vesicles and the cell-to-cell transfer of exosomes can't be assessed using this technique. Genetically encoded fluorescent CD63 are now being developed to illustrate the uptake of vesicles. Because CD63 is specifically expressed in exosomes, labelling of other extracellular vesicles is very unlikely, allowing the tracking of GFP-tagged exosomes uptake in cell-to-cell in live experiments[277].

2. Indirect communication: soluble ligand mediated signalling

Exosomes can mediate intercellular communication without direct contact with the recipient cell, by producing soluble ligand resulting from the cleavage of transmembrane protein – ligand that will then interact with its receptor at the surface of the targeted cell and activate multiple signalling pathways (Figure 9 – ligand signalling). For example, as part of the complement activation pathway, CD46 has been identified as one of the mediators of complement resistance of malignant cells by inactivating C3b and C4b

molecules[278]. CD46 can shed from the tumor cells via exosomes and cleaved by metalloproteinases to produce soluble form in ovarian cancer cells[278].

3. Exosomes uptake by target cells

Targeting the recipient cells, whether it is a specific and control process or stochastic, is the first step involved in the exosome uptake. This process requires the combination of specific molecules present at the surface of the cell and of the exosome (see Table 3), including proteins (glycoproteins, integrins or tetraspanins), lipids and sugar. Following interaction, exosomes either directly fuse with PM or are internalized by the recipient cell and deliver their content in the cytoplasm.

- **<u>Ligand – receptor interaction</u>**

Whether exosomes-cell interaction is a controlled and specific mechanism is still unknown, several studies investigated how exosomes could specifically target different cells in different physiological and pathological conditions[196,272,279]. For example, peripheral blood mononuclear cell-derived exosomes from lymphoma patients can specifically target B cells while exosomes derived from natural killer cells and T-lymphocytes cannot[196]. On the other hand, a single cell type can adsorb different exosomal populations [193]. Among the list of known ligand-receptor interaction, protein-protein interactions are the most abundant. For instance, when exosomes from human ovarian cells are pre-treated with proteinase K or trypsin to degrade the exosomal transmembrane protein, their uptake by the same cancerous cells is abolished [279–281]. Inhibiting specific interactions using antibodies or soluble ligand prior to treatment of cells with exosomes allowed to discover many specific ligand-receptor involved in the exosomes uptake. On the other hand, negative selection of exosomes can also occurs, as observed with exosomes bearing the CD47 transmembrane proteins inhibiting their phagocytosis by the recipient cells and contributing to a longer retention of exosomes in blood circulation[279].Targeting specific mediators in exosome-cell interactions would prevent the uptake of specific toxic exosomes allowing the development of therapeutic strategies (see IV. 6 Exosomes functions in intercellular communication).

	Exosome ligand	***Target cell ligand***	***References***
Glycoproteins	Fibronectin	Heparin sulfate proteoglycans (HSPGs) Integrins	197 282
	ICAM (CD54)	LFA-1	283–285
	MUC1	DC-SIGN	286
Integri	β1 and β2 integrins	ICAM-1 Collagen-I	287

	Integrin α4β1	Fibronectin	288
	αvβ3 / αvβ5 integrins	MFG-E8	289
	CD47	SIRPα	290
Lectin	C-type lectin	Mannose-rich C-type lectin receptor	291
	Galectin 5	Glycoproteins (CD7, α5β1-integrin, or laminin)	292
	Galectin 9	Tim 3	198
Tetraspanins	Tspan8-CD49d	ICAM-1 (CD54)	200
Lipid rafts	Phosphatidylserine	Tim-1/4	234
		MFG-E8	289
	Phosphatidylethanolamine		
	Annexin 2	Lipid raft domain	276
Sugar	α2,3-linked sialic acids	sialoadhesin (CD169)	293

Table 8 : Summary ligand – receptor interaction in exosomes/cell communication.
Known ligand/receptor interactions are listed and categorized according to the molecular origin of the exosomes' ligand. ICAM: InterCellular Adhesion Molecule, LFA-1: Lymphocyte Function-associated Antigen 1, MFG-E8: Milk Fat Globule-EGF factor 8 or lactadherin protein, SIRPα: SIgnal Regulatory Protein α, DC-SIGN: Dendritic Cell-Specific Intercellular adhesion molecule-3-Grabbing Non-integrin C type lectin receptor.

- **<u>Fusion of exosomes with PM</u>**

The exosome-recipient cell membrane fusion process is similar to the fusion taking place during a cell-cell fusion, with targeting – docking – fusion being the main required steps. One method developed to follow the fusion of exosomes with the PM is the use of self-quenching fluorescent lipid probe R18[230,294]. R18 lipid probe classically used to study the virus-cell fusion mechanims[295] can be applied to exosomes in order to track their direct fusion with the cell membranes[230,294]. Briefly, once R18 is incorporated in the vesicles, exosomes can be applied to the cell culture of interest. When the fusion occurs, R18 probe is diluted into the unlabelled membranes resulting in an increase of its fluorescence. The pH of the extracellular space is an important parameter vesicle-cell fusion process, as a tumorous environment with an acidic pH can enhance the fusion, while a pre-treatment with proton pump inhibitors reducing the extracellular space acidity reversed this phenomenon[294].

- **Endocytosis**

Exosomes uptake by the recipient cells can occur through the endocytic pathways including clathrin-or caveolin dependent endocytosis, and clathrin-independent mechanisms such as lipid-raft mediated endocytosis.

Clathrin-mediated and caveolin-dependent endocytosis

Various studies have highlighted the possibility of exosomes to be internalized by energy-dependent mechanisms involving the cytosqueleton of the recipient cells[275,292]. A well-known endocytosis pathway is the clathrin-mediated endocytosis (CME) involving the internalization of cytoplasm (including exosomes and cytosolic proteins) by means of clathrin coated vesicles[296]. The deformation of the limiting membrane of the cell induced by the clathrin protein, leads to the formation of inward buds growing into a larger vesicle that will mature and pinch off[297]. When chlopromazine was applied to ovarian cancer cells to inhibit CME, the uptake of exosomes by these cells was reduced[298]. Similarly, when dynamin inhibitor is applied to neurons or microglial cells – dynamin being a protein involved in the formation of a ring at the neck of the invaginating membrane to separate the vesicles from the PM – the exosomes uptake was dramatically decreased [157,292].

Exosomes can be internalized via caveolae, another endocytosis-mediated pathway. Caveolae are invaginations in the plasma membrane enriched in glycoproteins and cholesterol[299]. Caveolin rafts are internalized by the cell through dynamin activity[297]. Specific inhibition of caveolin-dependent endocytosis via the specific knock down of CAV gene reduce the uptake of exosomes in epithelial cells[300].

Micropinocytosis and phagocytosis

Exosomes can be secreted as a cluster [166], thus affecting the exosome incorporation through the classic clathrin- and caveolin-dependent mechanisms. In this context, both phagocytosis and micropinocytosis pathways can form large vacuoles[301] and can engulf large exosomes clusters and aggregates. Despite their resemblance, phagocytosis and micropinocytosis occur through two distinct cellular machineries. The phagocytosis relies on the association between the receptor from plasma membrane and the vesicle's ligand, while the micropinocytosis occurs constitutively and requires the cytoskeleton actin protein–dependent extension formation[271]. Macropinocytosis is characterized by the formation of ruffled extension from the PM around the extracellular space including extracellular fluid and component that will be further internalized by the cell. The macropinocytosis machinery requires multiple mediators such as PAK1 kinase, rac1, ras and src, cholesterol, cytoskeleton actin protein and Na+/H+ exchanger[301]. Inhibition of this machinery leads to a decrease in exosome uptake, supporting the role of macropinocytosis in the uptake of exosomes[271]. The drugs used to inhibit the micropinocytosis include: 1) dynasore (inhibitor of dynamin), 2) NSC23766 (suppressor of rac1 activity, 3) cytochalasin D (disruption of the actin cytoskeleton function), 4) amiloride (blocking of the Na+/H+ exchanger and 5) alkalinising drugs such bafilomycin A, chloroquine or monensin to increase pH. Similarly to macropinocytosis, phagocytosis requires the formation of

membrane invagination around the targeted cargo to be internalized. Phagocytosis is a major pathway for exosome internalization[302]. It involves actin cytoskeleton, PI3K, dynamin and phosphatidylserine (PS)[297,303]. When several phagocytosis mediators are inhibited using specific drugs (cytochalasin D / latrunculin B, wortmannin / LY294002) and siRNA-targetting dynamin expression, a decrease in exosome uptake is observed. Furthermore, when cells were pre-treated with a soluble analogue of PS, the exosomes uptake decreased suggesting a role for PS found in the bilayer of exosomes membranes to mediate the exosome uptake through phagocytosis pathway[297]. Accordingly, the treatment of recipient cells with TIM4 antibodies – TIM4 being a receptor involved in phagocytosis pathway through its association with PS[234] - led to the reduction of exosomes uptake via phagocytosis[302]. The pre-treatment of exosomes with annexin V, annexin V binding to PS of the vesicles' membranes, also reduced the exosome uptake[297]. Altogether, these studies the importance of the phagocytic capacity of the recipient cells in the exosomes uptake.

- **<u>Lipid raft-mediated endocytosis</u>**

Lipid rafts are formed by cholesterol and sphingolipid-rich microdomain and are phospholipid clusters enriched in transmembrane proteins and sphingolipids like sphingomyelin[297]. When classical endocytosis mechanisms such as clathrin-mediated endocytosis or macropinocytosis were not to part of the exosome uptake mechanisms, the colocalization of exosomes with a lipid raft marker pointed towards the role of lipid in the uptake of exosomes[273]. This non-clathrin dependent endocytosis of exosomes was confirmed by inhibiting vesicle uptake with cholesterol and specific lipid-raft dependent endocytosis inhibitor drugs[273].

4. Recycling or degradation: fate of exosomes inside the targeted cells

Following their internalization by the recipient cells, exosomes will integrate the endocytic pathway and most probably be targeted towards the lysosome for degradation[236,261,304,305]. For instance, the phagosome containing the exosomes up-taken through phagocytosis-dependent pathway will fuse with the lysosome and their content will be degraded[302] (Figure 9). The co-localization of exosomes with phagolysosome maturation markers (eg LBPA, Rab7 and LAMP proteins) strongly suggest the ability of phagocytic cells such as macrophages to internalize exosomes via phagocytosis forming large exosomes-containing vacuoles that are targeted towards lysosomes[302]. The exosome degradation by the lysosomes can then become a source of metabolites (such as amino acids, lipids, lactate or acetate) for the recipient cells[236,274]. Exosomal contents could be recycled by back fusion of the MVB with the PM releasing ILVs in the extracellular space[249].

5. How exosomes deliver functional content to the targeted cells

Late endosome accumulate vesicles that contain molecules not destined to be degraded by lysosomes[306]. To release functional content into the recipient cells' cytoplasm, exosomes escape the lysosomal degradation by back fusion, process where ILVs fuse with the limiting membrane of MVBs [307]. This back fusion process allows the vesicles to release their functional intraluminal content into the cytoplasm of the recipient cell[307]. The vesicular stomatitis virus (VSV) use a similar pathway to deliver its nucleocapsid into the cytoplasm of infected cells. The VSV virus is first internalized by the targeted cells, then directed toward the endocytic pathway where the virus is sorted into intraluminal vesicles. The virus capsid is subsequently released into cytoplasm by back fusion of the limiting membrane of the MVB with newly formed exosomes[308,309]. This virus can stay enclosed in the exosomes for several days, providing the viral content from any degradation before being released as exosomes by integration into new target cells[310]. Once internalized by targeted cells, the secreted VSV-containing exosomes can release their viral content by back fusion. The fusion of the limiting membrane of the MVB with the PM is a another opportunity for the exosomes to escape lysosomal degradation and deliver their functional content [236]. This phenomenon was described to occur with breast cancer cells-derived exosomes[249] and thus contribute to the in the propagation of the disease.

Soluble ligand- and juxtacrine signalling as well as direct fusion of the exosomes with the PM doesn't require the endocytosis of secreted vesicles to modify the phenotype of the recipient cells. In these contexts, exosomes will directly activate intercellular pathway responses.

6. Exosomes function in intercellular communication

Exosomes mediate multiple intercellular signalling within the recipient cell such as proliferation, angiogenesis, apoptosis and cytokine production among other. Soluble ligand- and juxtacrine signalling and direct fusion with the PM are more likely to induce a cellular signalling activation as a direct interaction between cell and exosomes or release of exosomal content occurs. Internalization of exosomes by endocytosis pathways can sometimes be followed by the release of exosome intraluminal content through back fusion (see Figure 2 and paragraph IV. 4. 4. Recycling or degradation: fate of exosomes inside the targeted cells). As previously described exosomes are composed of various molecules cargo that can be functionally delivered to recipient cells, inducing a cell-to-cell cascade signalling to transduce the exosomes function. Physiological functions of exosomes are variable and still not entirely understood. In the next sections will be listed known functions and signal transduction activation mediated through exosomes.

- **Role in development biology and cancer**

The internalization of exosomes by the targeted cell can, among others, activates the Wnt signalling pathway. This Wnt signalling pathway is a well-known signalling cascade involved in many processes during embryonic development, however less was known about the mechanisms involved in the transport of Wnt ligands to their targeted cells[311]. Canonical and non-canonical Wnts molecules have been identified in secreted vesicles from mammalian cells and are functionally transferred to cells to induce Wnt signalling activity[312].

Exosomes are also vehicle for pro- and anti-tumorigenic signalling molecules, acting as mediators of cell-cell crosstalk in the tumor environment. Mesenchymal stem cells-derived exosomes can promote tumor growth by mediating angiogenesis in tumor cells via the activation of extracellular signal –regulated kinase 1/2 (ERK1/2) and p38 MAPK pathways[313]. Promoting growth factor through improved vasculogenesis has been reported to be exosome-dependent in melanoma patients[270]. Briefly, the receptor kinase MET was transferred via melanoma cell-derived exosomes and activated ERK phosphorylation and other downstream effectors to induce the tumor growth and enhance the metastatic activity[270]. In endothelial cells, metastatic potential was stimulated through exosomal activation of MAPK/ERK signalling and stimulating the angiogenesis[314]. Moreover, the internalization of exosomes by monocytic cells induced the activation of NF-κB signalling, crucial step in IL6 production, activation of STAT3 and secretion of more cytokine contributing to the immune escape of tumor cells[281]. Contrary to a pro-tumorigenic potential of exosomes, other tumor cells-derived exosomes have been identified as mediators of tumor cell death through the activation of caspase pathways in an autocrine fashion. In this context, the caspases-3 and -9 are activated in tumor cells following the activation of GSK-3β neutralizing the PI3K/Akt survival signal transduction, and drive the tumor cells towards apoptosis[155].

- **Exosomes-induced signalling and role in the central nervous system**

In neuronal tissue, exosomes secreted by various cells including glia and neurons contribute to the physiology of the central nervous system[146,147,156,157,166,315]. Concerning stress protection, oligodendrocytes-derived exosomes have been demonstrated to support the metabolism activity of neurons under stress conditions suggesting a role of exosomes in neuroprotection[157]. In addition, through activation of several kinases such as CREB, GSK-3α/β and JNK, oligodendrocytes-derived exosomes mediate the transduction of pro-survival signalling as MEK/Erk and PI3K/Akt in neurons under physiological and stress conditions[156] further supporting the role of neuronal exosomes in the brain. Myelin is the insulating layer of neurons that helps conducting action potential along the axons of neurons. During the maturation of oligodendrocytes, neuronal axons are enwrapped by myelin, and the myelination process seems to be controlled by the exosomes secreted by the oligodendrocytes, activating in an autocrine manner the Rho-ROCK-myosin signalling pathway[146]. In addition to the axonal guidance role of oligodendrocytes-derived exosomes described above[146], these exosomes can enhance the action potential firing in cortical neurons[156],

but can also ensure a neuroprotective role. For instance, Hsp70 heat shock protein secreted through the oligodendrocytes-derived exosomes[147] that can be internalized by neurons axons mediating stress-protective signal. Finally, cortical neurons can also secrete exosomes[166,315] depending on the glutamatergic activity associated with Alpha-amino-3-hydroxy-5-methyl-4-isoxazolepropionic acid (AMPA) and N-methyl-D-aspartate (NMDA) glutamate receptors at the synapse. This cortical neurons-derived exosomes contain components of the synapse such as subunits of AMPA receptor and neuron cell adhesion L1, suggesting a role for these exosomes in the synapse plasticity.

In pathological conditions, exosomes have been identified as probable vehicle in disease progression within the nervous system. Alzheimer's disease (AD) is a neurodegenerative disorder characterized by loss of neurons and accumulation of amyloid plaques due to the loss of degradation of β-amyloid peptides in the brain. Aβ-peptides are accumulated in exosomes from AD patients, inducing its propagation in the extracellular space. Spreading of the disease to healthy cells has also been suggested by the colocalization of AD patients-derived exosomes and amyloid plaques[316]. Similarly, in Parkinson's disease (PD) - disease characterized by accumulation of α-synuclein - α-synuclein has been identified in exosomal content of neuroblastoma cells[317], exosomes that might also have a role in the propagation of the disease to healthy neurons.

- **<u>Role in protein recycling and intercellular communication</u>**

Original studies described the secretion of exosomes as a cellular mechanism to release excess and/or unnecessary proteins in the extracellular space. In early studies, analysis of reticulocyte maturation into erythrocyte unravelled the recycling of TfR through the secretion of exosomes[158,160]. Moreover, exosomes have been extensively studied for their role in immunology signal transduction. An early study by Raposo *et al* on B lymphocytes suggested a novel role of exosomes in antigen presentation[214] and stimulation of T cells activation. Finally, exosomes have also been identified as vehicle for infectious agents spreading such as HIV virus[150].

Altogether these results highlight the contribution of secreted exosomes in physiological and pathological conditions, suggesting the potential role of circulating exosomes in the communication between distant cells, but also their potential role in the propagation of toxic elements in different pathological context, including neurodegenerative diseases.

Chapter 3: Neurotoxic communication in ALS

I. Intercellular communication in ALS

Many pathological mechanisms are involved in ALS, as different cell types other than motor neurons also are altered and display dysregulations. In the SOD1 mutant murine model, neuroinflammation signs such as activated microglia and astrocytes were recorded before the symptom-onset[318]. Moreover, muscle cell defects are reported before the motor neuron loss[319,320]. Altogether, these results suggest that a non-cell autonomous toxicity could participate in disease onset and progression and thus be part of the ALS physio-pathological mechanism.

1. Evidence for non-neuronal cell toxicity

There has been several line of evidence implying non-neuronal cells-mediated toxicity. When G37R, G93A and G85R mutated forms of SOD1proteins were highly expressed in cortical and spinal motor neurons of transgenic murine model, no muscle denervation was observed, motor neuron death was minimal and not sufficient to induce motor deficits[321,322]. It is only in elderly mice (>1 year old) expressing a sufficiently high level of mutant SOD1 that neurodegenerative symptoms appears[323]. In a chimeric murine model, the expression of mutant SOD1 in neuronal cells was not toxic by itself unless the surrounding non-neuronal cells - astrocytes and microglial cells - expressed mutant SOD1[324]. Concordantly, ablating mutant SOD1 expression in motor neurons specifically only lightly the delay onset of symptoms without affecting the the mice survival [69,325]. In addition, when mutant SOD1 motor neurons were surrounded by healthy wild type cells, their death was delayed, while when they were surrounded by mutated SOD1 cells their death was exacerbated[324]. Similarly, when mutant SOD1 expression was decreased in microglial cells at late stage of the disease, symptoms progression declined[69] confirming the microglia-mediated toxicity contribution to the symptom evolution. *In vivo* and *in vitro* studies also confirmed that astrocytes expressing mutant SOD1 are toxicity towards motor neurons[326,327] Altogether these studies illustrate the role of glial cells such as astrocytes and microglia in non-autonomous toxicity in ALS patients. Therefore ALS-mediated toxicity is not strictly restricted to motor neurons and affected surrounding non-neuronal cells might contribute to pathogenesis.

2. Non-cell autonomous toxic mechanisms

In the central nervous system, microglia represent the immune cells pool[328]. Upon damage, microglial cells become active and secrete ROS and toxic molecules that may participate to the toxic environment of motor neurons in ALS [329,330]. In physiological conditions, astrocytes are supportive cells that will provide nutrients for motor neurons as well as ion buffering and neurotransmitter recycling[331]. In ALS patients, astrocytes undergo modifications switching from a neuroprotective to neurotoxic property against motor neurons[332]. Astrogliosis and microgliosis are the main pathological indications of neuroinflammation in ALS patients[328]

and signs of active microglia and astrocytes have been reported in numerous studies[333–335]. Oligodendrocytes also protect upper motor neurons by myelinating their axons and providing metabolic support such as lactate through the action of their monocarboxylate transporter 1 (MCT1). Expression of mutated form of SOD1 is accompanied by a reduction of the MCT1 expression in oligodendrocytes resulting in impaired axons and neuron loss[336]. Concordantly, deleting mutant SOD1 expression in oligodendrocytes of SOD1 mice re-establish their function and slow down symptoms progression[337].

II. Axonopathy mechanisms and muscle involvement

More recently there has been increasing interest in determining whether motor neuron degeneration is driven by toxic mechanisms arising from the cell body of neurons or by destruction of axonal projections. The role of muscle in keeping the neuromuscular junction hence suggest a possible role for muscle-mediated toxicity in motor neuron degeneration.

1. The neuromuscular junction

Motor neurons and skeletal muscle fibers interacts at the neuromuscular junction (NMJ), to transmit action potentials and induce muscular contraction. The NMJ is composed of the presynaptic cell (motor neuron), the postsynaptic cell (skeletal muscle cell) and the terminal glial cell providing support. The axons arising from the motor neuron innervate multiple skeletal muscle fibers ranging from 10 to over 1,000 fibers[338]. Each presynaptic cell contains many synaptic vesicles (50nm diameter vesicles), normally highly dense in presynaptic membrane structures called “active zone”[339]. Those specialized membrane section are particularly enriched in voltage-gated calcium channels involve in the release of the synaptic vesicles in the synaptic cleft. The muscle fibers at their membrane accumulates neurotransmitter receptors and voltage-gated sodium channels hollow projections that crosses the fiber called tubules T. The process of neurotransmission includes several mechanisms to transmit action potentials from motor neurons to muscle fibers and induce muscle contraction. 1) Acetylcholine, which is the neurotransmitter in vertebrates, is stored in the synaptic vesicles present in the motor neuron. 2) Following depolarization voltage-gated calcium channels opens resulting in an increase in intracellular calcium concentration. 3) Acetylcholine is released in the synaptic cleft and binds to its receptors at the muscle fiber membrane. 4) The induced depolarization results in a new action potential that propagates along the muscle fibers, allow the muscle to contract. 5) Acetylcholine is rapidly recycled from the synaptic cleft through the acetylcholinesterase activity, hence stopping the neuromuscular transmission (Figure 10).

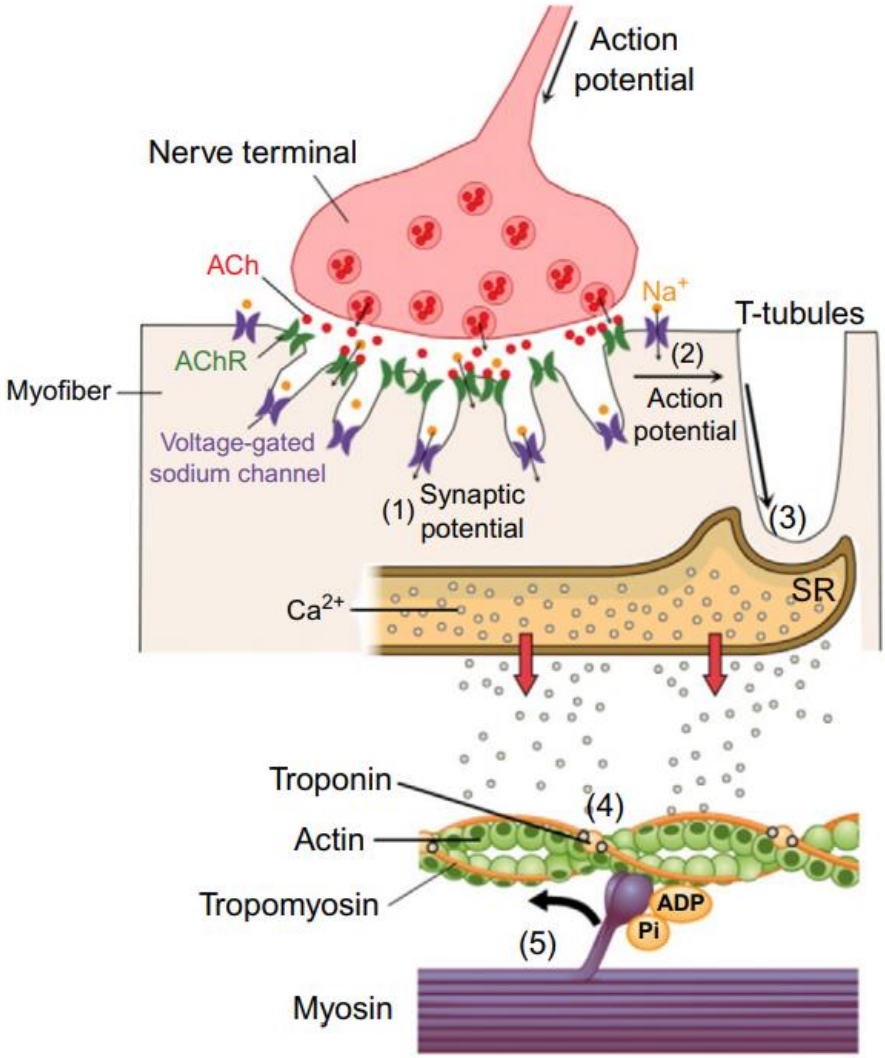

Figure 10 : The neuromuscular junction and muscle contraction.
Following an action potential that reaches the per-synaptic neuron, the neurotransmitter acetylcholine (ACh) is released in the synaptic cleft. Ach binds to its receptor on the post-synaptic nerve and triggers influx of Na^+ and 1) produce a synaptic potential that 2) activates voltage-gated sodium channels and produce an action potential that propagates along the membrane of the myofiber. 3) When it reaches the Tubule T invagination, calcium is released from the sarcoplasmic reticulum. 4) Finally calcium triggers muscle contraction through binding to troponin. 5) Myosin binds to the exposed binding site on the troponin protein and form a cross-bridge responsible for muscle contraction. Figure from Liu et al, 2018[340]

2. Distal axon degeneration

Any dysregulation of the NMJ impairs the synaptic transmission and is likely to induce muscle weakness or wasting[339]. Today it's still not clear whether the degeneration of motor neurons is a dying forward process, where the motor neuron lying in the cortex are the first impaired and then damages are transmitted to their axons, or if ALS is an axonopathy in which the primary injury starts at the neuron projection endings and extends toward the cell bodies (see Moloney et al[116] for review). It is likely that both anterograde and retrograde pattern of degeneration are taking place. In the SOD1 mouse model, pathological changes at the

NMJ are reported before the degeneration of motor neuron axons and cell bodies[341,342]. These results illustrate the progressive retrograde degeneration affecting distal regions earlier than neuronal degeneration, suggesting that muscle tissues could potentially be affected before the loss of motor neurons. Consequently, the muscle weakness and wasting observed in SOD1 mice could result from a combination of both independent and dependent-denervation features.

3. The role of skeletal muscle in ALS patients

Additionally to the trophic support of glial cell towards the motor neurons, skeletal muscle also appear to regulate the homeostasis of the NMJ. Muscle cells plays crucial role in maintaining neuronal survival and axonal growth, especially for developing neurons. A dysfunctional muscle metabolism may thus contribute to NMJ impairment[343,344]. Interestingly signs of muscles dysregulation have been reported in ALS patients[345–347], including early mitochondrial dysfunction[345], decrease in NMJ trophic support molecules such as the fibroblast growth factor binding protein 1 (FGFBP1) levels[346] or oxidative stress[347]. When human mutant SOD1 expression is restricted to the skeletal muscle, it induced an ALS-like phenotype in mice with progressive muscle weakness and wasting and mitochondrial dysfunction[347,348]. On the other hand, several studies tempted to knock down mutant SOD1 expression in skeletal murine muscle and show no significant decreases in the progression of symptoms [349,350]. However the silencing techniques used in both studies - lentivirus well known to be inefficient to target the skeletal muscle[351] and low dose of adeno-associated virus serotype 6 (10^{13} AAV particles as recommended for muscle gene therapy in DMD murine models[352]) were not efficient enough to completely knock down mutant SOD1 in all skeletal muscles, as mutated SOD1 expression level was reduced at the most by 60%. Similarly, in study conducted by Miller et al[349] the authors only decreased by ~20% the expression of mutant SOD1 in LoxSOD1^{G37R}/MCK-Cre murine model, rendering difficult to interpret the results obtain regarding survival and time on onset. In this context, the residual expression of SOD1 in muscle in both studies lead to a relentless progression of the symptoms[349,350] which is consistent with another study where the residual expression of mutant SOD1 was sufficient to support a pathological phenotype[347]. Altogether, these results suggest a possible muscle-mediated toxicity towards nerve in ALS pathogenesis.

4. Secreted vesicles and role in pathogenesis

Intercellular communications happens among neurons and their surrounding cells in the central nervous system through secretion of soluble molecules, the release of exosomes containing neurotrophic support molecules in the extracellular space[156,353]. Exosomes are secreted by many cells types including neurons[315], astrocytes[165], oligodendrocytes[147] and microglia[162] and may participate in the maintenance of physiological conditions in the brain[146,147,161,162,165,353]. However, increasing number of studies are reporting a pathological role of exosomes in neurodegenerative diseases such as Alzheimer's and Parkinson's disease[316,317] as

exosomes have a role in the propagation of neurotoxic proteins. In ALS patients, neuronal exosomes have been reported to contain ALS-associated proteins such as SOD1[354,355], FUS[356], TDP43[357,358] and C9orf72-mediated DPRs[359]. Interestingly, misfolded SOD1 seeds were identified in exosomes and are transmitted to recipient cells inducing propagation of the prion-like properties of SOD1[360]. In addition, astrocytes-derived exosomes contain mutant SOD1 and contribute to the death of motor neurons[355]. Likewise, TDP43 and C9orf72 DPRs spread from cell to cell and strengthen the propagation of misfolded proteins and toxic aggregates in recipient cells[358,359,361]. Similarly, skeletal muscle cells also acts as a secretory organ and release myokines[362] and extracellular vesicles under physiological[268] and physiopathological conditions[363], such as ectosomes (or microparticles) and exosomes.

5. Conclusion

Regarding 1) the emergence of ALS as a multisystemic disease, as pathological alteration are observed in different cell types including in muscles), 2) the distal axonal degeneration preceding loss of motor neurons implying a toxic intercellular communication between muscle and nerve and 3) the pathological potential of exosomes in ALS disease, we hypothesize that vesicle trafficking is disrupted in ALS muscle cells and influence the communication at the NMJ. This phenomenon could be a key element in disease progression.

Objectives

In addition to its classical role in locomotion, the skeletal muscles can act as a secretory organ. The muscle secretome is composed of exosomes, but also of microvesicles and secreted proteins called myokines[268,363]. Exosomes originate from multivesicular bodies or MVB (also called late endosome) that bud off internal vesicles. The MVB then fuse with the plasma membrane of the cell, releasing the exosomes in the extracellular space[364]. If they were first thought to be garbage vesicles, they are now seen as powerful intercellular messengers that can spread information from cell to cell[146–148,160,223,317,365,366]. Hence, exosome influence the homeostasis of recipient cells and interestingly muscle exosomes have been demonstrated to be able to deliver functional proteins, miRNA and microRNA to target cells[268,367].

ALS is an adult-onset fatal neurodegenerative disorder characterised by a progressive, rapid and fatal deterioration of both upper- and lower motor neurons[2]. ALS is mainly sporadic with 90% of ALS cases with no apparent family history, and only 5-10% of ALS cases are familial[7]. Today ALS remains incurable and the causes of muscle denervation are still unknown. Numerous mechanisms involving the neighbouring cells, including astrocytes and microglial cells are suggested to contribute to the motor neuron death in ALS patients and therefore is considered as multisystemic disease[69,324,326,327]. It has now been demonstrated that pathological molecular and cellular changes occur at the neuromuscular junction prior to motor neurons degenerations and symptom onset[342,368]. In addition, since the identification of SOD1 mutations in ALS patients[42] several gene associated with the vesicle trafficking have been described in ALS patients, such as the vesicle-associated membrane protein B gene[76] (*VABP*), alsin protein[64] or the valosin containing protein[129] (*VCP*). These results highlight the potential disruption of the exosomes biogenesis and secretion pathways in ALS patients. More recently hnRNA2B1 involved in the sorting of RNA into exosomes[243] has also been identified in ALS cases[369] suggesting a RNA processing dysregulation in ALS patients.

In light of these data, we hypothesise that vesicle trafficking is disturbed in ALS muscle cells and might influence the **intercellular communication** between the **muscle** and the **nerve**. This phenomenon could be a key element in the disease progression.

The purpose of this PhD project was to 1) confirm an altered exosomes secretion by ALS muscle cells, 2) determine the effects of the ALS exosomes on motor neuron survival, and 3) unravel the toxicity mechanism mediated by muscle ALS exosomes.

Material and methods

Experimental protocol n°1

Muscle stem cells extraction and culture (1) - Muscle biopsy dissection: micro- explant culture

Since 1961 the muscle fiber, the multinucleated contractile unit of muscle, is known to result from the fusion of numerous mononucleated myoblasts[370]. In adult healthy muscles, the muscle stem cells called satellite cells are the mononucleated muscle precursor responsible for muscle grow and repair following trauma. Satellite cells are located peripherally between the basal lamina and the muscle fibers. Following tissue damage, activation of these satellite cells induce their proliferation and are referred to as myoblasts. The myoblasts consequently differentiate and fuse into myotubes that will further elongate by fusing with other myotubes. The approach we used to extract the muscle stem cells from biopsy is the microexplant culture technique to allow cells to proliferate out the biopsy during culture[371]. To mimic a muscle trauma, the muscle biopsies are cut to trigger satellite cells activation, migration, and proliferation. This technique is an easy and reliable procedure that minimise primary cell extraction trauma and produce a cell population composed of approximatively 85% of proliferative myoblasts[371].

Dr G Oudaogo, Dr S D Duguez and L Le Gall extracted primary muscle stem cells from human biopsy as described below.

Procedure:

1. One 10cm petri dish is prepared for culture of explants:
    - 1-2ml of serum is added to the petri dish
    - The excess is removed by aspiration using a glass pipette.
2. To get rid of as much blood as possible the muscle biopsy is rinsed in DMEM 3 times in small 6cm petri dishes, and transfer in a petri dish containing serum
3. Leftover of skin and fat are gently removed using a pair of tweezers and scissors. The muscle biopsy is than roughly dissociated.
4. The entire muscle biopsy is transferred in a watch glass containing serum and cut into small explants
    - It's important to use a glass receptacle in order to avoid damages to the muscles explants due to scratches in plastic containers.

Products:

Foetal bovine serum (Gibco #10270-106)

DMEM (Gibco #41965-039)

Experimental protocol n°1

Muscle stem cells extraction and culture (1) - Muscle biopsy dissection: micro- explant culture

5. Using a small rubber pipette bulb and a glass pipette, the explants are moved to the 10cm petri dish prepared in step 1, while being careful not to create any scratches to the bottom of the dish.
6. Using a plastic tip, explants are gently and evenly spread out.
7. By gentle aspiration, the excess of serum is removed from around explants, and left to dry for approximatively 10-15mins.
8. Once dried, 6-7ml of proliferative medium (see experimental procedure n°2 for instructions) are slowly added to avoid detachment of the muscle explants. The muscle biopsy is transferred to the 37°C incubator.

Experimental protocol n°2

Muscle stem cells extraction and culture (2) - Myoblasts proliferation, sorting and differentiation

Following the microdissection of the muscle biopsy, myoblast migrate and proliferate. Once enough myoblasts have migrate outside the muscle explant, they are transferred into new petri dishes/flasks for proliferation, sorting and further differentiation into myotubes. Other cell types such as fibroblasts will migrate into the petri dish, however we call easily enrich the human skeletal muscle stem cells by perfoming a CD56 cell sorting. The CD56 antigen (or N-CAM, the neutral cell adhesion molecule) was used as a marker of myogenic cells[372].

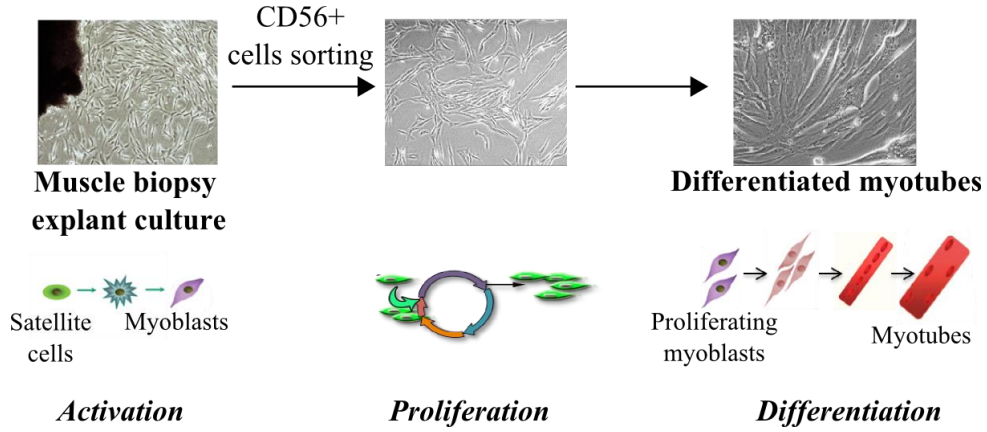

Procedure

I. Myoblasts proliferation:

Following the migration of cells out of the muscle biopsy explant, cells proliferate until the required number of cells is achieved.

9. Once approximatively 80% confluency is reached, cells are trypsinised for counting.
10. Myoblasts are washed 3 times in PBS to get rid of the serum
11. The corresponding volume of Trysin is added (see Table 1 below) and cells are incubated for 5min at 37°C.
12. Trypsin is inhibited by adding the corresponding volume of 5% FBS/PBS and centrifuged at 200g – 5min.

Products:

PBS (Gibco #10010-015)

0.25% Trypsin EDTA (Gibco #25200-056)

Moxi^Z Cassette (ORFLO #MXC012)

Instruments:

Moxi^Z Mini Automated Cell Counter

Experimental protocol n°2

Muscle stem cells extraction and culture (2) - Myoblasts proliferation, sorting and differentiation

13. Cells are resuspended in 1ml proliferative culture medium and counted using the cell counter moxi Z (ORFLO), and the number of divisions is evaluated as follows:

$$Division\ number = \frac{\log(\frac{Cell\ number\ at\ day\ n}{Cell\ number\ at\ day\ 0})}{\log 2}$$

14. Myoblasts are seeded in the appropriate flask for further proliferation.

Petri dish/Flask	Trypsin	5% SVF/PBS	Proliferation culture medium
6cm petri dish	300µl	5ml	5-7ml
10cm petri dish	1ml	9ml	10ml
Flask 175cm²	1ml	9ml	20ml
Flask 225cm²	2ml	13ml	25ml

Products:

BSA (Sigma #A9418-100G)

0.5M EDTA (Invitrogen #1861283)

CD56 magnetic beads (Miltenyl #130-050-401)

II. CD56+ MACS cell sorting:

Before performing a CD56 MACS cell sorting, cells count should reach at least 1.10^6 cells per culture.

Magnetic labelling

1. The cell number and division is determined as described above.
2. MACS buffer is prepared as follows : PBS pH7.2 – 0.5% BSA – 2nM EDTA.
3. Cells are washed in 2ml MACS buffer and centrifuged 200g – 5min.

The following volume are used for 1.10^6 cells

4. The cell pellet is resuspended in 80µl MACS buffer + 20µl CD56 magnetic beads and incubated for 15min at 4°C.
5. 1ml MACS buffer is added to dilute CD56 magnetic beads concentration and cells are centrifuged at 200g – 5min. Subsequently cells are resuspended in 500µl MACS buffer.

Experimental protocol n°2

Muscle stem cells extraction and culture (2) - Myoblasts proliferation, sorting and differentiation

Magnetic separation

1. An appropriate number of MACS columns are placed on the magnetic field of a MACS separator with collection tube and rinsed with 500µl MACS buffer.
2. The cell suspension is added to the MACS column and washed 3 times with 500µl MACS buffer.
3. The collection tube is removed and unlabelled $CD56^-$ cells (non-myogenic cells) which passed through the columns can be collected and counted for storage in -80°C freezer for further use.
4. A new collection tube is used to directly flush out the magnetic labelled $CD56^+$ cells (myogenic cells) with 1ml MACS buffer.
5. The cell number is determined and enriched myoblasts cell population are transferred into appropriate flask for further proliferation.

Products:

M199 (Gibco #41150-020)

Insulin (91077C-5G)

Fetuin (Millipore #341506-1GM)

bFGF (Millipore #GF407)

III. Myoblasts differentiation:

Once the cell count has reached the appropriate number of proliferative myoblasts per flask, differentiation into myoblasts is induced.

Differentiation induction:

1. The proliferative medium is carefully withdrawn from flasks.
2. Differentiation of myoblasts occurs in a serum-free medium, in order to get rid of most of the serum from the proliferative medium with minimum stress for the cells, cells are washed 5 times in DMEM
3. The suitable volume of DMEM is added and cells are left for differentiation for 3 days at 37°C (see table below).

Petri dish/Flask	Number of cells	Differentiation culture medium (DMEM)
6cm petri dish	$0{,}8.10^6$ cells	4ml
Flask 175cm²	5.10^6 cells	16ml
Flask 225cm²	$7{,}5.10^6$ cells	22ml

Experimental protocol n°2

Muscle stem cells extraction and culture (2) - Myoblasts proliferation, sorting and differentiation

Myotubes retrieval:

1. The 3 days differentiation medium is harvested and stored for further applications (see Exosomes extraction – experimental procedure n°5)
2. Adherent myotubes are washed once in PBS and appropriate volume of Trypsin is added (see Table above). Cells are incubated 5min at 37°C.
3. To inhibit the trypsin 5% FBS-PBS is added and cells are centrifuged at 200g – 5min.

Following volumes are used for 1.10^6 cells.

4. Harvested myotubes are resuspended in 100µl PBS and stored in eppendorf tubes at -80°C for further applications.

IV. Proliferative medium

1. DMEM/M199 medium is prepared by adding 125ml of M199 to 500ml of DMEM
2. 100ml of FBS is mixed with 400ml of DMEM/M199 and supplements are added to complete the proliferative medium:
    - 125µl Fetuin (final concentration of 25µg/ml)
    - 25µl bFGF (final concentration of 0.5ng/ml)
    - 25µl EGF (final concentration of 5ng/ml)
    - 250µl insulin (final concentration 5µg/ml)
3. The proliferative medium is filtered with a 0.22µm filter

Experimental protocol n°3

Human iPSCs motor neurons culture

Human iPSCs-derived motor neurons (iPSC MN) are obtained following Maury et al[373] protocol. iPSC MN progenitors and supplements were obtained from Dr C Martinat (I-Stem, INSERM/UEVE UMR 861, I-STEM, AFM, Corbeil-Essones, France).

Procedure

I. Poly-L-lysine / laminin coating (Day 1 and 2):

The experimental procedure from Maury et al.[373] was adapted to Ibidi® 8 well plates.

Day 1: Poly-L-ornithine (PLO) coating

1. PLO is diluted in PBS (final concentration 20µg/ml) and 150µL is added per well.
2. Plates are incubated at 37°C overnight.

Day 2: Laminin coating

1. PLO solution is removed and each well is rinsed 3 times with sterile water and once with PBS.
2. Laminin solution is prepared in PBS (final concentration 5µg/ml) and 150µL is added per well.
3. Plates are incubated at 37°C overnight.

II. iPSC MN culture (Day 3 to day 10)

iPSCs-derived MN are cultured in N2B27 differentiation medium for 7 days until reaching full differentiated state.

Day 3: iPSCs-MN progenitor's seeding

N2B27 culture medium preparation, N2B27$^{++}_{1}$:

1. N2B27 medium is prepared as described below:

	500mL	50mL
Neurobasal	250mL	25mL
DMEM/F12-Glutamax	250mL	25mL
N2	5mL	500µL
B27	10mL	1mL
Penicilin/Streptamicin	5mL	500µL
2-Mercaptoethanol	1,25mL	125µL
Glutamax	2,5mL	250µL

Products:

µ-Slide 8 Well ibidi treat (Thistle Scientific #80826)

Laminin (Gibco # 23017-015)

PLO (Sigma #P4957-50ml)

Neurobasal (Life Technologies #21103049)

DMEM/F12-Glutamax (Life Technologies # 31331028)

N2 (Life Technologies # 17502-048)

B27 (Life Technologies # A18956)

Penicilin/Streptamicin (Gibco #15070-063)

2-Mercaptoethanol (Life Technologies # 31350010)

Glutamax (Life Technologies #35050061

Experimental protocol n°3

Human iPSCs motor neurons culture

2. Additives including RI, RA, SAG, SAPT, GDNF and BDNF are diluted (1/1000) to the N2B27 medium. The supplemented N2B27 medium also contains laminin to promote cell adhesion of iPSCs-MN progenitors.

Products:

GDNF (Life Technologies #PHC7044)

BDNF (Life Technologies #10908010)

The $N2B27^{++}_{1}$ is prepared as described below:

$N2B27^{++}_{1}$	Dilution	Volume (µL)	Stock [X]	Final [X]
Rock Inhibitor (RI)	1/1000	6,4	100µM	100nM
Retinoic Acid (RA)	1/1000	6,4	100µM	100nM
SAG (Smoothened Agonist)	1/1000	6,4	500µM	500nM
DAPT	1/1000	6,4	10mM	10µM
GDNF	1/1000	6,4	10µg/mL	10ng/mL
BDNF	1/1000	6,4	10µg/mL	10ng/mL
Laminin	1/1000	6,4	5µg/mL	5ng/mL

iPSC-MN culture:

1. Progenitor are defrosted in N2B27 medium without additives and centrifuged at 260g for 5min.
2. Cells are resuspended in 1ml $N2B27^{++}_{1}$ and cell count is determined.
3. 6,000 progenitors are seeded per well in a final volume of 200µL $N2B27^{++}_{1}$ and incubated at 37°C for 2 days.

Day 5: N2B27 medium change n°1

N2B27 medium needs to be replaced regularly and different combination of additives are required depending on the differentiation step.

1. iPSCs-MN are very sensitive to any harsh medium flow so 75µL of $N2B27^{++}_{1}$ medium is gently removed to avoid cells to detach.
2. $N2B27^{++}_{2}$ medium is prepared as follows: RA, SAG, DAPT and BDNT additives are added to N2B27 medium (1/500 dilution factor)

Experimental protocol n°3

Human iPSCs motor neurons culture

3. Carefully, 100 of fresh 100µL $N2B27^{++}_{2}$ is added to each well and cells are incubated at 37°C for 3 days.

<u>Day 8</u>: N2B27 medium change n°2

1. Similarly, 75µL of $N2B27^{++}_{2}$ medium is gently removed from each well
2. $N2B27^{++}_{3}$ medium is prepared as follows: RA, GDNF, DAPT and BDNT are added to N2B27 medium (1/500 dilution factor)
3. Carefully, 100 of fresh 100µL $N2B27^{++}_{3}$ is added to each well and cells are incubated at 37°C for 2 days

<u>Day 10:</u> N2B27 medium change n°3

1. The last medium change occurs at day 10 when iPSC-MN are fully differentiated, $N2B27^{++}_{4}$ medium is prepared as follows; GDNF and BDNF are added to the N2B27 medium (1/500 dilution factor)
2. Cells can stay in culture for further applications

Experimental protocol n°4

Mycoplasma screening

Mycoplasma contamination screening have been performed regularly using the LookOut Mycoplasma PCR Detection kit from Sigma-Aldrich.

Procedure

Mycoplasma screening were performed using 600µl culture media from approximatively 80% confluent cells, cultivated without antibiotics for at least a week.

I. DNA extraction and purification

DNA extraction from culture media was completed with PureLink Genomic DNA Kits from Life Techologies.

Sample preparation

1. The culture media (600µl) is mixed with 20µl Proteinase K, and an equal volume (600µl) of PureLink genomic Lysis/Binding Buffer is added/
2. The mix is briefly vortexed and incubated at 55°C for 10min.
3. Lysed samples are centrifuged for 5sec and 200µl of 96-100% ethanol is added.

DNA purification

Wash Buffer I and Wash Buffer II are prepared as mentioned by supplier.

1. The lysate is added to the column and centrifuge at 10,000g for 1min at room temperature.
2. The column is placed on a new collection tube, and step 1 is repeated until the entire sample has been through the column.
3. DNA is washed with 500µl of Wash Buffer I and columns are centrifuged at 10,000g for 1min at room temperature.
4. The column is placed into a new collection tube, and DNA is washed with 500µl of Wash Buffer II.
5. Samples are centrifuged at maximum speed for 3mins and the collection tube is discarded.
6. Elution of DNA is performed with 50µl Elution Buffer, incubated for 1min at room temperature.
7. Columns were centrifuged at maximum speed for 1min at room temperature, and extracted DNA is used to perform PCR.

Products:

LookOut® Mycoplasma PCR detection kit (Sigma #MP0035)

PureLink Genomic DNA Kits (LifeTechnologies #K1820-02)

Jump Start taq DNA Polymerase (Sigma #D9307)

Agarose (Invitrogen #16500-100)

TAE 1X Buffer (Biosciences #786-060)

Proteinase K (Invitrogen #4485229)

Experimental protocol n°4

Mycoplasma screening

II. PCR setup

DNA Polymerase/Rehydration Buffer Preparation

1. DNA Polymerase/Rehydration Buffer (DNA-Pol/RB) volume determination

Per sample	23µL
1 Negative control	23µL
Positive control	25µL

$$Total\ volume\ of\ DNA-Pol/RB = (23 \times\ x\ samples) + 23\ (1\ Negative\ control) + 25\ (Positive\ control) + 23\ (1\ extra\ volume)$$

2. DNA Polymerase units determination
    - For JumpStart Taq Polymerase with 2,5units/µl, a volume of 0,5µl is required per reaction

$$Total\ volume\ of\ Jump\ Start\ Taq\ Polymerase = 0{,}5\mu l\ \times (\text{x samples} + 2\ \text{controls} + 1\ \text{extra volume})$$

3. The DNA Polymerase/Rehydration buffer are carefully mixed by flicking tubes.

Test Reaction tube rehydration

1. Appropriate number of tubes are prepared as follows:

$$(x\ samples) + (1\ negative\ control)$$

2. 23µl of the prepared DNA Polymerase/rehydration Buffer is added to each tube

Negative Control / Sample addition

1. 2µl of DNA free water is added to the negative control tube
2. 2µl of samples are added to the sample reaction tube

Positive control preparation

The positive tube contain positive mycoplasma DNA and are prepared last by adding 25µl of the prepared DNA polymerase/Rehydration Buffer.

Experimental protocol n°4

Mycoplasma screening

Incubation

1. Each tube is mixed by flicking them and quickly centrifuged
2. Samples are incubated at room temperature for 5min and are immediately processed with the thermal cycling.

III. PCR and results evaluation

Thermal cycle profile

The thermal cycle profile includes:

- 1 cycle 94°C for 2 min
- 40 cycles 94°C for 30 sec
  55°Cfor 30 sec
  72°C for 40 sec
- Cool down to 4-8°C

Agarose gel migration

1. 1,2% agarose gel is used for PCR products migration.
2. 8µl of PCR products are loaded into the gel and electrophoresis is run for approximatively 25 min at 100V.

Results evaluation

1. The negative control shows a unique band at 481bp indicating successfully performed PCR.
2. The positive control shows 2 distinct bands, one at 481bp the internal PCR efficiency control and one at 259bp corresponding to the mycoplasma DNA.
3. Mycoplasma-positive samples show a band around 260±8bp and depending on the contamination level a 481bp band for internal control.

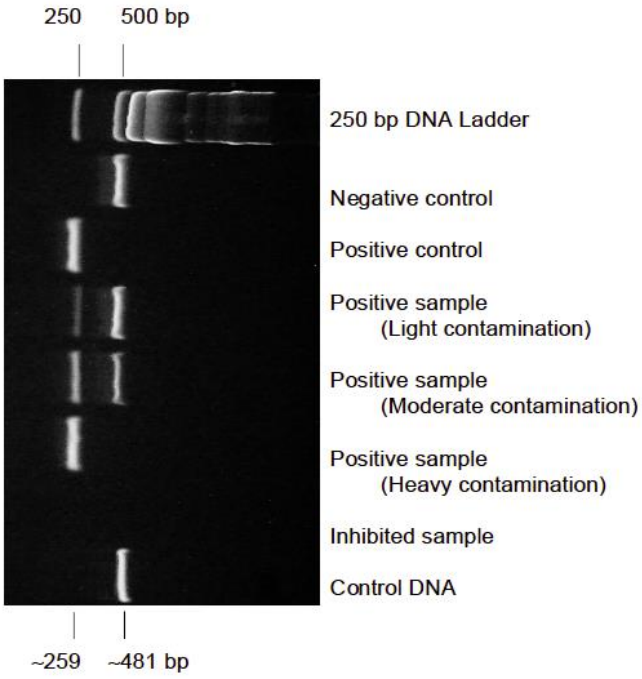

Experimental protocol n°5

Exosomes extraction from culture medium

Exosomes are 50-100nm secreted vesicles release by numerous cell types including skeletal muscle cells[268]. In order to have access to the secreted exosomes in culture medium of 3 days differentiated myotubes, the Total exosomes isolation kit from Life Technologies is used. This kit is based on polymers-containing preparations[221,222], allowing a rapid extraction of exosomes with low-speed centrifugations. However myotubes also secrete microparticles (or ectosomes) that are larger than exosomes (100-1000nm), so clearing the culture medium of larger vesicles and other cell debris is essential before performing extraction of exosomes.

Procedure

Products:

Total exosome isolation kit (Life technologies #4478359)

I. Culture medium preparation

Exosomes are extracted from culture medium from 3 days differentiated myotubes. To obtain pure exosomes pellets, larger vesicles and cell debris must be cleared from the culture medium.

1. Cell debris elimination is performed by differential centrifugations:
    - The culture medium is centrifuged at 300g for 10min
    - The supernatant is centrifuged at 4000g for 20min at 4°C
2. Removal of microparticles is performed by filtration of the obtained supernatant using 0.22µm filters. The conditioned culture medium is ready for exosomes extraction.

II. Exosomes extraction

1. The required volume of culture medium is transferred in a new tube and mixed with 0.5 volumes of Total exosomes isolation kit (2:1, v:v)
2. The culture medium/reagent is well mixed by pipetting up and down (or inverting the tube several times) until a homogeneous solution is obtained.
3. The mixture is incubated at 4°C overnight.
4. The next day exosomes are extracted by centrifuging the mixture at 10,000g for 1 hour at 4°C.
5. The exosome-free supernatant is removed and discarded, exosomes are in the pellet and are resuspended in 100µL PBS.

Experimental protocol n°6

Exosomes PKH26 labelling

PKH26 is fluorescent dye that possess a long aliphatic tails allowing its anchoring to lipid regions of cell membranes[374]. PKH26 staining has been used in a variety of in vivo and in vitro cell tracking experiments and has also proven effective for exosomes uptake monitoring. Extracted muscle exosomes are stained with PKH26 label before applied to cell cultures (muscle and nerve cultures) for treatment.

Procedure

1. A solution of 4µM PKH26 is prepared by mixing 3.2µL PKH26 with 800µL Diluent C.
2. 100µL of Diluent C are added to the 100µL exosomes suspension (see experimental protocol n°4 for exosomes extraction), immediately followed by 100µL of 4µM PKH26. The mixture should be immediately mixed to allow bright and uniform staining.
3. Exosomes suspension are incubated for 5min at room temperature.
4. The staining protocol of exosomes requires to wash the vesicles in concentrators to get rid of excess of PKH26 labelling reagent. The 100K concentrators are pre-rinsed with 500µL of PBS added to the sample chamber.
5. Concentrators are centrifuged at 15,000rpm for 10min at 4°C and the filtrate is discarded.
6. PKH26 labelling is diluted in 250µL PBS
7. The exosomes sample is added to the sample chamber of the concentrator and centrifuged at 15,000rpm for 10min at 4°C.
8. The filtrate is discarded and exosomes are washed by adding 500µL PBS to the sample and centrifuge at 15,000rpm for 10min at 4°C.
9. The filtrate is discarded and exosomes are washed again for a total of 3 PBS washings.
10. After the last centrifugation, exosomes can be resuspended in 100µL of PBS should kept in the sample chamber by gently scraping the column of the concentrator.
11. The labelled-exosomes are transferred to a new Eppendorf tube and immediately use for cell treatment.

Products:

PKH26 Red Fluorescent Cell Linker Kit for General Cell Membrane Labeling (Sigma # PKH26GL-1KT)

Pierce™ Protein Concentrators PES, 100K MWCO, 0.5 mL (Life Technologies #88503)

Experimental protocol n°7

Protein extraction and quantification from cell pellets sample

Total proteins quantification of muscle cells sample was performed using the bicinchoninic acid (BCA) assay, allowing for a colorimetric quantification of proteins. The BCA assay is based on the reduction of Cu^{2+} to Cu^{+} and the sensitivity of bicinchoninic acid to detect Cu^{+}.

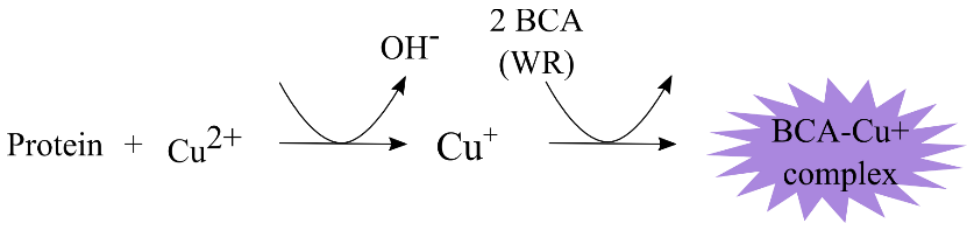

Procedure

Products:

RIPA buffer X (Thermo Scientific #89900)

Urea (Fischer Scientific # BP169-500)

Proteases and phosphatases inhibitors cocktail (Life Technologies #1861281)

BSA (Sigma #A9418-100G)

BCA quantification kit (Life Technologies #1859078)

I. Protein extraction

Protein extraction have been performed using different extraction buffer depending on further experiments.

1. Prepare appropriate extraction buffer:
    - RIPA buffer 1X
    - Urea 8M buffer
    - ½ RIPA 1X – ½ Urea 8M buffer
    - Each extracting buffer supplemented with 10µL/mL proteases and phosphatases inhibitors cocktail
2. 30µL of extraction buffer is added to the cell pellet and samples are incubated 15 to 30 min at 4°C for complete cell lysis.
3. Lysed cell samples are centrifuged at 14,000g for 10 min at 4°C.
4. Soluble proteins contained in the supernatant are transferred to a new Eppendorf tube and stored at -80°C for further applications.

II. Protein quantification

1. BSA standards are prepared as follows using a 2mg/ml BSA stock solution:

Experimental protocol n°7

Protein extraction and quantification from cell pellets sample

Vial	Volume of diluent (µL)	Volume and source of BSA (µL)	Final BSA concentration (µg/ml)
A	0	300 of Stock	2000
B	125	375 of Stock	1500
C	325	325 of Stock	1000
D	175	175 of Vial B dilution	750
E	325	325 of Vial C dilution	500
F	325	325 of Vial E dilution	250
G	325	325 of Vial F dilution	125
H	400	100 of Vial G dilution	25
I	400	0	0

2. Standards are prepared in PBS and same extraction buffer concentration is added to each vial:
    - Cell samples are rich in proteins, thus extracted proteins are usually diluted 1/10 in PBS before quantification.
    - 1/10 extraction buffer is thus added to each standards
3. Cell samples proteins are diluted in PBS (1/10 dilution factor)
4. BCA working reagent (WR) preparation:
    - Using the following formula, the required volume of WR is calculated

$$(\#standards + \#samples)\ x\ 3\ (triplicates)\ x\ 190\ (vol\ of\ WR\ per\ well) = Total\ volume\ WR\ required$$

    - WR is prepared by mixing BCA reagent A with BCA reagent B (50:1, v:v)
5. 10µL of standards and samples and 190µL of WR are to the corresponding wells of the 96 wells plate.
6. The plate is incubated at 37°C for 30 min before absorbance can be read at 562nm using a plate reader.

Experimental protocol n°8

Protein extraction and quantification from exosomal samples

Total proteins quantification from exosomes sample was performed using the bicinchoninic acid (BCA) based assay, allowing for a colorimetric quantification of proteins.

Procedure

I. Exosomes extraction and protein extraction

1. Exosomes are extracted as described previously (Experimental procedure n°5) and resuspended in 100µ PBS.
2. 25µl are used to perform quantification and 10µl of Urea 8M buffer (supplemented with 10µL/mL proteases and phosphatases inhibitors cocktail).
3. Exosome samples are incubated 15 min at 4°C for complete lysis.
4. Lysed exosomal samples are centrifuged at 14,000g for 10 min at 4°C.
5. Soluble proteins contained in the supernatant are transferred to a new Eppendorf tube and stored at -80°C for further applications.

II. Protein quantification

1. BSA standards are prepared as previously described using a 2mg/ml BSA stock solution
2. Standards are prepared in PBS and same extraction buffer concentration is added to each vial (28% of final volume, i.e. for 30µl of standards 12µl of Urea 8M is added)
3. BCA working reagent (WR) preparation:
    - Using the following formula, the required volume of WR is calculated

$$(\#standards + \#samples)\ x\ 3\ (triplicates)\ x\ 190\ (vol\ of\ WR\ per\ well) = Total\ volume\ WR\ required$$

    - WR is prepared by mixing BCA reagent A with BCA reagent B (50:1, v:v)
4. 10µL of standards and samples and 190µL of WR are to the corresponding wells of the 96 wells plate.
5. The plate is incubated at 37°C for 30 min before absorbance can be read at 562nm using a plate reader.

Experimental protocol n°9

Western blotting – Cell lysate samples

The western blotting, or immunoblotting (in reference to antibodies used to specifically detect proteins of interest) is a technique based on the separation of proteins on a gel and their subsequent transfer to a membrane for antibody-based detection. The first step includes preparation of proteins samples in reducing and denaturing condition to allow proteins to unfold and acquire a negative charge. Usually, ß-mercaptoethanol and DTT are common reducing agent responsible for the breaking of disulphide bonds. Moreover, sodium dodecyl sulfate SDS (SDS) is responsible for negatively charging the proteins by attachment of SDS anions to proteins samples. Following a boiling step at 70°C, proteins samples are fully unfolded and ready for electrophoresis, allowing their separation based on their molecular weight. The second step consists in transferring the proteins to a PVDF membrane using the iBlot 2 Dry Blotting System (Life Technologies). Finally, membrane are stained with primary antibodies specific for antigen of interest and Horseradish Peroxidase (HRP)-conjugated secondary antibodies targeting the primary antibody. In the presence of its substrate hydrogen peroxide and luminol, HRP produces a chemiluminescent signal that is acquired to detect proteins.

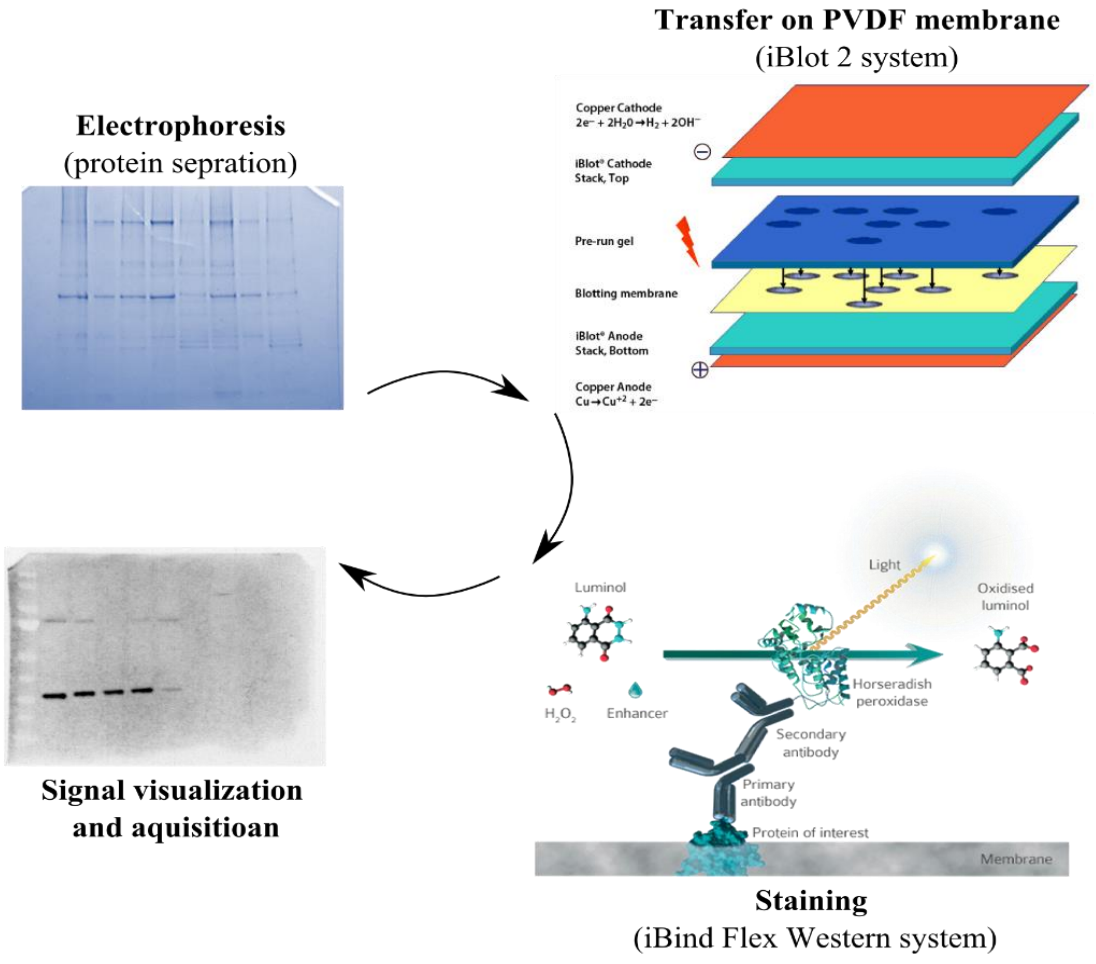

Experimental protocol n°9

Western blotting – Cell lysate samples

Procedure

I. Sample preparation

1. Proteins from cell lysates are extracted and quantified as needed (see experimental procedure n°7).
2. If samples are running under reducing conditions, a NuPAGE mix composed of 1 volume of NuPAGE reducing agent (10X) and 2.5 volumes of NuPAGE LDS sample buffer (4X) (1:2,5, v:v) is prepared, if non reducing conditions are required only NuPAGE LDS sample buffer (4X) is mixed with the samples.
   The required volume of NuPage to be added per sample is calculated as follows:
   $$NuPAGE\ volume\ for\ sample\ X = {Volume_{sample\ X}}/{2.85}$$
3. Samples are boiled at 70°C for 10min and quickly centrifuged.

II. Electrophoresis

The electrophoresis is performed using the XCell SureLock MiniCell and 4-12% polyacrylamide Bis Tris gels from LifeTechnologies.

1. The 1X SDS Running buffer is prepared as follows:
   - 50mL 20X NuPage SDS Running Buffer MOPS
   - 950mL deionized water
2. The cassette containing the gel is removed from the pouch and tape at the bottom of the cassette is detached. The cassette is quickly rinsed with 1X SDS Running Buffer.
3. The cassette is installed in the XCell SureLock Mini Cell and the inner chamber is filled with 1X SDS Running buffer and 500µL of Antioxidant.
4. 25µL (mini gels, 10 wells) or 45µL (midi gels, 12+2 wells) of samples are loaded and 7µL of molecular ladder is added to the gel.
5. The outer chamber is filled with 1X SDS Running Buffer and electrophoresis was run 45min at 200V.

Products:

Life technologies:

NuPAGE™ LDS Sample Buffer (4X) # NP0008

NuPAGE™ Sample Reducing Agent (10X) # NP0004

NuPAGE™ Antioxidant #NP0005

NuPAGE™ 4-12% Bis-Tris Midi Protein Gels, 12+2-well, w/adapters # WG1401A

NuPAGE™ 4-12% Bis-Tris Protein Gels, 1.0 mm, 10-well # NP0321BOX

NuPAGE™ MOPS SDS Running Buffer (20X) #NP0001

iBlot™ 2 Transfer Stacks, PVDF # IB24002

Instruments:

iBlot^2 Dry Blotting System (Life Technologies)

Experimental protocol n°9

Western blotting – Cell lysate samples

III. Transfer using iBlot™ 2 Dry Blotting system

The transfer stack provided with the iBlot 2 system includes a PVDF membrane.

1. Once electrophoresis is completed, the gel is removed from its cassette and is incubated in 20% ethanol for equilibration and optimal transfer.
2. One filter paper is soaked in deionized water and the transfer is assembled following the subsequent order:
    - The bottom stack is placed first in the iBlot 2 system, the PVDF membrane should be on top of the bottom stack.
    - The wet gel is carefully added to the stack followed by the pre-soaked filter paper. Air bubbles are gently removed.
    - The top stack is placed on top and air bubbles are removed.
    - The absorbent pad is finally added on top of the stack, making electrical contact with the iBlot 2 system.
3. The transfer of proteins to the PVDF membrane is run at 23V for 6min.

Following transfer, the PVDF membrane is removed from the transfer stack and Ponceau staining is performed to check transfer efficiency.

4. The PVDF membrane is quickly re-activated for 2 min in methanol.
5. The membrane is rinsed with distilled water for 10min.
6. The membrane is incubated in Red Ponceau staining until clear bands are visible. The excess of staining is washed by rinsing the membrane quickly with deionized water.
7. The membrane is ready for staining.

IV. Blotting membrane using iBind™ Flex Western system

The iBind Flex system allows an automated immunodetection of proteins.

1. The 1X iBind Flex solution is prepared as follows:
    - 500µL 100X additive
    - 10mL iBind™ Flex 5X Buffer
    - 39,5mL distilled water

Products:

Rouge Ponceau staining (Sigma #P7170-L)

Methanol (Honeywell 494437-2L-D)

Life technologies:

iBind™ Flex Solution Kit #SLF2020X4

iBind™ Flex Cards #SLF2010

Instrument:

iBind™ Flex Western system (Life Technologies)

Experimental protocol n°9

Western blotting – Cell lysate samples

Products:

Amersham ECL Prime Western blotting detection reagent (GE Healthcare # 16961637)

2. The PVDF membrane is incubated in the 1X iBind Flex solution for at least 10 mins, and continuously covered to avoid the membrane to dry out during preparation of antibodies solution.
3. Primary and secondary antibodies are diluted in the 1X iBind Flex solution.
4. The iBind Flex System is prepared for blotting by placing an iBind Flex Card in system and adding 10ml of 1X iBind Flex solution across the flow region as illustrated with picture below:

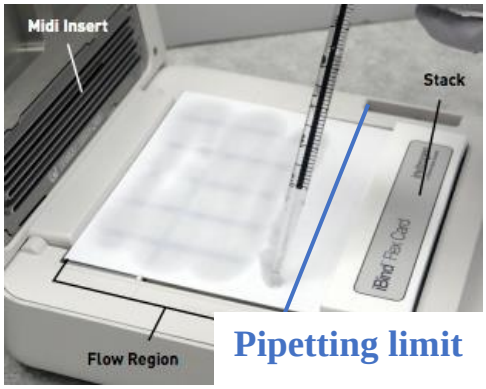

The 1X iBind Flex Solution shouldn't be added to close to the stack of the iBind card as it may decrease the efficiency of the blotting.

5. 2ml (for midi membranes) or 1ml (for mini membranes) of 1X iBind Flex solution are added in the middle of the iBind Flex Card, and the pre-incubated membrane is places protein-side down and the low molecular weight region closest to the card stack, and air bubbles are removed.

6. The lid is closed and antibodies solutions are added to the appropriate rows:

Experimental protocol n°9

Western blotting – Cell lysate samples

- Row 1: diluted primary antibody
- Row 2: 1X iBind Flex solution
- Row 3: Diluted secondary antibody
- Row 4: iBind Flex solution

Antibodies and appropriate dilutions used in western blotting are listed in Table from experimental procedure n°11)

V. Signal acquisition

1. Amersham ECL Prime Western blotting Detection Reagent was used for detection of signal. Solution A containing luminol, and solution B containing peroxide are mixed in a 1:1 ratio.
2. 2ml of Amersham ECL mix is added per midi membrane, 1ml per mini membrane, and incubated for 5 mins at room temperature.
3. Chemiluminescent signal is acquired using the UVP ChemiDoc-It² Imager and UVP software.

Experimental protocol n°10

Exosomes samples preparation for immunoblotting

The western blotting performed on exosomal samples requires supplemental steps to allow detection of antigens. The total exosomes isolation kit is a polymer based reagent and additional washings of exosomes are necessary to allow an efficient staining of samples.

Procedure

Products:

SDS (Sigma L3771-100G)

Exosomes protein extraction

1. Exosomes are extracted from cell culture medium using the total exosomes isolation kit from Life technologies as previously described (see experimental procedure n°4)
2. After extraction, exosomes are resuspended in 100µL PBS
3. Exosomes washing in PBS are performed in 100K Protein Concentrator before protein extraction. Concentrators are pre-rinsed by adding 500µL of PBS to the sample chamber and centrifuged at 15,000g for 10 min at 4°C.
4. The filtrate is discarded and the exosomes are added to the sample chamber and centrifuged at 15,000g for 10 min at 4°C.
5. Similarly the filtrate is discarded and exosomes are washed by adding 500µL PBS to the sample chamber and centrifuged at 15,000g for 10min at 4°C.
6. Exosomes samples are washed 3 times following step 5 directions.
7. Following the third wash, an extra centrifugation step is required to filtrate the entire the dead-stop volume of PBS.
8. After last centrifugation, extraction buffer is added to the sample chamber:
    - 30µL ½ 8M Urea + ½ RIPA 1X, supplemented with 2% SDS and 10µL/mL Proteases and Phosphatases inhibitor cocktail
9. Exosomal samples are immediately harvested from concentrators, columns are gently scraped to ensure to collect exosomes aggregated at the bottom of the sample chamber.
10. The 30µL of samples are transferred in a new Eppendorf tube and incubated 15 to 30 min at 4°C, and centrifuged at 14,000g for 10min at 4°C.

Experimental protocol n°10

Exosomes samples preparation for immunoblotting

11. The soluble exosomal proteins present in the supernatant are transferred in a new Eppendorf tube and ready for electrophoresis preparation similarly to cell lysate samples (see experimental procedure n°8).
    - If CD63 staining is required, samples are processed in non-reducing conditions (without Life technologies NuPAGE sample reducing agent).

Experimental protocol n°11

Immunocytochemistry (ICC)

Immunocytochemistry technique allows fluorescent labelling of a specific antigen in cultured cells. The antigen of interest is bound by a non-fluorescent primary antibody which is than targeted by a fluorescently-labelled secondary antibody that will amplify the signal. The signal produced by the fluorophore conjugated to the secondary antibody is detected using a fluorescent microscope.

Procedure

Products:

Formaldehyde (Sigma #252549-100ml)

Triton (Sigma T8787-50ml)

Tween 20 (Sigma P2287-500ml)

I. Cells fixation

Fixation of the cells using formaldehyde allows the preservation of cellular structures.

1. 4% formaldehyde solution is prepared in PBS, and cell culture are fixed for 10min.
2. Excess of formaldehyde is washed from cells with 3 times with approximatively 500µl PBS before staining.
3. If necessary, cultured cell can be stored in PBS (to avoid the wells to dry) at 4°C for several weeks until staining is performed.

II. Non-specific sites blocking.

To avoid the acquisition of background signal produced by non-specific binding of antibodies, a blocking step is required. The blocking buffer is composed of serum and BSA allowing the masking of all sites, and are replaced by the primary antibodies applied to cultured cells carrying a higher affinity for the antigen. The blocking buffer also includes detergents to permeabilize cell membrane and allow access to intercellular targets.

1. The blocking buffer is prepared as follows in PBS:
    - 20% FBS
    - 0.5% Triton
    - 0.5% Tween 20
    - 5% BSA
2. Cells are incubated in blocking buffer for 30 min at room temperature.

Experimental protocol n°11

Immunocytochemistry (ICC)

Products:

Ibidi® Mounting medium (Ibidi #50001)

Acridine Orange (Sigma #158550)

III. Antibodies staining

The table below summarizes the primary antibodies used.

1. The blocking buffer is gently removed and primary antibodies are diluted as required in blocking buffer. Primary antibodies solution are slowly added to the cells and incubated for 2 hours.
2. After 3 washes in PBS, labelled-secondary antibodies diluted in blocking buffer are added to the cells and incubated for 1h30 at room temperature and protected from the light.
3. Cells are washed with PBS, counter-stained with 1µg/ml DAPI for 1 min, and rinsed twice in PBS.
4. One drop of ibidi® mounting medium is added in each well to preserve fluorophores conjugated with secondary antibodies.
5. Pictures were acquired with Zeiss Axio Imager A2 microscope.

IV. Immunohistochemistry (IHC)

Similarly to cultured cells, tissue sections can be fluorescently labelled, technique known as immunohistochemistry. Muscles biopsies were embed in OCT prior to cryo-sectioning. 8µm transverse muscle sections were cut using a mircrotome-cryostat and were similarly permeabilised, blocked and stained as described above.

V. RNA staining

Acridine orange allows the differential labelling of DNA and RNA. In fact, when bound to double stranded nuclei acid such as DNA, acridine orange will emit a green fluorescence, while bound to single stranded nucleic acid such as RNA, acridine orange (AO) emits an orange fluorescence.

1. Following cell fixation, cell cultures were permeabilized for 1hr at room temperature.
2. Cells are stained with 20µg/ml AO diluted in PBS for 10 min.
3. Pictures were acquired using Zeiss Axio Imager A2 microscope.

Experimental protocol n°11

Immunocytochemistry (ICC)

Antibody	Clone	Manufacturer, Catalogue number	Species raised, Isotype	Dilution used	Application
Calnexin	AF18	Life Technologies MA3-027	Monoclonal, Mouse IgG1	1 : 100	WB
Caprin (GPIP137)		Life Technologies PA5-29514	Polyclonal, Rabbit IgG	1 : 200	ICC
CD63		BD Pharmingen	Monoclonal, Mouse IgG1	1 : 200	IHC, ICC
CD63	TS63	Life Technologies 10628D	Monoclonal, Mouse IgG1	2 µg/ml	WB
Desmin	D33	Life Technologies MA5-13259	Monoclonal, Mouse IgG1	1 : 50	ICC
Flotillin		Life Technologies PA5-18053	Polyclonal, Goat IgG	0.3 µg/ml	WB
FUS		Bethyl A300-302A	Polyclonal, Rabbit IgG	1 : 2000	ICC
FUS		Life Technologies PA5-23696 /PA5-52610	Polyclonal, Rabbit IgG	0.4 µg/ml	WB, ICC
H2AX		Cell Signalling 763J	Monoclonal, Rabbit IgG	1 : 50	ICC
Isl1/2	39.4D5	DSHB	Monoclonal, Mouse IgG2b	1 : 100	ICC
Myosin Heavy Chain	MF20	DSHB	Monoclonal, Mouse IgG2b	10 µg/ml	ICC
RPL5		Life Technologies PA5-26269 / PA5-27539	Polyclonal, Rabbit IgG	1 : 500	ICC
RPL5		Bethyl A303-933A	Polyclonal, Rabbit IgG	1 : 2000	WB
Tsg101	C-2	Santa Cruz, sc-7964	Monoclonal, Mouse IgG2a	1 : 200	ICC
Anti-Tubulin beta III isoform	TUJ1	Millipore, MAB-1637	Monoclonal, Mouse IgG1	1 : 250	ICC

Table 9 : Table of antibodies and their dilutions used in immunocytochemestry, immunohistochemistry or in western blotting.
(see experimental protocol n°9)

Experimental protocol n°12

RT-qPCR and relative gene expression analysis

The real time reverse transcriptase chain reaction (RT-qPCR) allows the quantification of mRNA in cell samples. RT-qPCR combines 3 steps: 1) following RNA extraction, reverse transcription is performed to convert RNA into cDNA, 2) the amplification of cDNA using the PCR technique, and 3) signal acquisition and quantification of PCR products in real time.

Procedure

Products:

TRIzol (Life Technologies #15596018)

Chloroform (Sigma #25666-100ml)

PureLink RNA Mini Kit (ThermoFisher #12183020)

I. RNA extraction and purification

RNA from muscle samples were prepared using TRIzol combines with PureLink RNA Mini Kit.

RNA extraction

1. Cell pellets were dissolved in 100µl TRIzol and complete cell lysis was achieved by adding 900µl TRIzol and pipetting up and down until mixture is homogeneous, and incubated at room temperature for 5min.
2. 200µl chloroform are added and tubes are vigorously shook before a 5min incubation.
3. Lysed cells are centrifuged at 12,000g for 15min at 4°C and the top aqueous phase containing RNA was transferred into a new Eppendorf tube for RNA purification.
4. One volume of 75% ethanol was added and mixed for a few seconds.

RNA purification

1. Up to 700µl of samples is transferred to the spin cartridge and centrifuged at 12,000g for 15sec. This step was repeated until the entire RNA sample was added.
2. The filtrate is discarded and 700µl of Wash Buffer is added to the spin cartridge and centrifuged at 12,000g for 15sec, filtrate is discarded.
3. RNA is washed a second time by adding 500µl of Wash Buffer II and spin cartridge centrifuged at 12,000g for 15 sec, twice.

Experimental protocol n°12

RT-qPCR and relative gene expression analysis

4. Spin cartridge were dried out by centrifuging it at 12,000g for 2min at room temperature and RNase free water was warmed up to 45°C.
5. RNA was eluted by adding 30µl warmed-up RNase free water. Spin columns were incubated for 2/3 min at room temperature before RNA was eluted at 12,000g for 2min at room temperature.
6. RNA purity, quantity, and quality was measured using the Nanodrop spectrophotometer (Thermo FisherScientific), and RNA was used for cDNA synthesis

Products:

M-MLV-RT (Invitrogen #28025-013)

RNase OUT (Invitrogen #10777-019)

10mM dNTP Mix (Invitrogen #18427-013)

Oligo(dT) (Invitrogen #18418012)

LightCycler 480 DNA SYBR Green Master 1 (Roche #04707516001)

Instrument:

LightCycler 480 Instrument Roche

II. cDNA synthesis

cDNA synthesis was achieved using the Moloney Murine Leukeia Virus Reverse Transcriptase (M-MLV-RT, Life Technologies).

1. 1µg of RNA was mixed with 0.5µl oligod(dT) (500µg/ml), 0.5µl random primers, 1µl 10nM dNTPs Mix (10nM each dATP, dGTP, dTTP, and dCTP at neutral pH) and 12µl of sterile and distilled water, and warmed at 65°C for 5 min before being quickly chilled an ice and centrifuged
2. 4µl First Strand Buffer, 2µl 0.1M DTT, and 1µl RNase OUT Recombinant Ribonuclease Inhibitor (40 units/µl) are gently added to the sample and incubated at 37°C for 2min.
3. Finally 1µl M-MLV-RT is added to the mix and incubated at 25°C for 10min and at 37°C for 50min.
4. The reaction was stopped by heating the samples at 70°C for 15min.
5. cDNA purity and quantity was checked using the Nanodrop, and the newly synthetize cDNA was used for RT-qPCR

III. RT-qPCR

Quantitative RT-PCR of exosomal markers analysis and housekeeping gene selection completed on muscles cells were performed on LightCycler 480 Instrument Roche using LightCycler 480 DNA SYBR Green I Master.

Experimental protocol n°12

RT-qPCR and relative gene expression analysis

Products:

Platinium SYBR Green qPCR Super-Mix (Life Technologies #11733-013)

1. RT-qPCR was performed in 384 wells plate, and each well contained 9µl
2. A SYBR Green mix was set-up for each gene, SYBR Green mix for 1 well is prepared as follows:
    - 0.14µl distiller water
    - 4.5µl SYBR Green
    - 0.36µl reverse and forward primers (20pmol/µl) for the gene of interest (see Table below).
3. 5µl of mix and 4µl of cDNA were added per well, in triplicate, and the plate was quickly centrifuged.
4. The cycling protocol includes:
    - Initial step: 94°C for 5 min
    - 50 cycles of : 94°C for 10sec, 60°C for 5sec, and 70°C for 5sec

Quantitative RT-PCR for FUS gene expression performed on muscles cells required the Light Cycler 480 Instrument Roche and Platinium® SYBR® Green qPCR SuperMix-UDG.

1. RT-qPCR was performed in 96 wells plate, and each well contained 15µl
2. A SYBR Green mix was set-up for each gene, SYBR Green mix for 1 well is prepared as follows:
    - 3.9µl distiller water
    - 7.5µl SYBR Green
    - 0.6µl reverse and forward primers (20pmol/µl) for the gene of interest (see Table 1 for primer sequence).
3. 12µl of mix and 3µl of cDNA were added per well, in triplicate, and the plate was quickly centrifuged.
4. The cycling protocol includes:
    - Initial step: 50°C for 2 min, and 95°C for 2min
    - 50 cycles of : 94°C for 15sec, 60°C for 30sec, and 72°C for 5sec

Experimental protocol n°12

RT-qPCR and relative gene expression analysis

IV. Comparative method analysis

The gene expression quantification was performed following the comparative C_t method, also referred to as $\Delta\Delta C_t$. The C_t value, or threshold cycle, corresponds to the cycle number for which a detectable fluorescent signal is measured, and thus used as a relative way of measuring the concentration of the target gene. A lower C_t value illustrates a higher concentration of starting material, or expression level. The comparative method allows to compare the differential gene expression between different samples.

One housekeeping gene, or endogenous gene is used to normalize data, one housekeeping gene should be expressed in constant fashion regardless of experiments conditions. In all samples, both gene of interest and endogenous genes expression levels are measured by RT-qPCR. We tested 7 housekeeping genes traditionally thought to have a stable expression: Beta-2-microglobulin (B2M), Glyceraldehyde-3-phosphate deshydrogenase (GAPDH), Glucoronidase (GUS), Hypoxanthine phosphoribosyltransferase 1 (HPRT1), Peptidylpropyl isomeras A (PPIA), Ribosomal protein large P0 (P0), Proteasome Subunit Alpha Type 2 (PSMA2) (see Table 2). B2M had a constant expression level regardless to the experimental conditions (Figure XX) and was thus used as housekeeping gene.

The PCR amplification efficiency of the reaction was calculated using the slope of the standard curve using PCR products from healthy muscle cells as reference samples (1:20, 1:100, 1:500, and 1:2500 dilutions were used) as follows:

$$Efficiency\ (E) = 10^{-1/slope}$$

The expression level in arbitrary unit was then calculated as follows:

$$E_{B2M}{}^{Ct_{B2M}} \Big/ E_{gene\ of\ interest}{}^{Ct_{gene\ of\ interest}}$$

Experimental protocol n°12

RT-qPCR and relative gene expression analysis

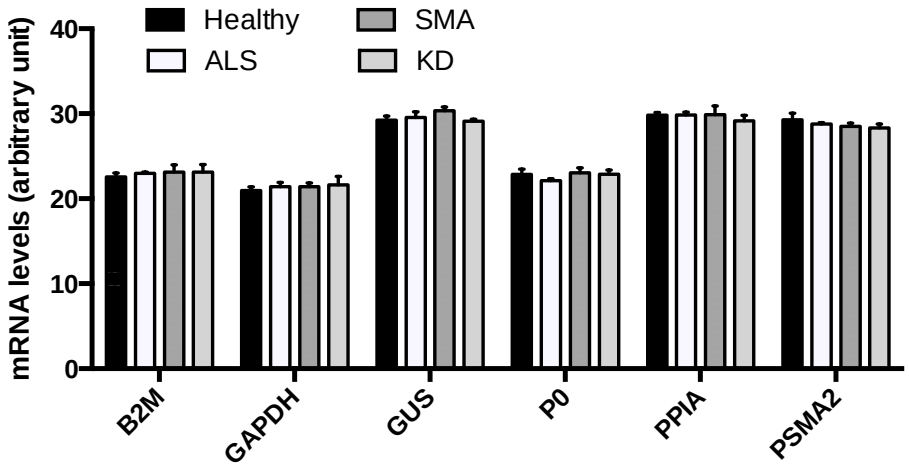

Figure 11 : Housekeeping gene expression level measurement.
RT-qPCR was performed on healthy, ALS SMA and KD muscle cells in order to test 7 housekeeping genes. The comparison of the different genes expression levels has led us to use B2M as housekeeping gene because of its consistent expression in all experimental condition.

Primers		Sequence (5' → 3')
β2M	Fw Primer	CTCTCTTTCTGGCCTGGAGG
	Rev Primer	TGCTGGATGACGTGAGTAAACC
GAPDH	Fw Primer	AAGGTGAAGGTCGGAGTCAACGG
	Rev Primer	TGACAAGCTTCCCGTTCTCAGCC
GUS	Fw Primer	CTCATTTGGAATTTTGCCGATT
	Rev Primer	CCGAGTGAAGATCCCCTTTTTA
HPRT1	Fw Primer	TGATAGATCCATTCCTATGACTGTAGA
	Rev Primer	CAAGACATTCTTTCCAGTTAAAGTTG
P0 (RPL0)	Fw Primer	TCCAGGCTTTAGGTATCACCAC
	Rev Primer	GCTCCCACTTTGTCTCCAGTC
PPIA	Fw Primer	CCTAAAGCATACGGGTCCTG
	Rev Primer	TTTCACTTTGCCAAACACCA
PSMA2	Fw Primer	CATTCAGCCCGTCTGGTAAA
	Rev Primer	GTTTTTTCTCAGTTGCTAATACCACA

Table 10 : Housekeeping gene primer sequences.

Experimental protocol n°12

RT-qPCR and relative gene expression analysis

Primers		Sequence (5' → 3')
Lamp1	Forward Primer	CAGATGTGTTAGTGGCACCCA
	Reverse Primer	TTGGAAAGGTACGCCTGGATG
Lamp2	Fw Primer	GAAAATGCCACTTGCCTTTATGC
	Rev Primer	AGGAAAAGCCAGGTCCGAAC
CD81	Fw Primer	TTCCACGAGACGCTTGACTG
	Rev Primer	CCCGAGGGACACAAATTGTTC
CD63	Fw Primer	CAGTGGTCATCATCGCAGTG
	Rev Primer	ATCGAAGCAGTGTGGTTGTTT
CD82	Fw Primer	GCTCATTCGAGACTACAACAGC
	Rev Primer	GTGACCTCAGGGCGATTCA
SCARB2	Fw Primer	GGCCGATGCTGCTTCTACA
	Rev Primer	GGTCTCCCCTCTGAGGATCTC
EPDR1	Fw Primer	GTCCAGGAGTGGTCGGACA
	Rev Primer	ACACCGAGGGGTCTTTAATACC
VPS29	Fw Primer	TGCAACAGTTTGCCAGCTAAA
	Rev Primer	CCTCTGCAACAGGGCTAAGC
RAB11FIP1	Fw Primer	GGACAAGGAGCGAGGAGAAAT
	Rev Primer	GTCGTGCTAGGGATGATGGC
CD44	Fw Primer	CTGCCGCTTTGCAGGTGTA
	Rev Primer	CATTGTGGGCAAGGTGCTATT
RAB5b	Fw Primer	TCACAGCTTAGCCCCCATGTA
	Rev Primer	CTTCACCCATGTCTTTGCTCG
HLA-G	Fw Primer	GAGGAGACACGGAACACCAAG
	Rev Primer	GTCGCAGCCAATCATCCACT
TSG101	Fw Primer	GAGAGCCAGCTCAAGAAAATGG
	Rev Primer	TGAGGTTCATTAGTTCCCTGGA
FUS	Fw Primer	TGGTCTGGCTGGGTTACTTT
	Rev Primer	TAACTGGTTGGCAGGTACGT

Table 11 : Exosomal marker and FUS primer sequences.

Experimental protocol n°13

siRNA-based FUS silencing

Protein synthesis follows 2 steps, transcription of DNA into mRNA and translation of mRNA into proteins. To silence a gene, small interfering RNA (siRNA) induce the degradation of mRNA before it can be translated into proteins. siRNA molecules are introduced to the cytoplasm of the recipient cells via cationic-lipid-dependent transfection. The transfectant reagent (Lipofectamine) forms liposomes containing the siRNA that will be uptaken by the cells via endocytosis and delivers the siRNA to the cytoplasm of the cell. Once in the cytoplasm, the double stranded siRNA that is complementary to the target mRNA forms a complex with the multiprotein complex RISC (RNA induced silencing complex). The RISC complex cuts the double stranded RNA into 2 single stranded RNA, the sense and antisense strands. RISC stays bound to the antisense strand to find complementary sequence with the mRNA. Once the target mRNA exits the nucleus for translation into proteins, the RISC complex identifies the complementary sequence and associate with the mRNA via complementary base pairing. The mRNA strand is cleaved by RISC and is rapidly degraded before translation into proteins can happen.

We performed Lipofectamine-mediated transfection on 1 day differentiated muscle cells to silence FUS gene. Three days after transfection induction and PKH26 labelled-exosomes treatment, fresh media is added to the 4 days differentiated muscle cells, and cells were cultured for 3 more days before fixation of cells.

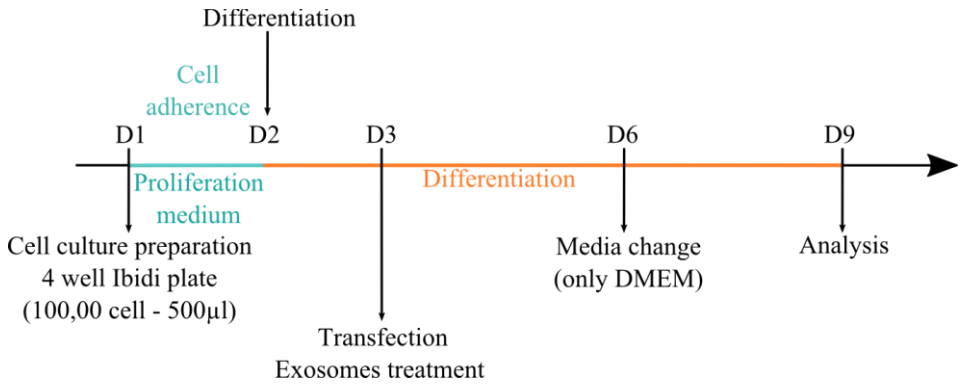

Procedure

Products:

siRNA FUS sS5401 (Ambion #4392420)

Negative Control Silencer - Scramble (Ambion AM4635)

Nucleases-free water (Ambion #AM9937)

I. siRNA preparation

1. 100µM siRNA solutions, including siRNA of target genes and negative control siRNA (siRNA with sequence that don't have any sequence target) are prepared in nuclease-free water from dried siRNA.
2. siRNA solution at 10µM are diluted for utilization during transfection.

Experimental protocol n°13

siRNA-based FUS silencing

II. Transfection procedure

Products:

Lipofectamine RNAiMAX (Invitrogen #13778-030)
OptiMEM (Gibco #31985-047)
µ-Slide 4 Well ibidi treat (Thistle Scientific #80426)

Day 1: Cell cultures preparation

Cells are seeded in appropriate plate 2 days before transfection induction to allow cells to adhere and differentiate for 1 day.

1. The day before differentiation, 100,000 cells are seeded in Ibidi 4 well plate.
2. Cells are cultured in 500µl per well and no antibiotics are added to the proliferation medium.

Day 2: Cell differentiation

1. As described in experimental procedure n°2, cells are washed 5 times in DMEM before differentiation induction
2. 500µl of DMEM are added to each well and cells are incubated at 37°C

Day 3: Transfection

Transfection of siRNA and Negative Control siRNA is performed with Lipofectamine® RNAiMAX Reagent to allow incorporation into muscle cells.

1. For each well a Lipofectamine/200nM siRNA mix is prepared. For Ibidi 4 well plate 50µl of mix for 500µl of culture medium is needed.
2. First the Lipofectamine RNAiMAX and siRNA molecules are diluted in OptiMEM medium following instruction in table:

Experimental protocol n°13

siRNA-based FUS silencing

		12wells plate (100 µL)	4wells plate (50 µL)
Mix Lipofectamine	*Lipofectamine*	6µL	3µL
	OptiMEM	94µL	47µL
Mix siRNA	*siRNA(10µL)*	2µL	1µL
	OptiMEM	98µL	49µL

3. The diluted siRNA is then added to the diluted Lipofectamine, and is gently mix by pipetting up and down a few times. The mix is incubated for 5min at room temperature.
4. The differentiation medium (DMEM) is removed from each well and replace by 450µl of fresh DMEM.
5. Slowly, 50µl of Lipofectamine/200nM siRNA mix is added drop by drop to the corresponding well. 50µl of DMEM is added to the non-transfected wells.
6. Cells are incubated for 3 days.

Alternative if exosomes treatment is performed as well:

1. The Lipofectamine/siRNA is prepared as described in step 2.
2. Exosomes samples are labelled with PKH26 and resuspended in 450µl of DMEM per well treated.
3. The differentiation medium is replaced by 450µl of exosomes resuspensed in DMEM. 450µl of only DMEM is added to the non-treated wells.
4. Slowly, 50µl of Lipofectamine/siRNA mix (or DMEM) is added to the corresponding well.
5. Cells are incubated for 3 days to allow integration of exosomes in the cells. On day 6 culture medium is replaced by fresh DMEM and cells are incubated for 3 more days before fixation.

Experimental protocol n°14

Exosomes treatment

I. Human muscle cells exosomes treatment

Healthy muscle cells treatment with ALS and healthy exosomes (1):

1. 200,000 healthy myoblasts are cultured in Ibidi 35mm µ-dishes
2. Exosomes are extracted from 200.000 ALS and healthy muscle cells cultures.
3. ALS and healthy exosomes are added to the culture of healthy myoblasts the same day the differentiation is induced. Exosomes absorption occurs for 3 days before fresh DMEM is added to the petri dishes.
4. Exosomes-treated myoblasts are fixed in 4% formaldehyde at day 3 or day 7 of differentiation.

Products:

35mm µ-Slide ibidi (Thistle Scientific #81856)

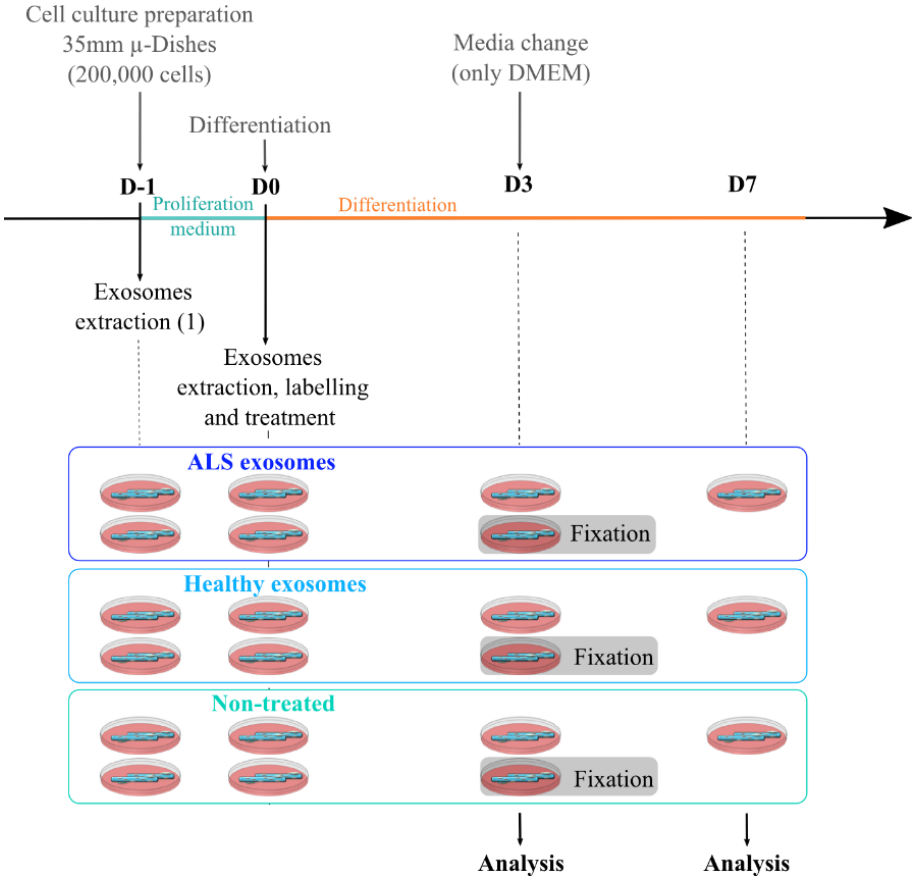

Experimental protocol n°14

Exosomes treatment

Analysis:

1. *Cell death*: Following fixation, cells are stained with DAPI and cell death after treatment is defined by nuclei loss, total nuclei were counted in each treatment conditions and compared to non-treated cells.
2. *Apoptosis*: apoptosis levels are measured with expression level of H2AX. Cells are stained with DAPI and H2AX and total number of nuclei and individual H2AX area are measured. The final H2AX are result from the individual H2AX sum normalized with the number of nuclei.
3. *Blebbing – cellular stress:* The number of cell blebs are counted on live pictures at 4hrs, 24hrs, 48hrs, 72hrs, 96hrs, and 168hrs and normalized per cell area.
4. *Fusion index:* Muscle cells are stained with DAPI and MF20 (myotube marker). Nuclei are counted in multinucleated myotubes and in mononucleated muscle cells and fusion index is determined using the following formula:

$$Fusion\ index = \frac{Number\ of\ mononucleated\ myotube\ nuclei}{Total\ number\ of\ myogenic\ nuclei}\ x\ 100$$

5. *Myonuclear domain:* The myonuclear domain illustrating the atrophic level of myoblasts is calculated using the following formula:

$$Myonuclear\ domain = \frac{\Sigma\ MF20\ area}{\Sigma\ nuclei\ in\ myotubes}$$

6. *Exosomes integration*: Exosomes integration was assessed on live pictures following integration of PKH26 staining in cytoplasm of myotubes.

Healthy muscle cells treatment with ALS and healthy exosomes (2):

1. 100,000 healthy muscle cells are cultured in ibidi 4 well plate.
2. ALS and healthy exosomes are extracted and exosomal proteins are quantified (see experimental protocol n°8)
3. 4µg or 8µg of exosomes are applied to the muscle cells cultures and differentiation is induced.
4. Cells were fixed at 6 days of differentiation.

Experimental protocol n°14

Exosomes treatment

Analysis:

1. *Cell death and apoptosis levels*: Similarly, cell death and apoptosis levels were assessed following directions explained above.
2. *RNA localisation*: Cells are stained with acridine orange (see experimental protocol n°11) and total nuclei is determined for each picture. The percentage of nuclear and cytoplasmic RNA accumulation is calculated.

Muscle cell lines overexpressing wild type forms of FUS, SOD1 and TDP43 treatment:

Dr J Dumoncaux and Dr V Mariot (NIHR Biomedical Research Centre, University College London, Great Ormond Street Institute of Child Health and Great Ormond Street Hospital NHS Trust, London, UK) generated the immortalized cell lines expressing FUS_{FLAG}, SOD1 $SOD1_{FLAG}$ or $TDP43_{FLAG}$.

1. Healthy muscle cell lines are transduced with plasmid coding for a tagged (FLAG tag) of wild type FUS (FUS_{FLAG}), SOD1 ($SOD1_{FLAG}$) or TDP43 ($TDP43_{FLAG}$), and selected with hygromycin.
2. 50,000 cells were plated in ibidi 8 well plate and treated with 0.5µg of ALS or healthy exosomes at the time of differentiation.
3. After 3 days of differentiation, fresh DMEM is added to each well and cells were fixed at 6 days of differentiation.

Experimental protocol n°14

Exosomes treatment

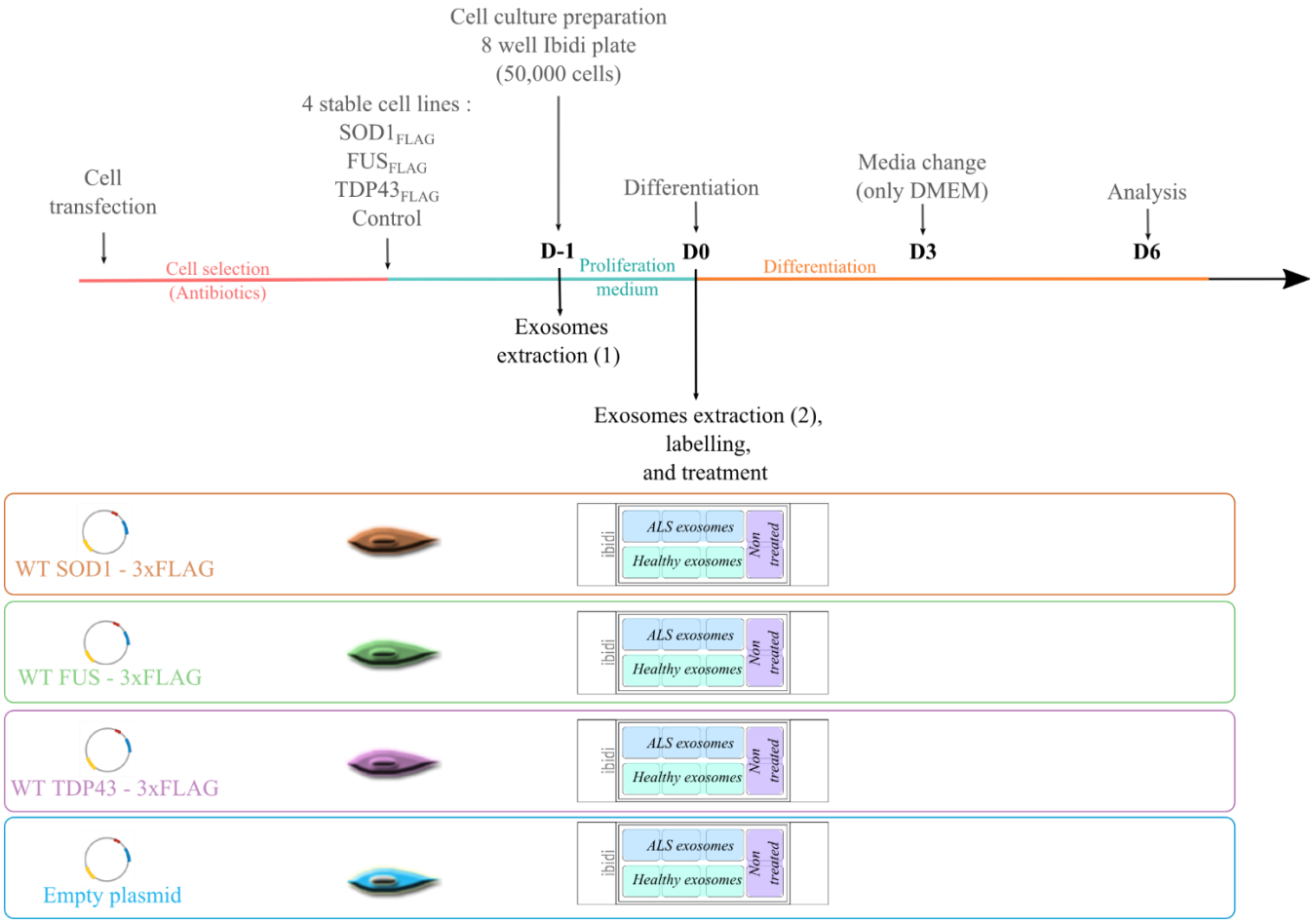

Analysis:

Cell death and cell blebbing levels are determined as described above.

KO-FUS muscle cells treatment:

1. 100,000 healthy muscle cells are plated in 4 well Ibidi and transfected with either a 200nM s5401 FUS siRNA (experimental protocol n°13) or a negative control siRNA and treated with 4µg of ALS or healthy exosomes at day 1 of differentiation (see experimental protocol n° 8 for protein quantification).
2. Exosomes are integrated for 3 days before fresh DMEM is added.
3. Cells were fixed at 7 days of differentiation.

Experimental protocol n°14

Exosomes treatment

Analysis:

1. *Cell death and RNA localisation*: Analysis are following instructions as previously described.
2. *RPL5 aggregation:* Cells are stained for RPL5 and percentage of RPL5 aggregates-positive nuclei is determined.

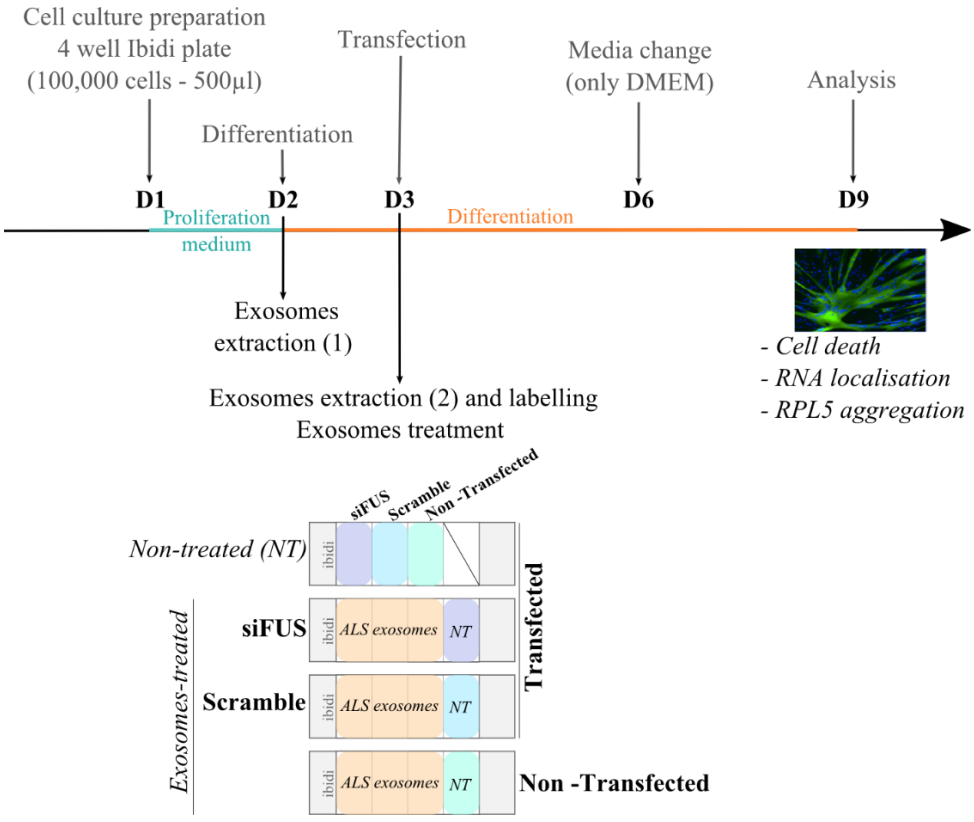

II. iPSCs MN treatment

1. 9 days MN progenitors are differentiated for 7 days as previously described (see experimental protocol n°3), in either 96 well plate (3,000 cells per plate) or 8 well plate ibidi (6,000 well plate).
2. 16 days differentiated MN are either treated with ALS or healthy exosomes resuspended in $N2B27^{++}_{4}$ medium:
   - 0.5µg exosomes per well in 96 well plate
   - 2µg exosomes per well in 8 well plate
3. Cultures are fixed after 2 or 3 days of treatment.

Experimental protocol n°14

Exosomes treatment

Analysis:

- *Cell death*: Nuclei loss defining cell death is calculated following staining of cell cultures with DAPI as previously described.
- *Neurites length*: Cells are stained with anti-tubulin, beta III isoform antibody, or TUJ1 to label neurites. The length of all the neurites per picture is manually measured for each motor neuron and compared to non-treated cells.
- *Neurites branching*: Similarly, the number of branching for each motor neuron is manually counted and compared to non-treated cells.
- *Isl1/2 proportion*: To characterize the proportion neuronal cells altered by exosomes treatment, cell cultures are stained with a motor neuron marker (Isl1/2) and is used to calculate the number of motor neurons per picture. The percentage of motor neuron death is normalized by the total number of nuclei per picture.

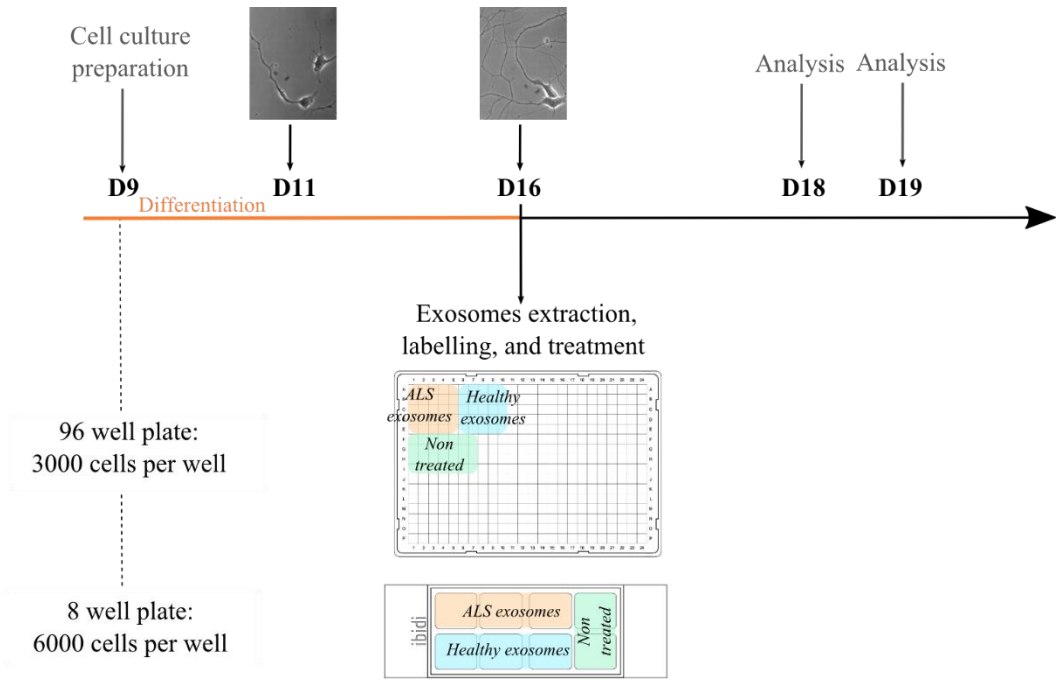

Experimental protocol n°14

Exosomes treatment

Table 12 : Table summarizing experimental conditions and analysis performed on MN cultures treatment.

		MN treatment #1	MN treatment #2
Experimental conditions		1- ALS exosomes treatment 2- Healthy exosomes treatment 3- Non treated MN	1- ALS exosomes treatment 2- Healthy exosomes treatment 3- Non treated MN
		10 wells per condition	3 wells per condition
Analysis performed	*Cell death*	10 pictures per well = 100 pictures per condition	10-12 pictures per well = 30 pictures per condition
	RNA staining		20 pictures per well = 60 pictures per condition
	Isl1/2 staining		100 pictures per well = 300 pictures per condition
	Neurite length and branching	5 pictures per well = 50 pictures per conditions	
Number of cells plated		3,000 MN	6,000 MN
Amount of labelled exosomes applied for treatment (per well)		0.5µg	2µg
Plate used for cell cultures		96 wells plate	Ibidi 8 well plate

Table 13 : Table summarizing experimental conditions and analysis performed on muscles cells treatment with exosomes.

See following page.

		Healthy muscle treatment		WT FUS/SOD1/TDP43 overexpressing muscle cells treatment	KO-FUS muscle cells treatment
Experimental conditions		1- ALS exosomes treatment 2- Healthy exosomes treatment 3- Non treated cells	1- ALS exosomes treatment 2- Healthy exosomes treatment	**4 different cell lines:** - ALS exosomes treatment (triplicate) - Healthy exosomes treatment (triplicate) - Non treated cells (duplicate)	**4 conditions** ALS exosomes treatment (triplicate) or non-treated (single well) : - KO-FUS muscle cells - KO-SOD1 muscle cells - Scramble treated muscle cells - Non transfected muscle cells
		Each condition in triplicate	Each condition in duplicate		
Analysis performed	*Cell death*	10 pictures per petri-dish = 30 pictures per condition	5 pictures per well = 20 pictures per condition	10 pictures per well = 80 pictures per cell line	20 pictures per well = 80 pictures per condition
	Apoptosis		20 pictures per well 80 pictures per condition		
	RNA staining		15 pictures per well =60 pictures per condition		15 pictures per well = 60 pictures per condition
	RPL5 aggregation				20 pictures per well = 80 pictures per condition
	Myonuclear domain	10 pictures per petri-dish = 30 pictures per condition			
	Fusion index				
Number of cells plated		200,000 cells	100,000 cells	50,000 cells	100,000 cells
Amount of labelled exosomes applied for treatment (per well)		Exosomes from 200,000 cells	4µg or 8µg	0.5µg	4µg
Plate used for cell cultures		35mm µ-dishes	4 well plate	8 well plates	4 well plate

Results

To date, ALS pathogenesis is still unknown and several studies suggest involvement of neighbouring cells such as astrocytes and microglial cells responsible for the degeneration of motor neurons in ALS patient[69,324,326,327]. Hence it is believed that ALS is a multisystemic disease. The primary involvement of muscle is still controversial, however multiple signs for an axonopathy in ALS patients prior to MN degeneration and symptom onset[116,342,368] suggest that in addition to its role in NMJ stabilization[346], the muscle could participate to a toxic MN environment[343,344]. It is known that the muscle is acting as an endocrine organ via its secretory properties[154], so we hypothesised that the muscle secretome contribute to the degeneration of motor neurons in ALS.

Thanks to the *in silico* secretome performed using transcriptomic data from two independent previously published studies[375,376], the team observed that both endosome and lysosomes pathways were significantly enriched in ALS muscle - pathways known to be part of the exosomes genesis and secretion. The team then confirmed by electron microscopy imaging and immunostaining that there is a significant accumulation of MVB (TSG101) and exosomes (CD63) under the sarcolemma on muscle sections from sporadic ALS. Exosomes originate from the inward budding of late endosomes and accumulate in endosomes called multivesicular bodies or MVB[152,377]. The MVBs full of exosomes then fuses either with the lysosome for degradation or with the plasma membrane to release their intraluminal vesicles in the extracellular space. First thought to be the "cell's garbage"[158,159], the role of exosomes in intercellular signalling was rapidly unravelled[147–150], suggesting their important function in physiology and homeostasis. Thus we hypothesized that ALS muscle might influence intercellular communication between muscle and nerve through a disrupted exosomes pathway.

I. Exosomal pathway disruption in ALS patients.

ALS patients are characterized by progressive degeneration of upper and lower motor neurons leading to a gradual denervation responsible for muscle weakness and wasting[2]. In order to determine if the exosomal pathway up-regulation in ALS patients is dependent, or not, from muscle denervation, we extracted muscle stem cells (also known as satellite cells) - cells located at the surface of the myofiber[378] and naïve for any innervation/denervation process. To conduct this project, the team had access to muscle biopsies from sporadic ALS patients (including three C9orf72 mutation- and one ATXN2 mutation-associated patients) and healthy subjects (including control diseases such as polyneurithis, SBMA and SMA patients, see Table 14). Because of the limited lifespan of human primary cells, cells from different patients were used for different experiment along the study: transcriptomic analysis, or for imaging (including electron microscopy and histology), or for exosomes extraction and cell treatments (muscle cells and iPSCs-derived

MN cultures), with some overlap between different experiments (See Supplementary Table 2 in manuscript). For each experiments conducted, samples were randomly picked- as we did not know at the time, the genetic results for the ALS patients.

66 Subjects	Age at the time of the biopsie	Gender	ALS/FRS	Genetic	Muscle testing	Site of onset 0=spinal; 1=Upper limb; 2=Lower limb; 3=bulbar; 4=respiratory	Duration of disease (months)	Histology	Electron microscopy	Cell culture	Transcriptome	Immunostaining cell culture	RT-qPCR	exosome treatment MN	exosome treatment myotubes
24 ALS (35-76y: 58.54±8.28; 7F, 17M)	58	F	38		130	1	13								
	67	M	45		146	2	25,2								
	56	M	41		140	2	26,7								
	59	F	39	*C9orf72*	146	3	16,5								
	53	F	28	C9orf72	119	3	6								
	61	M	38	*ATXN2*	130	2	11,3								
	64	M	40		130	1	39,3								
	70	M	37		126	3	48,3								
	68	M	33		123	1	53,4								
	76	M	32		104	1	28								
	59	F	23		103	3	33								
	61	M	40		97	1	11								
	61	M	38		88	1	52								
	53	M	31		94	2	40								
	52	H	37		No data	0	101								
	35	F	32		No data	0	85								
	52	F	43		135	1	33,6								
	49	M	41		111	2	44.1								
	53	M	40		130	2	17,4								
	57	M	37	*C9orf72*	145	3	20,6								
	66	M	41		147	2	28.7								
	51	M	36		139	2	12								
	66	M	43		149	1	12								
	58	F	40		98	3	14								
24 Healthy (21-75y: 48.29 ± 17.56; 7F, 17M)	61	M													
	75	M													
	56	F													
	64	F													
	51	M													
	52	F													
	47	F													
	59	M													
	19	M													
	59	M													
	54	M													
	59	F													
	49	F													
	53	M													
	70	M													
	21	M													
	21	M													
	53	M													
	69	F													
	66	M													
	21	M													
	33	M													
	22	M													
	25	M													
2 Polyneuritis (70 & 45 y; 1F, 1M)	70	M					13								
	45	F					8								
10 SBMA (43-71y: 58.18 ± 9.65; 10M)	60	M	42	47 repeats	132	2	420								
	43	M	44	48 repeats	148	2	60								
	57	M	44	44 repeats	148	2	72								
	71	M	35	45 repeats	136	2	324								
	45	M	39	50 repeats	134	2	168								
	71	M	40	41 repeats	149	1	372								
	66	M	40	49 repeats	142	2	144								
	56	M	36	46 repeats	121	2	324								
	62	M	38	47 repeats	143	2	156								
	64	M	37	45 repeats	138	2	108								
6 SMA-III/IV (30-61y: 42.5 ± 10.27; 1F, 5M)	48	M	42		140	2	156								
	36	M	41		106	2	276								
	61	M	40		122	2	588								
	45	M	41		124	2	324								
	30	M	43		139	2	84								
	35	F	44		142	2	384								

Table 14 : Table summarizing samples characteristics.
Muscle biopsies were isolated from deltoid muscles. The table summarizes the age of onset, ALSFRS-R score, muscle testing results and genetics when applicable. Each sample is associated to every experimental procedure it has been used in.

The ALS and healthy muscle stem cells have the same mitotic age[379] as no differences in their proliferative capacities were observed. ALS muscle stem cells had a lower fusion index (~10% less) and formed thinner myotubes, characteristics already established by two studies[379,380]. The transcriptomic analysis of differentiated myoblasts performed by the team show that all ALS patient myotubes cluster together and are separated not only from the healthy subjects but also from the disease controls. ALS myotubes present thus a specific gene expression profile. Cell Where is an online tool developed by the team that allows a graphical display of protein subcellular localization (https://sys-myo.com/cellwhere/). Following the groundbreaking transcriptomic analysis results and using the Cell Where tool, the list of top 30 genes mostly contributing to this ALS-specific signature, revealed among others an enrichment of genes encoding for proteins that are secreted through exosomes proteins. The present study shows for the first time that: 1) the ALS signature is shared across muscle stem cells from ALS patients (including monogenic form of ALS and ALS with non-known causes) and 2) this strong signature has never been observed in motor neurons, astrocytes or inflammatory cells[381,382]. Accordingly, a specific gene expression profile was observed in muscles cells of an ALS murine model and was different from axotomy-induced dennervated muscles transcriptome profile[383].

II. Muscle exosomes characterization and toxicity study

This project is based on extraction of exosomes from muscle cells cultures. There is no gold standard protocol for optimal separation of exosomes, classically exosomes extraction is performed by differential centrifugation[148]. Because the exosomes extracted after ultracentrifugation form a loose invisible pellet and consequently lead to the loss of most of the exosomal material, it thus requires a large volume of starting material, approximatively 100-250 million muscle stem cells[268], to assure an efficient exosomal extraction for one experiment without any replicates. Our muscle stem cells are primary cells possessing a limited maximum number of division (38-46 divisions) before reaching senescence (Table 15). In order to avoid working with pre-senescent cells, we are working with a limited number of cells forcing us to use a polymer based extraction kit from Life technologies that allows a rapid exosomes isolation from smaller starting material samples.

	Number of divisions	Total number of extracted cells	Number of muscle cells (10%)
Sufficient cell for exosomes analysis	0	3,000	300
	1	6,000	600
	2	12,000	1,200
	3	24,000	2,400
	4	48,000	4,800
	5	96,000	9,600
	6	192,000	19,200
	7	384,000	38,400
	8	768,000	76,800
	9	1,536,000	153,600
Optimal range of cell amplification for experiments	10	3,072,000	307,200
	11	6,144,000	614,400
	12	12,288,000	1,228,800
	13	24,576,000	2,457,600
	14	49,152,000	4,915,200
	15	98,304,000	9,830,400
	16	196,608,000	19,660,800
	17	393,216,000	39,321,600
	18	786,432,000	78,643,200
	19	1,572,864,000	157,286,400
Pre-senescent stage	20	3,145,728,000	314,572,800
	21	6,291,456,000	629,145,600
	22	12,582,912,000	1,258,291,200

Table 15 : Number of cells extracted per biopsy and proportion of muscle cells.
Table summarizing total number of cells after each amplification step. Muscles cells represents approximatively 10.91% and are enriched by CD56 MACS sorting.

Absolute purification of exosomes is not achievable, however several procedures allows concentration of exosomes, such as ultracentrifugation that is the used separation technique in exosomes field. If it is assume that low protein contaminant are isolated with exosomes during ultracentrifugation, the high speed (100,000g[213] to 140,000g[217,218]) during ultracentrifugation can induce mechanical damage. During cell treatment it is primordial to keep the integrity of exosomes by avoiding damaging them. Importantly ultracentrifugation requires large volume of starting material and working with primary cells doesn't suit this requirement. Density-gradient separation is another well-known exosomes isolation procedure however only a sub-population of vesicles at a particular buoyant density is studied and in order to illustrate the heterogeneity of secreted vesicles in ALS patients we want to study the whole muscle exosome population. It also require a first step to isolate total exosomes by ultracentrifugation, and again requires a large amount of cell culture media as described above. Size-exclusion chromatography or ultrafiltration allows the separation of exosomes depending on their size, exosomes as well as non-vesicular component sharing

similar sizes with exosomes are co-purified[384]. Moreover exosomes can easily aggregates and block the filtrate and may cause loss of vesicles[385].

For many years virus extraction are successfully performed using polymer-based isolation techniques[221,384,386,387]. Polymer-based exosomes extraction kit are now commercially available, but still raise controversy in the exosomes field. It has been demonstrated that polymer-based exosomes extraction from blood samples co purify contaminants such as immunoglobulins or larger proteins such as albumin[385]. Culture media is not as rich in contaminants as blood samples, and precipitated exosomes are labelled and washed in PBS multiple time before further application allowing withdrawal of any possible contaminants as illustrated on polyacrylamide gel from healthy and ALS exosomes extracted using LifeTechnologies extraction kit (See Figure supplemental 3F in paper). Important critics about the use of polymer-based extraction technique is based on the observation of residual gel matrix in exosomes pellet[388]. It is important to note that this study, contrary to ours is conducted on blood samples richer in contaminants to start with. Authors declared that the extraction kit influences the uptake of exosomes, however approximatively same amount of vesicles were monitored in recipient cells treated either with exosomes extracted with the polymer-based kit or by ultracentrifugation, in accordance with other studies[389]. Importantly authors demonstrated that washing exosomes with PBS allows the removal of residual polymer[389], and during our exosomes staining procedure, exosomes samples are washed several times in PBS suggesting that the extraction kit is washed away and can't interfere with the further applications.

Single vesicle analysis, including electron microscopy immunostaining, and NanoSight analysis and protein content composition through western blotting allowed us to validate that the extraction kit isolate cup-shaped vesicles, positive for exosome markers as recommended by the field[390]. The quantity of exosomes secreted by ALS muscle cells was greater than the healthy cells (see Figure 2H and supplemental Figure 3F in paper). To follow the integration of exosomes by recipient cells, we labelled exosomes with an organic fluorescent dye PKH26. We first studied the effect of ALS muscles exosomes on muscle cells in a muscle-to-muscle ratio of 1:1. Labelled ALS and healthy exosomes were rapidly uptaken by the muscle cells, four hours after adding the exosomes to the culture medium. The differentiation of myoblasts into myotubes was not affected by the exosome treatment, as the fusion index and the number of myonuclei per myotube were similar in all conditions (Figure 11).

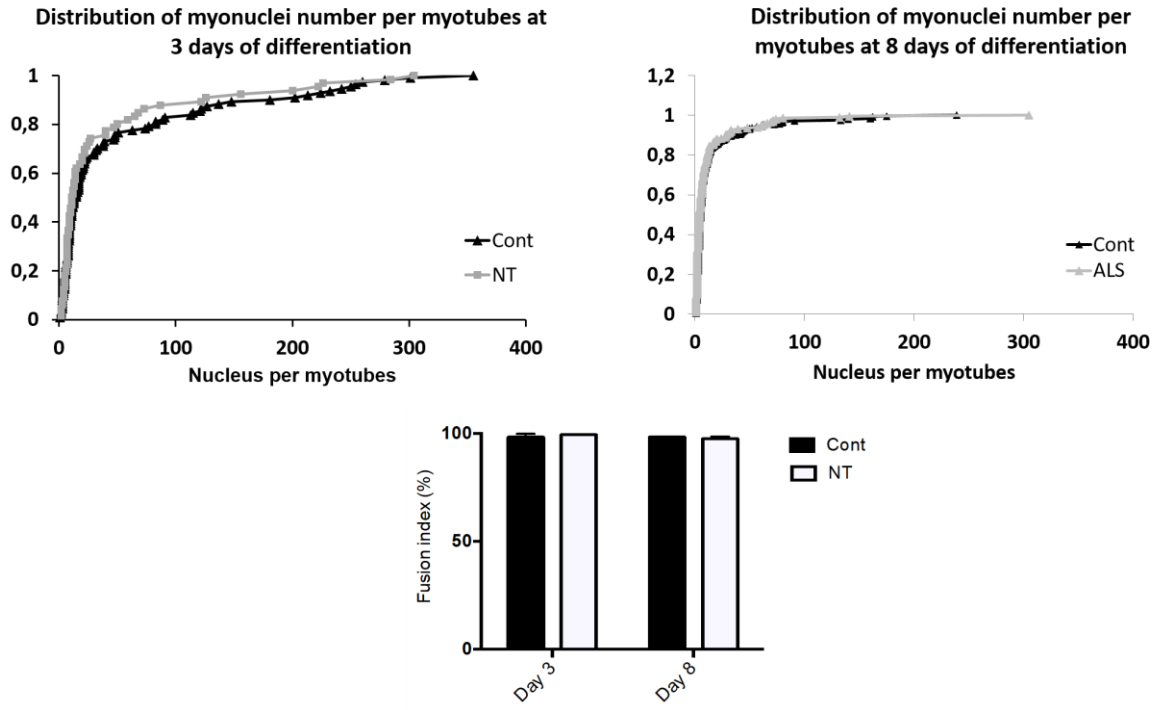

Figure 12 : Similar myotubes differentiation after ALS and control exosomes treatment.
At 3 days or 7 days of exosomes treatment the number of myonuclei per myotubes was measured as illustrated by cumulative rank plot showing a similar distribution in both conditions and time points. The fusion index was calculated as previously described, and was about 96% in both ALS- and healthy exosomes.

ALS exosomes were toxic for muscle cells by inducing muscle atrophy, cell stress and cell death (see supplemental Figure 4A-E in paper). When we loaded either 8µg or 4µg of ALS and healthy exosomes, we consistently observed a lower death when myotubes were treated with 4µg ALS exosomes compare to 8 µg. In addition, the lowest concentration of ALS exosomes - 4µg - induced a greater cell death than the highest concentration of healthy exosomes - 8µg-, suggesting that both quantity and quality of exosomes are important for the toxicity of ALS exosomes.

As ALS is a motor neurone disease affecting motor neuron survival, we next characterized the effect of muscle exosomes on healthy human iPSC-MN. For this purpose we had to determine how much exosomes amount would be added to the MN cultures. A single motor neuron innervates several muscle fibers, forming together one motor unit. However, the number of muscle fibers per motor unit is highly variable[338,391], ranging from 180 muscle fibers in the soleus muscle[392] to several hundred in the gastrocnemius muscle[338]. Moreover, a single myofiber contains in average 500 myonuclei [393,394]. If we take the example of the soleus muscle, one motor unit would contain approximatively 90,000 myonuclei. Translated to cell cultures where 3,000 MN are seeded in a single well from a 384 well plate, exosomes isolated from the culture medium of 270,000,000 myoblasts would be necessary for a single well treatment. Because it is technically impossible to meet these criteria we decided to apply a muscle-to-neuron ratio of

10:1. Similarly MN were treated with ALS and healthy muscle exosomes and 72h after treatment 60% of neuronal death was observed. In collaboration with Dr Hélène Blasco and Dr Blandine Madjihounoum, we treated primary murine motor neurons with ALS and healthy human exosomes and observed 96hrs after treatment a higher cell death (see Figure 13).

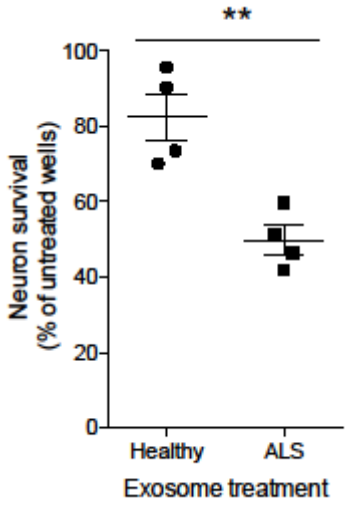

Figure 13 : Primary motor neuron survival after ALS or healthy exosomes treatment

To further study the role the toxic effect of exosomes, we treated the human iPSCs motor neurons with equal amount of ALS and healthy exosomes following BCA-based protein quantification. The same low dose corresponding to 0.5µg of exosomes was added to the culture medium of 3,000 iPSCs MN per well. Likewise, both ALS and healthy exosomes were integrated by the recipient cells, and 72h after the treatment of the motor neurons with exosomes we observed signs of cell stress such as shorter neurites and reduced branching in iPSCs MN treated with ALS muscle exosomes. Interestingly, even low concentrations of ALS muscle exosomes induced a higher cell death compare with healthy exosomes treatments. As previously described[373], during the motor neuron progenitors' differentiation other neuronal cell type such as interneurons can be find among the motor neurons population. Approximatively 80% of the progenitors will differentiate into motor neurons. To characterize the proportion of motor neurons affected by the ALS exosomes treatment, we used a motor neuron specific marker Isl1/2. Our results show that treatment of MN with ALS exosomes didn't affect the proportion of non-neuronal cells or Isl1/2 negative cells suggesting that ALS exosomes are specifically targeting MN. The cell death we measured (approximatively 65%) is representing the loss of MN. In addition, these exosomes also induced shortened, less branched neurites.

Numerous studies have described protein aggregation in ALS patients either positive for SOD1, FUS or TDP43 and others[43,53,63,99,102,103]. Based on these data we wanted to explore whether 1) we could detect these proteins in muscle exosomes, and 2) determine if these ALS candidate proteins are involved in ALS muscle exosomes toxicity. Interestingly only FUS was found in ALS muscle exosomes. Based on these data we investigated the role of exosomes on the FUS pathway. We then generated four stable cell lines expressing

either a Flagged form of wild-type FUS (FUS_{FLAG}), or wild-type $SOD1_{FLAG}$ or wild-type $TDP43_{FLAG}$. At equal low concentration (0.5µg of exosomes per well), we observed a greater cell stress and death after treatment with ALS exosomes in all four cell lines, but the effect was markedly greater in the FUS-overexpression cells (see Figure 4G in the paper).

The toxic effect of ALS exosomes is thus exacerbated in the presence of an over-expression of FUS (see Figure 4G in the paper). On the other hand, when we knock down FUS expression in the recipient cells, the cells were less sensitive to ALS exosomes (see Figure 4H in the paper). These data suggest that cells that express a high level of FUS will be more sensitive to ALS muscle exosomes. Interestingly iPSCs MN express higher level of FUS further highlighting the role of FUS in exosomes toxicity (See figure 4I in the Human proteome database). FUS is a multifunctional DNA/RNA-binding protein involved in multiples steps of gene expression, including mRNA transcription and RNA transport[53] and many RNA metabolism pathways are believed to be disrupted in ALS patients. Interestingly, when we treated the cells with ALS exosomes, we observed a significant increased number of nuclei positive for RNA (see Figure 4D and supplemental Figure 5B in the paper), suggesting a disruption of RNA transport following ALS muscle exosomes treatment.

In parallel, we also observed that ALS myotubes present an altered distribution of FUS (FUS granulation study performed using FindFoci algorithm on ImageJ/Fiji software[395]) and TDP43 (see Figure 12), they accumulate RNA in their myonuclei, and they present a mislocalization of the two FUS partners, RPL5 and Caprin-1 (see Figure 4C and supplemental Figure 5A in the paper). Altogether, these data suggest that RNA transport is affected in ALS muscle cells – phenomenon described to be affected in different ALS models[396].

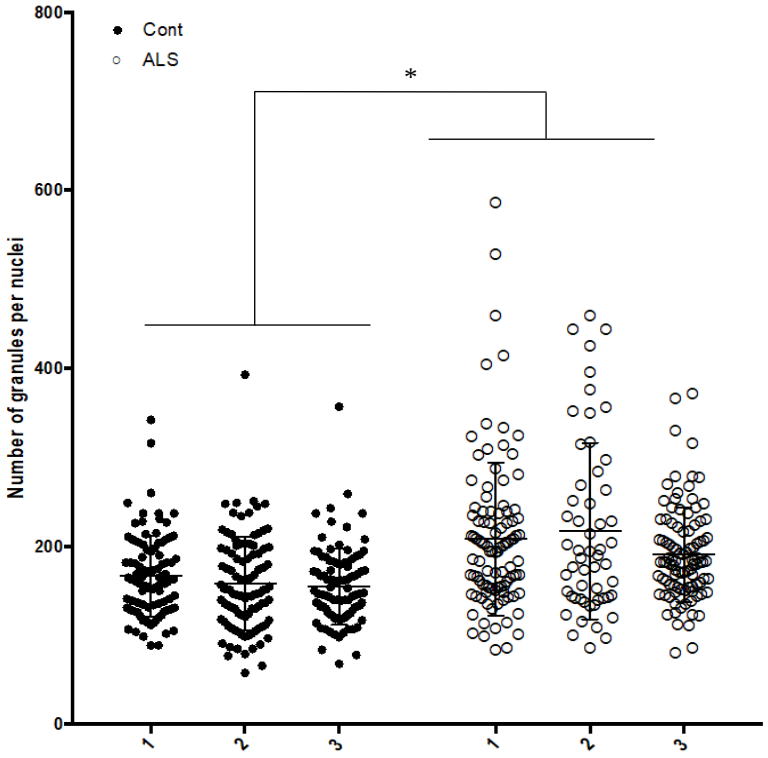

Figure 14 : TDP43 granulation in ALS and healthy muscle cells.
Similarly to Figure 4A from paper, TDP43 granulation was assessed in ALS and healthy muscle cells. Each circle represents one myonuclei, 100 nuclei were analysed per patient (x axis, n=3). A greater accumulation of TDP43 granules were measured in ALS muscle compared to. *, P<0,05 significantly different from healthy myonuclei.

In summary, the present study we show that (1) ALS myotubes present a specific signature with accumulation and over-secretion of exosomes and (2) these muscle exosomes induce toxic effects on both human healthy muscle cells and iPSCs MN. We also unraveled that ALS muscle exosomes toxicity involves the FUS pathway.

Title: FUS-dependent neurotoxicity of vesicles secreted by muscle cells of ALS patients

Authors: Stephanie Duguez[1,‡,*,†,c], Laura Le Gall[1,2*], William J Duddy[1,‡,**], Cecile Martinat[3,**], Virginie Mariot [4,‡], Stephanie Millecamps[5], Jeanne Lainé[2], Gisele Ouandaogo[2], Udaya Geetha Vijayakumar[1], Susan Knoblach[6], Cedric Raoul[7], Olivier Lucas[7], Jean Philippe Loeffler[8], Peter Bede[9,10,11], Anthony Behin[12], Helene Blasco[13], Gaelle Bruneteau[2,11,], Maria Del Mar Amador[11], David Devos[14], Anne Cecile Durieux[15], Damien Freyssenet[15], Alexandre Henriques[8], Adele Hesters[11], Lucette Lacomblez[10,11], Pascal Laforet[16], Timothee Langlet[11], Pascal Leblanc[17], Nadine Le Forestier[11], Thierry Maisonobe[11], Vincent Meininger[18], Alexandre Mejat[17], Franscesca Ratti[17], Laura Robelin[8], Francois Salachas[11], Tanya Stojkovic[12], Giorgia Querin[9,10], Julie Dumonceaux[4,‡], Gillian Butler Browne[2], Jose-Luis González De Aguilar[8], Pierre Francois Pradat[1,10,11,†].

Affiliations:

1- Northern Ireland Center for Stratified Medicine, Biomedical Sciences Research Institute, Londonderry, UK.

2- Sorbonne Université, Institut National de la Santé et de la Recherche Médicale, Association Institut de Myologie, Centre de Recherche en Myologie, UMRS974, Paris, France.

3- I-Stem, INSERM/UEVE UMR 861, I-STEM, AFM, Corbeil-Essones, France

4- NIHR Biomedical Research Centre, University College London, Great Ormond Street Institute of Child Health and Great Ormond Street Hospital NHS Trust, London, UK.

5- Inserm U1127, CNRS UMR7225, Sorbonne Universités, UPMC Univ Paris 6 UMRS1127, France.

6- George Washington University, Genetic Medicine, Children's National Medical Center, Washington, US.

7- The Neuroscience Institute of Montpellier, Inserm UMR1051, Univ Montpellier, Saint Eloi Hospital, Montpellier, France.

8- Mécanismes Centraux et Périphériques de la Neurodégénérescence, Université de Strasbourg, INSERM UMR_S 1118, Strasbourg, France.

9- Computational Neuroimaging Group, Academic Unit of Neurology, Trinity College Dublin, Ireland

10- Sorbonne Université, CNRS, INSERM, Laboratoire d'Imagerie Biomédicale, Paris, France

11- APHP, Département de Neurologie, Hôpital Pitié-Salpêtrière, Centre référent SLA, Paris, France

12- APHP, Centre de référence des maladies neuromusculaires Nord/Est/Ile de France, Institut de Myologie, Hôpital Pitié-Salpêtrière, Paris, France

13- Laboratoire de Biochimie et Biologie Moléculaire, Hôpital Bretonneau, CHRU de Tours, Tours, France

14- INSERM U1171, Pharmacologie Médicale & Neurologie Université, Faculté de Médecine, CHU de Lille, Lille, France

15- Univ Lyon - University Jean Monnet of Saint Etienne- EA7424 – Laboratoire Interuniversitaire de Biologie de la Motricité, Saint-Etienne, France

16- Département de Neurologie, Centre de Référence Maladies Neuromusculaires Paris-Est, Hôpital Raymond-Poincaré, Garches, France.

17- Laboratory of Molecular Biology of the Cell, Ecole Normale Supérieure de Lyon, Lyon, France.

18- Hôpital des Peupliers, Ramsay Générale de Santé, F-75013 Paris, France

Short title : Neurotoxic vesicles secreted by ALS muscle cells

‡ Previous address: Sorbonne Université, Institut National de la Santé et de la Recherche Médicale, Association Institut de Myologie, Centre de Recherche en Myologie, UMRS974, Paris, France

† Scientific lead: S. Duguez; Clinical lead: PF Pradat

* contributed equally to this work

** contributed equally to this work

C corresponding author: s.duguez@ulster.ac.uk

Abstract: The abstract should be about 100-150 words, and organized in this structure: An opening sentence that sets the question that you address and is comprehensible to the general reader, background content specific to this study, results, and a concluding sentence. It should be one paragraph only.

The cause of the motor neuron death that drives terminal pathology in Amyotrophic Lateral Sclerosis (ALS) remains unknown, and is increasingly thought to result from the interplay of multiple mechanisms and cell types. We report that the skeletal muscle of ALS patients secretes exosomal vesicles that are specifically toxic to motor neurons. Among muscle biopsies and biopsy-derived denervation-naïve differentiated muscle stem cells (myotubes) from 66 human subjects, including healthy and disease controls, ALS myotubes had a consistent signature of disrupted exosome biogenesis and RNA-processing. Exosomes from ALS myotubes induced shortened, less branched neurites, cell death, and disrupted localization of RNA and RNA-processing proteins, in motor neurons. Some 37% of known protein binding partners of the RNA-processing protein FUS were present in the proteome of ALS muscle exosomes, and exosomal toxicity was dependent on the presence of FUS, which is highly expressed in recipient motor neurons.

One Sentence Summary: Muscle cells of ALS patients secrete exosomal vesicles that are toxic to motor neurons

Amyotrophic lateral sclerosis (ALS) is a fatal adult-onset motor neuron disorder affecting 3-5/100,000 individuals per year (*1*). The cause of pathology is likely complex with onset resulting from some combination of genetic mutations, DNA damage, environmental risk factors, viral infections, or other factors (*2–4*), leading to diverse cellular dysfunction such as glutamate-mediated excitotoxicity (*5*), abnormal protein aggregation (*6*), and mitochondrial disorganization and dysfunction (*7*, *8*) contributing to oxidative stress (*9*).

Not only motor neurons (MN) are affected in ALS, but also glial cells, muscle fibers (*10*) and immune cells (*11*), each of which may participate actively to ALS onset and progression. In a FUS murine model of motor neurone disease, where the FUS mutation is expressed in all tissues except the MN, the motor deficits still appear at a late stage (*12*). In addition, when the human mutated SOD1(hSOD1) is selectively knocked-down in MN and astrocytes of newborn transgenic hSOD1 mice, their life expectancy is prolonged by only 65-70 days, and there is still significant astrogliosis and microglial activation (*13*). These studies suggest that the local environment has a key role in "non-cell autonomous" MN death (*14*).

Numerous cell and tissue types, including skeletal muscle, can secrete exosomes and other types of vesicle (*15*, *16*). Such extracellular vesicles may be involved in cell-cell communication in the central nervous system (*17*, *18*), where they can carry out intercellular transport of functional proteins, mRNA, miRNA, and lipids, and may have key roles in spreading of proteinopathies (*17*, *18*) or neurotoxic elements (*19*). For instance, astrocytes extracted from the SOD1 murine model of ALS secrete exosomes that contain hSOD1, and propagate this toxic protein to neighboring MNs (*20*). As intensive efforts remain underway to determine the role of cell to cell

communication in ALS, we hypothesized that the muscle secretome may be an important component of the disease, based on long-standing observations that disassembly of the neuromuscular junction is an early critical event in the onset of the clinical pathology of ALS (*10*), and that motor neuron degeneration may start at the neuromuscular junction (*21–26*).

Accumulation of exosomes in ALS muscle biopsies

To explore previous data for evidence of muscle vesicle involvement in ALS, we tested for dysregulation of secretory compartments in a reanalysis of two published independent studies of gene expression in muscle biopsies from sporadic ALS patients (*27*, *28*). These showed a significant enrichment in endosomal and lysosomal compartments (Fig.S1A, Table S1) – two structures that are implicated in exosomal biogenesis and secretion. Prompted by this finding, we analysed patient muscle biopsies, and observed an increased frequency of multi-vesicular bodies (MVBs) in ALS muscles (1 MVB for every 62.09±13.3 sarcomeres, vs 1 MVB for every 330.8±127 sarcomeres in healthy controls; Fig.S1B) and an accumulation of exosomal markers at the periphery of the myofibers (Fig.1, Fig. S1C-D).

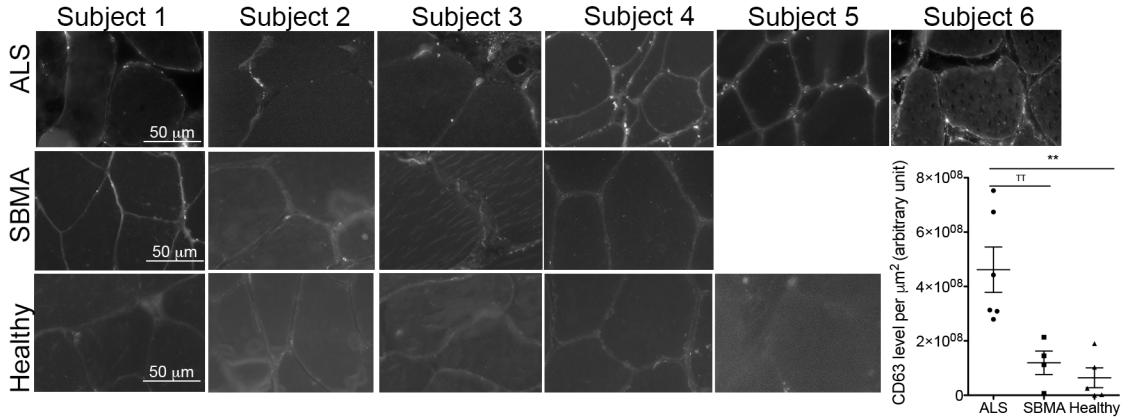

Figure 1: Accumulation of exosomal markers in muscle of ALS patients. Panel showing representative images of CD63 immunostaining performed on muscle biopsies from different subjects. Right insert: Quantification of exosomal marker CD63 in muscle biopsies (Pixel per μm^2 n= 6 ALS, 4 SBMA, 5 Healthy; ** significantly different from healthy subjects, $P<0.01$; ^{TT} significantly different from SBMA patients, $P<0.01$).

ALS patient muscle cells accumulate and secrete exosomes

To investigate the pathological consequences of increased exosomal accumulation in ALS muscle, we extracted myoblast cells from biopsies of confirmed ALS patients at an early stage of pathology. These were compared to healthy subjects, and to SMA-III/IV and SBMA which are two lower motor neuron disorders that mimic ALS clinically (see Table S2 for patient description, and a breakdown of which samples were used in which experiment). Transcriptomic analysis showed that ALS myotubes had gene expression patterns significantly different not only from healthy control subjects but also from SMA-III/IV and SBMA (Fig. 2A), and many of the dysregulated mRNAs encode proteins known to be secreted or localized in exosomes (Fig. 2B). Differentiated ALS myoblasts formed smaller myotubes with less nuclei per myotube (Fig. S2C), a smaller nuclear domain (Fig. S2E) and lower fusion index (Fig. S2F), compared to controls, whereas mitotic age and proliferative capacity were the same as controls (Fig. S2A and B). These observations suggest that ALS muscle cells are not subject to increased rates of regeneration throughout patient lifespan, and that observed differences with healthy controls are not due to age- or disease-induced cell senescence (*29*).

Immunostaining (Fig. 2C and Fig. S2G), RT-qPCR (Fig. 2D) and electron microscopy (Fig. 2E) all showed a consistent accumulation of exosomal markers in ALS myotubes. This feature is not a characteristic of muscle denervation or repeated re-innervation as no accumulation of exosomal markers was observed in SBMA, SMA-III/IV and polyneuritis cells by immunostaining (Fig. 2C). Similarly, no upregulation of exosomal markers was observed in either murine cachectic muscle or muscle denervated for 7 days (Fig. S3A-C). Exosome secretion by ALS myotubes was confirmed by electron microscopy (Fig. 2F). Both ALS and healthy vesicles were positive for exosomal markers CD63, CD82, Flotillin and both were negative for calnexin, an endoplasmic

reticulum marker normally absent in exosome fraction (Fig. 2G and S3D). The size of the exosomes was also typical (90-200 nm) (Fig. S3E). The exosome-enriched fraction secreted by ALS myotubes contained twice as much protein as that secreted by an equal number of healthy control myotubes (Fig. 2H, Fig. S3F).

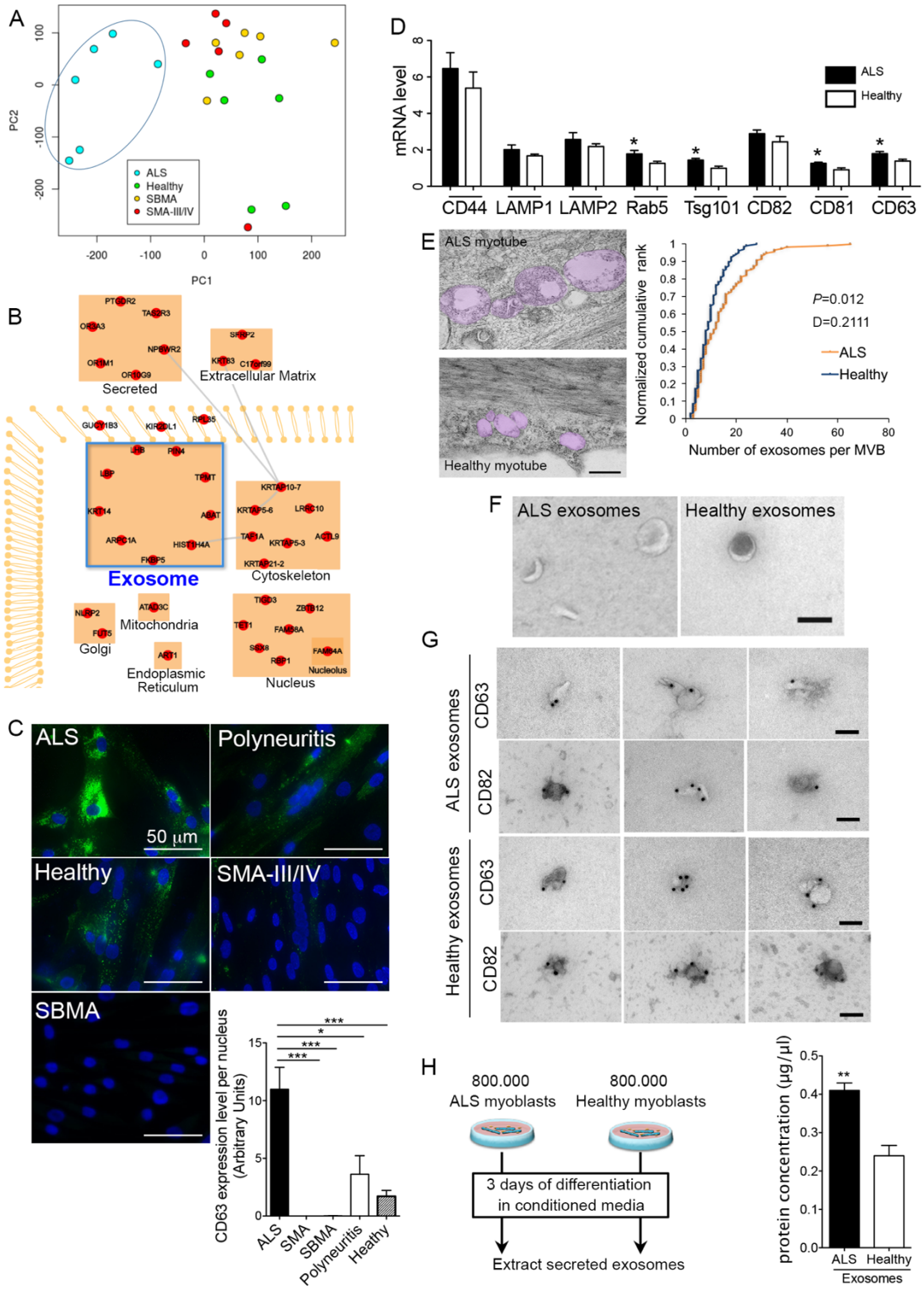

Figure 2: Increased accumulation and secretion of exosomes by ALS myotubes. (A) PCA plot showing separation of ALS patients on the 1st component (x-axis), ALS: blue, SBMA: pink, SMA-III/IV: red, Healthy: green. The transcriptomic analysis was performed on primary human myoblasts differentiated for three days to form myotubes.

Myoblasts were extracted from muscle biopsies of patients and healthy subjects (all male, 30-67 years old, n=5/6 per group, see Material and Methods for details). (B) Of the 30 genes having expression signatures most strongly specific to ALS, many have been observed at exosomally-relevant subcellular localizations, according to analysis by the CellWhere tool. (C) Immunostaining of myotubes for the exosomal marker CD63. Left and upper panels: Representative images of differentiated myoblasts from ALS, SMA-III/IV, SBMA and polyneuritis patients, and from healthy controls. Lower right Panel: quantification of CD63 fluorescence signal normalized per myonucleus (70-108 myonuclei were analysed per individual, with n=5, 2, 3, 2, 6 ALS, SMA-III/IV, SBMA, polyneuritis and healthy subjects, respectively). * and ***, significantly different from ALS with $P<0.05$ and P<0.001, respectively. (D) mRNA encoding for exosomal proteins normalized per B2M mRNA level are upregulated in ALS myotubes compared to healthy (n=7 ALS, 6 Healthy). * significantly different from Healthy with P<0.05. (E) Multi-vesicular bodies that are present in ALS myotubes contain more exosomes than those of healthy controls. Left panel: Representative electron micrographs showing an accumulation of exosomes in multi-vesicular bodies (MVBs; highlighted in pink). Scale bar = 500 nm. Right panel: quantification of the number of exosome-like vesicles in the MVBs (100 MVBs per condition were analysed). Two sample Kolmogorov-Smirnov test confirmed the visual impression that the MVBs of ALS muscle contain a greater number of exosome-like vesicles compared to healthy controls (P<0.05). (F) Representative electron micrographs of exosomes extracted from the culture medium of ALS or healthy myotubes. Scale bar = 100 nm. The extracted vesicles have the typical cup-shape of exosomes. (G) Representative electron micrographs of exosome immunostaining showing that both ALS and healthy exosomes express CD63 and CD82. bar = 100 nm. Exosomes also expressed CD81, and presented a size distribution between 80-100 nm (see Fig. S2D and S2E). (H) The exosome-enriched fraction secreted by ALS myotubes contained twice as much protein as that of healthy control myotubes. Left panel: schema summarizing the experimental procedure. Briefly the same number of ALS and healthy myoblasts were differentiated, and after 3 days the culture medium was harvested to extract the exosomes as described in material and methods. Right panel: Protein quantification of exosomes. 800,000 differentiated myoblasts per subject, with n=4 subjects per group. ** significantly different from healthy myotubes (P<0.01). (See also Fig. S2F).

Secreted ALS exosomes are toxic and their toxicity is driven by FUS

To test exosomal toxicity, 0.5 μg of ALS or healthy exosomes were added to the culture medium of healthy human iPSC-derived motor neurons (hiPSC-MN). Following exosomal uptake (Fig.

3A), only ALS exosomes and not healthy exosomes resulted in shorter neurites (Fig. 3B), with less branching (Fig. 3C) and a greater cell death (Fig. 3D) 72h post-treatment. Similarly, when added to the culture medium of healthy human myotubes, ALS exosomes induced myotube atrophy (Fig. S4A), and cell stress (Fig. S4B) leading to cell death (Fig. S4C-D). The quantity of cell death was decreased when less exosomal protein was loaded, though ALS exosome toxicity remained greater than healthy exosome toxicity at either dose (Fig. S4E-G), suggesting that toxicity is dependent on both the quantity and content of exosomes.

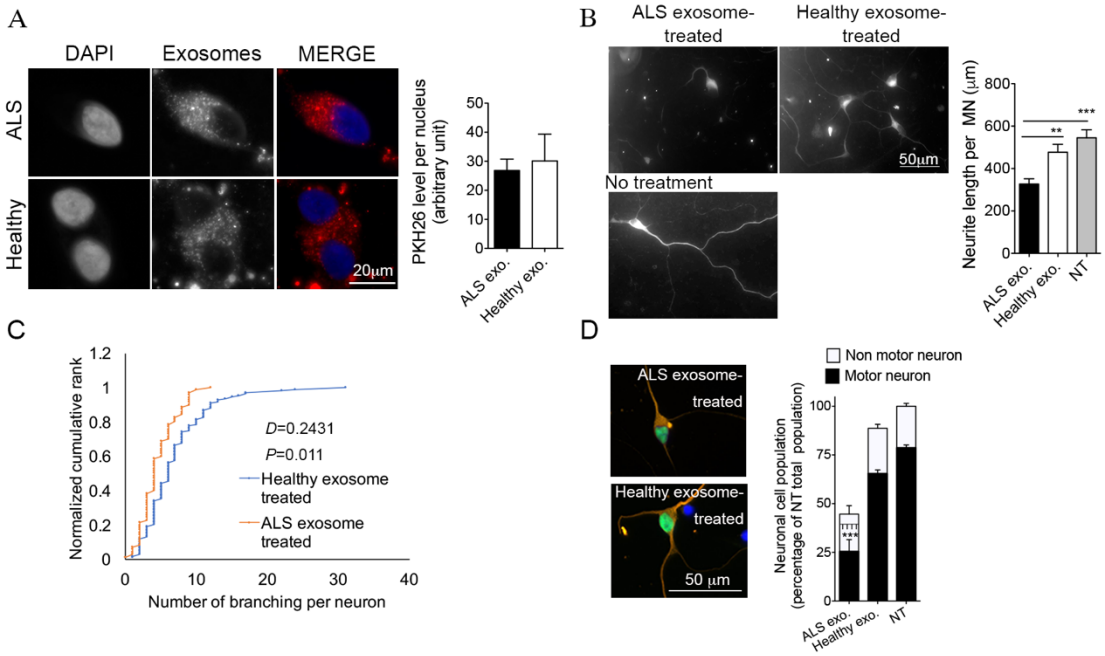

Figure 3: ALS exosomes induce decreased neurite length and branching, and increased death, of human induced pluripotent stem cells derived motor neurons. (A) Equal quantities of ALS and healthy exosomes are taken up by motor neurons. (B) Neurite lengths of motor neurons are shortened when treated with ALS exosomes compared to healthy exosomes. Left panel: representative images of exosome-treated motor neurons. Right panel: quantification of neurite length (8 to 15 motor neurons analysed per well, with n=5 wells per treatment). ** and *** significantly different from ALS values $P<0.01$ and $P<0.001$, respectively. (C) Neurites of iPSC-MN cells have fewer neurite branch-points following treatment with ALS exosomes compared to treatment with healthy exosomes; two-sample Kolmogorov-Smirnov test confirmed the visual impression that the number of branches per neurite is decreased

(P=0.011). (D) Neurotoxicity of ALS exosomes is specific to motor neurons. Right panel: representative images of human iPSC-MN treated with ALS or healthy exosomes. iPSC-MN are positive for motor neuron marker Islet1/2 (green) and neuronal marker Tuj1 (orange). Right panel: quantification of human iPSC neuron and MN cells (10 frames per well, n=3 wells per condition). ***, P<0.001 and ^{TTT}, P<0.001, significantly different from healthy-exosome-treated and non-treated cells, respectively.

Since a leading theory is that disruption of RNA metabolism, including of its translation, transport, storage, and degradation, contributes to ALS physiopathology by affecting neuronal function and viability (*30*), we hypothesized an involvement of RNA processing in exosome toxicity. Human ALS myotubes presented a greater granulation of the RNA-processing protein FUS within the nucleus (Fig. 4A), as well as a nuclear accumulation of RNA (Fig. 4B), and mislocalization of two FUS protein binding partners, RPL5 and caprin 1, that are involved in RNA processing and stress granule formation (Fig. 4C and S5A) (*31*). Furthermore, proteomic analysis revealed that ALS muscle exosomes contain many known protein binding partners of the RNA-processing proteins FUS (*31*) and TDP43 (*32*) (P< 0.00001; Fig. S6A), with some 37% (40 of 109) of FUS binding partners being detected. Genes encoding FUS and TDP43 binding proteins were upregulated in the myotubes of ALS patients and these genes were shared with many RNA-processing pathways that were similarly upregulated (Fig. S6B and S6C). Interestingly, when human iPSC-MNs were treated with ALS exosomes, RNA accumulated in their nuclei (Fig. 4D), an event that could lead to cell death (*33*). Similar results were obtained when ALS exosomes were added to cultures of healthy human myotubes (Fig. S5B). Furthermore, exosomes contained FUS and FUS binding partners (Fig. 4E-F, Fig. S5C, Fig.S6). Therefore, ALS exosomal toxicity in recipient cells may be mediated through the FUS pathway. To test this, we added 0.5 μg of ALS or healthy exosomes to the culture medium of a human muscle cell line that over-expressed a previously published tagged

form of wild-type FUS (FUS-$_{FLAG}$, (*34*)). This induced a dramatic increase in cell death (Fig. 4G), accompanied with greater cellular stress (Fig. S5D) – the same was not observed in cell lines that over-expressed tagged forms of wild-type TDP43 and SOD1 (Fig. 4G). Conversely, when ALS exosomes were added to the culture medium of cells in which FUS was knocked down, a lower proportion of RPL5 granules was observed (Fig. S5E) and the quantity of cell death was reduced (Fig. 4H), suggesting that the toxicity of ALS exosomes was partially reduced in the absence of FUS expression in the recipient cells. These data implicate the FUS pathway in exosome toxicity. Consequently, cells that express a high level of FUS, as observed in hiPSC-MN (Fig. 4I), may be particularly sensitive to ALS muscle exosome toxicity.

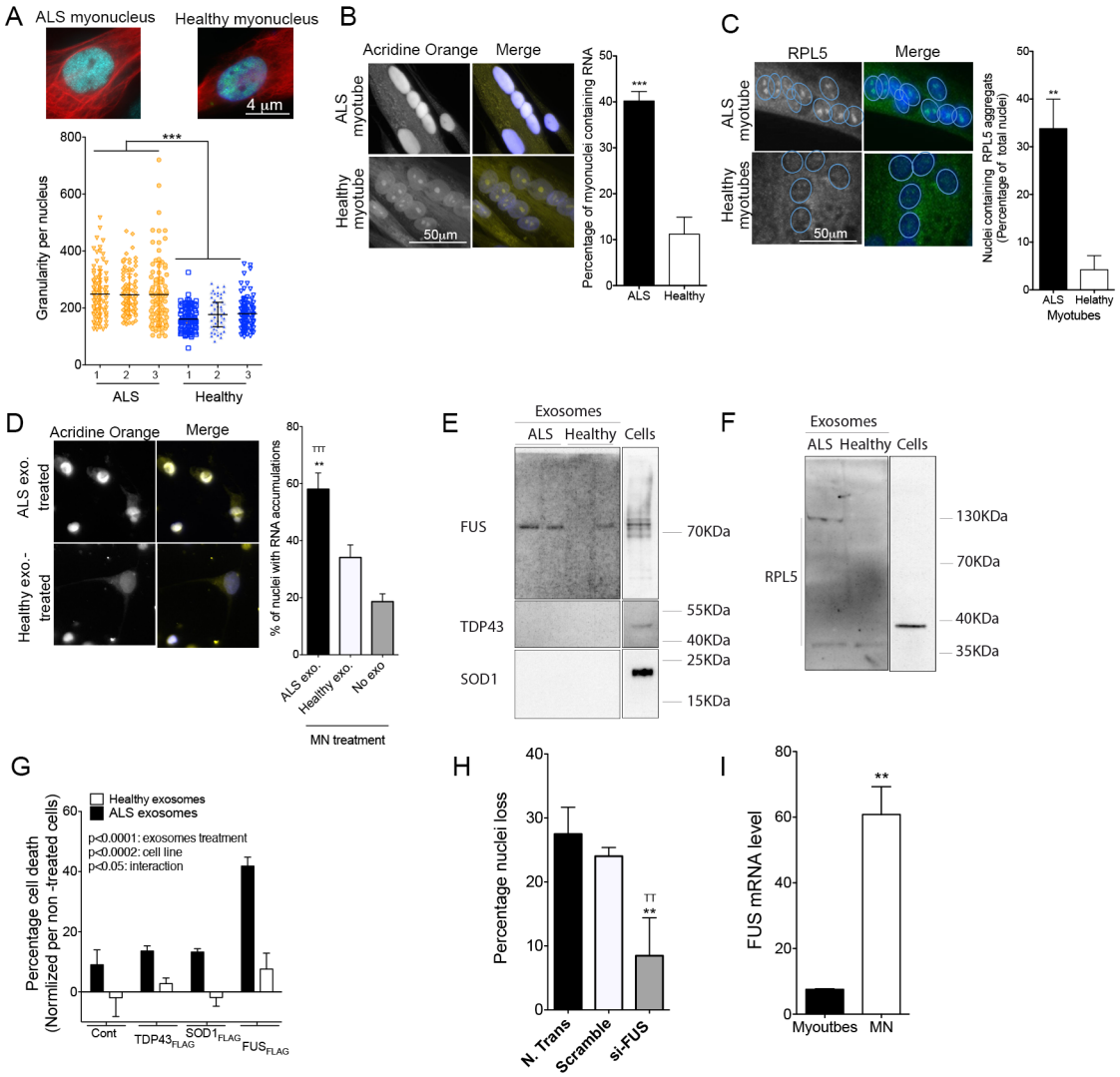

Figure 4: The toxicity of ALS muscle exosomes to healthy motor neurons involves the FUS protein and RNA processing. (A) ALS myonuclei present an increased granulation of FUS compared to healthy controls. Upper panel: representative images of FUS immunostaining in ALS and healthy myonuclei. Lower panel: quantification of granulation (100 myonuclei analysed per subject, with n=3 subjects per group). ***, *P*<0.001 significantly different from healthy myonuclei. (B) ALS myotubes present an accumulation of RNA in their nuclei. Left panel: representative images of RNA localisation in ALS and healthy myotubes. Right panel: percentage of myonuclei with high levels of RNA, assayed by acridine orange staining (50 myonuclei analysed per subject, with n=5 subjects per group). ***, *P*<0.001 significantly different from healthy myotubes. (C) RPL5, a protein involved in RNA transport and stress granules, is granulated in ALS myonuclei. Left panel: representative images of RPL5 localisation in ALS and healthy myotubes. Right panel: percentage of myonuclei with RPL5 granules (500 to 2,000 nuclei analysed per subject, with

n=4 subjects per group). **, $P<0.01$ significantly different from healthy myotubes. (D) ALS exosomes induce an accumulation of RNA in MN nuclei. Left panel: representative images of RNA localisation in MN nuclei. Right panel: percentage of nuclei with accumulations of RNA (150 to 260 nuclei analysed per well, with n=3 wells per condition). **, $P<0.01$ and ^{TTT}, $P<0.001$ significantly different from MN treated with healthy exosomes and untreated MN, respectively. (E) FUS and (F) RPL5 are detected in exosomes. Representative images of western blot showing the presence of FUS and RPL5 in exosomes. Two bands are observed for RPL5 in ALS exosomes only at 130 and 37 kDa. (G) Cell death induced by 0.5 μg of ALS exosomes is exacerbated in the presence of over-expression of FUS. ANOVA 2 factors was performed, showing the effect of ALS exosomes ($P<0.0001$), the effect varying due to cell line ($P<0.0002$), and an interaction between the two parameters ($P<0.05$) (10 frames per well analysed, with n=3 wells per condition). (H) Percentage of cell death is decreased when ALS exosomes are added to the culture medium of cells deficient for FUS (FUS expression level was reduced by 79.5% with siRNA strategy, see Material and Methods, 10 frames per well analysed, with n=3 wells per condition). (I) FUS mRNA level is significantly higher in MN compared to myotubes. **, $P<0.01$ significantly different from human myotubes (n=3 per group).

Discussion

Exosomes are suspected to carry toxic elements from astrocytes towards motor neurons (*13*), and pathological proteins have recently been identified in the extracellular vesicles of sALS patients (*35*). Here muscle exosomes are shown to be toxic to motor neurons, thereby establishing the skeletal muscle as a participant to a vesicle-mediated toxicity model of ALS pathology. The observation that ALS muscle exosomes act on RNA transport, and that RNA transport protein mislocalization is partially corrected and cell death reduced when FUS expression was abolished in recipient cells, is consistent with a body of literature suggesting an RNA processing blockade mechanism in ALS MN (*36*, *37*). High expression levels of FUS in motor neurons may render them especially susceptible to the toxic contents of exosomes, corroborating with the previously observed selective vulnerability of motor neurons to endocytosis of pathogenic proteins (*38*, *39*). The proportionate abundance of muscle tissue in the body would suggest that, as a source of exosomal toxicity, muscle could make an important contribution to motor neuron pathology.

The accumulation and secretion of neurotoxic muscle exosomes was observed across all sporadic ALS patients of our cohort, including patients carrying mutations in *C9orf72* or *ATXN2*, suggesting that this is a common feature across most or all genetic backgrounds of ALS. The consistent observation of a pronounced RNA processing and protein mislocalization phenotype in the ALS myotubes suggests that these cells recapitulate aspects of the disease mechanism that have been observed in motor neurons. Since this phenotype was preserved in primary myoblasts after several divisions and differentiation ex vivo, it must be due to some property of the cells that is heritable between generations of cell division, suggesting DNA mutation or epigenetic imprinting, but it is also possible that some transmissible agent is responsible. Moreover, muscle vesicle-mediated toxicity may represent a common target for novel ALS therapeutics, and muscle exosomes, which have the advantage of being released outside of the blood-brain barrier, and their contents may act as biomarkers with mechanistic links to this toxicity.

References:

1. R. H. Brown, A. Al-Chalabi, Amyotrophic Lateral Sclerosis. *N. Engl. J. Med.* **377**, 1602–1602 (2017).
2. R. Chia, A. Chiò, B. J. Traynor, *Novel genes associated with amyotrophic lateral sclerosis: diagnostic and clinical implications* (Elsevier, 2018; https://www.sciencedirect.com/science/article/pii/S1474442217304015), vol. 17.
3. Y. C. Xue, R. Feuer, N. Cashman, H. Luo, Enteroviral Infection: The Forgotten Link to Amyotrophic Lateral Sclerosis? *Front. Mol. Neurosci.* **11**, 63 (2018).
4. C. Armon, From Snow to Hill to ALS: An epidemiological odyssey in search of ALS causation. *J. Neurol. Sci.* (2018), doi:10.1016/j.jns.2018.05.016.
5. H. Blasco, S. Mavel, P. Corcia, P. H. Gordon, The glutamate hypothesis in ALS: pathophysiology and drug development. *Curr. Med. Chem.* **21**, 3551–75 (2014).
6. C. A. Ross, M. A. Poirier, Protein aggregation and neurodegenerative disease. *Nat. Med.* **10**, S10–S17 (2004).
7. V. Delic *et al.*, Discrete mitochondrial aberrations in the spinal cord of sporadic ALS patients. *J. Neurosci. Res.* **96**, 1353–1366 (2018).
8. E. Onesto *et al.*, Gene-specific mitochondria dysfunctions in human TARDBP and C9ORF72 fibroblasts. *Acta Neuropathol. Commun.* **4**, 47 (2016).
9. A. Anand, K. Thakur, P. K. Gupta, ALS and oxidative stress: The neurovascular scenario. *Oxid. Med. Cell. Longev.* **2013** (2013), pp. 1–14.
10. V. Cappello, M. Francolini, Neuromuscular Junction Dismantling in Amyotrophic Lateral Sclerosis. *Int. J. Mol. Sci.* **18** (2017), doi:10.3390/ijms18102092.
11. F. Rizzo *et al.*, Cellular therapy to target neuroinflammation in amyotrophic lateral sclerosis. *Cell. Mol. Life Sci.* **71** (2014), pp. 999–1015.
12. J. Scekic-Zahirovic *et al.*, Motor neuron intrinsic and extrinsic mechanisms contribute to the pathogenesis of FUS-associated amyotrophic lateral sclerosis. *Acta Neuropathol.* **133**, 887–906 (2017).
13. E. Dirren *et al.*, SOD1 silencing in motoneurons or glia rescues neuromuscular function in ALS mice. *Ann. Clin. Transl. Neurol.* **2**, 167–84 (2015).

14. H. Ilieva, M. Polymenidou, D. W. Cleveland, Non-cell autonomous toxicity in neurodegenerative disorders: ALS and beyond. *J. Cell Biol.* **187**, 761–72 (2009).

15. S. Duguez *et al.*, Dystrophin deficiency leads to disturbance of LAMP1-vesicle-associated protein secretion. *Cell. Mol. Life Sci.* **70** (2013), doi:10.1007/s00018-012-1248-2.

16. M.-C. Le Bihan *et al.*, In-depth analysis of the secretome identifies three major independent secretory pathways in differentiating human myoblasts. *J. Proteomics*. **77**, 344–356 (2012).

17. F. Ciregia, A. Urbani, G. Palmisano, Extracellular Vesicles in Brain Tumors and Neurodegenerative Diseases. *Front. Mol. Neurosci.* **10**, 276 (2017).

18. F. N. Soria *et al.*, Exosomes, an Unmasked Culprit in Neurodegenerative Diseases. *Front. Neurosci.* **11**, 26 (2017).

19. G. Scesa, A. L. Moyano, E. R. Bongarzone, M. I. Givogri, Port-to-port delivery: Mobilization of toxic sphingolipids via extracellular vesicles. *J. Neurosci. Res.* **94**, 1333–40 (2016).

20. M. Basso *et al.*, Mutant copper-zinc superoxide dismutase (SOD1) induces protein secretion pathway alterations and exosome release in astrocytes: Implications for disease spreading and motor neuron pathology in amyotrophic lateral sclerosis. *J. Biol. Chem.* **288**, 15699–15711 (2013).

21. L. R. Fischer *et al.*, Amyotrophic lateral sclerosis is a distal axonopathy: evidence in mice and man. *Exp. Neurol.* **185**, 232–40 (2004).

22. G. Bruneteau *et al.*, Endplate denervation correlates with Nogo-A muscle expression in amyotrophic lateral sclerosis patients. *Ann. Clin. Transl. Neurol.* **2**, 362–372 (2015).

23. G. Dobrowolny *et al.*, Muscle Expression of *SOD1* ^{G93A} Triggers the Dismantlement of Neuromuscular Junction *via* PKC-Theta. *Antioxid. Redox Signal.* **28**, 1105–1119 (2018).

24. C. Tallon, K. A. Russell, S. Sakhalkar, N. Andrapallayal, M. H. Farah, Length-dependent axo-terminal degeneration at the neuromuscular synapses of type II muscle in SOD1 mice. *Neuroscience*. **312**, 179–89 (2016).

25. M. Wong, L. J. Martin, Skeletal muscle-restricted expression of human SOD1 causes motor neuron degeneration in transgenic mice. *Hum. Mol. Genet.* **19**, 2284–302 (2010).

26. J.-P. Loeffler, G. Picchiarelli, L. Dupuis, J.-L. Gonzalez De Aguilar, The Role of Skeletal Muscle in Amyotrophic Lateral Sclerosis. *Brain Pathol.* **26**, 227–236 (2016).

27. P.-F. Pradat *et al.*, Muscle gene expression is a marker of amyotrophic lateral sclerosis severity. *Neurodegener. Dis.* **9**, 38–52 (2012).

28. M. Bakay *et al.*, Nuclear envelope dystrophies show a transcriptional fingerprint suggesting disruption of Rb-MyoD pathways in muscle regeneration. *Brain*. **129**, 996–1013 (2006).

29. A. Bigot *et al.*, Age-Associated Methylation Suppresses SPRY1, Leading to a Failure of Re-quiescence and Loss of the Reserve Stem Cell Pool in Elderly Muscle. *Cell Rep.* **13**, 1172–82 (2015).

30. K. Talbot, E. Feneberg, J. Scaber, A. G. Thompson, M. R. Turner, Amyotrophic lateral sclerosis: the complex path to precision medicine. *J. Neurol.* **265**, 2454–2462 (2018).

31. M. Kamelgarn *et al.*, Proteomic analysis of FUS interacting proteins provides insights into FUS function and its role in ALS. *Biochim. Biophys. Acta - Mol. Basis Dis.* **1862**, 2004–2014 (2016).

32. B. D. Freibaum, R. K. Chitta, A. A. High, J. P. Taylor, Global Analysis of TDP-43 Interacting Proteins Reveals Strong Association with RNA Splicing and Translation Machinery. *J. Proteome Res.* **9**, 1104–1120 (2010).

33. D. K. Rajani, M. Walch, D. Martinvalet, M. P. Thomas, J. Lieberman, Alterations in RNA processing during immune-mediated programmed cell death. *Proc. Natl. Acad. Sci.* **109**, 8688–8693 (2012).

34. T. Yamazaki *et al.*, FUS-SMN protein interactions link the motor neuron diseases ALS and SMA. *Cell Rep.* **2**, 799–806 (2012).

35. D. Sproviero *et al.*, Pathological Proteins Are Transported by Extracellular Vesicles of Sporadic Amyotrophic Lateral Sclerosis Patients. *Front. Neurosci.* **12** (2018), doi:10.3389/fnins.2018.00487.

36. M. Zhao, J. R. Kim, R. van Bruggen, J. Park, Molecules and Cells RNA-Binding Proteins in Amyotrophic Lateral Sclerosis. *Mol. Cells*. **41** (2018), doi:http://dx.doi.org/10.14348/molcells.2018.0243.

37. S. Rossi *et al.*, Nuclear accumulation of mRNAs underlies G4C2-repeat-induced translational repression in a cellular model of C9orf72 ALS. *J. Cell Sci.* **128**, 1787–1799 (2015).

38. C. Benkler *et al.*, Aggregated SOD1 causes selective death of cultured human motor neurons. *Sci. Rep.* **8**, 16393 (2018).

39. N. Wächter, A. Storch, A. Hermann, Human TDP-43 and FUS selectively affect motor neuron maturation and survival in a murine cell model of ALS by non-cell-autonomous mechanisms. *Amyotroph. Lateral Scler. Frontotemporal Degener.* **16**, 431–41 (2015).

40. S. Millecamps *et al.*, Phenotype difference between ALS patients with expanded repeats in *C9ORF72* and patients with mutations in other ALS-related genes. *J. Med. Genet.* **49**, 258–263 (2012).

41. S. Lattante *et al.*, Contribution of ATXN2 intermediary polyQ expansions in a spectrum of neurodegenerative disorders. *Neurology*. **83**, 990–995 (2014).

42. S. Duguez *et al.*, Dystrophin deficiency leads to disturbance of LAMP1-vesicle-associated protein secretion. *Cell. Mol. Life Sci.* **70**, 2159–74 (2013).

43. L. Zhu *et al.*, CellWhere: Graphical display of interaction networks organized on subcellular localizations. *Nucleic Acids Res.* **43** (2015), doi:10.1093/nar/gkv354.

44. Y. Maury *et al.*, Combinatorial analysis of developmental cues efficiently converts human pluripotent stem cells into multiple neuronal subtypes. *Nat. Biotechnol.* **33**, 89–96 (2014).

45. J. C. Stevens *et al.*, Modification of Superoxide Dismutase 1 (SOD1) Properties by a GFP Tag – Implications for Research into Amyotrophic Lateral Sclerosis (ALS). *PLoS One.* **5**, e9541 (2010).

46. B. S. Johnson, J. M. McCaffery, S. Lindquist, A. D. Gitler, A yeast TDP-43 proteinopathy model: Exploring the molecular determinants of TDP-43 aggregation and cellular toxicity. *Proc. Natl. Acad. Sci. U. S. A.* **105**, 6439–44 (2008).

Acknowledgments:

We thank the Human Cell Culture Platform of The Institute of Myology, and the "Plateforme Biopuces et Séquençage de l'IGBMC". This work was financed by Target-ALS (ViTAL consortium, PI: S Duguez), ARsLA (TEAM consortium, PI: S Duguez ; PULSE, PI: D Devos), European Union Regional Development Fund (ERDF) EU Sustainable Competitiveness Programme for N. Ireland, Northern Ireland Public Health Agency (HSC R&D) & Ulster University (PI : T Bjourson). LLG is a recipient from ArSLA. It was also partially supported by European Community's Health Seventh Framework Programme under grant agreement No.

259867 (Euro-MOTOR), INSERM, Sorbonne University, and the AFM. The study was sponsored by APHP.

The authors declare that they have no conflict of interest.

SD, LLG, SR, VM, and UV performed the myoblast and motor neuron cell cultures and measurements, SK performed the nanosight and proteomic analysis on exosomes. JLGDA generated the transcriptome data on differentiated myoblasts. WJD performed the computational analysis, JL performed the electron microscopy analysis, SM performed genetic analysis. PB, AB, HB, GB, MDMA, DD, ACD, DFr, AH, AdHes, LL, PL, TL, PLeb, NLF, TM, VM, AM, GO, FR, LR, FS, TS, GQ and PFP generated the samples, and had some input into data generation. SD with the help of WJD took the lead in interpretation of results and writing the manuscript. CM, SK, JD, JLGDA, CR, GBB, OL discussed the results and provided critical feedback on the manuscript. SD and PFP conceived the original idea. SD supervised the project.

Supplemental Table S1

	No. altered		As %		% expected		Enrichment (Fisher test)	
	Ref 1	Ref 2	Ref 1	Ref 2	Ref 1	Ref 2	Ref 1	Ref 2
Secreted	41	16	5.0	8.3	10.3	10.0	-	-
Secreted (not TM)	31	13	3.8	6.6	9.0	8.8	-	-
Golgi + secreted	3	2	0.4	1.0	0.2	0.2	-	0.078
Clathrin	0	0	0.0	0.0	0.3	0.3	-	-
Endosome	**27**	**8**	**3.3**	**4.0**	**2.0**	**2.0**	**0.012**	**0.057**
Lysosome	**11**	**8**	**1.3**	**4.0**	**1.2**	**1.2**	**-**	**0.003**
Autophagosome	4	1	0.5	0.5	0.2	0.2	0.074	-
All secretion-related (union of above)	75	28	9.6	15.5	14	13.6	-	-

Table summarizing the number of genes dysregulated in different secretory compartments in ALS muscles, by re-analysis of data of Bakay et al (2006) and Pradat et al (2012) – referred to in the table as Ref 1 and Ref 2 respectively. The GEO repository accession number for Bakay et al. is GDS2855, and the ArrayExpress repository number for Pradata at al. is E-MEXP.3260 The column '% expected' shows the percentage expected by chance based on the proportion of genes of that study's microarray chip that are annotated to the respective cell compartment.

A Fisher's exact test was performed for each compartment to determine if it was significantly enriched (Fisher p value is given).

Supplemental Table. S2

66 Subjects	Age at the time of the biopsie	Gender	ALS/FRS	Genetic	Muscle testing	Site of onset 0=spinal; 1=Upper limb; 2=Lower limb; 3=bulbar; 4=respiratory	Duration of disease (months)	Histology	Electron microscopy	Cell culture	Transcriptome	Immunostaining cell culture	RT-qPCR	exosome treatment MN	exosome treatment myotubes
24 ALS (35-76y: 58.54±8.28; 7F, 17M)	58	F	38	.	130	1	13								
	67	M	45	.	146	2	25.2								
	56	M	41	.	140	2	26.7								
	59	F	39	*C9orf72*	146	3	16.5								
	53	F	28	C9orf72	119	3	6								
	61	M	38	*ATXN2*	130	2	11.3								
	64	M	40	.	130	1	39.3								
	70	M	37	.	126	3	48.3								
	68	M	33	.	123	1	53.4								
	76	M	32	.	104	1	28								
	59	F	23	.	103	3	33								
	61	M	40	.	97	1	11								
	61	M	38	.	88	1	52								
	53	M	31	.	94	2	40								
	52	H	37	.	No data	0	101								
	35	F	32	.	No data	0	85								
	52	F	43	.	135	1	33.6								
	49	M	41	.	111	2	44.1								
	53	M	40	.	130	2	17.4								
	57	M	37	*C9orf72*	145	3	20.6								
	66	M	41	.	147	2	28.7								
	51	M	36	.	139	2	12								
	66	M	43	.	149	1	12								
	58	F	40	.	98	3	14								
24 Healthy (21-75y: 48.29 ± 17.56; 7F, 17M)	61	M	.	.	.	.	.								
	75	M	.	.	.	.	.								
	56	F	.	.	.	.	.								
	64	F	.	.	.	.	.								
	51	M	.	.	.	.	.								
	52	F	.	.	.	.	.								
	47	F	.	.	.	.	.								
	59	M	.	.	.	.	.								
	19	M	.	.	.	.	.								
	59	M	.	.	.	.	.								
	54	M	.	.	.	.	.								
	59	F	.	.	.	.	.								
	49	F	.	.	.	.	.								
	53	M	.	.	.	.	.								
	70	M	.	.	.	.	.								
	21	M	.	.	.	.	.								
	21	M	.	.	.	.	.								
	53	M	.	.	.	.	.								
	69	F	.	.	.	.	.								
	66	M	.	.	.	.	.								
	21	M	.	.	.	.	.								
	33	M	.	.	.	.	.								
	22	M	.	.	.	.	.								
	25	M	.	.	.	.	.								
2 Polyneuritis (70 & 45 y; 1F, 1M)	70	M	.	.	.	.	13								
	45	F					8								
10 SBMA (43-71y: 58.18 ± 9.65; 10M)	60	M	42	47 repeats	132	2	420								
	43	M	44	48 repeats	148	2	60								
	57	M	44	44 repeats	148	2	72								
	71	M	35	45 repeats	136	2	324								
	45	M	39	50 repeats	134	2	168								
	71	M	40	41 repeats	149	1	372								
	66	M	40	49 repeats	142	2	144								
	56	M	36	46 repeats	121	2	324								
	62	M	38	47 repeats	143	2	156								
	64	M	37	45 repeats	138	2	108								
6 SMA-III/IV (30-61y: 42.5 ± 10.27; 1F, 5M)	48	M	42		140	2	156								
	36	M	41		106	2	276								
	61	M	40		122	2	588								
	45	M	41		124	2	324								
	30	M	43		139	2	84								
	35	F	44		142	2	384								

Table summarizing the subject samples used for each type of experiment. Subject age at time of biopsy is indicated in the column “Age”. All ALS patients were confirmed to be ALS according to El Escorial. The ALSFRS-R and Muscle Testing results measured at the time of the biopsies are given. Manual muscle testing was scored from 0, representing total paralysis, to 5, representing normal strength, according to the Medical Research Council Score.

Supplementary figures:

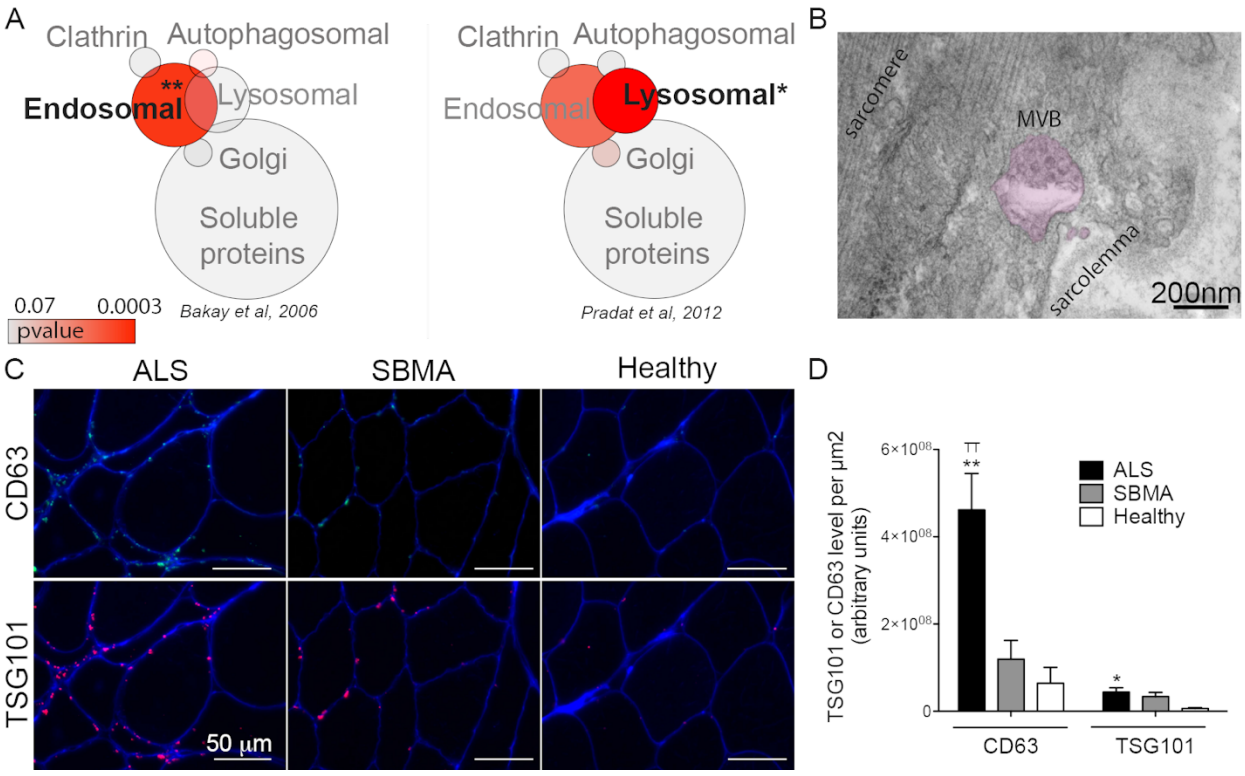

Figure S1: Disruption of the exosomal pathway in sporadic ALS muscles. (A) Dysregulation of secretory compartments in a reanalysis of two previously published gene expression studies of ALS muscle biopsies (*27*, *28*). Each circle represents a compartment related to a secretory pathway. The size of each circle is proportional to the number of genes related to each compartment. Red colour indicates that the gene expression of the compartment is altered in ALS muscle compared to healthy (* and **, $P<0.05$ and $P<0.01$, respectively). See Table S1A for more details. (B) Representative electron micrograph of sALS muscle longitudinal section. Multivesicular bodie (MVB) is highlighted in purple. The MVBs contain exosome-like vesicles. MVBs were observed every 62.09±13.3 sarcomere in ALS muscle whereas 1 MVB was observed every 330.8±127 in healthy muscles (500 to 5,000 sarcomeres were analysed per subject, with n = 3 subjects per group). (C) Representative images of exosomal markers CD63

and TSG101 immunostaining in ALS, SBMA, and healthy muscle. Scale bar 50 μm. (D) Quantification of exosomal markers CD63 and TSG101 in muscle biopsies (Pixel per μm^2, n= 6 ALS, 4 SBMA, 5 Healthy for CD63, and n=4 per group for TSG101; * and ** significantly different from healthy subjects, $P<0.05$ and $P<0.01$, respectively; ^{TT} significantly different from SBMA patients, $P<0.01$). CD63 in green, TSG101 in red, Dystrophin in blue.

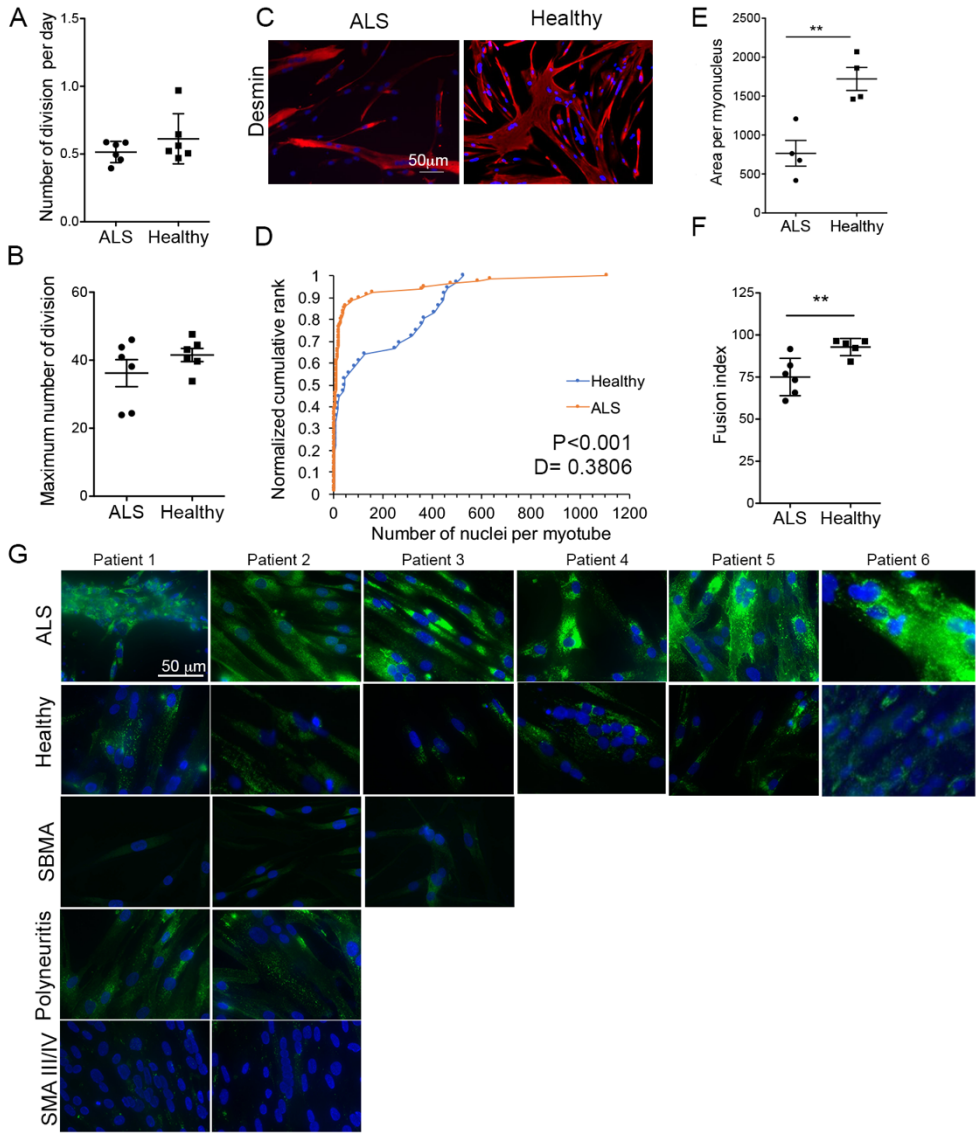

Figure S2: ALS myoblasts form thinner myotubes with fewer myonuclei. (A) ALS myoblasts have the same division speed as healthy myoblasts (n= 6 subjects per group). (B) ALS myoblasts can reach the same maximum number of divisions as healthy myoblasts (n= 6 subjects per group). (C) Representative images of differentiated ALS and healthy myoblasts. Myotubes were immunostained with desmin, red. Scale bar = 50 μm. (D) ALS myoblasts form smaller myotubes with less nuclei. Kolmogorov-Smirnov test was used to compare the distribution of myotube nuclear numbers in ALS and healthy cell cultures, $P<0.001$ and the maximum difference between the cumulative distribution is D=0.3806. (E) ALS myotubes are thinner as shown by the measurement of desmin area per myonucleus. (n= 4 subjects per group). **, significantly different from healthy group, $p<0.01$. (F) ALS myoblasts show a lower fusion index. (n=6 subjects per group). **, significantly different from healthy group, $P<0.01$. (G) Panel showing representative images of CD63 immunostaining performed on cultured myotubes from different patients. Of note, ALS patient 6 is *C9orf72* mutated.

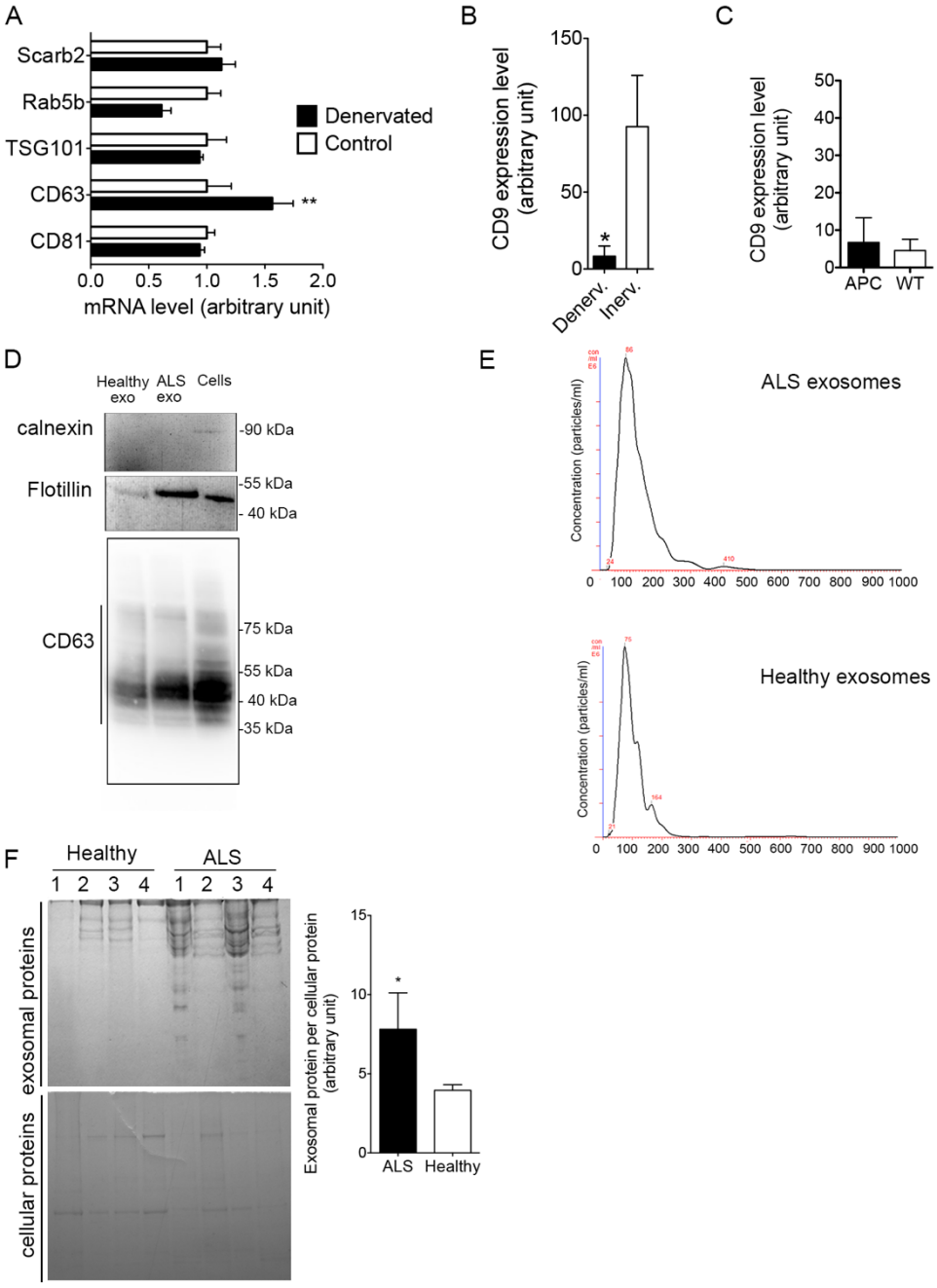

Figure S3: ALS myotubes secrete exosomes. Denervated murine muscles do not show a global upregulation of the exosomal pathway, neither by RT-qPCR (A), nor by immunostaining (B). CD9 immunostaining was used to labelled murine exosomes on muscle sections. **,

significantly different from innervated muscle, $P<0.01$. (C) No upregulation of exosomal markers was observed in cachectic murine muscles. *, significantly different from innervated muscle, $P<0.05$. (D) ALS and healthy exosomes are positive for CD63 and flotillin, and negative for calnexin. (E) NanoSight analysis showing that ALS and healthy exosomes sizes range between 90-200 nm. (F) SDS-PAGE analysis showing a greater quantity of protein in exosomally enriched fraction secreted by 800,000 ALS myotubes compared to healthy controls. Left panel: representative image of SDS-PAGE. Exosomes were extracted from the culture medium of 800,000 myoblasts differentiated into myotubes for 3 days. Right panel: quantification of protein levels per well. *, significantly different from healthy, $P<0.05$.

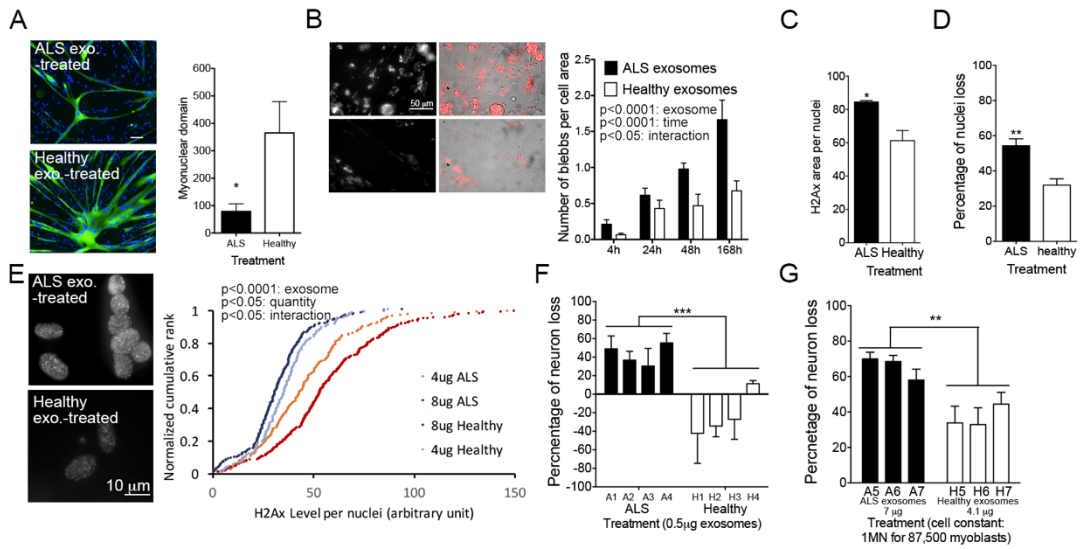

Figure S4: ALS exosomes are toxic toward healthy human iPSC-MN and myotubes. (A) ALS exosomes induce muscle cell atrophy. Left panel: Representative images of healthy myotubes treated with ALS or Control exosomes. Myotubes are stained with myosin heavy chain (green). Right panel: quantification of myonuclear domain size (area of myosin heavy chain staining divided by the number of nuclei). The ALS-exosome treated myotubes have a smaller myonuclear domain. * $P<0.05$, significantly different from healthy values. 2,000 to 4,000 myonuclei were analysed per subject, with n=3 subjects per group. (B) ALS exosomes induce cell stress. Counts of blebs per healthy myotube at different time-points after treatment with ALS or control exosomes. Five myotubes per time point per subject were analysed, with n=3 subjects per group. ANOVA 2 factor interaction, time and treatment $P<0.001$. (C) Levels of cell death marker H2Ax are increased in myonuclei of ALS-exosome-treated myotubes compared to Healthy-exosome-treated myotubes. Two hundred to 400 myonuclei per subject were analysed, with n=3 subjects per group. * $P<0.05$, significantly different from healthy values. (D) A greater loss of myonuclei is observed in cultures treated with ALS exosomes compared to healthy exosomes. n=3 subjects per group. ** $P<0.01$, significantly different from healthy controls. (E) Decreasing ALS exosome quantity leads to decreased cell death. Left panel: representative immunostaining of H2-Ax immunostaining of healthy myotubes treated

with ALS or control exosomes. Right panel: The graph represents a distribution of H2Ax level in myonuclei treated with either 4 or 8 μg of ALS exosomes (curves in orange and red), or with 4 or 8 μg of healthy exosomes (curves in light and dark blue). One hundred and eighty to 300 nuclei were analysed per subject and per condition, with n = 3 per subject. Two factor ANOVA was performed, showing the effect of ALS exosomes (P<0.0001), the effect varying due to quantity (P=0.0110), and an interaction between the two parameters (P=0.0301). (F) Quantification of the death of human IPSC-motor neurons treated with equal amounts (by protein content: 0.5 μg) of ALS or healthy exosomes. Exosomes were extracted from sporadic ALS patients negative for known mutations (each bar represents a different subject: n=4 subjects per group, each in triplicate). *** P<0.001, significantly different from healthy values. (G) Quantification of the death of human IPSC-motor neurons treated with ALS or control exosomes extracted from the culture medium of equal numbers (262,500) of differentiated myoblasts (ratio of 1 MN per 87,500 myoblasts). Each bar represents one subject (five replicates per subject). One subject was C9orf72 mutated, one was Sca2 mutated and one subject had no known ALS-associated gene mutations. ** P<0.01, significantly different from healthy values.

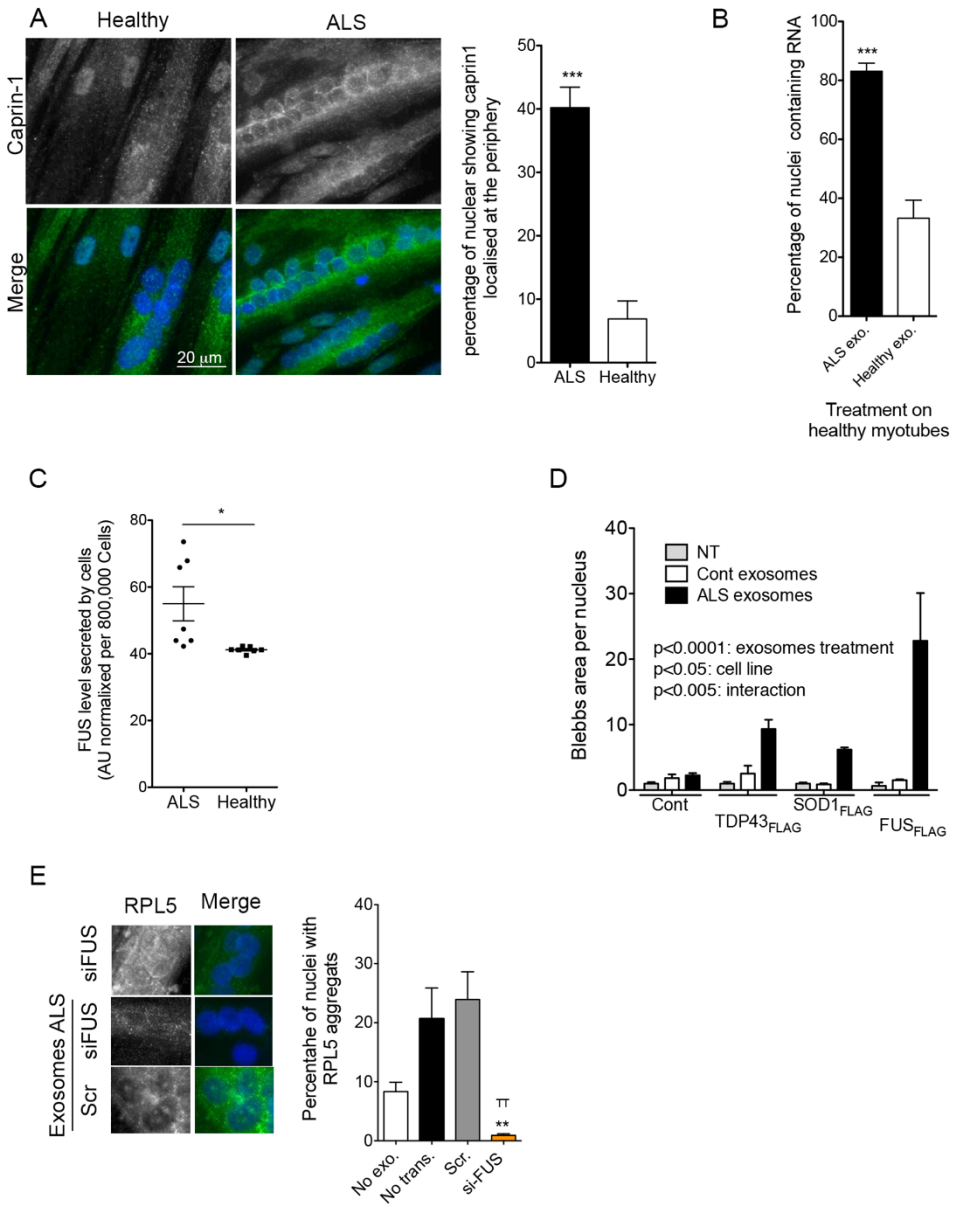

Figure S5: RNA transport is affected in ALS myotubes, and in cells treated with ALS exosomes. (A) Caprin 1, a FUS partner protein involved in RNA transport, accumulated at the myonuclei of sALS myotubes. Left panel: Representative images of healthy myotubes treated with ALS or Control exosomes. Myotubes are stained with myosin heavy chain (green). Right panel: percentage of myonuclei that had an accumulation of caprin 1 at their periphery. *** $P<0.001$, significantly different from healthy values. Six hundred to 1,000 nuclei per subject were analysed, with n=4 subjects per group. (B) Percentage of myonuclei positive for

accumulation of RNA in myotubes treated with ALS or healthy exosomes. Accumulation of RNA is increased in the myonuclei of ALS-exosome-treated myotubes. *** $P<0.001$, significantly different from healthy values. Seventy to 100 myonuclei per subject were analysed, with n=4 subjects per group. (C) Quantification by Western blot of FUS level in exosomes secreted from 800,000 differentiated myoblasts. * $P<0.05$, significantly different from healthy values. n=7 subjects per group. (D) Cell stress induced by ALS exosomes is exacerbated in presence of over-expression of FUS. ANOVA 2 factors was performed, showing the effect of ALS exosomes ($P<0.0001$), the effect varying due to cell line ($P<0.005$), and an interaction between the two parameters ($P<0.005$). (E) RPL5-aggregates are no longer observed following ALS-exosome-treatment when the recipient cells do not express FUS. Left panel: Representative images of myotubes treated with siFUS or siScrambled control, and with addition or not of ALS exosomes. Myotubes are immunostained for RPL5 (green). Right panel: Percentage of myotube nuclei with RPL5 aggregates in untreated ('No exo.'), ALS-exosome-treated with no knockdown ('No trans'), ALS-exosome-treated with siScrambled knockdown ('Scr.'), or ALS-exosome-treated with siFUS knockdown ('si-FUS'). Eight hundred to 1,000 nuclei were analysed per well, with n=3 wells per condition. ANOVA 1 factor was performed, showing the effect of ALS exosomes on the two different knock-down conditions, with ** and ^{TT} representing significant difference from 'No trans.' and 'Scr.', respectively, $P<0.01$.

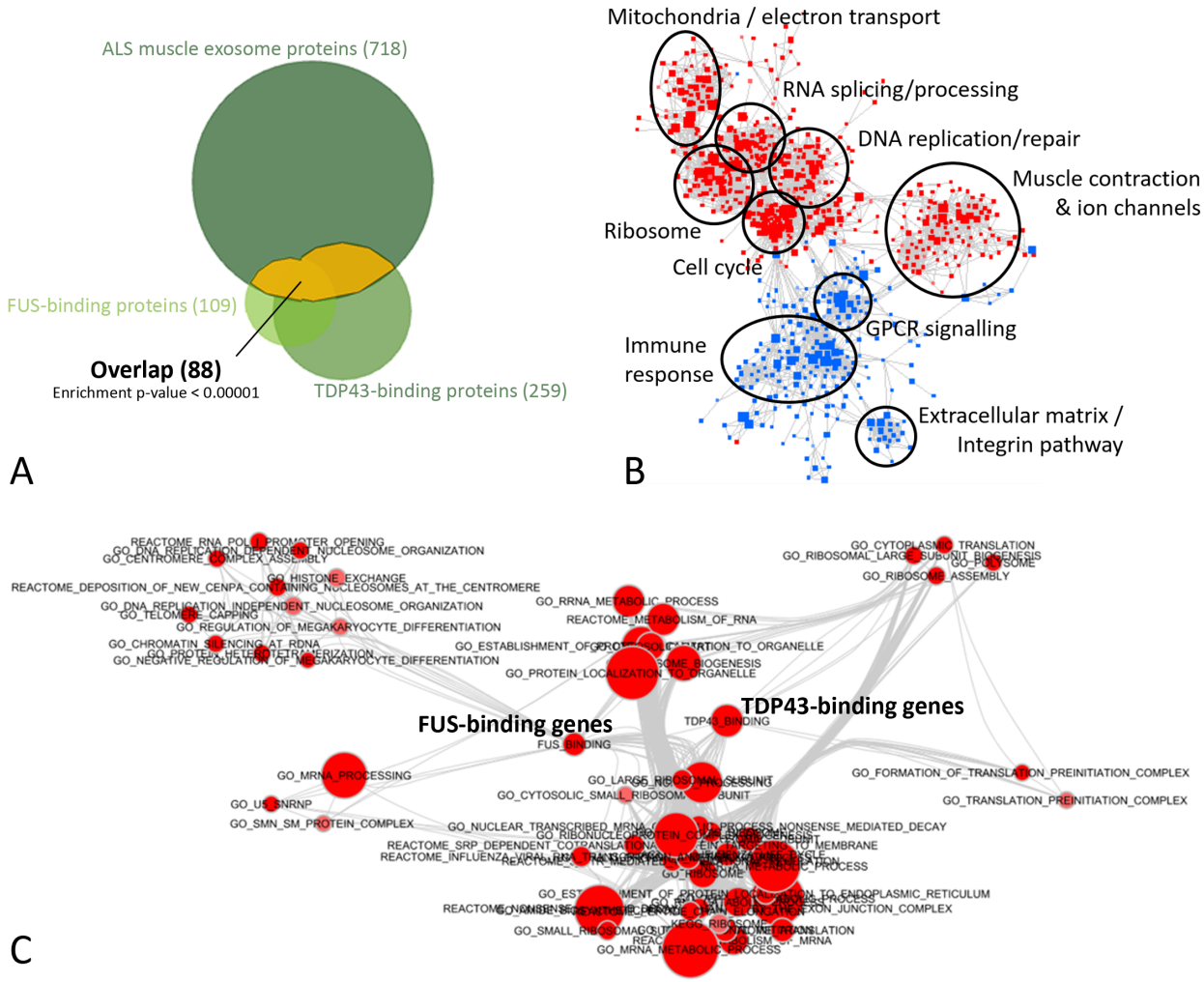

Figure S6: The proteomic content of exosomes is enriched for FUS and TDP43 binding proteins, and the genes encoding FUS and TDP43 binding proteins are upregulated and contribute to the upregulation of RNA-processing in the myotubes of ALS patients. (A) Whereas only 1.5% of all proteins are known binding partners of FUS and/or TDP43, they represent 12.7% (88 of 718) of the proteins detected by proteomic analysis of exosomal contents (Fisher's test $P<0.00001$). (B) Enrichment map representing overlap and clustering of the cellular processes and pathways for which gene expression is dysregulated in ALS myotubes compared to healthy controls (red = upregulated; blue = downregulated). (C) Enrichment map showing that genes encoding FUS and TDP43 binding proteins are upregulated in ALS myotubes compared to healthy controls, and that these genes are shared

with many RNA-processing pathways that are similarly upregulated (red = upregulated).

Material and Methods

Participants and ethical approvals

An open biopsy was performed on deltoid muscles of 18 ALS patients with probable or definite ALS according to the revised El Escorial criteria (Brooks BR et al, Amyotroph Lateral Scler Other Motor Neuron Disord 2000; 1: 293-299), who attended the Motor Neuron Diseases Center (Pitié Salpétrière, Paris). Genetic analyses were carried out on DNA extracted from blood samples for all ALS patients to screen several ALS related genes: the *C9orf72* hexanucleotide repeat expansion (using gene scan and repeat primed PCR procedures described in(*40*)), *ATXN2* repeat length (*41*) and the coding regions of *SOD1, TARDBP, FUS*, *UBQLN2* and *TBK1*(sequences of the used primers are available upon request). An open deltoid biopsy was also obtained from 6 patients with SMN1-linked adult Spinal Muscular Atrophy (SMA type III/IV) and 10 patients with genetically confirmed Spinal and Bulbar Muscular Atrophy (SBMA, also known as Kennedy's Disease) recruited in the Paris MND Center or the Institute of Myology (Pitié Salpétrière, Paris).

Two peroneal muscle biopsies were obtained from patients affected by sensorimotor polyneuropathy. Twenty-four deltoid muscle biopsies from healthy age and gender-matched subjects were obtained from the BTR (Bank of Tissues for Research, a partner in the EU network EuroBioBank) in accordance with European recommendations and French legislation. The main demographic, clinical, and genetic characteristics of the subjects are indicated in table S1.

The protocols (NCT01984957) and (NCT02360891) were approved by the local Ethical Committee and all subjects signed an informed consent in accordance with institutional guidelines.

Immunolabelling

- *Immunocytochemistry:* 200,000 cells or 100,000 cells were respectively plated on u-dish 35mm high ibidiTreat or 4 wells plate ibidiTreat (ibidi®) in proliferative medium. The following day, muscle stem cells were washed with PBS and myogenic differentiation was induced by cultivating the cells in DMEM only. Muscle cells were fixed at 3 days of differentiation using 4% formaldehyde. The cells were permeabilised, blocked and stained as described (*42*).
- *Immunohistology:* 8 µm muscle transverse sections were cut from human biopsies on a cryostat microtome at -20ºC, permeabilised, blocked and stained as previously described (*29*)

Primary antibodies used are listed in the Table below and the secondary antibodies used were goat anti-mouse IgG1 or anti-mouse IgG2a, or mouse IgG2b or anti-rabbit tagged with AlexaFluor 355 or AlexaFluor 488 or Alexa Fluor 555 or AlexaFluor 594 or AlexaFluor 647 (1:400, Invitrogen™). The slides were washed, counter-stained with 1μg.ml^{-1} DAPI for 1 min, rinsed 2 times and mounted with ibidi mounting medium (ibidi®).

Ten to 20 non-overlapping pictures were acquired in a line along the diameter of the slide with an Olympus IX70, and an Olympus UPlan FI 10x/0.30 Ph1 and an Olympus BX60 objectives equipped with a Photomatics CoolSNAP™ HQ camera. For the human muscle sections, pictures were taken with an Olympus LCPlan FI 40x/0.60 Ph2 objective. Images were acquired using Zeiss software and analysed using either Fiji or ImageJ 1.37v.

Antibody	**Clone**	**Manufacturer, Catalogue number**	**Species raised, Isotype**	**Dilution used**	**Application**
Calnexin	AF18	Life Technologies	Monoclonal,	1 : 100	WB

		MA3-027	Mouse IgG1		
Caprin (GPIP137)		Life Technologies PA5-29514	Polyclonal, Rabbit IgG	1 : 200	ICC
CD63		BD Pharmingen	Monoclonal, Mouse IgG1	1 : 200	IHC, ICC
CD63	TS63	Life Technologies 10628D	Monoclonal, Mouse IgG1	2 µg/mL	WB
Desmin	D33	Life Technologies MA5-13259	Monoclonal, Mouse IgG1	1 : 50	ICC
Flotillin		Life Technologies PA5-18053	Polyclonal, Goat IgG	0.3 µg/mL	WB
FUS		Bethyl A300-302A	Polyclonal, Rabbit IgG	1 : 2000	ICC
FUS		Life Technologies PA5-23696 /PA5-52610	Polyclonal, Rabbit IgG	0.4 µg/mL	WB, ICC
H2AX		Cell Signalling 763J	Monoclonal, Rabbit IgG	1 : 50	ICC
Isl1/2	39.4D5	DSHB	Monoclonal, Mouse IgG2b	1 : 100	ICC
Myosin Heavy Chain	MF20	DSHB	Monoclonal, Mouse IgG2b	10 µg/mL	ICC
RPL5		Life Technologies PA5-26269 / PA5-27539	Polyclonal, Rabbit IgG	1 : 500	ICC

RPL5		Bethyl A303-933A	Polyclonal, Rabbit IgG	1 : 2000	WB
Tsg101	C-2	Santa Cruz, sc-7964	Monoclonal, Mouse IgG2a	1 : 200	ICC
Anti-Tubulin Antibody, beta III isoform	TUJ1	Millipore, MAB-1637	Monoclonal, Mouse IgG1	1 : 250	ICC

Electron microscopy

- *Electron Microscopy for extracted exosomes* - Purified vesicles were fixed in 2% paraformaldehyde and were counterstained with uranyl and lead citrate and analysed as previously described (*16*).
- *Electron microscopy for human myotubes* – Human myotubes were plated on plastic (Thermanox, Nalge Nunc, Rochester, NY, USA) coverslips and fixed in 2.5% glutaraldehyde in 0.1 M phosphate buffer (v/v), pH 7.4 and further post-fixed in 2% OsO4 (w/v). They were gradually dehydrated in acetone including a 1% uranyl en-bloc staining step in 70% acetone (w/v), and embedded in Epon resin (EMS, Fort Washington, PA, USA). Ultrathin sections were counterstained with uranyl and lead citrate. Observations were made using a CM120 transmission electron microscope (Philips, Eindhoven, The Netherlands) at 80 kV and images recorded with a Morada digital camera (Olympus Soft Imaging Solutions GmbH, Münster, Germany).
- *Electron microscopy for human muscle biopsies* – Human muscles biopsies were fixed in 2% glutaraldehyde, 2% paraformaldehyde, 0.1 M phosphate

buffer. After abundant washes and 2% OsO4 post-fixation samples were dehydrated at 4 °C in graded acetone including a 1% uranyl acetate in 70° acetone step and were finally embedded in Epon resin. Thin (70 nm) sections were stained with uranyl acetate and lead citrate, observed using a Philips CM120 electron micro- scope (Philips Electronics NV) and photographed with a digital SIS Morada camera.

Muscle stem cell extraction and culture.

Briefly, muscles biopsies were dissociated mechanically as previously described in (*29*), and plated in proliferation medium [1 volume of M199, 4 volumes of Dulbecco's modified Eagle's medium (DMEM), 20% foetal bovine serum (v:v), 25 ug.ml^{-1} Fetuin, 0.5 ng.ml^{-1} bFGF, 5 ng.ml^{-1} EGF, 5 ug.ml-1 Insulin]. The myogenic cell population was enriched using CD56 magnetic beads, and for their myogenicity using anti-desmin antibodies as described before (*29*). A minimum of 80% of the cell population were positive for desmin. After rinsing 3 times the proliferative myoblasts with PBS, and 3 times with DMEM to remove any FBS residual, the human muscle stem cells were differentiated into myotubes by culturing them in DMEM for 3 days.

Number of divisions per day and life span.

Primary myoblast proliferation was followed until proliferative exhaustion. The number of divisions was calculated as follows:

$$Division\ number = \frac{\log\left(\frac{Cell\ number\ at\ day\ n}{Cell\ number\ at\ day\ 0}\right)}{\log 2}$$

RNA extraction.

Purified muscle stem cells were differentiated for 3 days into myotubes. RNA from muscle cells was extracted as described in (*29*). The quality of RNA samples was assessed with Agilent 2100 Bioanalyzer (Agilent Technologies Inc., Santa Clara, CA).

Gene expression profiling.

- *mRNA gene expression profiling* - Aliquotes of high-quality total RNA from each sample (ALS n=6, SBMA n=6, SMA n=5, and healthy n=6, muscle stem cells) were used for mRNA expression profiling using GeneChip Human Exon 1.0 ST arrays (Affymetrix) as previously described (*27*).
- *Analysis of gene expression data* – Expression data were uploaded to the GEO repository at accession number GSE122261. Raw data (.CEL Intensity files) were processed using R/Bioconductor packages. Briefly, sample quality was verified by assessment of MA plots, normalized unscaled standard error (NUSE; all samples had median <1.1), and relative log expression (RLE; all sample had divergence <0.2), using the oligo package. Background-corrected normalized log2-transformed probe set signal intensities were obtained by Robust Multi-array Averaging (RMA) using default settings. Affycoretools and huex10stprobeset.db were used to annotate probeset IDs. For exon-level analysis, probesets were retained if oligo's paCalls function declared them present with $p<0.05$ in all samples of at least one experimental group. For gene-level analysis, probesets were retained if they had expression level $>\log_2 50$ in at least 4 of the 23 samples. A design matrix (~0 + condition; condition = ALS, SBMA, SMA, or Healthy) was created, to which Limma was used to fit a linear model to the normalized expression values, and differentially expressed genes were identified using Limma's empirical Bayes method. Genes that were dysregulated in the same direction in all comparisons of ALS v SBMA, SMA-

III/IV, and Healthy, were identified, and the top 50 ranked by fold-change in ALS v Healthy were uploaded to CellWhere (*43*). CellWhere was used to identify secretory-related subcellular localization annotations of proteins encoded by these genes, and to visualize these proteins and their localizations on a schema of the cell. For enrichment mapping, the GSEA tool (http://software.broadinstitute.org/gsea/index.jsp) was used to assess the distribution of gene sets across the differential expression profile of ALS compared to Healthy myotubes. 6,349 gene sets were tested, including all of the Gene Ontology Biological Process and Cellular Component collections, and all of the Canonical Pathways from MSigDB. In addition, custom gene sets were created listing genes encoding the known protein binding partners of FUS (*31*) and TDP43 (*32*). Cytoscape v3 and the enrichment map plugin were used to create a graph representing as nodes the gene sets identified by GSEA to be significantly enriched with FDR < 0.05, with edges shown for those pairs of gene sets having overlap coefficient >0.5. Cytoscape's selection features were used to isolate a sub-graph of the enrichment map showing only the FUS and TDP43 binding gene sets and those gene ontology or canonical pathway gene sets with which they shared genes (overlap coefficient >0.5).

-

Quantitative RT-qPCR

- *cDNA synthesis:* RNA from 3 days differentiated muscle cells was extracted as described above. 1 ug of RNA was used to synthesise cDNA using M-MLV Reverse Transcriptase (LifeTechologies™). Quantitative PCR was performed on LightCycler® 480 Instrument (Roche) using LightCycler® 480 DNA SYBR Green I Master (Roche).

- *Housekeeping genes*: Out of the 7 housekeeping genes listed in the table below and tested, Beta-2-microglobulin (B2M) showed a constant expression level in all samples, and was used to normalize the gene expression levels of exosomal markers.

Primers	**Sequence (5' → 3')**
β2M	Fw Primer CTCTCTTTCTGGCCTGGAGG Rev Primer TGCTGGATGACGTGAGTAAACC
GAPDH	Fw Primer AAGGTGAAGGTCGGAGTCAACGG Rev Primer TGACAAGCTTCCCGTTCTCAGCC
GUS	Fw Primer CTCATTTGGAATTTTGCCGATT Rev Primer CCGAGTGAAGATCCCCTTTTTA
HPRT1	Fw Primer TGATAGATCCATTCCTATGACTGTAGA Rev Primer CAAGACATTCTTTCCAGTTAAAGTTG
P0 (RPL0)	Fw Primer TCCAGGCTTTAGGTATCACCAC Rev Primer GCTCCCACTTTGTCTCCAGTC
PPIA	Fw Primer CCTAAAGCATACGGGTCCTG Rev Primer TTTCACTTTGCCAAACACCA
PSMA2	Fw Primer CATTCAGCCCGTCTGGTAAA

	Rev Primer	GTTTTTTCTCAGTTGCTAATACCACA

- *Exosomal markers and FUS expression level:* Quantitative PCR was performed on LightCycler® 480 Instrument (Roche) using LightCycler® 480 DNA SYBR Green I Master (Roche). Primers used are listed in table below. The amplification efficiency of the reaction was calculated using data from a standard curve using RT products from control cells as reference samples (1:20, 1:100, 1:500 and 1:2500 dilutions used). The gene expression level was estimated using the comparative Ct method - Ct representing the cycle at which the fluorescence signal crosses the threshold as previously described (*29*).

Primers		Sequence (5' → 3')
Lamp1	Forward Primer	CAGATGTGTTAGTGGCACCCA
	Reverse Primer	TTGGAAAGGTACGCCTGGATG
Lamp2	Fw Primer	GAAAATGCCACTTGCCTTTATGC
	Rev Primer	AGGAAAAGCCAGGTCCGAAC
CD81	Fw Primer	TTCCACGAGACGCTTGACTG
	Rev Primer	CCCGAGGGACACAAATTGTTC
CD63	Fw Primer	CAGTGGTCATCATCGCAGTG
	Rev Primer	ATCGAAGCAGTGTGGTTGTTT
CD82	Fw Primer	GCTCATTCGAGACTACAACAGC
	Rev Primer	GTGACCTCAGGGCGATTCA
SCARB2	Fw Primer	GGCCGATGCTGCTTCTACA
	Rev Primer	GGTCTCCCCTCTGAGGATCTC

EPDR1	Fw Primer	GTCCAGGAGTGGTCGGACA
	Rev Primer	ACACCGAGGGGTCTTTAATACC
VPS29	Fw Primer	TGCAACAGTTTGCCAGCTAAA
	Rev Primer	CCTCTGCAACAGGGCTAAGC
RAB11FIP1	Fw Primer	GGACAAGGAGCGAGGAGAAAT
	Rev Primer	GTCGTGCTAGGGATGATGGC
CD44	Fw Primer	CTGCCGCTTTGCAGGTGTA
	Rev Primer	CATTGTGGGCAAGGTGCTATT
RAB5b	Fw Primer	TCACAGCTTAGCCCCCATGTA
	Rev Primer	CTTCACCCATGTCTTTGCTCG
HLA-G	Fw Primer	GAGGAGACACGGAACACCAAG
	Rev Primer	GTCGCAGCCAATCATCCACT
TSG101	Fw Primer	GAGAGCCAGCTCAAGAAAATGG
	Rev Primer	TGAGGTTCATTAGTTCCCTGGA
FUS	Fw Primer	TGGTCTGGCTGGGTTACTTT
	Rev Primer	TAACTGGTTGGCAGGTACGT

Exosome extraction

Cells were differentiated into myotubes for 3 days in DMEM. The conditioned media were then harvested, centrifuged at 260 g for 10 min at room temperature, and then at 4000 g for 20 min at 4°C to remove any dead cells and cell debris. The subsequent supernatant was filtered through 0.22 um filter to remove microparticles. The filtered medium was then mixed with total exosome isolation reagent (Life technologies™; 2:1, v:v), incubated overnight at 4°C, and then centrifuged at 10,000 g at 4°C for 1 h. The supernatant was discarded and the pellet containing the exosomes was

resuspended in 100 µl PBS. The exosome suspensions were kept at -80°C until needed. Exosomal protein was extracted using 8M Urea and quantified using BCA kit.

NanoSight

Size and distribution of ALS and control exosomes (n=3 per group) were evaluated by a NanoSight LM10 instrument (NanoSight) equipped with NTA 2.0 analytic software.

Exosome labelling

The exosomes were labelled using PKH26 kit (Sigma-Aldrich®). Briefly, after adding 100 µl of Diluent C to the exosome suspension, 100 µl of 4 µM PKH26 solution were added to the sample. After 5 min of incubation, 1 ml PBS was added and the exosomes were washed using a 100K concentrators, 15,000 g at 4°C for 10 min. The exosomes were washed 3 times in PBS using the 100K concentrators before being mixed with the cell media for treatment.

Exosomes added to iPSC motor neurons

hiPSC-derived motor neurons were obtained as previously described (*44*). 6,000 MN progenitors differentiated for 9 days were then plated in poly-l-ornithine (SIGMA) Laminin (LifeTechnologies) coated 8 well plates in differentiation medium N2B27 (DMEM F12, Neurobasal v:v, supplemented with N2, B27, Pen-Strep, βMercaptoethanol 0,1%, Glutamax) supplemented with 100nM Rock Inhibitor (RI), 100nM Retinoic Acid (RA), 500nM SAG, 100nM DAPT, 10ng/mL BDNF and Laminin. The medium was replaced at 11 days of differentiation with N2B27 supplemented with 200nM RA, 1µM SAG, 20ng/mL BDNF and 200nM DAPT and again at 14 days of differentiation with N2B27 supplemented with 200nM RA, 20ng/mL GDNF, 20ng/mL BDNF and 200nM DAPT. 16 days differentiated motor neurons were either treated with ALS exosomes or healthy exosomes resuspended in N2B27 differentiation medium supplemented with 20ng/mL GDNF and 20ng/mL BDNF. Cultures were fixed

with 4% formaldehyde at 3 days of treatment. The MN were labelled for Tuj1, Islet ½ and analysed as described in the immuno-labelling section. MN loss was normalized to untreated MN cultures.

Exosomes added to healthy human muscle cells.

Labelled exosomes were added to the differentiation medium of 200,000 control cells cultured in Ibidi 35mm µ-Dishes. Exosome absorption occurred during the first 3 days of differentiation. The myotubes were then rinsed 3 times with PBS, and fresh DMEM was added to the petri-dishes. The cells were fixed with 3,6% formaldehyde for 15min at room temperature at day 3 or day 7 of differentiation, then washed 3 times in PBS and stored at 4C until subsequent analysis:

- *Exosome integration* - The exosome integration was checked by live imaging at 4h, 24h, 48h, 72h, 96h and 168h.
- *Myonuclear domain* - The myotubes were fixed and stained for DAPI and MF20 as described above.
    - The myonuclear domain was calculated using the following formula:

$$\text{Myonuclear domain} = \frac{(\Sigma\ \text{MF20 area})}{(\Sigma\ \text{nuclei in myotubes})}$$

- *Stress blebbing* - Blebs were counted on live images.
- *Cell death inducing an increase in H2Ax expression level* - The myotubes were fixed and stained for DAPI and H2AX as described above. To measure H2AX signal per myonucleus, the total area of H2AX signal was divided by the total number of myonuclei.
- *Cell loss* - The total number of nuclei were counted in each field using ImageJ 1.37v, and summed for each well.

RNA staining

ALS and healthy muscle cells were differentiated for 3 days before being fixed using 4% paraformaldehyde and permeabilized for 1 hour at RT (5% BSA; 20% FBS; 0,5% Triton X100; 0,5% Tween20). Cells were then stained with a 20 µg/mL acridine orange solution for 10 min at RT.

Muscle cell lines overexpressing wild type forms of FUS, SOD1 and TDP43.

Healthy human muscle cell lines were transduced with previously published plasmid coding either for a tagged form of wild type FUS (FUS-3xFLAG, (*34*)), or wild type SOD1 (SOD1-3xFLAG, modified WT-SOD1 plasmid from (*45*)) or TDP43 (TDP43-3xFLAG, modified WT-TDP43-YFP plasmid from (*46*)) and a selection was done with hygromycin. 50,000 Cont, FUS_{FLAG}, $TDP43_{FLAG}$ and $SOD1_{FLAG}$ muscle cells were plated in 8 well Ibidi® plates in proliferative medium. The next day, myogenic differentiation was induced by replacing the medium with DMEM, and cells were treated with 0.5µg of healthy and ALS exosomes. Exosomes were applied for 3 days, before fresh DMEM medium was applied to the cultures. At 6 days of differentiation, cells were fixed and analyzed for cell death and cell blebbing as described above.

Proteomic

- *Protein extraction from exosomes* - A volume of cell culture medium was mixed to 0.5 volumes of Total Exosome Isolation Reagent from cell culture media (lifeTechnologies®) and incubated overnight at 4°C. The samples were then centrifugated at 10,000 × g for 1 hr at 4°C. The exosome pellets were re-suspended in 25 µl 8M Urea, 50 mM ammonium bicarbonate, pH 8.5, and reduced with DTT for 1 h at 4˚C. Protein concentrations were then quantified

using Pierce BCA Protein Assay kit (ThermoFisher®). Exosomal proteins were kept at -80°C.

- *Proteome profile determined by Mass spectrometry* - Approximately 20 μg of exosome protein were trypsin digested using a SmartDigest column (Thermo) for 2 hours at 70oC and 1400 rpm. Peptides were then fractionated into 8 fractions using a high pH reverse phase spin column (Thermo). Fractioned peptides were vacuum dried, resuspended and analyzed by data-dependent mass spectrometry on a Q Exactive HF (Thermo) with the following parameters: Positive Polarity, m/z 400-2000 MS Resolution 70,000, AGC 3e6, 100ms IT, MS/MS Resolution 17,500, AGC 5e5, 50ms IT, Isolation width 3 m/z, and NCE 30, cycle count 15.
- *Database Search and Quantification* - Resulting mass spectral files were searched for protein identification using ProteomeDiscoverer (Thermo) against the Uniprot human database for semi tryptic peptides and filtered based on a false discovery rate of <1%. 718 proteins were detected in at least 1 sample

Knockdown of FUS with siRNA

100,000 cells were plated in μ-Slide 4 Well ibiTreat (Ibibi®) one day before differentiation was induced. On day 2 of differentiation, cells were transfected using Lipofectamine RNAiMAX Reagent with 200nM s5401 FUS siRNA (LifeTechnologies™) and treated with a low dose of PKH26-labelled ALS exosomes. Exosomes were integrated by the cells for 3 days before fresh differentiation medium was added to the 5 days differentiated cells. The cells were harvested at day 8 of differentiation to check for RNA levels by RT-qPCR and to perform cell death analysis,

immunostaining for RPL5, and distribution analysis of RNA/DNA using acridine orange staining.

Western Blotting

Extracted ALS and healthy exosomes were washed three times with PBS using 100K MWCO concentrator columns (LifeTechnologies™) and resuspended in lysis buffer (8M urea; 2% SDS; 10 µL/mL protease inhibitor cocktail). Extracted proteins were loaded into NuPage polyacrylamide 4-12% BisTris gels for electrophoresis under reducing conditions (Calnexin, Flotillin) and non-reducing conditions (CD63). Transfer on polyvinylidene difluoride (PVDF) membrane was performed using the iBlot® Dry Blotting System (Life Technologies™) and upon transfer polyacrylamide gels were stained with Blue Coomassie Gel Code Blue Stain Reagent (LifeTechnologies™) to visualize proteins. Immunoblotting was carried out using the iBind™ Flex Western System and primary antibodies (Calnexin, CD63, Flotillin and RPL5 see Table S3) with respective secondary antibodies (Goat anti Mouse HRP, Donkey anti Goat HRP, Goat anti Rabbit HRP). The signal was detected using the Amersham ECL™ Prime Western blotting Detection Reagent and the UVP ChemiDoc-It^2 Imager.

Statistics

All values are presented as means ± SEM. Student's T-Test was used to compare differences between ALS and control samples for all the protein quantifications, electron microscopy quantifications, exosome integration, immunostaining (FUS, Acridine Orange, RPL5, Caprin1), FUS expression level, exosome-treated MN and myotube death, myotube atrophy. A Kolmogorov-Smirnov test was used to compare the distribution of number of vesicles per MVBs in ALS and healthy myotubes, the distribution of neurites branching in ALS and healthy exosomes-treated MN, the

distribution of H2AX expression levels in myonuclei treated with different doses of exosomes, and the distribution of myotube nuclear numbers in control myotubes treated with ALS and control exosomes. One-way ANOVA followed by a Dunnet's multiple comparison test was used to evaluate the differences in the in silico secretome, in the immunostaining for exosomal markers, RT-qPCR, neurites length, and MN treatments. Two-way ANOVA was used to evaluate changes in bleb counts, and cell death in different cells lines (Cont, FUS_{FLAG}, $SOD1_{FLAG}$, $TDP43_{FLAG}$). Differences were considered to be statistically different at $P < 0.05$.

Discussion

Knowing that neuromuscular junction disassembly is a key step in the pathology[341,342], we investigated the role of muscle and reported that the skeletal muscle of ALS patients secretes exosomal vesicles that are specifically toxic to motor neurons. The increased secretion of exosomes by ALS muscle cells might be related to an increased calcium concentration in ALS muscle[397], calcium known to stimulate the exosome secretion in cells[398].

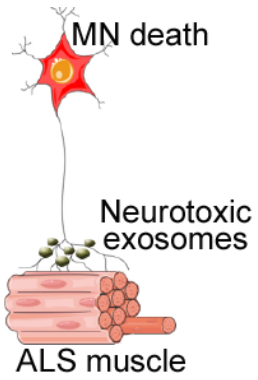

Figure 15 : ALS muscle cells secrete neurotoxic exosomes.
These vesicles disrupt the RNA-processing in MN. Potential role of muscle exosomes in body-wide propagation of disease.

Do muscle exosomes contribute to the proteinopathy observed in ALS?

Numerous proteins pathways dysregulation have been reported such as proteins aggregation in the cytoplasm of the cells, misfolded proteins, proteasome activity defects and autophagy failure[85,86] and correspond to key pathogenesis pathways in ALS patients.

Exosomes have already been suggested in other neurological diseases to propagate neurotoxic elements such as β-amyeloide peptides or synuclein in Alzheimers's and Parkinson's diseases[317,366], respectively. Similarly, ALS associated proteins such as SOD1, FUS, TDP43 are observed in circulating extracellular vesicles from ALS serum[399] and CSF samples[400]. These vesicles could thus participate to the propagation of protein aggregates – aggregates that are a common feature among ALS patients[43,53,63,99,102,103] – and contribute to motor neuron death.

Muscle atrophy has been generally linked with dysregulated proteasome activity[401] and several studies have demonstrated that exosomes contain components of the proteolytic machinery[363,402]. In ALS patients, a protein homeostasis dysregulation has been studied in many ALS associated mutations and sporadic cases[70,84,85,88,89,403], and muscles exosomes could deliver proteasome components to nearby muscle cells and contribute to this abnormal proteolytic activity. Concordantly, in our study ALS exosomes induced myotube atrophy once added to the culture medium of healthy myotubes (See Figure supplemental 4A).

How exosomes contribute to RNA processing disruption?

Following the identification of mutations in two RNA binding protein in ALS patients, FUS and TDP43, RNA metabolism has been vastly studied. Among the RNA processing pathways that are altered in ALS is transcription defects, splicing dysregulation and nucleoplasmic transport impairment[22,46,78,81,404]. RNA accumulation in the nuclei has already been demonstrated in SOD1 mutant and C9orf72 mutation associated ALS patients[405,406]. Interestingly, when ALS muscle exosomes are added to the culture medium of motor neurons, they contribute to an increase level of RNA accumulation in MN nuclei (Figure 16).

ALS exosomes contain FUS and binding partners (see Figure 4E and Figure supplemental 5C and 6). An increase in wild type FUS expression level is sufficient to induce ALS pathogenesis in motor neuron[407]. Moreover FUS contribute to DNA damage response[408,409], as a knock down of FUS is responsible for an increase in DNA damage levels. FUS is also suggested to be involved in the formation of D-loops, essential for homologous recombination and DNA damage response[410]. Interestingly, the treatment of healthy muscle cells with ALS exosomes have a high level of H2AX (see Figure supplemental 4C & 4E). Altogether these results suggests that the treatment with ALS exosomes might influence the DNA damage response, contributing to the dysregulation of RNA processing and transport observed in ALS patients.

It is noteworthy that ALS exosome treatment allows the reproduction of ALS pathogenesis observed in patients and might represent a good ALS model. Importantly this PhD study was based on sporadic ALS patients samples (with known and unknown gene mutations) suggesting a common toxic pathway in ALS muscle stem cells.

How can exosomes participate to the propagation of disease?

Knowing that the pathology starts in one member before spreading to the other non-affected limb, and then ultimately into the entire body, one can hypothesize that exosomes toxicity could be spread towards healthy part of the body through the bloodstream (Figure 16). Indeed, muscle exosomes have been isolated from blood samples[411] (and results in the team) (Figure 16, 7-). Moreover several studies have already demonstrated the ability of exosomes to cross the blood-brain-barrier[267,412] suggesting that once in the bloodstream, ALS muscle exosomes can easily target non-affected UMN and by extend LMN or muscle fibers contributing to the relentless and fast progression of symptoms in ALS patients. Furthermore, muscle exosomes could possibly exploit viral routes to target the CNS (Figure 16, 5-). The NMJ is a highly specialized synapse between nerve and muscles, and most motor neurons synapsing with muscle have their soma in the spinal cord where a synaptic contact with a motor neuron that have their cell body in the cortex[413]. It is not surprising that viruses and bacteria take advantage of the NMJ as a gateway to spread in the CNS. The Rabies virus (RABV) is a neurotrophic virus that induce a fatal and acute myeloencephalitis in human following infection[413]. The RABV transport depends on long distance axonal spread between synaptically connected neurons using retrograde transport machinery as well as endosomal trafficking pathway[414,415]. This infection mechanism allows the spreading of the infection from post-synaptic to pre-synaptic motor neuron until reaching the CNS. Similarly it has been demonstrated that the canine adenovirus type 2 once injected in the muscles is transduced in motor neurons in the same manner[416]. Hence, muscles exosomes once secreted in the extracellular milieu could spread from LMN to UMN by retrograde

transport along axons, and the same way could be further transported to non-affected limb muscles through an anterograde transport manner.

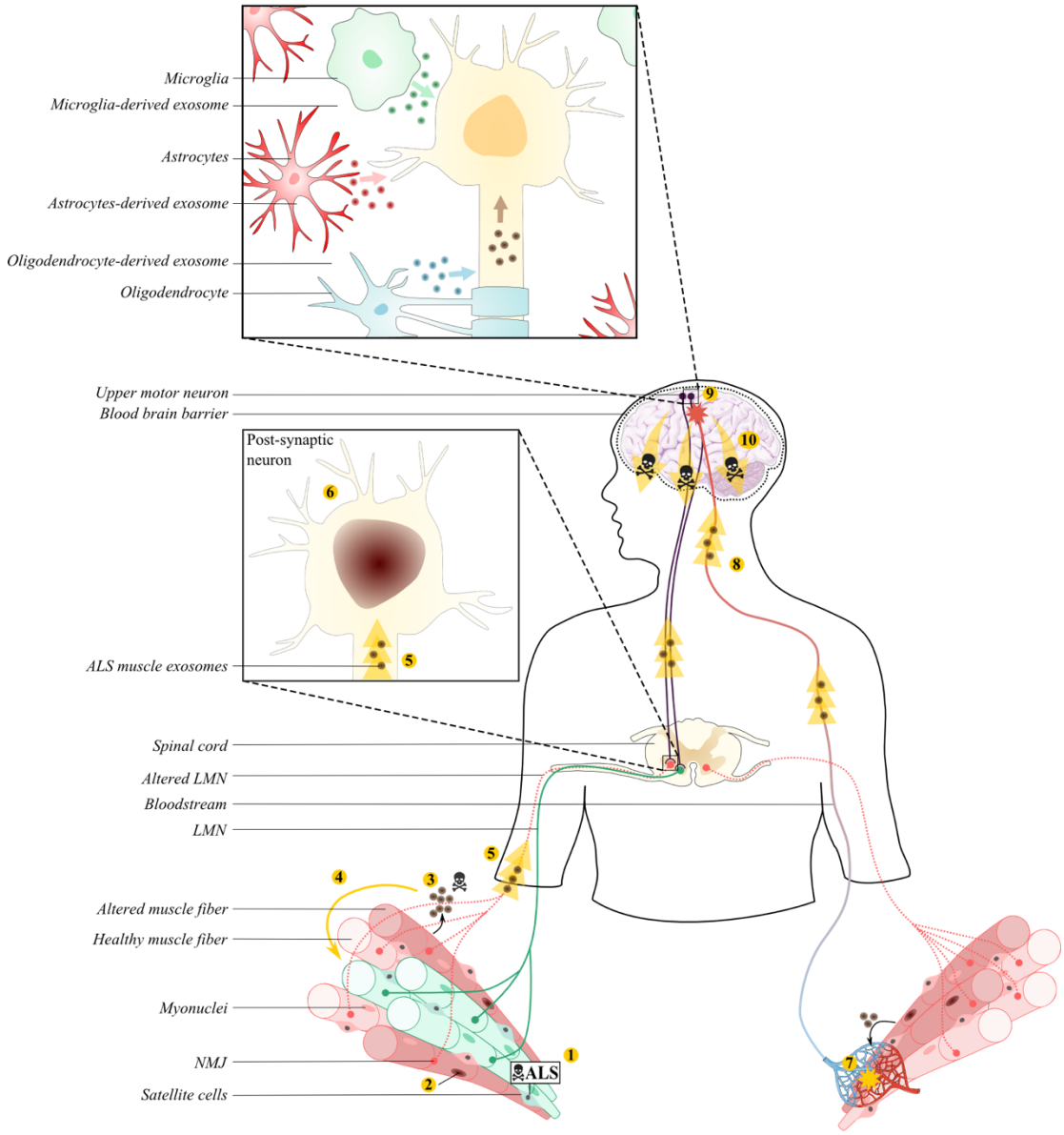

Figure 16 : Graphical abstract. Speculation on how muscle exosomes can have a role in the propagation of the disease.

This project demonstrated that 1) ALS muscle stem cells share a specific ALS signature that is independent from any innervation/denervation process. 2) Multiple RNA processing dysregulation have been observed in ALS muscle cells such as nuclear accumulation of RNA, high FUS nuclear granulation, and aggregation of FUS partner, RPL5 in myonuclei. Here illustrated as brown nuclei from altered muscle fiber in dark red colour. 3) We showed a toxic secretion of exosomes by muscle cells of ALS patients that are toxic and induce cell death in 4) muscle cells and 5) motor neurons. 5) ALS muscle exosomes are toxic towards MN and could potentially be retrogradely transported towards to cell body of the affected MN (here in red dashed line versus green full line for healthy non-altered MN) and 6) induce an accumulation of RNA in MN nuclei. On the other hand, exosomes have been isolated from blood samples meaning they can 7) have access to the bloodstream and 8) pass the brain-blood-barrier. 9) Exosomes from motor neuron neighbouring cells such as astrocytes, microglia and oligodendrocytes also secrete exosomes that

participate in the toxic motor neuron environment. 10) Once the upper motor neurons are altered by ALS muscle cells, toxicity could easily be spread to non-affected motor neurons and/or muscle cells and contribute to the progression of ALS pathology.

Conclusion

For many years now the muscle involvement in ALS has been controversial and several studies have suggested contradictory effects of muscles. This project based on human primary muscle cells from sporadic ALS, healthy subjects and control diseases has demonstrated for the first time the significant role of muscle stem cells in exosomes in ALS pathology. During this study, we analysed bulk isolations of muscle exosomes from ALS patients, however multiples exosomes subpopulations are secreted at the same time by the same cell[178,224,225,227–230]. Using immunoaffinity-based isolation technique we could determine if the entire population of ALS muscle exosomes or a specific sub-population is toxic and would allow future studies to specifically target the muscle-induced toxicity.

Publications

Journal of Neuromuscular Diseases 2 (2015) 205–217
DOI 10.3233/JND-150097
IOS Press

Review

Changes in Communication between Muscle Stem Cells and their Environment with Aging

Matthew Thorley[a,b,c,d,1], Apostolos Malatras[a,b,c,d,1], William Duddy[a,b,c,d,1], Laura Le Gall[a,b,c,d], Vincent Mouly[a,b,c,d], Gillian Butler Browne[a,c,b,c,d] and Stéphanie Duguez[a,b,c,d,*]
[a]*Sorbonne Universités, UPMC Univ Paris 06, Center of Research in Myology UMRS 974, F-75013, Paris, France*
[b]*INSERM UMRS 974, F-75013, Paris, France*
[c]*CNRS FRE 3617, F-75013, Paris, France*
[d]*Institut de Myologie, F-75013, Paris, France*

Abstract. Aging is associated with both muscle weakness and a loss of muscle mass, contributing towards overall frailty in the elderly. Aging skeletal muscle is also characterised by a decreasing efficiency in repair and regeneration, together with a decline in the number of adult stem cells. Commensurate with this are general changes in whole body endocrine signalling, in local muscle secretory environment, as well as in intrinsic properties of the stem cells themselves. The present review discusses the various mechanisms that may be implicated in these age-associated changes, focusing on aspects of cell-cell communication and long-distance signalling factors, such as levels of circulating growth hormone, IL-6, IGF1, sex hormones, and inflammatory cytokines. Changes in the local environment are also discussed, implicating IL-6, IL-4, FGF-2, as well as other myokines, and processes that lead to thickening of the extra-cellular matrix. These factors, involved primarily in communication, can also modulate the intrinsic properties of muscle stem cells, including reduced DNA accessibility and repression of specific genes by methylation. Finally we discuss the decrease in the stem cell pool, particularly the failure of elderly myoblasts to re-quiesce after activation, and the consequences of all these changes on general muscle homeostasis.

Keywords: Aging, adult stem cells, muscles, skeletal, myoblasts, intercellular signaling peptides and proteins, homeostasis

INTRODUCTION

Over the last 60 years, work performed on animal models, chiefly mouse, rat, and avian, and on human samples, has revealed and explored the capacity of adult stem cells - also called somatic stem cells – to self-renew and to differentiate into unipotent progeny within their residing tissue [1], generally for the purpose of repair. Resident stem cell populations have now been described in most tissues, including bone marrow [2], blood vessels [3], peripheral blood [4], skin [5], teeth [6], gut [7], liver [8], heart [9], brain [10] and skeletal muscle [11]. Once body growth has stopped and adulthood is reached, most of these stem cells become quiescent, and will only be activated for tissue turnover. Although this turnover can be very active as in circulating blood or gut epithelium in other tissues such as liver the stem cells usually remain unsolicited as hepatic damage rarely occurs in healthy adults [8]. Despite this heterogeneity, a decline in number and properties is universally observed in aged stem cells, a phenomenon which alters the maintenance of tissue homeostasis with aging. In aged skeletal muscle, a tissue with low turnover, this decline in the adult stem

[1]Co first author.

[*]Correspondence to: Stéphanie Duguez. Tel.: +33 1 42 16 57 19; Fax: +33 1 42 16 57 00; E-mail: stephanie.duguez@upmc.fr.

ISSN 2214-3599/15/$35.00

cell (also called satellite cell), which is responsible for muscle repair [12], is associated with muscle atrophy and muscle weakness [13–15], although their depletion in the mouse has differential effects depending on the muscle [12].

Muscle stem cells or satellite cells are localized beneath the basal lamina, peripheral to the muscle fibers [11], and express Pax7 [16] and Notch3 [17]. After muscle injury, satellite cells are driven out of their quiescent state, and start to proliferate. Most of the activated satellite cells rapidly co-express MyoD or Myf5 [16, 18]. The proliferating satellite cells - also called myogenic precursor cells or myoblasts - expand under the control of Notch3 [17] and Notch1/Hey1 pathways [19, 20]. They divide asymmetrically, with self-renewal of the stem cell pool being maintained by a minor population of myogenic precursor cells that down-regulate their expression of MyoD and Myf5 and return to a quiescent state [18, 21–23]. This asymmetrical division involves Numb, an antagonist of the Notch signalling pathway [19, 24]. Numb is asymmetrically localized during myoblast mitosis and it is the cell that has a high level of Numb that goes back to quiescence for self-renewal [19, 24–26]. After several rounds of proliferation, activated myoblasts decrease their expression levels of Pax7, Myf5 [16, 18] and Notch3 [17]. The Notch1 pathway is then repressed by Stra13 [20] through the CBF1 pathway [20, 27]. Simultaneously, the Wnt pathway is activated and promotes myoblast differentiation through β-catenin [28]. Myoblasts exit the cell cycle by expressing p57 [29], and then cyclin inhibitors - p21 and hypophosphorylated pRb [30–32] - together with higher levels MyoD followed by myogenin, a driver which triggers the expression of the differentiation genes [33, 34]. The myoblasts consequently undergo differentiation into myocytes, and fuse either with each other or with existing multi-nucleated myofibers in order to repair injured muscle [35, 36]. The differentiation and maturation process is regulated by MEF2, MEF3, and Mrf4 pathways [37–39], while other factors, such as Myomaker, are involved in fusion [40]. Muscle precursor cell proliferation, fusion and differentiation are tightly orchestrated by circulating hormones (*e.g.* growth hormone [41], testosterone [42, 43] and thyroid hormones [44, 45]), growth factors (*e.g.* IGF system [41], FGF system [46–48], TGF-b [49, 50]), G-CSF [51], chemokines (*e.g.* interleukines [52–55], MPC [55, 56]) and other secreted components (*e.g.* vesicles [57, 58]) present in the muscle stem cell environment.

Aged human [59] or murine [60–62] muscle can regenerate and repair, although the rate of regeneration declines [60–62]. This slower regeneration can be explained by: (1) changes in the muscle stem cell environment (growth factors, growth hormones, inflammation, and extracellular matrix content); (2) a lowered responsiveness of progenitor cells to repair stimuli; and (3) decrease in the number of muscle stem cells with aging. Each of these factors may impact on muscle homeostasis and each may both participate to, and be affected by, age-associated changes in intercellular communication. The subsequent sections will describe the different roles that intercellular communication may play in muscle aging, from hormonal and other circulating endocrine factors to local paracrine and autocrine secretory environment of the stem cell niche that may also modify the intrinsic properties of the stem cells themselves.

HORMONAL AND OTHER CIRCULATING FACTORS: CHANGE IN ENDOCRINE COMMUNICATION WITH AGING

The decline in muscle regenerative capacity with age [63] has been partly attributed to a decline in extrinsic environmental cues (see Fig. 1). Levels of circulating hormones, such as testosterone or IL-6 or growth hormone (GH) or IGF-1, are low in serum samples of aged subjects [64–66].

The endocrine hypothalamic-pituitary axis is altered with aging, leading to changes in hormone secretion that can contribute to cognitive decline or depression. Epidemiological studies have also shown a correlation between the decrease in growth hormone (GH) secretion and sarcopenia as well as other signatures of aging (e.g. intra-abdominal adiposity, osteopenia, etc.) [67]. GH is a stress hormone produced by the hypothalamus. It plays a key role in muscle mass maintenance through life [66]. It acts on myoblasts through its receptor GHR and activates NFATc2 that in turn stimulates the expression and secretion of IL-4 [41, 68, 69] - IL-4 being critical for myoblast fusion [68, 69]. GH also stimulates IGF-1 secretion by both liver and muscle [66]. IGF-1 and its splice variants - IGF-1Ea and IGF-1Eb - modulate myoblast proliferation [70] and differentiation [71] through MAPK and ERK1/2 signalling [70]. The latter regulates myogenesis, for example by interacting with p38αβ MAPK and the asymmetric division and self-renewal of satellite cells [72].

These age-associated changes in the endocrine hypothalamic-pituitary axis can have further effects on the gonadotropic axis. Sex-steroid privation associated with age participates to, among other phenomena,

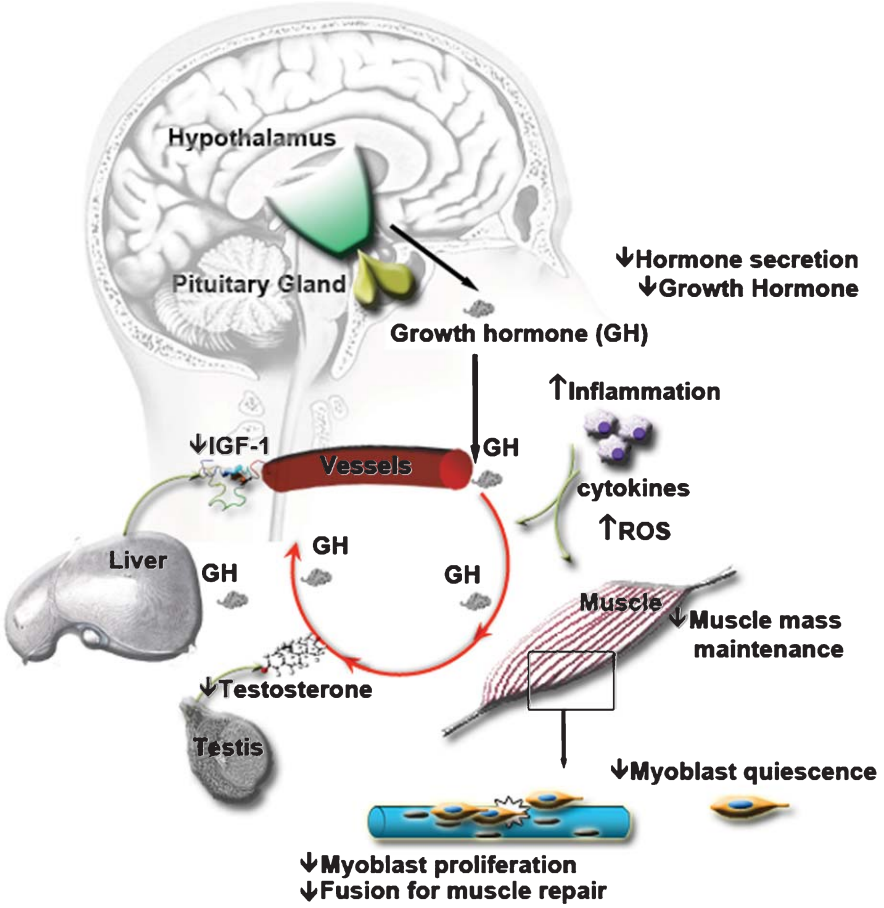

Fig. 1. Age alters serum composition and thereby affects intercellular communication at distance. The endocrine hypothalamic-pituitary axis is altered with aging, affecting the composition of circulating hormones in the serum. For instance, the secretion of growth hormone is decreased, leading to loss of muscle mass. In addition, the lower level of growth hormone will also stimulate less the secretion of IGF-1 - IGF-1 being involved in muscle mass maintenance and in the satellite cell myogenic program. The endocrine hypothalamic-gonadotropic axis is also affected, leading to a decrease of sex steroids such as Testosterone, another hormone involved in muscle mass maintenance. Similarly, a decrease in oestrogen can act on the myogenic program through IGF-1 signaling. The decrease in circulating hormones affects the capacity of the satellite cells to respond to muscle damage. Aging is also associated with an increase in inflammation. The cytokines secretion by aged inflammatory cells as well as their ROS production is modified and can also affect the capacity of the satellite cells to respond to muscle damage. The modification of the entire serum composition with aging has negative effects on muscle mass and on muscle regeneration capacity.

loss of muscle mass [67]. The sex-steroid testosterone, secreted by the testis, has been extensively studied in muscle, and can be considered as a double-sided blade, acting both on myoblast proliferation and differentiation. It acts on myoblasts through the androgen receptor localized in the nucleus [73] or through G protein-coupled receptors [74]. It promotes myoblast proliferation through protein kinase C (PKC) signaling [74] - for instance through nPKCδ and extracellular signal-regulated kinases 1 and 2 (ERK1/2) activation [75]. Once ERK1/2 is phosphorylated, it is accompanied by an increase in cyclin E and Cdk2 – which are involved in myoblast proliferation [76]. Testosterone acts also on myoblast differentiation via protein kinase A (PKA) signaling [74] - PKA being required for myoblast fusion [77, 78]. Interestingly, oestrogens act similarly on the myogenic program through IGF-1 signaling [79].

Aging is associated with an increase in low grade chronic and systemic inflammation, also called inflammaging [80]. Inflammaging could be due to microbial infection, cell debris, over-activated coagulation system, or an increase in cellular senescence with the associated changes in secretion [80]. This increased inflammation is generally attributed to a modified immune partner. Indeed, while young macrophages

have been shown to have a beneficial effect to clear muscle debris after injury and stimulate myogenesis [81–83], aged macrophages can release a higher level of osteopontin that inhibits the muscle regeneration process [84]. Not only macrophages are involved in the muscle regeneration process, but also neutrophils, lymphocytes, dendritic cells, etc. These inflammatory cells secrete numerous chemokines and cytokines, but little is known about the impact of aging on cytokine secretion [85]. In the literature, it is described that IL-6 serum level is decreasing during aging [65]. IL-6 originates from the inflammatory cells, but also from the skeletal muscle itself [86]. It has been shown to be an important regulator of muscle stem cells [53], as it activates janus kinase 2 (Jak2) that will in turn phosphorylate STAT3 [52]. Once STAT3 is phosphorylated, it homodimerizes and translocates to the nucleus to bind to the γ-interferon activation sequence [87] in the promoter regions of genes involved in myoblast proliferation such as c-myc [52]. IL-6 not only regulates myoblast proliferation, but also promotes myoblast differentiation through the p38 MAPK pathway [88]. A decrease in IL-6 serum level could thus impact muscle regeneration efficacy.

The tissues from which circulating factors originate, such as muscle, hypothalamus, gonads, and liver, become atrophic and less active with age [8, 66, 89]. This change in body composition and activity with aging can thus participate to the decrease in circulating hormones (see Fig. 1). Consequently, when muscle damage occurs in an aged person, satellite cells be less prone to activation and differentiation, leading to a less efficient repair. Ten years ago, Conboy et al. elegantly showed that muscle regeneration could be partly rescued in aged mice exposed to serum from young mice through a parabiosis system [90]. Similarly, hormones released during pregnancy rescued the muscle regenerative capacity of aged female mice [91]. When aged subjects are trained, a rejuvenating effect is observed on muscle. This benefit effect could probably be due to a decrease of the inflammation for instance, as observed in exercised patients affected by myositis [92, 93]. When aged muscle stem cells were engrafted into young mice [94], their capacities to proliferate and differentiate were partly restored. Together these data suggest that circulating agents, which can originate from different tissues, impinge on muscle regeneration efficiency. Aging affects both the size and function of each tissue and consequently tissue secretory capacity. This alters the composition of circulating serum effecting intercellular communication at distance.

SECRETORY ENVIRONMENT OF THE STEM CELL NICHE: CHANGE IN PARACRINE AND AUTOCRINE CELL-CELL COMMUNICATION WITH AGING

In addition to its classical role as a locomotive system, skeletal muscle has recently been shown to have a secretory activity. For instance, IL-6 [86] and musculin [95] have been identified to originate from and be secreted by skeletal muscle *in vivo*. *In vitro*, the secretome profile of C2C12 myotubes [55, 56], human myotubes [57] and rat muscle explants [96] suggest that muscle cells secrete numerous growth factors (*e.g.* follistatin like protein 1, IGF-2, TGF, etc) and cytokines. Secreted proteins - also named myokines [95] - may act in an autocrine/paracrine manner on neighboring muscle cells and contribute to muscle growth and regeneration. This local muscle secretome can be altered with aging. For instance, Chakkalakal et al. have shown that an increased secretion of FGF-2 by aged myofibers in mice inhibits sprouty1 expression in satellite cells, and consequently reduces their capacity to go back to quiescence and replenish the pool of the muscle stem cell [47]. The muscle secretome includes not only hormones, but also extracellular matrix components (ECM, *e.g.* TIMP2, fibronectin), miRNAs, and vesicles (exosomes and microvesicles) [57, 58, 97, 98]. Interestingly, exosomes originating from differentiated myocytes stimulate the myogenic program of proliferating myoblasts [58]. Myocyte exosomes contain miRNAs that inhibit Sirtuin expression, and thus stimulate the myoblast differentiation into myotubes [98]. A decrease in muscle mass with aging may thus reduce muscle secretory output. In a transcriptomic analysis performed on quadriceps muscle from young (15–24 years old) and elderly (72–80 years old) subjects, we indeed observed down-regulation of secretome markers in aged muscle [99]. However, little is known about the changes in the composition of the muscle secretome of aged muscle and further investigation is needed.

The local niche of muscle stem cells includes growth factors and cytokines secreted not only by the myofibers themselves, but also potentially by other cell types present within muscle, such as fibroblasts, endothelial or peri-endothelial cells [100, 101]. This local secretome can also be altered with aging (Fig. 2). For instance, fibroblasts present in aged skeletal muscle express a high level of TGF-β [101] – a growth factor that inhibits differentiation of myoblasts [102], and thus slows down the regeneration process. In addition, aging is described to be associated with an increase

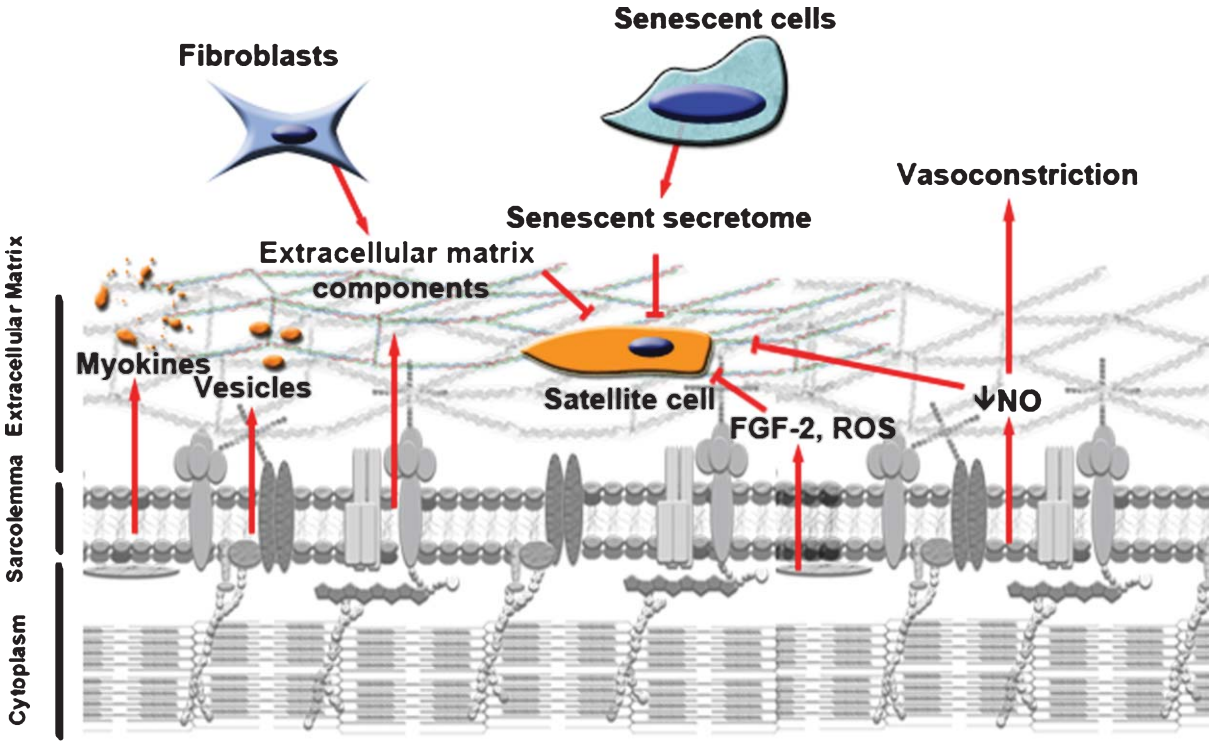

Fig. 2. Aging changes the microenvironment of the satellite cell. Decreased muscle mass can be accompanied by a decrease in myokines and vesicles secreted into the microenvironment of the satellite cells. Aged myofibers produce more ROS and FGF-2, factors that can change epigenetic marking of the satellite cells and shut down their myogenic program and their capacity to re-quiesce. They also release less NO into their environment, stimulating vasoconstriction which may inhibit serum tissue perfusion. Aged fibroblasts present in the muscle can secrete more fibrous proteins, thickening the ECM. In turn, this decreases the diffusion of growth factors toward the satellite cells and thus their responsiveness to muscle repair cues. Increase in senescent cells with age can secrete factors that inhibit tissue regeneration. The microenvironment of the satellite cells is thus altered and affects their capacity to respond to any muscle damage.

in senescent or pre-senescent cells in muscle and other tissue [103, 104]. During the last decade, the secretome of senescent cells from different tissues has been investigated and has been described to have an impact on the inflammatory response (by stimulating it in chronic obstructive pulmonary disease [105]) and to be instrumental in poor tissue regeneration (as observed in aged skin [106]). Altogether, these data suggest that the presence of senescent cells distinct from satellite cells within muscle tissue could alter these microenvironment of the satellite cells, and thus their behavior.

Muscle perfusion is decreased with aging [107], which may render myofibers and satellite cells less accessible to circulating hormones. This loss of perfusion may be maintained by the muscle loss itself. Indeed, sarcopenic muscle presents a disruption of the dystroglycan complex [108], leading to NOS-1 mislocalization, due to the link of NOS-1 to the dystrophin protein [109]. The mis-localization of NOS-1 results in decreased NO production, thereby diminishing muscle perfusion [110]. A second effect of decreased NO production is a reduction in satellite cell activation [111].

Aged skeletal muscle presents a thickening of the ECM and a general increase in fibrosis [112]. Even if muscle fibers can secrete collagens and other components of the ECM [57, 97], little is known about their role in ECM thickening. A recent study shows that fibroblasts present in aged rat muscles express a higher level of collagen IVa2 and laminin 2 – which may participate in the thickening of the ECM [101]. This increase in the ECM thickness can interfere with the muscle regeneration process by modifying myoblast activation, proliferation and migration [48, 113]. Finally, a thickened ECM may act as a partial barrier, reducing the accessibility of the satellite cells to circulating growth factors, as observed for smooth muscle cells [114], and thus impair satellite cell activation and differentiation during muscle repair.

Together, these data suggest that the changes in the secretory composition of the muscle stem cell's local niche with aging can slow down the regeneration process and decrease the replenishment of the pool of reserve cells. Repetitive iterations of this could contribute to the loss of muscle stem cells with aging.

CHANGE IN THE INTRINSIC PROPERTIES OF STEM CELLS WITH AGING

Exposure to a young environment by engraftment into young subjects or by parabiosis experiments only partly rescues the properties of aged satellite cells [90]. For instance their capacity to replenish the pool of reserve cells is not rescued (our unpublished data and [115]). These data suggest that some intrinsic properties of satellite cells are altered with aging and are not easily manipulated by external cues.

Intrinsic properties rely at least partly on DNA methylation, which may regulate gene expression in two ways [116]: (1) the accessibility of methylated enhancer regions to transcription factors is reduced, resulting in gene expression repression; (2) methyl-CpG-binding proteins bind to methylated DNA and alter the activity of histone deacetylases and methyltransferases. Consequently, local histones are hypermethylated, stabilizing the nucleosomes, so that DNA in methylated regions is tightly packed preventing binding of transcription factors or RNA polymerases. A recent study shows that histone methylation patterns are different between aged and young satellite cells in mice [117], and that the methylation profile can be modified by the presence of local growth factors such as FGF-2 [118]. The authors associated this histone methylation profile to a slower capacity of aged satellite cells to re-enter the cell cycle for aged satellite cells [117]. Interestingly, this study [117], as well as our own observations on culture of aged human muscle stem cells, show that once activated, aged satellite cells have a similar myogenic potential to young satellite cells. This indicates that muscle stem cells do not lose their differentiation potency with age, suggesting that the decrease with aging in the differentiation program during muscle regeneration is strongly related to changes in circulating factors.

DNA methylation has been shown to be increased in several tissues with aging, and the skeletal muscle is no exception [119, 120]. We have observed a higher level of DNA methylation in satellite cells of aged subjects (unpublished data). This hypermethylation could impact on the satellite cell fate and interfere with their capacity for self-renewal as observed in previously published studies (our data and [47, 115]). How DNA methylation is regulated with aging is not well known. Repeated stress over time can be one of the parameters implicated [121], involving for instance reactive oxygen species (ROS) [122]. Increased ROS production with age can be due to an increase in inflammation with aging [80] or to mitochondrial dysfunction in aged muscle [123, 124]. A decrease of circulating GH is also associated with a higher level of ROS and a lower level of anti-oxidants [125]. This overproduction of ROS could participate to increased DNA damage observed with aging [126]. Consequently, DNA methyltransferases (DNMT) are recruited to the DNA damage site, potentially inducing DNA silencing of the region nearby [127]. When we re-analyzed the transcriptome data available online (GSE9103), we indeed confirm a significant enrichment in the cellular response to oxidative stress in aged muscles (Fig. 3), suggesting a higher stress in aged muscle. ROS diffuse easily through membranes of fibers, thus potentially affecting DNA damage in neighboring satellite cells, and modifying their methylation status.

Factors discussed above - changes in the composition of circulating hormones in serum, as well as in the microenvironment - could also modify the epigenetic status of satellite cells and thus their behavior during regeneration, slowing satellite cell activation and decreasing their capacity to go back to quiescence

THE LOSS OF MUSCLE STEM CELLS WITH AGING AND ITS CONSEQUENCES ON MUSCLE HOMEOSTASIS

The number of muscle stem cells declines with age in mouse [13, 47, 90, 94] and humans [128, 129]. Although this loss can be caused by an increase in cell death, cellular senescence, or a deficiency in re-quiescence, apoptosis is rarely observed in aged murine and human muscle stem cells [94, 130, 131], suggesting that this cannot by itself explain the loss of muscle stem cells with aging. However, we cannot exclude the fact that apoptosis is a short punctual event that may be missed experimentally. Cellular senescence - also called replicative senescence - is defined as a phenomenon by which normal diploid cells cease to divide. It can be induced by telomere shortening that occurs during cell proliferation, and has been proposed to contribute to the loss of satellite cell function with aging [103]. However, shortened telomere length has not been reported in aged human satellite cells.

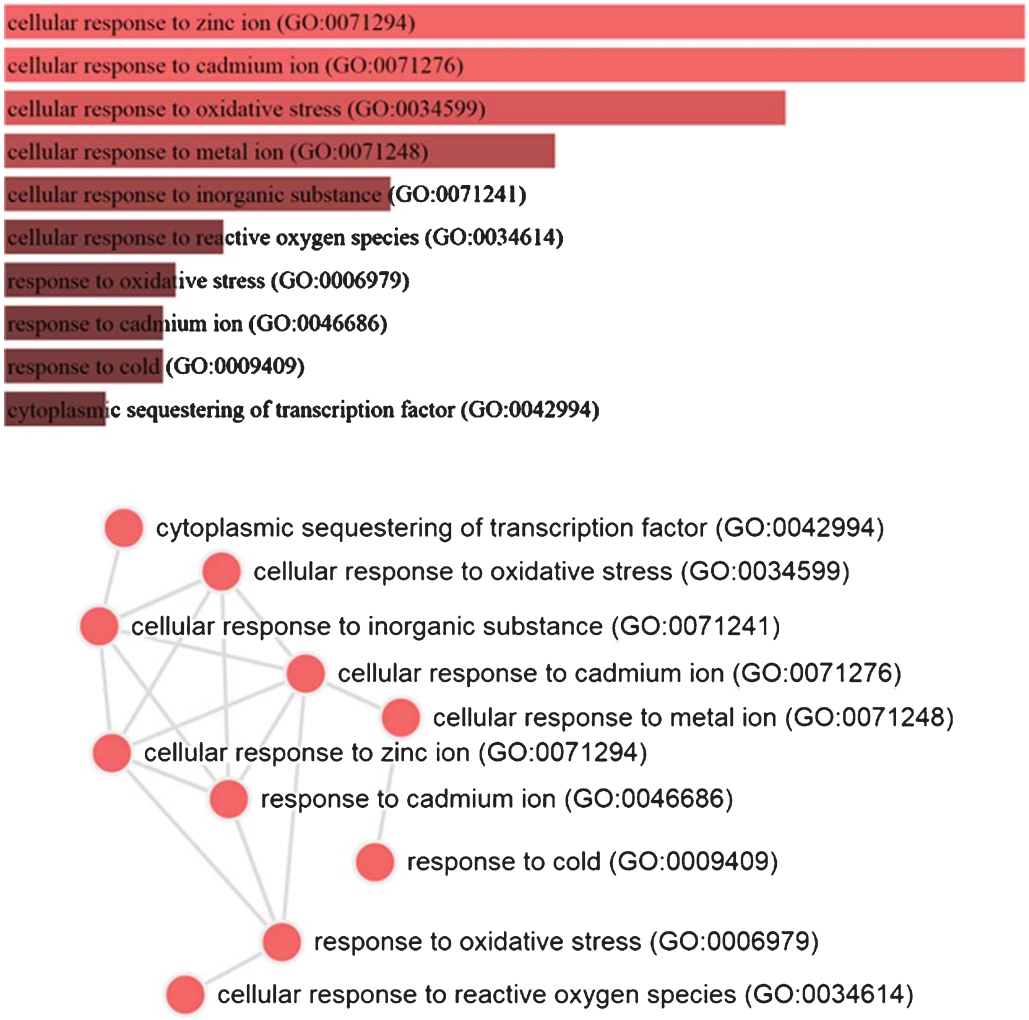

Fig. 3. Increase of oxidative stress response in aged muscles. For this analysis we retrieved the gene expression matrix of old and young muscles of sedentary subjects (series GSE9103 from the Gene Expression Omnibus [139]). We discarded three samples as they did not pass the quality control threshold. To identify differentially expressed genes we used the characteristic direction method [140] followed by gene set enrichment with Enrichr [141]. The top figure depicts a bar graph from the top 10 up-regulated GO Biological Processes (combined score: *p*-value multiplied by z-score) and the bottom figure a network of the same Processes, where each node represents the enriched term and the edges represent the gene content similarity between the nodes.

Furthermore, there may be insufficient activation and turnover of satellite cells to allow senescence to be a major contributor to stem cell decline. Satellite cells are rarely activated in healthy adult human or mouse, and once muscle growth is complete in young human adults [14], subsequent myonuclear turnover is slow, being estimated at 15 years during adulthood [132]. In mouse models, myofiber growth by the addition of new nuclei through satellite cell fusion is completed by 21 days postnatally [133], and there is little evidence to suggest significant turnover. As discussed earlier, the capacity to re-quiesce through the sprouty1 pathway is decreased in aged stem cells [47, 117]. Consequently, when satellite cells are activated for muscle repair in elderly subjects, they do not replenish the pool of reserve cells. This failure of re-quiescence is a likely contributor to stem cell population decline.

The decrease in the number of satellite cells with aging can affect muscle homeostasis by altering the ECM composition. Indeed, aged muscle depleted in satellite cells in a $Pax7^{CreER}$-DTA murine model shows an increase in fibrotic deposition [134], while fiber size was unaffected [135]. Resulting thickening of the ECM may increase myofiber fragility, and reduce the response of satellite cells to muscle damage, as discussed earlier. Therefore a loss of satellite cells could

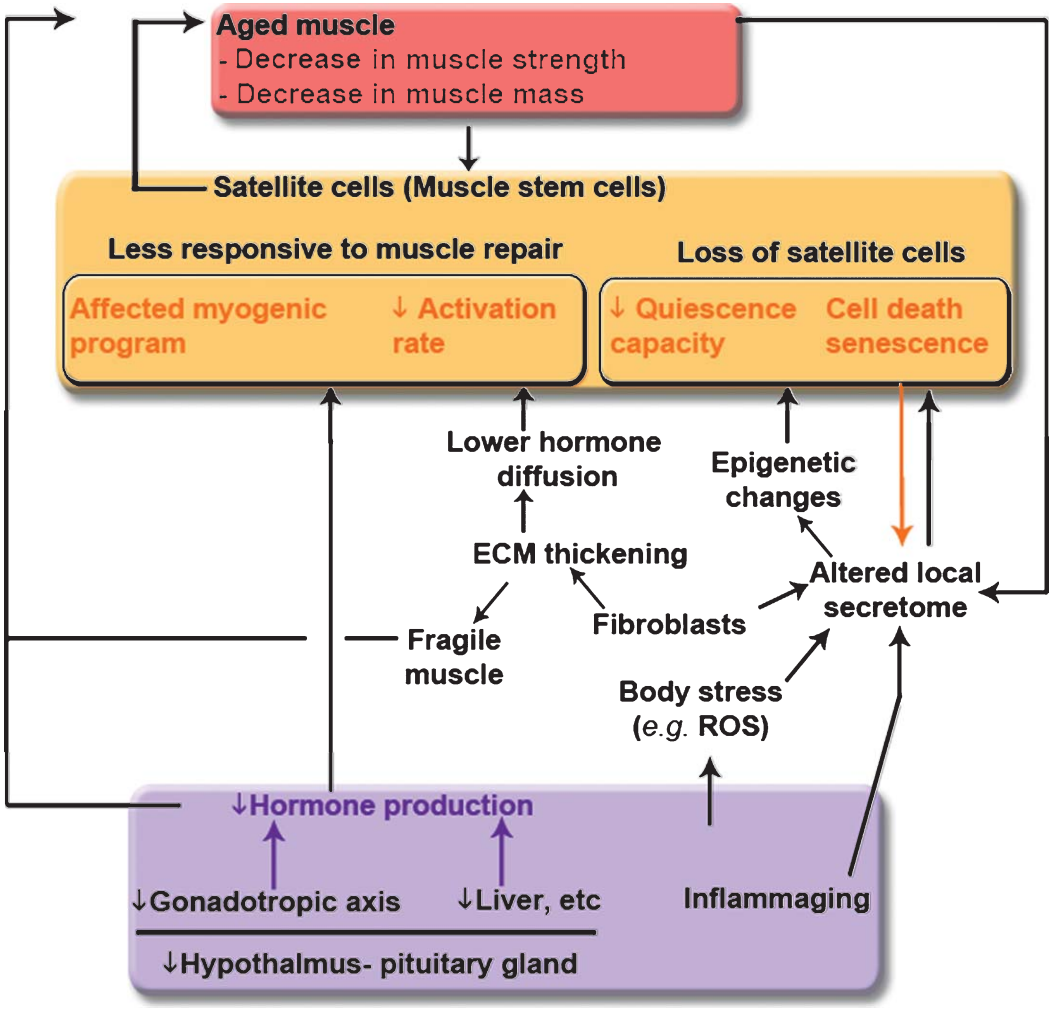

Fig. 4. Links between whole-body composition changes, the decline of muscle size and function, and the loss of muscle stem cells and their functions with aging. Modifications with age of the endocrine systems (hypothalamus-pituitary system, gonad glands, liver, etc.) affect the quantity and the content of circulating serum hormones and impact muscle mass maintenance (atrophy of the muscle fibers and decrease in the regenerative capacity of the muscle). Increased inflammation with age - also called inflammaging - affects whole body stress level and is accompanied by modification in secreted cytokine content. Increased oxidative stress of the muscle leads to DNA damage and epigenetic changes, and consequently affects the regenerative capacity of the muscle. The composition of the microenvironment of the satellite cells is affected with age, through the presence of aged fibroblasts, of senescent cells, and aged myofibers. These local changes contribute to the fragility of the myofibers and to a decrease in the regenerative potency.

impinge directly upon muscle homeostasis, and exacerbate muscle fragility with aging.

CONCLUSION

The interplay between whole-body tissue composition, the quantity and content of circulating serum hormones, and whole-body stress, such as ROS production, changes with age, and contributes to the decline in muscle mass and function (Fig. 4). Increased stress can act through epigenetic marking of satellite cells, changing their intrinsic properties with age - aged satellite cells show a decrease in their activation rate due to epigenetic changes. In addition, satellite cell number is decreased during aging, a loss that can contribute not only to a decreased regenerative capacity, but also to an increase in fibrotic deposition and ECM thickening. Increased muscle stiffness renders myofibers more fragile, requiring the activation of an already reduced and less responsive satellite cell population. Age-associated changes in the local signalling environment can affect the myogenic program causing a lower regeneration efficacy, a decrease in myonuclear

turnover, and a failure in replenishing the pool of reserve cells, further contributing to the loss of muscle mass. Changes in the whole system of intercellular communication – both at the whole-body scale and in muscle microenvironment – may thus act as a vicious circle to exacerbate sarcopenia as the body ages. It is noteworthy that most studies on muscle aging in the literature have been done on muscle stem cells, rather than myofibers, and thus emphasize the role of satellite cells in muscle mass maintenance. The effect of hormones and cytokines and more generally the effect of aging on myofibers is difficult to assess directly and should not be neglected. The myofibers themselves comprise the bulk of the muscle mass and are clearly a key part of the maintenance of their own mass with aging, as indicated by disequilibrium of protein synthesis and degradation or the expression of micropeptides such as myoregulin that have a key role in muscle performance [138].

ACKNOWLEDGMENTS

This work was financed by the EU FP7 Programme project MYOAGE (contract HEALTH-F2-2009-223576), the ANR Genopath-INAFIB, the AFLD, the CNRS, INSERM, the University Pierre and Marie Curie Paris 6 and the AFM (Association Française contre les Myopathies).

CONFLICTS OF INTEREST

All authors declare no conflicts of interest.

REFERENCES

[1] Hosseinkhani M, Shirazi R, Rajaei F, Mahmoudi M, Mohammadi N, Abbasi M. Engineering of the embryonic and adult stem cell niches. Iran Red Crescent Med J. 2013;15(2):83-92.

[2] Thomas ED, Lochte HL, Cannon JH, Sahler OH, Ferrebee JW. Supralethal whole body irradiation and isologous marrow transplantation in man. J Clin Invest. 1959;38:1709-16.

[3] Baddour LM, Wilson WR, Bayer AS, Fowler VG, Bolger AF, Levison ME, et al. Infective endocarditis: Diagnosis, antimicrobial therapy, and management of complications. Circulation. 2005;111(23):e394-434.

[4] McCredie KB, Hersh EM, Freireich EJ. Cells capable of colony formation in the peripheral blood of man. Science. 1971;171(968):293-4.

[5] Potten CS. Cell replacement in epidermis (keratopoiesis) via discrete units of proliferation. Int Rev Cytol. 1981;69:271-318.

[6] Miura M, Gronthos S, Zhao M, Lu B, Fisher LW, Robey PG, et al. SHED: Stem cells from human exfoliated deciduous teeth. Proc Natl Acad Sci U S A. 2003;100(10):5807-12.

[7] Potten CS, Owen G, Booth D. Intestinal stem cells protect their genome by selective segregation of template DNA strands. J Cell Sci. 2002;115(Pt 11):2381-8.

[8] Dollé L, Best J, Mei J, Al Battah F, Reynaert H, van Grunsven LA, et al. The quest for liver progenitor cells: A practical point of view. Journal of Hepatology. 2010, pp. 117-29.

[9] Beltrami AP, Barlucchi L, Torella D, Baker M, Limana F, Chimenti S, et al. Adult cardiac stem cells are multipotent and support myocardial regeneration. Cell. 2003;114(6):763-76.

[10] Altman J, Das GD. Autoradiographic and histological evidence of postnatal hippocampal neurogenesis in rats. J Comp Neurol. 1965;124(3):319-35.

[11] MAURO A. Satellite cell of skeletal muscle fibers. J Biophys Biochem Cytol. 1961;9:493-5.

[12] Keefe AC, Lawson JA, Flygare SD, Fox ZD, Colasanto MP, Mathew SJ, et al. Muscle stem cells contribute to myofibres in sedentary adult mice. Nat Commun. 2015;6:7087.

[13] Brack AS, Bildsoe H, Hughes SM. Evidence that satellite cell decrement contributes to preferential decline in nuclear number from large fibres during murine age-related muscle atrophy. J Cell Sci. 2005;118(Pt 20):4813-21.

[14] Verdijk LB, Snijders T, Drost M, Delhaas T, Kadi F, van Loon LJC. Satellite cells in human skeletal muscle; from birth to old age. Age (Dordr). 2014;36(2):545-7.

[15] Barberi L, Scicchitano BM, De Rossi M, Bigot A, Duguez S, Wielgosik A, et al. Age-dependent alteration in muscle regeneration: The critical role of tissue niche. Biogerontology. 2013;14(3):273-92.

[16] Zammit PS, Golding JP, Nagata Y, Hudon V, Partridge TA, Beauchamp JR. Muscle satellite cells adopt divergent fates: A mechanism for self-renewal? J Cell Biol. 2004;166(3):347-57.

[17] Kitamoto T, Hanaoka K. Notch3 null mutation in mice causes muscle hyperplasia by repetitive muscle regeneration. Stem Cells. 2010;28(12):2205-16.

[18] Yablonka-Reuveni Z. The skeletal muscle satellite cell: Still young and fascinating at 50. J Histochem Cytochem. 2011;59(12):1041-59.

[19] Conboy IM, Rando TA. The regulation of Notch signaling controls satellite cell activation and cell fate determination in postnatal myogenesis. Dev Cell. 2002;3(3):397-409.

[20] Sun H, Li L, Vercherat C, Gulbagci NT, Acharjee S, Li J, et al. Stra13 regulates satellite cell activation by antagonizing Notch signaling. J Cell Biol. 2007;177(4):647-57.

[21] Zammit PS, Relaix F, Nagata Y, Ruiz AP, Collins CA, Partridge TA, et al. Pax7 and myogenic progression in skeletal muscle satellite cells. J Cell Sci. 2006;119(Pt 9):1824-32.

[22] Day K, Shefer G, Richardson JB, Enikolopov G, Yablonka-Reuveni Z. Nestin-GFP reporter expression defines the quiescent state of skeletal muscle satellite cells. Dev Biol. 2007;304(1):246-59.

[23] Gayraud-Morel B, Chrétien F, Jory A, Sambasivan R, Negroni E, Flamant P, et al. Myf5 haploinsufficiency reveals distinct cell fate potentials for adult skeletal muscle stem cells. J Cell Sci. 2012;125(Pt 7):1738-49.

[24] Shinin V, Gayraud-Morel B, Gomès D, Tajbakhsh S. Asymmetric division and cosegregation of template DNA strands in adult muscle satellite cells. Nat Cell Biol. 2006;8(7):677-87.

[25] Kuang S, Gillespie MA, Rudnicki MA. Niche regulation of muscle satellite cell self-renewal and differentiation. Cell Stem Cell. 2008;2(1):22-31.

[26] George RM, Biressi S, Beres BJ, Rogers E, Mulia AK, Allen RE, et al. Numb-deficient satellite cells have regeneration and proliferation defects. Proc Natl Acad Sci U S A. 2013;110(46):18549-54.

[27] Zhou S, Fujimuro M, Hsieh JJ, Chen L, Miyamoto A, Weinmaster G, et al. SKIP, a CBF1-associated protein, interacts with the ankyrin repeat domain of NotchIC To facilitate NotchIC function. Mol Cell Biol. 2000;20(7):2400-10.

[28] Brack AS, Conboy IM, Conboy MJ, Shen J, Rando TA. A temporal switch from notch to Wnt signaling in muscle stem cells is necessary for normal adult myogenesis. Cell Stem Cell. 2008;2(1):50-9.

[29] Bigot A, Jacquemin V, Debacq-Chainiaux F, Butler-Browne GS, Toussaint O, Furling D, et al. Replicative aging down-regulates the myogenic regulatory factors in human myoblasts. Biol Cell. 2008;100(3):189-99.

[30] Duguez S, Sabido O, Freyssenet D. Mitochondrial-dependent regulation of myoblast proliferation. Exp Cell Res. 2004;299(1):27-35.

[31] Ciavarra G, Zacksenhaus E. Rescue of myogenic defects in Rb-deficient cells by inhibition of autophagy or by hypoxia-induced glycolytic shift. J Cell Biol. 2010;191(2):291-301.

[32] Heron-Milhavet L, Franckhauser C, Fernandez A, Lamb NJ. Characterization of the Akt2 Domain Essential for Binding Nuclear p21cip1 to Promote Cell Cycle Arrest during Myogenic Differentiation. PLoS One. 2013;8(10): e76987.

[33] Weintraub H, Davis R, Tapscott S, Thayer M, Krause M, Benezra R, et al. The myoD gene family: Nodal point during specification of the muscle cell lineage. Science. 1991;251(4995):761-6.

[34] Sassoon D, Lyons G, Wright WE, Lin V, Lassar A, Weintraub H, et al. Expression of two myogenic regulatory factors myogenin and MyoD1 during mouse embryogenesis. Nature. 1989;341(6240):303-7.

[35] Duguez S, Féasson L, Denis C, Freyssenet D. Mitochondrial biogenesis during skeletal muscle regeneration. Am J Physiol Endocrinol Metab. 2002;282(4):E802-9.

[36] Chargé SBP, Rudnicki MA. Cellular and molecular regulation of muscle regeneration. Physiol Rev. 2004;84(1):209-38.

[37] Naya FJ, Olson E. MEF2: A transcriptional target for signaling pathways controlling skeletal muscle growth and differentiation. Current Opinion in Cell Biology. 1999. pp. 683-8.

[38] Rhodes SJ, Konieczny SF. Identification of MRF4: A new member of the muscle regulatory factor gene family. Genes Dev. 1989;3(12 B):2050-61.

[39] McGeachie AB, Koishi K, Andrews ZB, McLennan IS. Analysis of mRNAs that are enriched in the post-synaptic domain of the neuromuscular junction. Mol Cell Neurosci. 2005;30(2):173-85.

[40] Millay DP, O'Rourke JR, Sutherland LB, Bezprozvannaya S, Shelton JM, Bassel-Duby R, et al. Myomaker is a membrane activator of myoblast fusion and muscle formation. (Supp). Nature. 2013;499(7458):301-5.

[41] Mavalli MD, DiGirolamo DJ, Fan Y, Riddle RC, Campbell KS, Van Groen T, et al. Distinct growth hormone receptor signaling modes regulate skeletal muscle development and insulin sensitivity in mice. J Clin Invest. 2010;120(11): 4007-20.

[42] Serra C, Tangherlini F, Rudy S, Lee D, Toraldo G, Sandor NL, et al. Testosterone improves the regeneration of old and young mouse skeletal muscle. Journals Gerontol - Ser A Biol Sci Med Sci. 2013;68(1):17-26.

[43] Sinha-Hikim I, Roth SM, Lee MI, Bhasin S. Testosterone-induced muscle hypertrophy is associated with an increase in satellite cell number in healthy, young men. American Journal of Physiology Endocrinology and Metabolism. 2003. E197-205

[44] Dentice M, Ambrosio R, Damiano V, Sibilio A, Luongo C, Guardiola O, et al. Intracellular inactivation of thyroid hormone is a survival mechanism for muscle stem cell proliferation and lineage progression. Cell Metab. 2014;20(6):1038-48.

[45] Leal ALRC, Albuquerque JPC, Matos MS, Fortunato RS, Carvalho DP, Rosenthal D, et al. Thyroid hormones regulate skeletal muscle regeneration after acute injury. Endocrine. 2014;233-40.

[46] Han D, Zhao H, Parada C, Hacia JG, Bringas P, Chai Y. A TGF-Smad4-Fgf6 signaling cascade controls myogenic differentiation and myoblast fusion during tongue development. Development. 2012. pp. 1640-50.

[47] Chakkalakal JV, Jones KM, Basson MA, Brack AS. The aged niche disrupts muscle stem cell quiescence. Nature. 2012;490(7420):355-60.

[48] Grounds MD. Age-associated changes in the response of skeletal muscle cells to exercise and regeneration. Ann N Y Acad Sci. 1998;854:78-91.

[49] Blokzijl A, Dahlqvist C, Reissmann E, Falk A, Moliner A, Lendahl U, et al. Cross-talk between the Notch and TGF-β signaling pathways mediated by interaction of the Notch intracellular domain with Smad3. J Cell Biol. 2003;163(4):723-8.

[50] McFarlane C, Hui GZ, Amanda WZW, Lau HY, Lokireddy S, Xiaojia G, et al. Human myostatin negatively regulates human myoblast growth and differentiation. Am J Physiol Cell Physiol. 2011;301(1):C195-203.

[51] Hara M, Yuasa S, Shimoji K, Onizuka T, Hayashiji N, Ohno Y, et al. G-CSF influences mouse skeletal muscle development and regeneration by stimulating myoblast proliferation. J Exp Med. 2011;208(4):715-27.

[52] Toth KG, McKay BR, De Lisio M, Little JP, Tarnopolsky MA, Parise G. IL-6 induced STAT3 signalling is associated with the proliferation of human muscle satellite cells following acute muscle damage. PLoS One. 2011;6(3): e17392.

[53] Serrano AL, Baeza-Raja B, Perdiguero E, Jardí M, Muñoz-Cánoves P. Interleukin-6 is an essential regulator of satellite cell-mediated skeletal muscle hypertrophy. Cell Metab. 2008;7(1):33-44.

[54] Chazaud B, Sonnet C, Lafuste P, Bassez G, Rimaniol A-C, Poron F, et al. Satellite cells attract monocytes and use macrophages as a support to escape apoptosis and enhance muscle growth. J Cell Biol. 2003;163(5):1133-43.

[55] Chan CYX, Masui O, Krakovska O, Belozerov VE, Voisin S, Ghanny S, et al. Identification of differentially regulated secretome components during skeletal myogenesis. Mol Cell Proteomics. 2011;10(5):M110.004804.

[56] Henningsen J, Rigbolt KTG, Blagoev B, Pedersen BK, Kratchmarova I. Dynamics of the skeletal muscle secretome during myoblast differentiation. Mol Cell Proteomics. 2010;9(11):2482-96.

[57] Le Bihan M-C, Bigot A, Jensen SS, Dennis J, Rogowska-Wrzesinska A, Lainé J, et al. In-depth analysis of the secretome identifies three major independent secretory pathways in differentiating human myoblasts. J Proteomics. 2012;77:344-56.

[58] Forterre A, Jalabert A, Berger E, Baudet M, Chikh K, Errazuriz E, et al. Proteomic analysis of C2C12

myoblast and myotube exosome-like vesicles: A new paradigm for myoblast-myotube cross talk? PLoS One. 2014;9(1):e84153.
[59] Clarkson PM, Dedrick ME. Exercise-induced muscle damage, repair, and adaptation in old and young subjects. J Gerontol. 1988;43(4):M91-6.
[60] Gutmann E, Carlson BM. Regeneration and transplantation of muscles in old rats and between young and old rats. Life Sci. 1976;18(1):109-14.
[61] Sadeh M. Effects of aging on skeletal muscle regeneration. J Neurol Sci. 1988;87(1):67-74.
[62] Smythe GM, Shavlakadze T, Roberts P, Davies MJ, McGeachie JK, Grounds MD. Age influences the early events of skeletal muscle regeneration: Studies of whole muscle grafts transplanted between young (8 weeks) and old (13-21 months) mice. Exp Gerontol. 2008;43(6):550-62.
[63] Carlson ME, Conboy IM. Loss of stem cell regenerative capacity within aged niches. Aging Cell. 2007;6(3): 371-82.
[64] Kojo G, Yoshida T, Ohkawa S, Odamaki M, Kato A, Takita T, et al. Association of serum total testosterone concentration with skeletal muscle mass in men under hemodialysis. Int Urol Nephrol. 2014;46(5):985-97.
[65] Gordon SE, Kraemer WJ, Looney DP, Flanagan SD, Comstock BA, Hymer WC. The influence of age and exercise modality on growth hormone bioactivity in women. Growth Horm IGF Res. 2014;24(2-3):95-103.
[66] Sattler FR. Growth hormone in the aging male. Best Pract Res Clin Endocrinol Metab. 2013;27(4):541-55.
[67] Veldhuis JD. Aging and hormones of the hypothalamo-pituitary axis: Gonadotropic axis in men and somatotropic axes in men and women. Ageing Research Reviews. 2008. pp. 189-208.
[68] Sotiropoulos A, Ohanna M, Kedzia C, Menon RK, Kopchick JJ, Kelly PA, et al. Growth hormone promotes skeletal muscle cell fusion independent of insulin-like growth factor 1 up-regulation. Proc Natl Acad Sci USA. 2006;103(19):7315-20.
[69] Horsley V, Jansen KM, Mills ST, Pavlath GK. IL-4 acts as a myoblast recruitment factor during mammalian muscle growth. Cell. 2003;113(4):483-94.
[70] Brisson BK, Barton ER. Insulin-Like Growth Factor-I E-Peptide Activity Is Dependent on the IGF-I Receptor. PLoS One. 2012;7(9):e45588.
[71] Matheny RW, Nindl BC. Loss of IGF-IEa or IGF-IEb impairs myogenic differentiation. Endocrinology. 2011;152(5):1923-34.
[72] Troy A, Cadwallader AB, Fedorov Y, Tyner K, Tanaka KK, Olwin BB. Coordination of satellite cell activation and self-renewal by par-complex-dependent asymmetric activation of p38??/?? MAPK. Cell Stem Cell. 2012;11(4): 541-53.
[73] Sinha-Hikim I, Taylor WE, Gonzalez-Cadavid NF, Zheng W, Bhasin S. Androgen receptor in human skeletal muscle and cultured muscle satellite cells: Up-regulation by androgen treatment. J Clin Endocrinol Metab. 2004;89(10): 5245-55.
[74] Fu R, Liu J, Fan J, Li R, Li D, Yin J, et al. Novel evidence that testosterone promotes cell proliferation and differentiation via G protein-coupled receptors in the rat L6 skeletal muscle myoblast cell line. J Cell Physiol. 2012;227(1):98-107.
[75] Czifra G, Szöllősi A, Nagy Z, Boros M, Juhász I, Kiss A, et al. Protein kinase Cδ promotes proliferation and induces malignant transformation in skeletal muscle. J Cell Mol Med. 2015;19(2):396-407.
[76] Wei C, Ren H, Xu L, Li L, Liu R, Zhang L, et al. Signals of Ezh2, Src, and Akt Involve in Myostatin-Pax7 Pathways Regulating the Myogenic Fate Determination during the Sheep Myoblast Proliferation and Differentiation. PLoS One. 2015;10(3):e0120956.
[77] Mukai A, Hashimoto N. Localized cyclic AMP-dependent protein kinase activity is required for myogenic cell fusion. Exp Cell Res. 2008;314(2):387-97.
[78] Han SY, Park DY, Lee GH, Park SD, Hong SH. Involvement of type I protein kinase A in the differentiation of L6 myoblast in conjunction with phosphatidylinositol 3-kinase. Mol Cells. 2002;14(1):68-74.
[79] Ahtiainen M, Pöllänen E, Ronkainen PHA, Alen M, Puolakka J, Kaprio J, et al. Age and estrogen-based hormone therapy affect systemic and local IL-6 and IGF-1 pathways in women. Age (Omaha). 2012;34(5):1249-60.
[80] Franceschi C, Capri M, Monti D, Giunta S, Olivieri F, Sevini F, et al. Inflammaging and anti-inflammaging: A systemic perspective on aging and longevity emerged from studies in humans. Mech Ageing Dev. 2007;128(1):92-105.
[81] Zhang J, Xiao Z, Qu C, Cui W, Wang X, Du J. CD8 T Cells Are Involved in Skeletal Muscle Regeneration through Facilitating MCP-1 Secretion and Gr1high Macrophage Infiltration. J Immunol. 2014;193(10):5149-60.
[82] Wang H, Melton DW, Porter L, Sarwar ZU, McManus LM, Shireman PK. Altered macrophage phenotype transition impairs skeletal muscle regeneration. Am J Pathol. 2014;184(4):1167-84.
[83] Chazaud B. Macrophages: Supportive cells for tissue repair and regeneration. Immunobiology. 2014;219(3):172-8.
[84] Paliwal P, Pishesha N, Wijaya D, Conboy IM. Age dependent increase in the levels of osteopontin inhibits skeletal muscle regeneration. Aging (Albany NY). 2012;4(8): 553-66.
[85] Ebersole JL, Steffen MJ, Pappo J. Secretory immune responses in ageing rats. II. Phenotype distribution of lymphocytes in secretory and lymphoid tissues. Immunology. 1988;64(2):289-94.
[86] Pedersen BK, Febbraio M. Muscle-derived interleukin-6–a possible link between skeletal muscle, adipose tissue, liver, and brain. Brain Behav Immun. 2005;19(5):371-6.
[87] Ivanova AV., Ivanov SV., Zhang X, Ivanov VN, Timofeeva OA, Lerman MI. STRA13 interacts with STAT3 and modulates transcription of STAT3-dependent targets. J Mol Biol. 2004;340(4):641-53.
[88] Baeza-Raja B, Muñoz-Cánoves P. p38 MAPK-induced nuclear factor-kappaB activity is required for skeletal muscle differentiation: Role of interleukin-6. Mol Biol Cell. 2004;15(4):2013-26.
[89] Nilwik R, Snijders T, Leenders M, Groen BBL, van Kranenburg J, Verdijk LB, et al. The decline in skeletal muscle mass with aging is mainly attributed to a reduction in type II muscle fiber size. Exp Gerontol. 2013;48(5): 492-8.
[90] Conboy IM, Conboy MJ, Wagers AJ, Girma ER, Weissman IL, Rando TA. Rejuvenation of aged progenitor cells by exposure to a young systemic environment. Nature. 2005;433(7027):760-4.
[91] Falick Michaeli T, Laufer N, Sagiv JY, Dreazen A, Granot Z, Pikarsky E, Bergman Y, Gielchinsky Y. The rejuvenating effect of pregnancy on maternal regeneration. Aging Cell. 2015;14(4):698-700.
[92] Nader GA, Lundberg IE. Exercise as an anti-inflammatory intervention to combat inflammatory diseases of muscle. Curr Opin Rheumatol. 2009;21(6):599-603.

[93] Lundberg IE, Nader GA. Molecular effects of exercise in patients with inflammatory rheumatic disease. Nat Clin Pract Rheumatol. 2008;4(11):597-604.
[94] Collins CA, Zammit PS, Ruiz AP, Morgan JE, Partridge TA. A population of myogenic stem cells that survives skeletal muscle aging. Stem Cells. 2007;25(4):885-94.
[95] Engler D. Hypothesis: Musculin is a hormone secreted by skeletal muscle, the body's largest endocrine organ. Evidence for actions on the endocrine pancreas to restrain the beta-cell mass and to inhibit insulin secretion and on the hypothalamus to co-ordinate the neuroendocrine and appetite responses to exercise. Acta Biomed. 2007;78 Suppl 1:156-206.
[96] Roca-Rivada A, Al-Massadi O, Castelao C, Senín LL, Alonso J, Seoane LM, et al. Muscle tissue as an endocrine organ: Comparative secretome profiling of slow-oxidative and fast-glycolytic rat muscle explants and its variation with exercise. J Proteomics. 2012;75(17):5414-25.
[97] Duguez S, Duddy W, Johnston H, Lainé J, Le Bihan MC, Brown KJ, et al. Dystrophin deficiency leads to disturbance of LAMP1-vesicle-associated protein secretion. Cell Mol Life Sci. 2013;70(12):2159-74.
[98] Forterre A, Jalabert A, Chikh K, Pesenti S, Euthine V, Granjon A, et al. Myotube-derived exosomal miRNAs downregulate Sirtuin1 in myoblasts during muscle cell differentiation. Cell Cycle. 2014;13(1):78-89.
[99] Baraibar MA, Gueugneau M, Duguez S, Butler-Browne G, Bechet D, Friguet B. Expression and modification proteomics during skeletal muscle ageing. Biogerontology. 2013;14(3):339-52.
[100] Abou-Khalil R, Mounier R, Chazaud B. Regulation of myogenic stem cell behavior by vessel cells: The "ménage à trois" of satellite cells, periendothelial cells and endothelial cells. Cell Cycle. 2010;9(5):892-6.
[101] Zwetsloot KA, Nedergaard A, Gilpin LT, Childs TE, Booth FW. Differences in transcriptional patterns of extracellular matrix, inflammatory, and myogenic regulatory genes in myofibroblasts, fibroblasts, and muscle precursor cells isolated from old male rat skeletal muscle using a novel cell isolation procedure. Biogerontology. 2012;13(4):383-98.
[102] Liu D, Black BL, Derynck R. TGF-β inhibits muscle differentiation through functional repression of myogenic transcription factors by Smad3. Genes Dev. 2001;15(22):2950-66.
[103] Sousa-Victor P, Gutarra S, García-Prat L, Rodriguez-Ubreva J, Ortet L, Ruiz-Bonilla V, et al. Geriatric muscle stem cells switch reversible quiescence into senescence. Nature. 2014;506(7488):316-21.
[104] Fukada S, Ma Y, Uezumi A. Adult stem cell and mesenchymal progenitor theories of aging. Front Cell Dev Biol. 2014;2(March):1-9.
[105] Kumar M, Seeger W, Voswinckel R. Senescence-associated secretory phenotype and its possible role in chronic obstructive pulmonary disease. Am J Respir Cell Mol Biol. 2014;51(3):323-33.
[106] Demaria M, Desprez PY, Campisi J, Velarde MC. Cell Autonomous and Non-Autonomous Effects of Senescent Cells in the Skin. J Invest Dermatol. 2015;1722-6.
[107] Behringer EJ, Segal SS. Spreading the signal for vasodilatation: Implications for skeletal muscle blood flow control and the effects of ageing. J Physiol. 2012;590(Pt 24):6277-84.
[108] Leiter JRS, Upadhaya R, Anderson JE. Nitric oxide and voluntary exercise together promote quadriceps hypertrophy and increase vascular density in female 18-mo-old mice. AJP: Cell Physiology. 2012. pp. C1306-15.
[109] Lai Y, Thomas GD, Yue Y, Yang HT, Li D, Long C, et al. Dystrophins carrying spectrin-like repeats 16 and 17 anchor nNOS to the sarcolemma and enhance exercise performance in a mouse model of muscular dystrophy. J Clin Invest. 2009;119(3):624-35.
[110] Song W, Kwak HB, Kim JH, Lawler JM. Exercise training modulates the nitric oxide synthase profile in skeletal muscle from old rats. Journals Gerontol-Ser A Biol Sci Med Sci. 2009;64(5):540-9.
[111] Anderson JE. A role for nitric oxide in muscle repair: Nitric oxide-mediated activation of muscle satellite cells. Mol Biol Cell. 2000;11(5):1859-74.
[112] Goldspink G, Fernandes K, Williams PE, Wells DJ. Age-related changes in collagen gene expression in the muscles of mdx dystrophic and normal mice. Neuromuscul Disord. 1994;4(3):183-91.
[113] Ferreira MM, Dewi RE, Heilshorn SC. Microfluidic analysis of extracellular matrix-bFGF crosstalk on primary human myoblast chemoproliferation, chemokinesis, and chemotaxis. Integr Biol. 2015;569-79.
[114] Fannon M, Forsten-Williams K, Zhao B, Bach E, Parekh PP, Chu CL, et al. Facilitated diffusion of VEGF165 through descemet's membrane with sucrose octasulfate. J Cell Physiol. 2012;227(11):3693-700.
[115] Bernet JD, Doles JD, Hall JK, Kelly Tanaka K, Carter T a, Olwin BB. p38 MAPK signaling underlies a cell-autonomous loss of stem cell self-renewal in skeletal muscle of aged mice. Nat Med. 2014;20(3):265-71.
[116] Saini A, Mastana S, Myers F, Lewis M. "From death, Lead me to immortality"- mantra of ageing skeletal muscle. Curr Genomics. 2013;14(4):256-67.
[117] Liu L, Cheung TH, Charville GW, Hurgo BMC, Leavitt T, Shih J, et al. Chromatin modifications as determinants of muscle stem cell quiescence and chronological aging. Cell Rep. 2013;4(1):189-204.
[118] Li J, Han S, Cousin W, Conboy IM. Age-Specific Functional Epigenetic Changes in p21 and p16 in Injury-Activated Satellite Cells. Stem Cells. 2015;33(3):951-61.
[119] Horvath S. DNA methylation age of human tissues and cell types. Genome Biol. 2013;14(10):R115.
[120] Bocker MT, Hellwig I, Breiling A, Eckstein V, Ho AD, Lyko F. Genome-wide promoter DNA methylation dynamics of human hematopoietic progenitor cells during differentiation and aging. Blood. 2011;117(19):e182-9.
[121] Blaze J, Roth TL. Evidence from clinical and animal model studies of the long-term and transgenerational impact of stress on DNA methylation. Semin Cell Dev Biol. 2015;S1084-9521.
[122] Cencioni C, Spallotta F, Martelli F, Valente S, Mai A, Zeiher AM, et al. Oxidative stress and epigenetic regulation in ageing and age-related diseases. Int J Mol Sci. 2013;14(9):17643-63.
[123] Claflin DR, Jackson MJ, Brooks S V. Age affects the contraction-induced mitochondrial redox response in skeletal muscle. Front Physiol. 2015;6.
[124] Liu D, Sartor M, Nader G, Pistilli EE, Tanton L, Lilly C, et al. Microarray analysis reveals novel features of the muscle aging process in men and women. J Gerontol A Biol Sci Med Sci. 2013;68(9):1035-44.
[125] Brioche T, Kireev R a, Cuesta S, Gratas-Delamarche A, Tresguerres J a, Gomez-Cabrera MC, et al. Growth hormone replacement therapy prevents sarcopenia by a dual mechanism: Improvement of protein balance and of antioxidant defenses. J Gerontol A Biol Sci Med Sci. 2013;(7):1-13.

[126] Signer RAJ, Morrison SJ. Mechanisms that regulate stem cell aging and life span. Cell Stem Cell. 2013;12(2): 152-65.
[127] Zampieri M, Ciccarone F, Calabrese R, Franceschi C, Bürkle A, Caiafa P. Reconfiguration of DNA methylation in aging. Mech Ageing Dev. 2015; pii:S0047-6374(15)00007-X.
[128] Renault V, Thornell L-E, Eriksson P-O, Butler-Browne G, Mouly V, Thorne L-E. Regenerative potential of human skeletal muscle during aging. Aging Cell. 2002;1(2):132-9.
[129] Malmgren LT, Fisher PJ, Jones CE, Bookman LM, Uno T. Numerical densities of myonuclei and satellite cells in muscle fiber types in the aging human thyroarytenoid muscle: An immunohistochemical and stereological study using confocal laser scanning microscopy. Otolaryngol Head Neck Surg. 2000;123(4):377-84.
[130] Cousin W, Ho ML, Desai R, Tham A, Chen RY, Kung S, et al. Regenerative capacity of old muscle stem cells declines without significant accumulation of DNA damage. PLoS One. 2013;8(5):e63528.
[131] Alsharidah M, Lazarus NR, George TE, Agley CC, Velloso CP, Harridge SDR. Primary human muscle precursor cells obtained from young and old donors produce similar proliferative, differentiation and senescent profiles in culture. Aging Cell. 2013;12(3):333-44.
[132] Spalding KL, Bhardwaj RD, Buchholz BA, Druid H, Frisén J. Retrospective birth dating of cells in humans. Cell. 2005;122(1):133-43.
[133] White RB, Biérinx A-S, Gnocchi VF, Zammit PS. Dynamics of muscle fibre growth during postnatal mouse development. BMC Dev Biol. 2010;10:21.
[134] Lee JD, Fry CS, Mula J, Kirby TJ, Jackson JR, Liu F, et al. Aged muscle demonstrates fiber-type adaptations in response to mechanical overload, in the absence of myofiber hypertrophy, Independent of satellite cell abundance. J Gerontol A Biol Sci Med Sci. 2015;1-7.
[135] Fry CS, Lee JD, Mula J, Kirby TJ, Jackson JR, Liu F, et al. Inducible depletion of satellite cells in adult, sedentary mice impairs muscle regenerative capacity without affecting sarcopenia. Nat Med. 2014;76-80.
[136] Takeuchi F, Yonemoto N, Nakamura H, Shimizu R, Komaki H, Mori-Yoshimura M, et al. Prednisolone improves walking in Japanese Duchenne muscular dystrophy patients. J Neurol. 2013;260(12):3023-9.
[137] Hussein MRA, Abu-Dief EE, Kamel NF, Mostafa MG. Steroid therapy is associated with decreased numbers of dendritic cells and fibroblasts, and increased numbers of satellite cells, in the dystrophic skeletal muscle. J Clin Pathol. 2010;63(9):805-13.
[138] Anderson DM, Anderson KM, Bassel-duby R, Olson EN, Mcanally JR, Kasaragod P, et al. Article a micropeptide encoded by a putative long noncoding RNA regulates muscle performance article a micropeptide encoded by a putative long noncoding RNA regulates muscle performance. Cell. 2015;1-12.
[139] Barrett T, Wilhite SE, Ledoux P, Evangelista C, Kim IF, Tomashevsky M, et al. NCBI GEO: Archive for functional genomics data sets - Update. Nucleic Acids Res. 2013;41(D1).
[140] Clark NR, Hu KS, Feldmann AS, Kou Y, Chen EY, Duan Q, et al. The characteristic direction: A geometrical approach to identify differentially expressed genes. BMC Bioinformatics. 2014;15(1):79.
[141] Chen EY, Tan CM, Kou Y, Duan Q, Wang Z, Meirelles GV, et al. Enrichr: Interactive and collaborative HTML5 gene list enrichment analysis tool. BMC Bioinformatics. 2013;14(1):128.

Poster communications

1. European Alliance for Personalized Medicine (EAPM) Congress – Belfast / UK:

« Secretion of toxic exosomes by muscle cells: role in ALS physiopathology »

Best Poster Award

Authors: **Laura Le Gall**[1,2], William J Duddy[1], Sylvain Roquevière[3], Mariot Virginie[4], Blandine Madji Hounoum[5], Jeanne Lainé[2], Romain Joubert[6], Julie Dumonceaux[4], Pascal Leblanc[7], Gisele Ouandaogo[2], Laura Robelin[8], Franscesca Ratti[7], Alexandre Mejat[7], Gillian Butler Browne[2], Jean Philippe Loeffler[8], Anne Cecile Durieux[9], Jose-Luis Gonzales De Aguilar[8], Helene Blasco[5], Cecile Martinat[3], Pierre Francois Pradat[10*], Stephanie Duguez[1*]

***Co-last authors**

Affiliations:

1- Northern Ireland Center for Stratified Medicine, Biomedical Sciences Research Institute, Londonderry, UK.
2- Myologie Centre de Recherche, Université Sorbonne, UMRS 974 UPMC, INSERM, FRE 3617 CNRS, AIM, Paris, France.
3- I-Stem, INSERM/UEVE UMR 861, I-STEM, AFM, Evry, France.
4- NIHR Biomedical Research Centre, University College London, Great Ormond Street Institute of Child Health and Great Ormond Street Hospital NHS Trust, London, UK.
5- Université François-Rabelais, INSERM U930 "Imagerie et Cerveau", CHRU de Tours, 10 Bv Tonnellé, 37044 Tours, France.
6- Unité Physiologie et Pathologie Moléculaires des Rétrovirus Endogènes et Infectieux, CNRS UMR 9196, Institut Gustave Roussy, Villejuif, France.
7- Laboratory of Molecular Biology of the Cell, Ecole Normale Supérieure de Lyon, Lyon, France.
8- Mécanismes Centraux et Périphériques de la Neurodégénérescence, Université de Strasbourg, INSERM U1118, Strasbourg, France.
9- LPE, Université Jean Monnet de Saint Etienne, Faculté de Médecine Jacques Lisfranc, Saint Etienne, France.
10- Département des Maladies du Système Nerveux, Hôpital de la Pitie-Salpetriere, Paris, France.

Introduction: Amyotrophic lateral sclerosis (ALS) is a neurodegenerative disorder with an adult onset and characterized by a rapid and lethal deterioration of cortical, brainstem and spinal cord motor neurons. This denervation leads to a gradual muscle weakness characterized by muscle atrophy and stiffness, and muscle cramps. Patients experience paralysis and die within 3 to 5 years after the symptoms have reached the intercostal and the diaphragm muscle. To date, numerous mutations have been identified such as SOD1, FUS and the intronic hexanucleotide expansion in C9orf72 gene. Today ALS remains incurable and the causes of muscle denervation are still unknown. Numerous mechanisms involving the neighbouring non-neuronal cells are suggested to affect motor neurons death in ALS. It has been demonstrated that pathological molecular and cellular changes occur at the neuromuscular junction prior to motor neurons degeneration and symptom onset. Based on these studies we hypothesised that muscle can participate to the ALS pathogenesis. Moreover, using transcripomic data previously published we performed an in-silico secretome revealing that the endosome and lysosome secretion compartments are significantly enriched in ALS muscle. These pathways are known to be part of the exosomes genesis and

secretion. Thus, we hypothesised that the vesicle trafficking is disturbed in ALS muscle and might influence intercellular communication between muscle and nerve.

Methods: We extracted human primary cells from deltoid muscle biopsies from ALS (n=18), SBMA (n=12), SMA (n=12) and healthy subjects (n=15). The muscle cells were sorted using CD56 MACS beads. Muscle exosomes were extracted after removing cell debris and microparticles using the Life Technologies kit.

Results: We demonstrated that there is an ALS signature in muscle stem cells as we observed an accumulation of MVBs is independent from the denervation process that is a characteristic of the ALS myotubes. The disruption of the exosomal pathway is associated with a 2 fold higher amount of secreted exosomes by ALS muscle cells. And finally we could demonstrate that ALS exosomes are toxic for muscle cells and toward neurons as they can induce a greater cellular stress, nuclear loss and cell death after treatment with healthy muscle stem cells or healthy human iPSC-motor neurons or healthy primary motor neuron.

Discussion Altogether, the present study suggests that muscle cells from sporadic patient secrete toxic agents through their exosomes. The secretion of toxic exosomes may influence the intercellular communication between the muscle and its environment, including motor neurons, and may have a key role in the ALS pathology

Secretion of toxic exosomes by muscle cells: role in ALS pathogenesis

Laura Le Gall[1,2], William J Duddy[1], Sylvain Roquevière[3], Mariot Virginie[4], Blandine Madji Hounoum[5], Jeanne Lainé[2], Romain Joubert[6], Julie Dumonceaux[4], Pascal Leblanc[7], Gisele Ouandaogo[2], Laura Robelin[8], Franscesca Ratti[7], Alexandre Mejat[7], Gillian Butler Browne[2], Jean Philippe Loeffler[8], Anne Cecile Durieux[9], Jose-Luis Gonzales De Aguilar[8], Helene Blasco[5], Cecile Martinat[3], Pierre Francois Pradat[10*], Stephanie Duguez[1*]

***Co-last authors**

1- Northern Ireland Center for Stratified Medicine, Biomedical Sciences Research Institute, Londonderry, UK.
2- Myologie Centre de Recherche, Université Sorbonne, UMRS 974 UPMC, INSERM, FRE 3617 CNRS, AIM, Paris, France.
3- I-Stem, INSERM/UEVE UMR 861, I-STEM, AFM, Evry, France.
4- NIHR Biomedical Research Centre, University College London, Great Ormond Street Institute of Child Health and Great Ormond Street Hospital NHS Trust, London, UK.
5- Université François-Rabelais, INSERM U930 "Imagerie et Cerveau", CHRU de Tours, 10 Bv Tonnellé, 37044 Tours, France.
6- Unité Physiologie et Pathologie Moléculaires des Rétrovirus Endogènes et Infectieux, CNRS UMR 9196, Institut Gustave Roussy, Villejuif, France.
7- Laboratory of Molecular Biology of the Cell, Ecole Normale Supérieure de Lyon, Lyon, France.
8- Mécanismes Centraux et Périphériques de la Neurodégénérescence, Université de Strasbourg, INSERM U1118, Strasbourg, France.
9- LPE, Université Jean Monnet de Saint Etienne, Faculté de Médecine Jacques Lisfranc, Saint Etienne, France.
10- Département des Maladies du Système Nerveux, Hôpital de la Pitie-Salpetriere, Paris, France.

Amyotrophic Lateral Sclerosis

- ✓ Rare neurodegenarative disorder
- ✓ Adult onset neurodegenerative disorder
- ✓ 90% sporadic cases

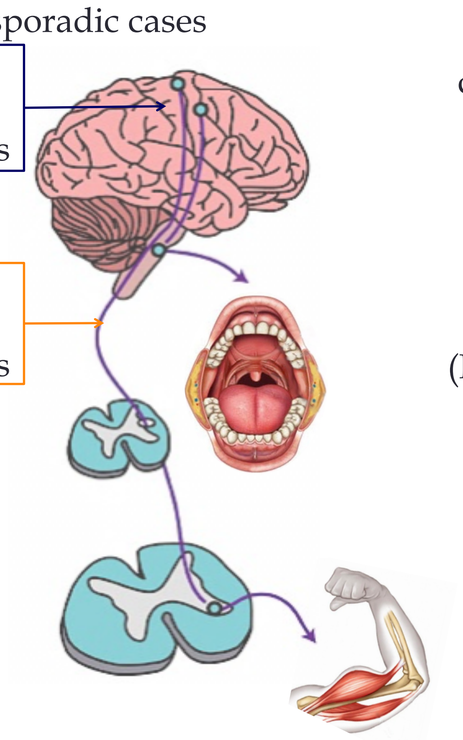

Rapid and fatal deterioration of the **lower** and **upper** motor neurons

↓ Muscle denervation

↓ Muscle damage (Muscle weakness & atrophy)

↓ Death (respiratory failure)

Hypothesis :

Toxic cellular environment

Published data suggest a disruption of the exosome pathway

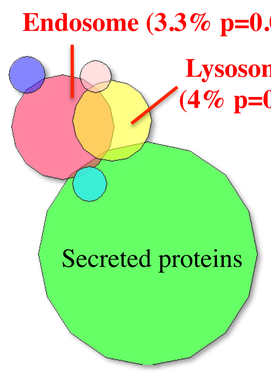

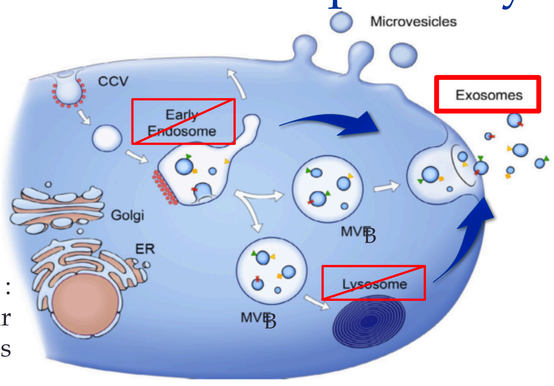

MVB : Multivesicular bodies

Axo-terminal degeneration at the neuromuscular junction

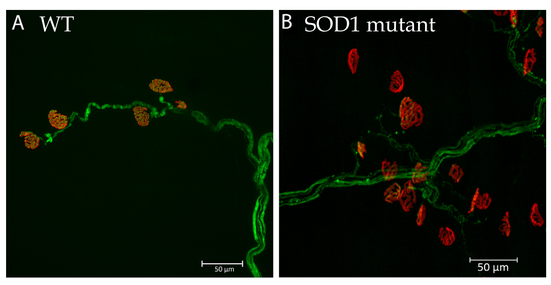

C Tallon et al., Neuroscience 312 (2016) 179-189

Hypothesis: Muscle exosomes altered & involved in ALS pathology

Muscle exosomes

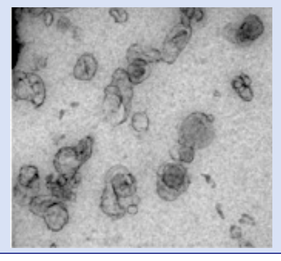

I. Accumulation of MVBs & exosomes in ALS muscles

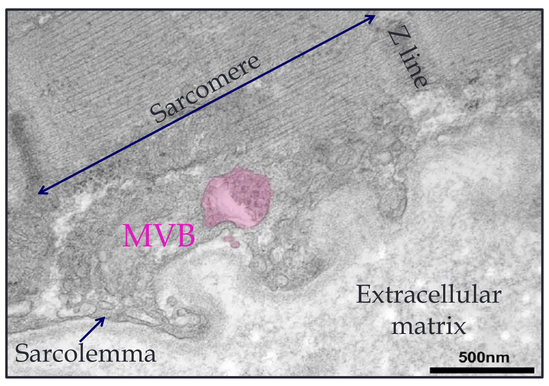

ALS: 1 MVB/69 sarc. Cont: 1 MVB/323 sarc.

Quantification of exosome immunostaining

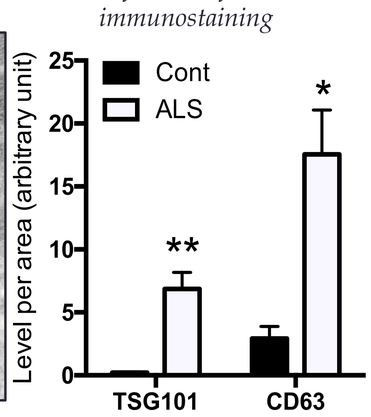

N=3 /group

II. ALS Signature in muscle stem cells

Transcriptome analysis of ALS, SMA, SBMA and Cont Cells

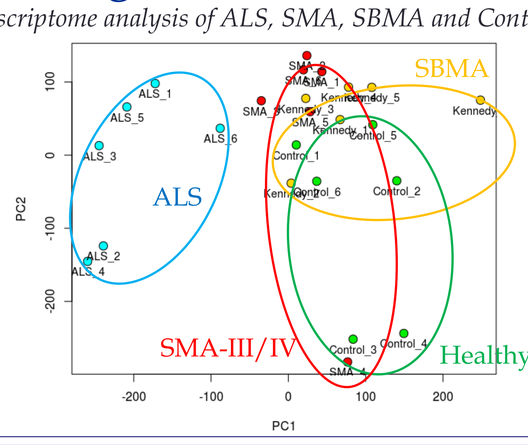

N=6 /group

ALS muscle markers can be associated with vesicles trafficking and exosomes

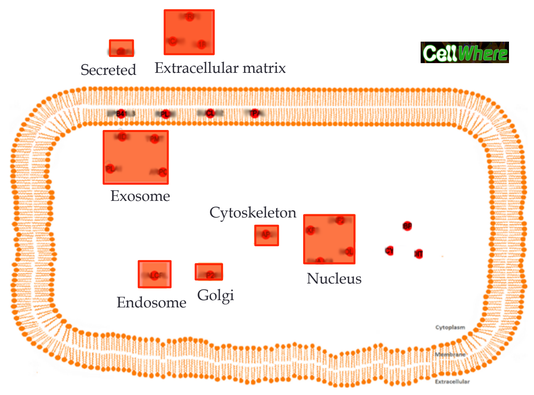

III. Accumulation of exosomes in ALS muscle cells

- **ALS exosomes accumulation in MVBs**

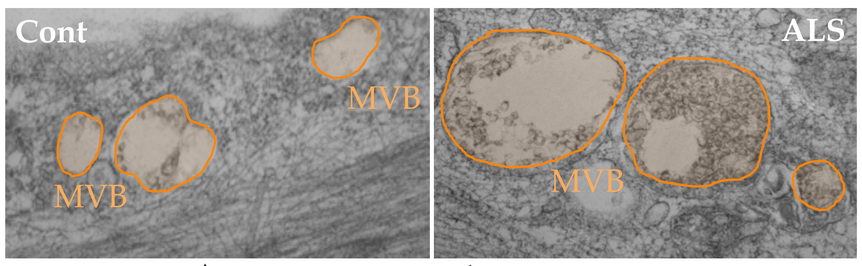

Electron microscopy of 3 days differentiated myotubes from ALS patients and healthy subjects (n=3 per group)

Quantifications of exosomes per MVB

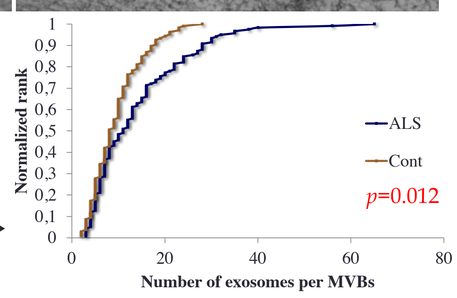

- **ALS exosomes accumulation in muscle cells**

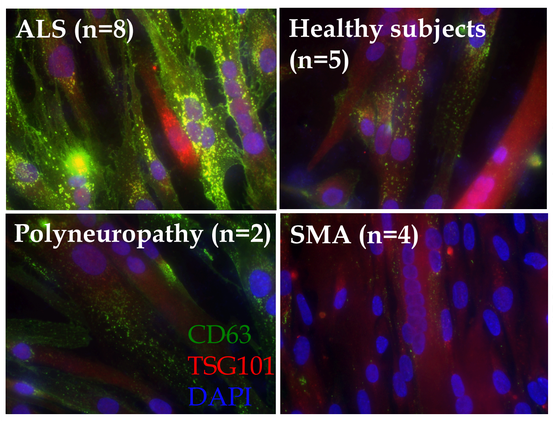

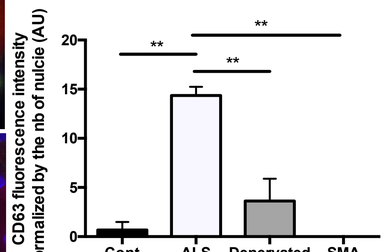

- **Up-regulation of the exosomal pathway in ALS muscle cells (RT-qPCR)**

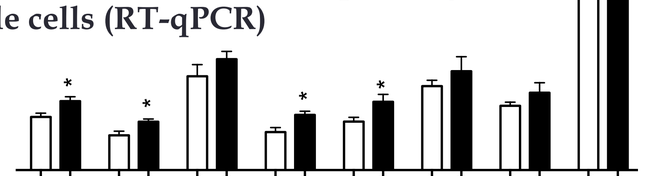

IV. ALS exosomes are over-secreted

- **Accumulation of ALS exosomes in the culture medium**

2.4 M ALS cells

2.4 M healthy cells

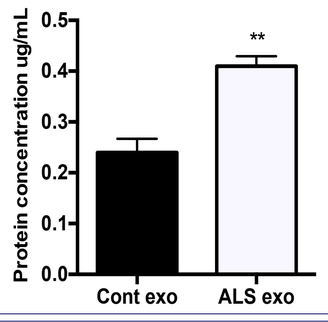

N=6 / group

V. Toxic autocrine and paracrine effects of ALS exosomes

#1 Muscular atrophy

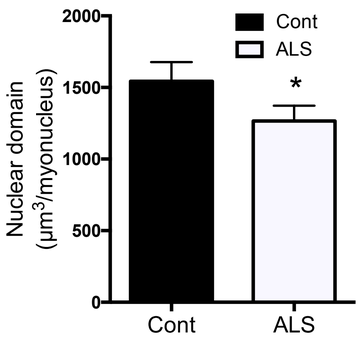

#2 Cell stress (blebbing)

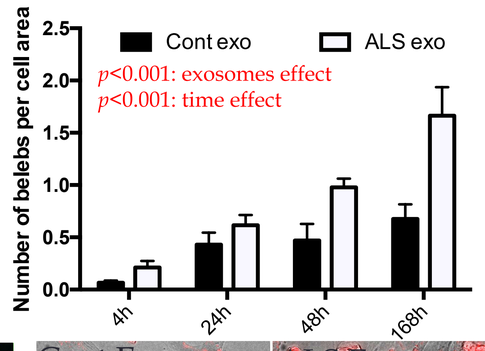

#3 Cell Death

- **Nuclei loss**

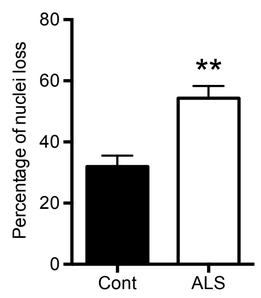

- **H2Ax staining**

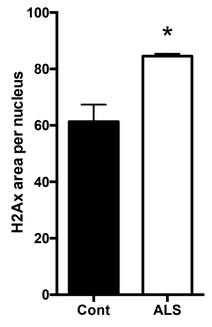

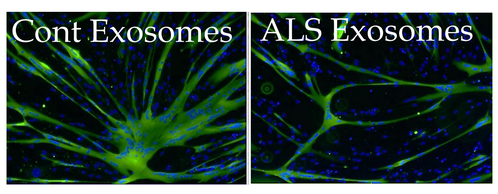

Myosin heavy chain
Nuclei

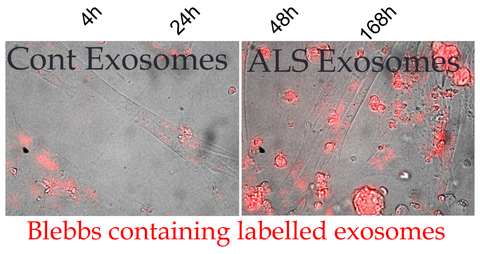

Blebbs containing labelled exosomes

#1 Cell stress (72h):

- **Neurite length**

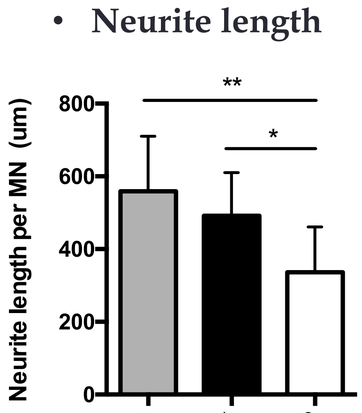

- **Branching**

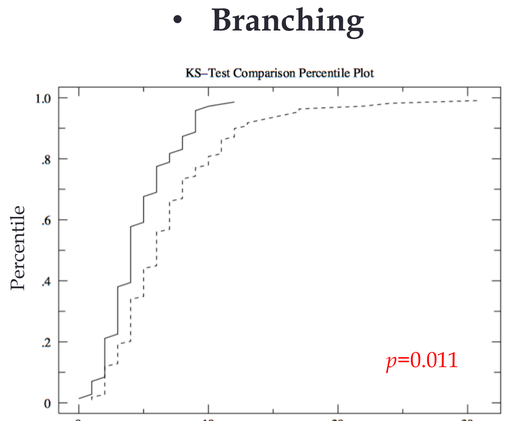

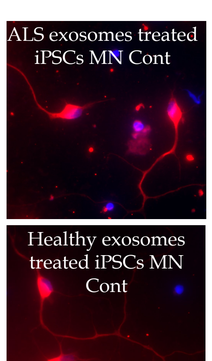

#3 Cell Death

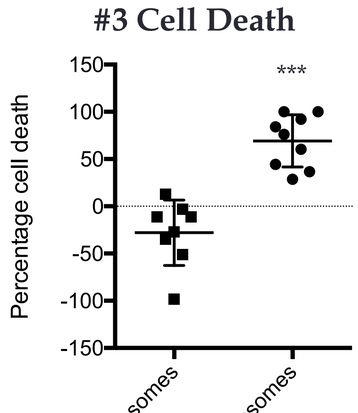

Aknowledgement

This work was supported by:

- the Association pour la Recherche sur la Sclérose Latérale Amyotrophique (ARSLA),
- INSERM &Direction Générale de l'Organisation des Soins (DGOS)
- the Association Française contre les myopathies (AFM),
- Target-ALS association and
- £11.5M grant awarded to Professor Tony Bjourson from European Union Regional Development Fund (ERDF) EU Sustainable Competitiveness Programme for N. Ireland; Northern Ireland Public Health Agency (HSC R&D) & Ulster University.

Material & methods

Human primary cells extracted from Deltoid muscle biopsies:

- SBMA(n=12), ALS (n=18), SMA (n=12), Healthy subjects (n=15).
- All Male, 20-76 years old.
- Muscle cells sorted using CD56 MACS beads: >86% myogenic cells
- Transcriptome analysis of the muscle stem cells using GeneChip Human Exon 1.0ST Array (Affimetrix ; n=6/group)
- After removing cell debris and microparticles (centrifugation 200g,10 min RT; 2,000g 20 min 4C and filtration 0.22 mm), exosomes were extracted using Life Technologies kit (we validated the quality of the kit by electron microscopy and immunostaining and western blot)
- Labelled ALS or control exosomes were added to healthy human muscle stem cells or healthy human iPSC-motor neuron n=6/3 per group

2. 28th International Symposium on ALS/MND – Boston, MA

« Secretion of toxic exosomes by muscle cells: role in ALS pathology »

Authors: **Laura Le Gall**[1,2], William J Duddy[1], Sylvain Roquevière[3], Mariot Virginie[4], Blandine Madji Hounoum[5], Jeanne Lainé[2], Romain Joubert[6], Julie Dumonceaux[4], Pascal Leblanc[7], Gisele Ouandaogo[2], Laura Robelin[8], Franscesca Ratti[7], Alexandre Mejat[7], Gillian Butler Browne[2], Jean Philippe Loeffler[8], Anne Cecile Durieux[9], Jose-Luis Gonzales De Aguilar[8], Helene Blasco[5], Cecile Martinat[3], Pierre Francois Pradat[10*], Stephanie Duguez[1*]

***Co-last authors**

Affiliations:

1- Northern Ireland Center for Stratified Medicine, Biomedical Sciences Research Institute, Londonderry, UK.
2- Myologie Centre de Recherche, Université Sorbonne, UMRS 974 UPMC, INSERM, FRE 3617 CNRS, AIM, Paris, France.
3- I-Stem, INSERM/UEVE UMR 861, I-STEM, AFM, Evry, France.
4- NIHR Biomedical Research Centre, University College London, Great Ormond Street Institute of Child Health and Great Ormond Street Hospital NHS Trust, London, UK.
5- Université François-Rabelais, INSERM U930 "Imagerie et Cerveau", CHRU de Tours, 10 Bv Tonnellé, 37044 Tours, France.
6- Unité Physiologie et Pathologie Moléculaires des Rétrovirus Endogènes et Infectieux, CNRS UMR 9196, Institut Gustave Roussy, Villejuif, France.
7- Laboratory of Molecular Biology of the Cell, Ecole Normale Supérieure de Lyon, Lyon, France.
8- Mécanismes Centraux et Périphériques de la Neurodégénérescence, Université de Strasbourg, INSERM U1118, Strasbourg, France.
9- LPE, Université Jean Monnet de Saint Etienne, Faculté de Médecine Jacques Lisfranc, Saint Etienne, France.
10- Département des Maladies du Système Nerveux, Hôpital de la Pitie-Salpetriere, Paris, France.

The cause of ALS remains unknown, and several studies performed on muscle cells from patients have suggested an involvement of skeletal muscle. We hypothesized that the muscle secretome was disrupted in ALS patients. To test this hypothesis, we extracted primary muscle stem cells from the deltoid muscle biopsies of sporadic ALS patients (n=18) and aged-matched healthy subjects (n=21). After differentiating the cells for 3 days into myotubes, we observed by RT-qPCR a significant upregulation of CD81, CD63, TSG101 and Rab5 – genes that are involved in exosomal biogenesis. When muscle stem cells were differentiated into myotubes, we observed a significantly greater amount of exosomes that were released into the culture medium of ALS myotubes. To test the effect of the exosomes on surrounding cells, we labelled them with PKH26 and tested their effect on healthy muscle cells over time. ALS and healthy exosomes started to be integrated into muscle cells as soon as 4 h – integration that gradually increased over 48h. Cell blebs – a signature of cellular stress – appeared as soon as 4h in ALS exosome-treated muscle cells and increased until 168h. Consequently, we observed a greater cell death at day 3 after treatment – as shown by a significantly higher level of H2Ax in nuclei and a greater loss of nuclei. In addition, we observed an atrophy in myotubes as the myonuclear domain was smaller in myotubes treated with ALS exosomes. Together the present data suggest that muscle stem cells have a disruption of exosomal biogenesis, and that ALS muscle exosomes are toxic to muscle cells – phenomena that are independent to muscle denervation.

We are now characterizing the content of these exosomes and determining whether the exosome content can act with a prion-like effect.

Secretion of toxic exosomes by muscle cells : role in ALS pathogenesis

Laura Le Gall[1,2], William J Duddy[1], Sylvain Roquevière[3], Mariot Virginie[4], Blandine Madji Hounoum[5], Jeanne Lainé[2], Romain Joubert[6], Julie Dumonceaux[4], Pascal Leblanc[7], Gisele Ouandaogo[2], Laura Robelin[8], Franscesca Ratti[7], Alexandre Mejat[7], Gillian Butler Browne[2], Jean Philippe Loeffler[8], Anne Cecile Durieux[9], Jose-Luis Gonzales De Aguilar[8], Helene Blasco[5], Cecile Martinat[3], Pierre Francois Pradat[10*], Stephanie Duguez[1*]

***Co-last authors**

1- Northern Ireland Center for Stratified Medicine, Biomedical Sciences Research Institute, Londonderry, UK.
2- Myologie Centre de Recherche, Université Sorbonne, UMRS 974 UPMC, INSERM, FRE 3617 CNRS, AIM, Paris, France.
3- I-Stem, INSERM/UEVE UMR 861, I-STEM, AFM, Evry, France.
4- NIHR Biomedical Research Centre, University College London, Great Ormond Street Institute of Child Health and Great Ormond Street Hospital NHS Trust, London, UK.
5- Université François-Rabelais, INSERM U930 "Imagerie et Cerveau", CHRU de Tours, 10 Bv Tonnellé, 37044 Tours, France.
6- Unité Physiologie et Pathologie Moléculaires des Rétrovirus Endogènes et Infectieux, CNRS UMR 9196, Institut Gustave Roussy, Villejuif, France.
7- Laboratory of Molecular Biology of the Cell, Ecole Normale Supérieure de Lyon, Lyon, France.
8- Mécanismes Centraux et Périphériques de la Neurodégénérescence, Université de Strasbourg, INSERM U1118, Strasbourg, France.
9- LPE, Université Jean Monnet de Saint Etienne, Faculté de Médecine Jacques Lisfranc, Saint Etienne, France.
10- Département des Maladies du Système Nerveux, Hôpital de la Pitie-Salpetriere, Paris, France.

Amyotrophic Lateral Sclerosis

- ✓ Rare neurodegenarative disorder
- ✓ Adult onset neurodegenerative disorder
- ✓ 90% sporadic cases

Upper motor neurons

Lower motor neurons

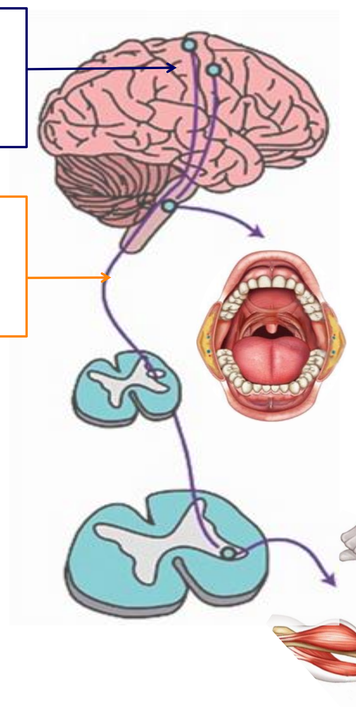

Rapid and fatal deterioration of the **lower** and **upper** motor neurons

↓ Muscle denervation

↓ Muscle damage (Muscle weakness & atrophy)

↓ Death (respiratory failure)

Hypothesis :

Toxic cellular environment

Published data suggest a disruption of the exosome pathway

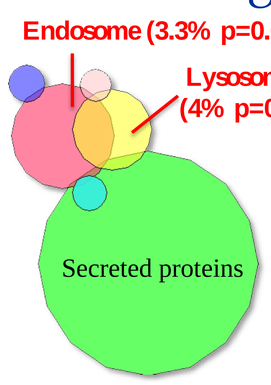

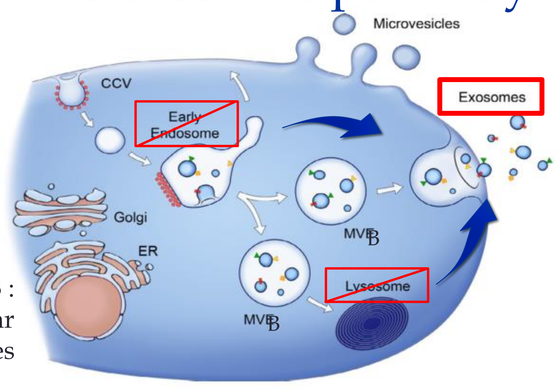

MVB : Multivesicular bodies

Axo-terminal degeneration at the neuromuscular junction

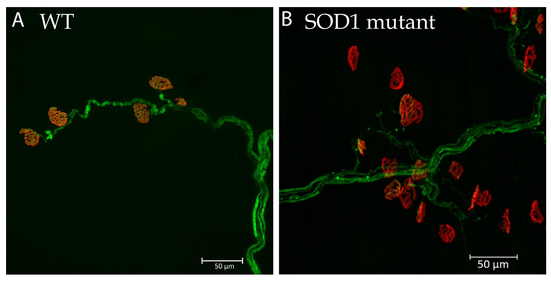

C Tallon et al., Neuroscience 312 (2016) 179-189

Hypothesis:

Muscle secretome– exosomes - disrupted in ALS pathology

Muscle exosomes

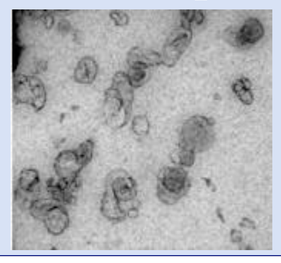

I. Primary muscle stem cells (MSCs) extraction

Healthy subjects (n=21) | Sporadic ALS patients (n=18)

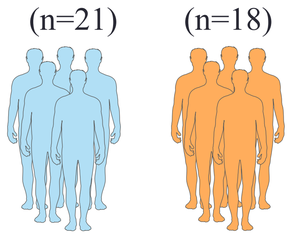

Deltoid muscle biospy

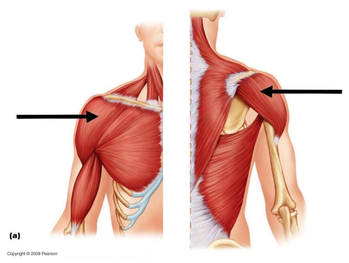

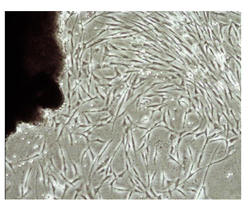

MSCs activation

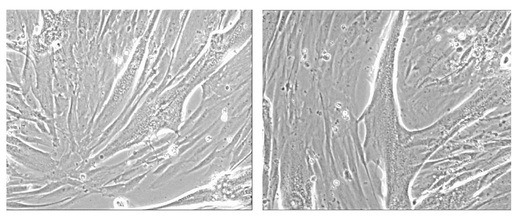

Myotube formation

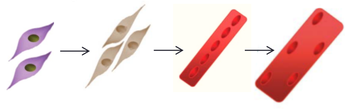

II. Up-regulation of exosomal markers in ALS muscle cells

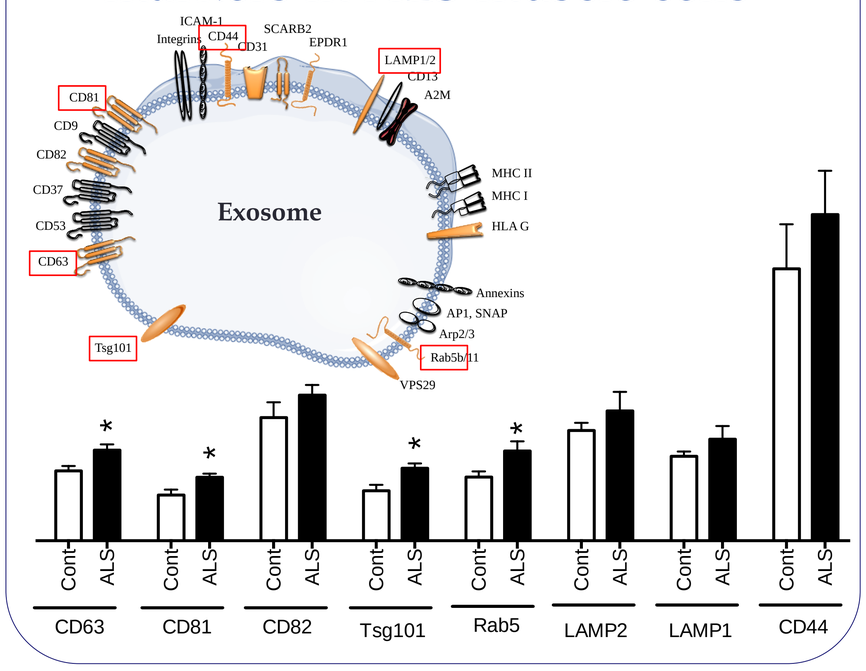

III. Accumulation of ALS exosomes in the culture medium

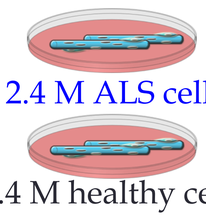

2.4 M ALS cells

2.4 M healthy cells

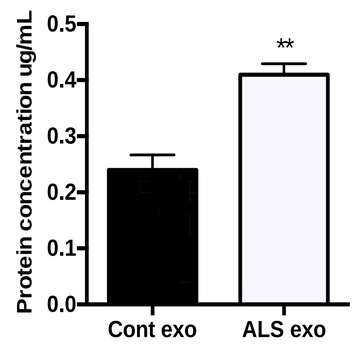

N=6 / group

V. Toxic autocrine and paracrine effects of ALS exosomes

3 days differentiation ALS myotubes

3 days differentiation healthy myotubes

Exosome extraction

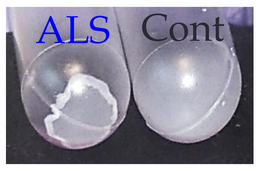

PKH26 labelling

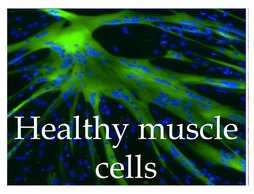

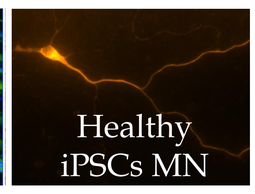

#1 Exosomes integration

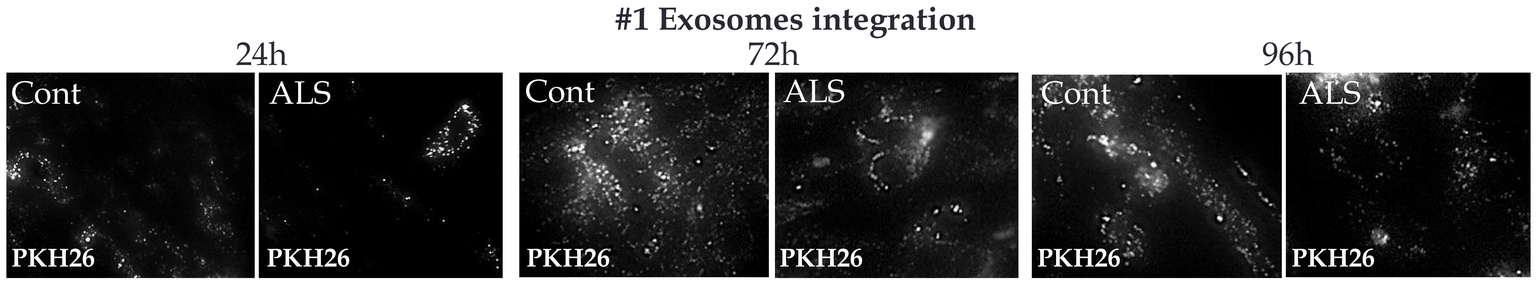

#2 Muscular atrophy

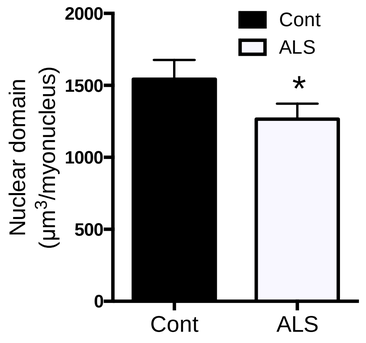

#3 Cell stress (blebbing)

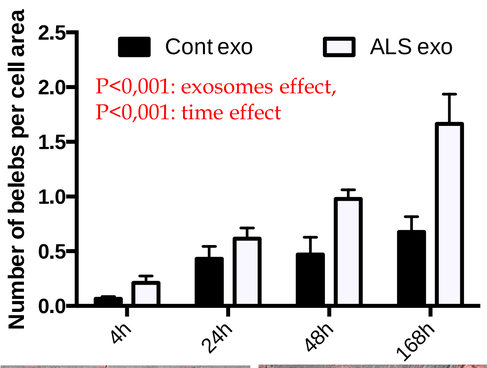

#4 Cell Death

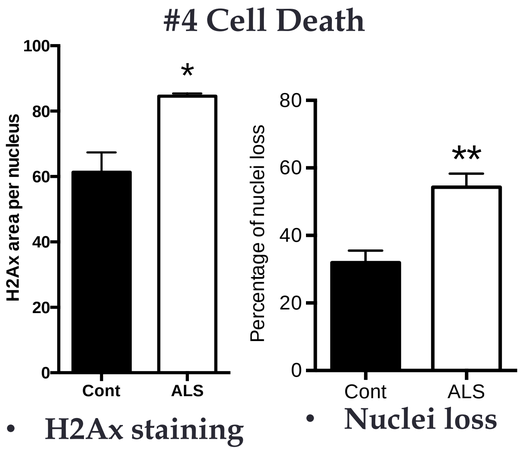

- H2Ax staining
- Nuclei loss

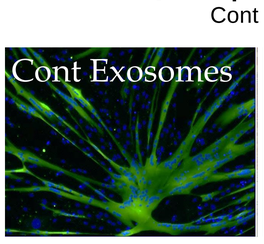

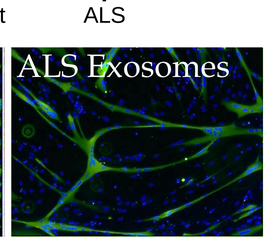

Myosin heavy chain Nuclei

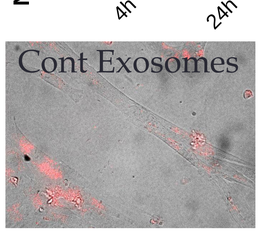

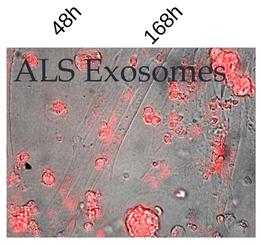

Blebbs containing labelled exosomes

#1 Cell stress (72h):

- Neurite length
- Branching

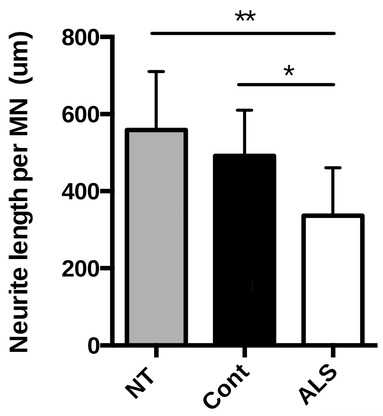

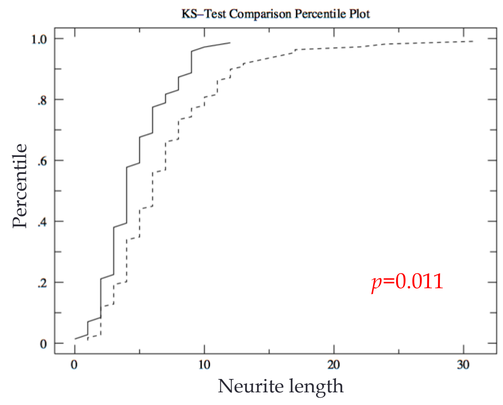

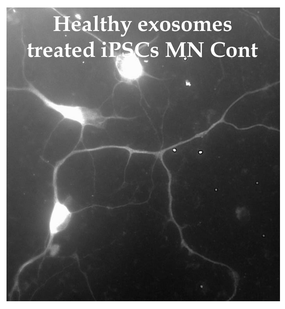

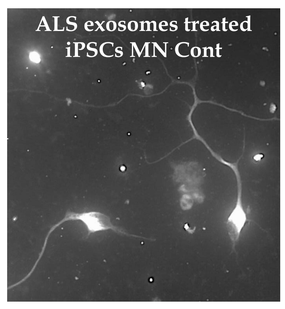

#2 Cell Death

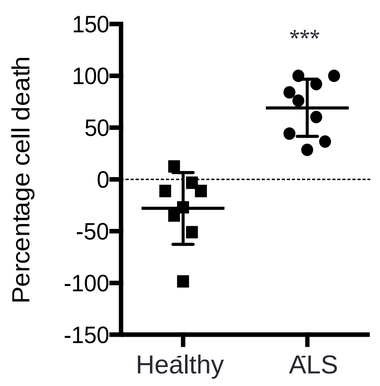

Aknowledgement

This work was supported by:

- the Association pour la Recherche sur la Sclérose Latérale Amyotrophique (ARSLA),
- INSERM &Direction Générale de l'Organisation des Soins (DGOS)
- the Association Française contre les myopathies (AFM),
- Target-ALS association and
- European Union Regional Development Fund (ERDF) EU Sustainable Competitiveness Programme for N. Ireland; Northern Ireland Public Health Agency (HSC R&D) & Ulster University.

Material & methods

Human primary cells extracted from Deltoid muscle biopsies:

- SBMA(n=12), ALS (n=18), SMA (n=12), Healthy subjects (n=15).
- All Male, 20-76 years old.
- Muscle cells sorted using CD56 MACS beads: >86% myogenic cells

- After removing cell debris and microparticles (centrifugation 200g,10 min RT; 2,000g 20 min 4C and filtration 0.22 mm), exosomes were extracted using Life Technologies kit (we validated the quality of the kit by electron microscopy and immunostaining and western blot)
- Labelled ALS or control exosomes were added to healthy human muscle stem cells or healthy human iPSC-motor neuron n=6/3 per group

3. 29th International Symposium on ALS/MND – Glasgow – UK

"Alteration of FUS pathway leading to a communication breakdown in ALS"

Laura Le Gall[1,2], William J Duddy[1], Sylvain Roquevière[3], Mariot Virginie[4], Julie Dumonceaux[4], TRANE group study, Olivier Lucas[5], Cedric Raoul[35], Susan Knoblach[6], Cecile Martinat[3], Jose-Luis Gonzales De Aguilar[7], Pierre Francois Pradat[8*], Stephanie Duguez[1*]

***Co-last authors**

Affiliations:

1- Northern Ireland Center for Stratified Medicine, Biomedical Sciences Research Institute, Londonderry, UK.
2- Myologie Centre de Recherche, Université Sorbonne, UMRS 974 UPMC, INSERM, FRE 3617 CNRS, AIM, Paris, France.
3- I-Stem, INSERM/UEVE UMR 861, I-STEM, AFM, Evry, France.
4- NIHR Biomedical Research Centre, University College London, Great Ormond Street Institute of Child Health and Great Ormond Street Hospital NHS Trust, London, UK.
5- Équipe Pathologies du motoneurone : inflammation et thérapie, INSERM U1051 – INM, Montpellier, France.
6- Children's National Medical Center, George Washington University, Washington, US.
7- Mécanismes Centraux et Périphériques de la Neurodégénérescence, Université de Strasbourg, INSERM U1118, Strasbourg, France.
8- Département des Maladies du Système Nerveux, Hôpital de la Pitie-Salpetriere, Paris, France.

Study group:
Gillian Butler Brown[1], Vincent Mouly[1], Gisele Ouandaogo[1] , Alexandre XX[2], Laura Robelin[2], Franscesca Ratti[3], Alexandre Mejat[3], Pascal LeBlanc[3], Salachas Francois[4], Anne Cecile Durieux[5], Loeffler jean Philippe[2]

1- Myologie Centre de Recherche, Université Sorbonne, UMRS 974 UPMC, INSERM, FRE 3617 CNRS, AIM, Paris, France
2- Mécanismes Centraux et Périphériques de la Neurodégénérescence, Université de Strasbourg, INSERM U1118, Strasbourg, France
3- Laboratory of Molecular Biology of the Cell, Ecole Normale Supérieure de Lyon, Lyon, France.
4- Département des Maladies du Système Nerveux, Hôpital de la Pitie-Salpetriere, Paris, France.
5- LPE, Université Jean Monnet de Saint Etienne, Faculté de Médecine Jacques Lisfranc, Saint Etienne, France.

Background :

To date ALS remains incurable and the primary involvement of muscle in ALS pathogenesis is still controversial. However, there is now evidence implying a perturbation of pathways involved in the exosomal pathway in sporadic as well as familial cases. Moreover, it has been demonstrated that pathological molecular and cellular changes occur at the neuromuscular junction prior to motor neuron degeneration and symptoms onset. Altogether these data suggest that the skeletal muscle could participate to ALS.

Secretion of neurotoxic vesicles by muscle cells of ALS patients Laura Le Gall

Objectives:

So far, our data has demonstrated an altered exosomal secretion occurring from muscle of sporadic ALS patients. We further explored the function of exosomes in ALS pathology, and more particularly how the muscle exosomes interact with the FUS pathways.

Methods:

To explore this in a way that is independent and upstream of muscle denervation we used primary muscle stem cells extracted from deltoid muscles biopsies from sporadic ALS patients (n=18) and aged-matched healthy subjects (n=21). After differentiating the cells for 3 days, exosomes were extracted from the culture medium. Exosomal proteins were extracted using 8M Urea buffer and quantified using the BCA Protein Assay. Equal amounts of PKH26-labelled ALS and healthy exosomes were added to the culture medium of healthy muscle cells and IPS-derived motor neurons. We created healthy muscle cell lines expressing tagged form of wild type FUS (FLAG-FUS), TDP43 (FLAG-TDP43) or SOD1 (FLAG-SOD1).

Results:

ALS exosomes induce an increased cell death when added to the culture medium of healthy human muscles and IPS-derived motor neurons. A consistently greater cell death was observed when muscle cells were treated with ALS exosomes - no matter the amounts of exosomes loaded – suggesting that both quantity and quality of exosomes are important for the toxicity of ALS exosomes.

Recently, we detected the presence of FUS in exosomes. To further investigate the role of exosomes on the FUS pathway, all FLAG-FUS/TDP43/SOD1 cell lines were treated with equal amounts of exosomes. ALS exosomes induced greater cell stress and cell death than healthy exosomes, in all cell lines, but the effect was markedly greater in FLAG-FUS cell line. Interestingly, FUS distribution is also altered in ALS muscle cells.

Discussion:

Together, these data demonstrate that the muscle cells from sporadic patients secrete toxic agents - for muscle cells and motor neurons - through their exosomes. The increased toxicity of ALS exosomes with FLAG-FUS cell line is suggesting that ALS exosomes toxicity is exacerbated in the presence of FUS over-expression. Moreover, results are showing that FUS function is impacted in ALS muscle cells. We are now further exploring the impact of ALS muscle exosomes with the FUS pathway.

Aknowledgements:

Target-ALS (ViTAL consortium, PI: S Duguez), ARsLA (TEAM consortium, PI: S. Duguez ; PhD fellowship: L. Le Gall), Invest NI (PI: T. Bjourson) and Sorbonne University.

Secretion of neurotoxic vesicles by muscle cells of ALS patients

Laura Le Gall[1,2], William J Duddy[1*], Cecile Martinat[3*], Sylvain Roquevière[3], Mariot Virginie[4], Jeanne Lainé[2], Udayageetha Vijayakumar[1], Susan Knoblach[5], Cedric Raoul[6], Olivier Lucas[6], Study group TRANE, Giorgia Querin[7,8], Thomas Voit[4], Julie Dumonceaux[4], Gillian Butler Browne[2], Jose-Luis Gonzales De Aguilar[9], Pierre Francois Pradat[1,7,8], Stephanie Duguez[1]

1- Northern Ireland Center for Stratified Medicine, Biomedical Sciences Research Institute, Londonderry, UK.
2- Myologie Centre de Recherche, Université Sorbonne, UMRS 974 UPMC, INSERM, FRE 3617 CNRS, AIM, Paris, France.
3- I-Stem, INSERM/UEVE UMR 861, I-STEM, AFM, Evry, France
4- NIHR Biomedical Research Centre, University College London, Great Ormond Street Institute of Child Health and Great Ormond Street Hospital NHS Trust, London, UK.
5- George Washington University, Genetic Medicine, Children's National Medical Center, Washington, US.
6- INSERM U1051-Institut des Neurosciences de Montpellier - Déficits sensoriels et moteurs, Montpellier, France.
7- Sorbonne Université, CNRS, INSERM, Laboratoire d'Imagerie Biomédicale, Paris, France
8- APHP, Département de Neurologie, Hôpital Pitié-Salpêtrière, Centre référent SLA, Paris, France
9- Mécanismes Centraux et Périphériques de la Neurodégénérescence, Université de Strasbourg, INSERM U1118, Strasbourg, France.

Motor neuron environment is toxic in ALS

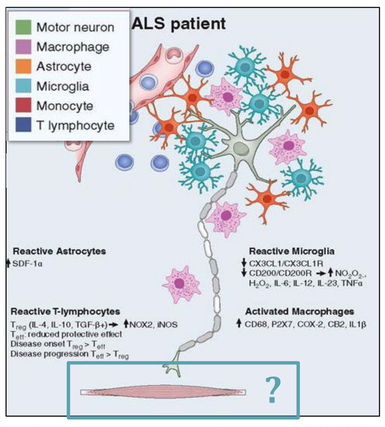

Rizzo et al., Cell Mol Life Sci (2014) Mar;71(6):999-1015

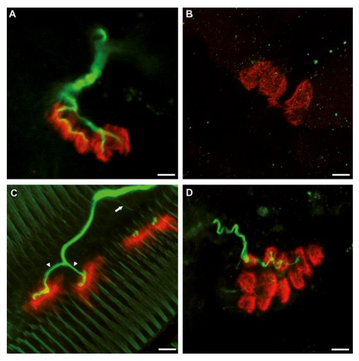

Bruneteau G et al., Ann Clin Transl Neurol. 2015 Apr;2(24):362-72

Hypothesis:
Muscle is participating to motor neuron degeneration and death

Subject samples table : summarizing the subject samples used for each type of experiment.

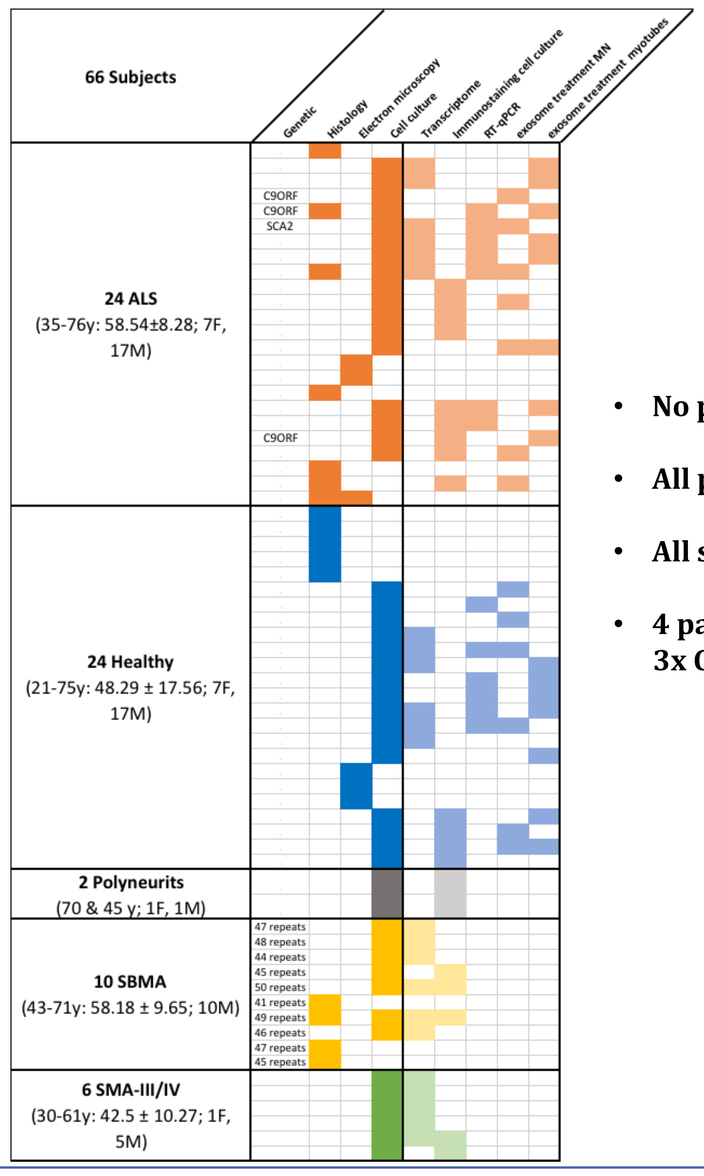

- **No post-mortem tissue**
- **All primary cells**
- **All sporadic ALS patients**
- **4 patients with mutations: 3x C9ORF72, 1x Sca2**

Increased accumulation and secretion of exosomes by ALS myotubes

- Accumulation of exosomal markers at the periphery of the myofibers

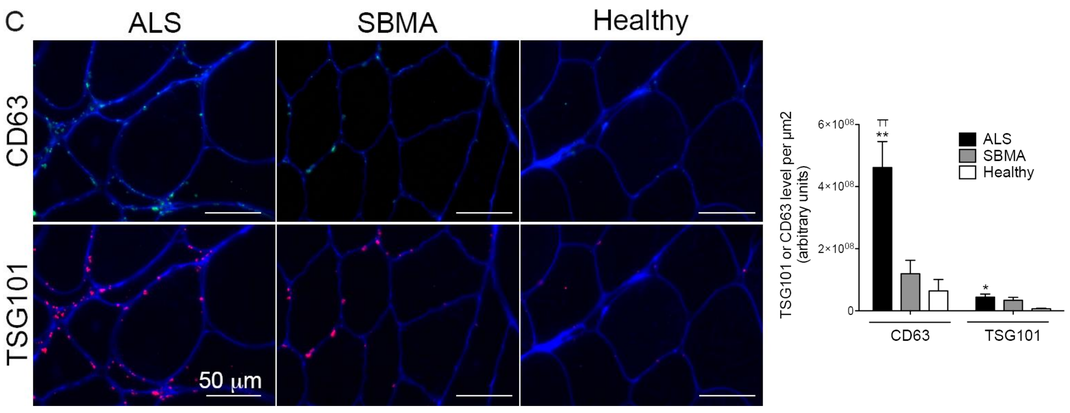

- Accumulation of exosomal markers in ALS myotubes

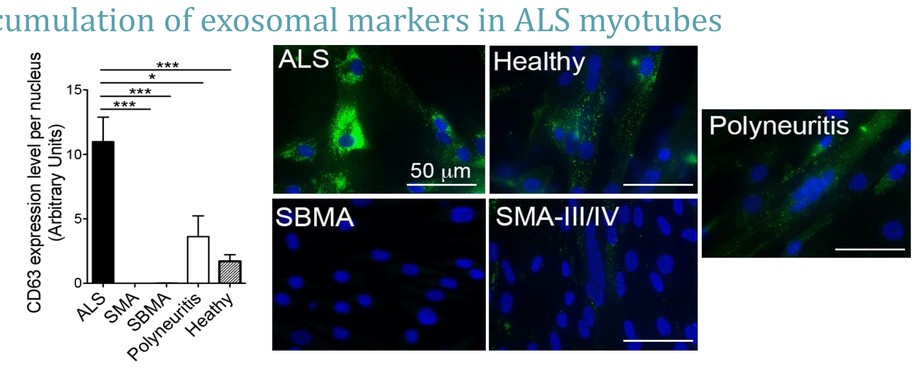

- ALS myotubes secrete exosomes

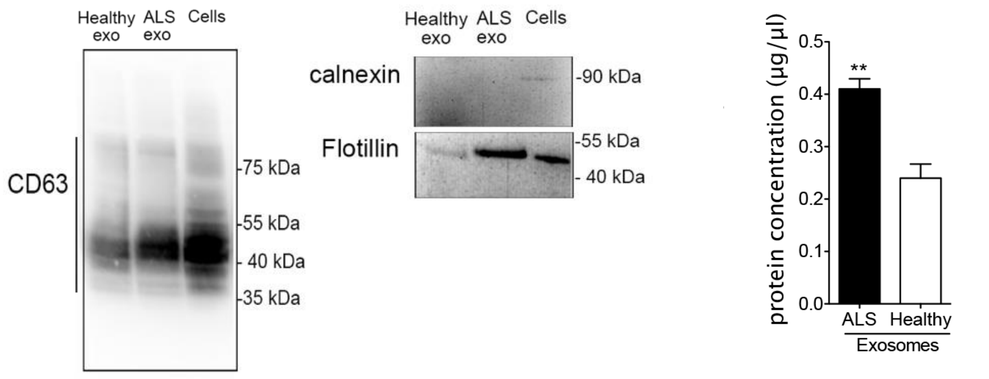

ALS muscle cells secrete exosomes toxic towards motor neurons

3 days differentiation ALS myotubes

3 days differentiation healthy myotubes

Exosome extraction

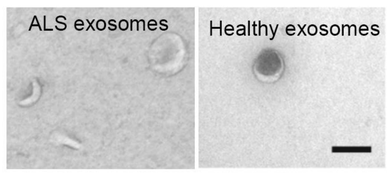

PKH26 labelling

Equal amount : 0.5 µg ALS / healthy exosomes

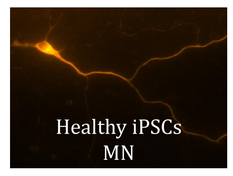

- ALS exosomes integration by iPSCs MN

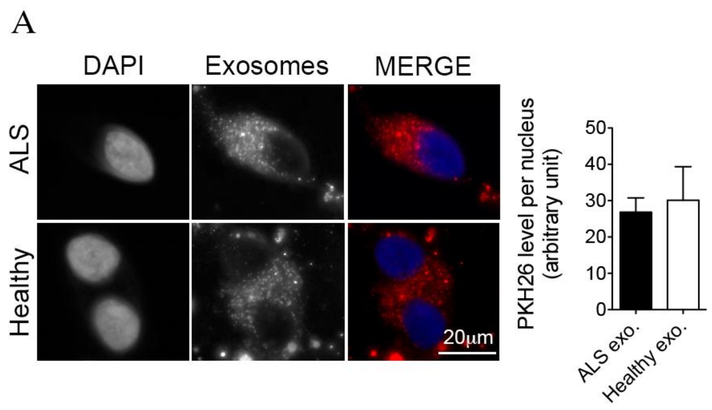

- ALS exosomes induce shorter neurites

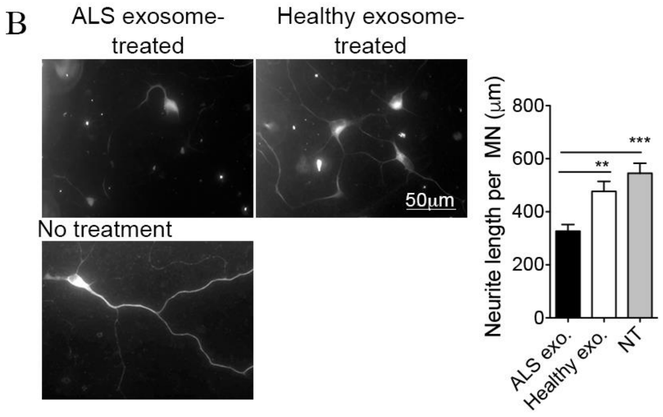

- ALS exosomes induce less branching

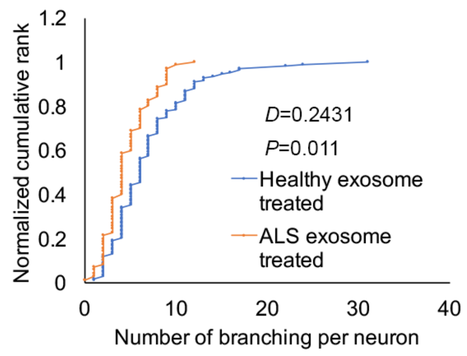

- ALS exosomes induce greater cell death

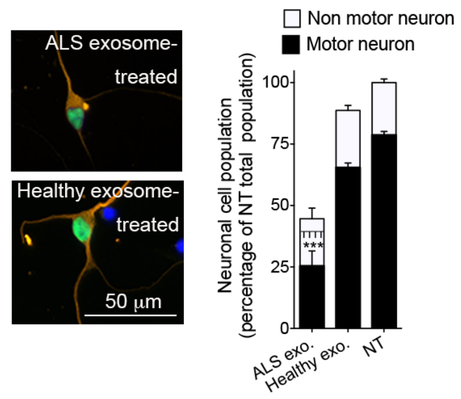

Involvement of RNA processing in exosome toxicity

- ALS exosomes induce nuclear RNA accumulation

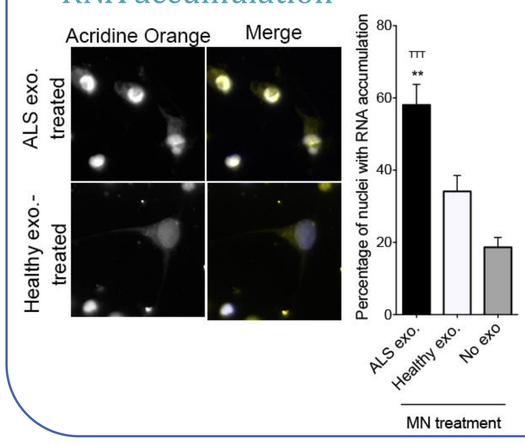

- Exosomes contained FUS and FUS binding partners

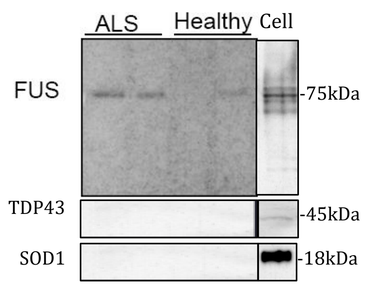

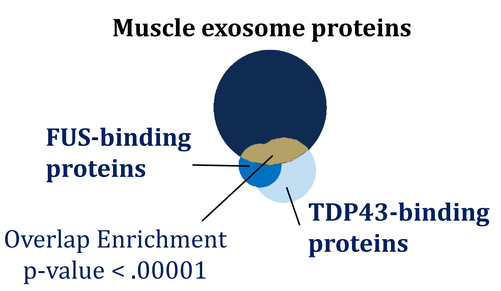

Toxicity of ALS muscle exosomes to healthy motor neurons involves the FUS protein

- Cells with high expression level of FUS are more sensitive to ALS exosomes
- Cells with low expression level of FUS are less sensitive to ALS exosomes
- MN express a greater level of FUS

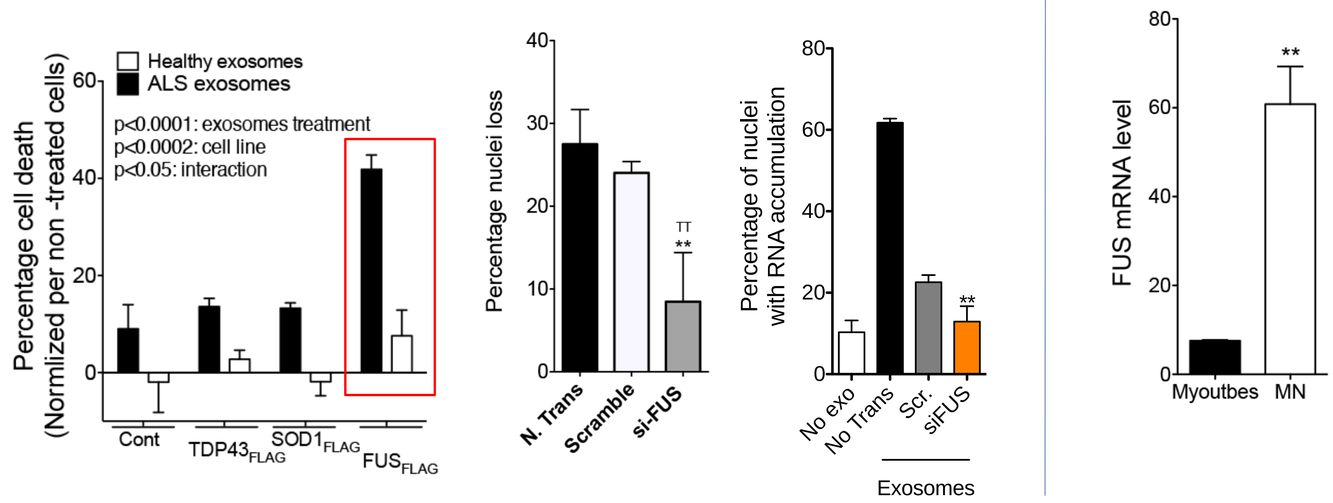

Conclusion

- **ALS muscle secrete neurotoxic exosomes**
- **ALS exosomes induce a RNA processing disruption**
- **FUS dependant toxicity**
- **Exosomes might be involved in propagation of ALS**

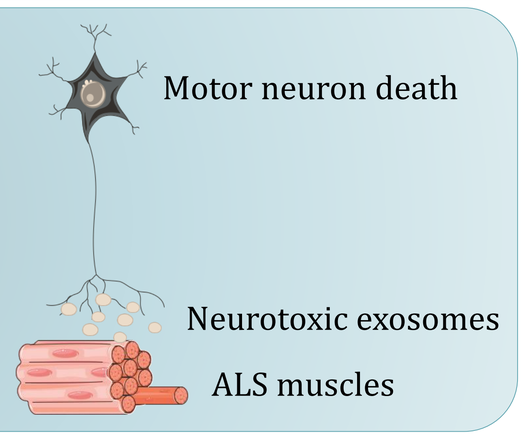

Acknowledgement

This work was supported by:
- the Association pour la Recherche sur la Sclérose Latérale Amyotrophique (ARSLA),
- INSERM &Direction Générale de l'Organisation des Soins (DGOS)
- the Association Française contre les myopathies (AFM),
- Target-ALS association and
- European Union Regional Development Fund (ERDF) EU Sustainable Competitiveness Programme for N. Ireland; Northern Ireland Public Health Agency (HSC R&D) & Ulster University.

Oral communications

1. **2ème Journées de la recherche sur la SLA et les maladies du neurone moteur – Paris – France**
   « Jeune chercheur ARsLA 2016 » Award

2. **3ème Journées de la recherche sur la SLA et les maladies du neurone moteur – Paris – France**

3. **3MT Competition – Ulster University, Derry/Londonderry – UK**
   People's Choice Award 2018

Burning bridges between will and action :
A communication breakdown in ALS

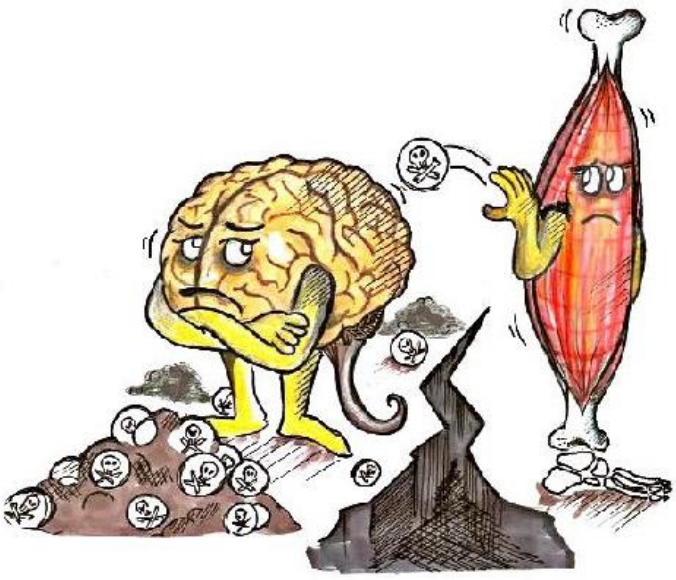

For many years now, a vicious serial killer is attacking the nerves of ALS patients. What is ALS? ALS stands for Amyotrophic Lateral Sclerosis but I'm sure that some of you have already heard about this disease during summer 2014 when the ALS ice bucket challenge went viral. Today, many investigators are trying to solve the "ALS case" and here are the facts.

It is easy for us to move our legs when we want to, right? We can stimulate our muscles by impulses that travel from our brain towards our muscles. Critically important are the nerves that innervate our muscles, called motor neurons as they create a valuable bridge between our brain and muscles. These neurons are essential, they allow us to walk, talk, speak and more importantly breathe.

Unfortunately for ALS patients, these motor neurons are killed, breaking this vital line of communication. Eventually, the ability to start and control voluntary movement is lost, patients' muscles no longer receive stimulation and will gradually weaken, resulting in paralysis and ultimately death. It is challenging to predict how fast ALS will progress, in fact Dr Stephen Hawking's longevity was quite rare since ALS patients are only given 2 to 5 years to live.

Today there is no cure available for ALS and it is critical to identify the murderer among a long list of suspects. As a PhD student I am now taking part in this investigation and my work aims to determine if the muscle is indeed a prime suspect.

You may be wondering, "why the muscle?" when many researchers are more interested in other cells surrounding the motor neurons in the brain. Well, as surprising as it may sound, your muscles are very chatty and one way for them to communicate is by releasing molecules packaged inside vesicles. A vesicle could be compared to a very small soap bubble that is surrounded by a membrane and filled with molecules, just like a soap bubble is surrounded by a film of soap and filled with air.

My PhD project aims to investigate the effect of vesicles released by ALS muscle and more particularly, identify whether their contents are toxic. If this is the case, then my project may provide an explanation of how the muscle may be involved in the death of motor neurons in ALS.

ALS is not an incurable disease! It is just a misunderstood one and our best chances to identify a cure is to catch the killer.

References

1. Bäumer, D., Talbot, K. & Turner, M. R. *Advances in motor neurone disease*. *Journal of the Royal Society of Medicine* **107**, 14–21 (SAGE PublicationsSage UK: London, England, 2014).

2. Gordon, P. H. Amyotrophic Lateral Sclerosis: An update for 2013 Clinical Features, Pathophysiology, Management and Therapeutic Trials. *Aging Dis.* **4**, 295–310 (2013).

3. Goldstein, L. H. & Abrahams, S. Changes in cognition and behaviour in amyotrophic lateral sclerosis: Nature of impairment and implications for assessment. *The Lancet Neurology* **12**, 368–380 (2013).

4. Brooks, B. R. *et al.* El Escorial World Federation of Neurology criteria for the diagnosis of amyotrophic lateral sclerosis. in *Journal of the Neurological Sciences* **124**, 96–107 (1994).

5. Brooks, B. R., Miller, R. G., Swash, M. & Munsat, T. L. El Escorial revisited: Revised criteria for the diagnosis of amyotrophic lateral sclerosis. *Amyotroph. Lateral Scler. Other Mot. Neuron Disord.* **1**, 293–299 (2000).

6. de Carvalho, M. *et al.* Electrodiagnostic criteria for diagnosis of ALS. *Clin. Neurophysiol.* **119**, 497–503 (2008).

7. Talbott, E. O., Malek, A. M. & Lacomis, D. The epidemiology of amyotrophic lateral sclerosis. *Handb. Clin. Neurol.* **138**, 225–238 (2016).

8. Hardiman, O. *et al.* The changing picture of amyotrophic lateral sclerosis: lessons from European registers. *J. Neurol. Neurosurg. Psychiatry* **88**, 557–563 (2017).

9. Chiò, A. *et al.* Global Epidemiology of Amyotrophic Lateral Sclerosis: A Systematic Review of the Published Literature. *Neuroepidemiology* **41**, 118–130 (2013).

10. Benjaminsen, E., Alstadhaug, K. B., Gulsvik, M., Baloch, F. K. & Odeh, F. Amyotrophic lateral sclerosis in Nordland county, Norway, 2000–2015: prevalence, incidence, and clinical features. *Amyotroph. Lateral Scler. Front. Degener.* 1–6 (2018). doi:10.1080/21678421.2018.1513534

11. Paul Mehta, M. *et al.* Prevalence of Amyotrophic Lateral Sclerosis — United States, 2014. doi:10.1001/jama.2014.9799

12. Arthur, K. C. *et al.* Projected increase in amyotrophic lateral sclerosis from 2015 to 2040. (2016). doi:10.1038/ncomms12408

13. Salameh, J., Brown, R. & Berry, J. Amyotrophic Lateral Sclerosis: Review. *Semin. Neurol.* **35**, 469–476 (2015).

14. Kiernan, M. C. *et al.* Amyotrophic lateral sclerosis. *Lancet* **377**, 942–955 (2011).

15. Turner, M. R., Barnwell, J., Al-Chalabi, A. & Eisen, A. Young-onset amyotrophic lateral sclerosis: historical and other observations. *Brain* **135**, 2883–2891 (2012).

16. Sabatelli, M. *et al. Natural history of young-adult amyotrophic lateral sclerosis*. *Neurology* **71**, 876–881 (2008).

17. Forbes, R. B., Colville, S., Swingler, R. J. & Scottish ALS/MND Register. *The epidemiology of amyotrophic lateral sclerosis (ALS/MND) in people aged 80 or over*. *Age and Ageing* **33**, 131–134 (2004).

18. Liu, X., He, J., Gitler, A. D. & Fan, D. The epidemiology and genetics of Amyotrophic lateral sclerosis in China. *Brain Res.* **1693**, 121–126 (2018).

19. Couratier, P. *et al.* Epidemiology of amyotrophic lateral sclerosis: A review of literature. *Rev. Neurol. (Paris).* **172**, 37–45 (2016).

20. Tard, C., Defebvre, L., Moreau, C., Devos, D. & Danel-Brunaud, V. Clinical features of amyotrophic lateral sclerosis and their prognostic value. *Rev. Neurol. (Paris).* **173**, 263–272 (2017).

21. Hardiman, O. *et al.* Amyotrophic lateral sclerosis. *Nat. Rev. Dis. Prim.* **3**, 17071 (2017).

22. van Es, M. A. *et al.* Amyotrophic lateral sclerosis. *Lancet* **390**, 2084–2098 (2017).

23. Swinnen, B. & Robberecht, W. The phenotypic variability of amyotrophic lateral sclerosis. *Nature Reviews Neurology* **10**, 661–670 (2014).

24. Lillo, P. & Hodges, J. R. Frontotemporal dementia and motor neurone disease: Overlapping clinic-pathological disorders. *J. Clin. Neurosci.* **16**, 1131–1135 (2009).

25. Chiò, A. *et al. Prognostic factors in ALS: A critical review*. *Amyotrophic Lateral Sclerosis* **10**, 310–323 (Taylor & Francis, 2009).

26. D'Amico, E., Pasmantier, M., Lee, Y.-W., Weimer, L. & Mitsumoto, H. Clinical evolution of pure upper motor neuron disease/dysfunction (PUMMD). *Muscle Nerve* **47**, 28–32 (2013).

27. Al-Chalabi, A. *et al.* Amyotrophic lateral sclerosis: moving towards a new classification system. *The Lancet Neurology* **15**, 1182–1194 (2016).

28. Rowland, L. P. Progressive muscular atrophy and other lower motor neuron syndromes of adults. *Muscle Nerve* **41**, 161–165 (2010).

29. Crockford, C. *et al.* ALS-specific cognitive and behavior changes associated with advancing disease stage in ALS. *Neurology* **91**, e1370–e1380 (2018).

30. Neary, D. *et al. Frontotemporal lobar degeneration: A consensus on clinical diagnostic criteria*. *Neurology* **51**, 1546–54 (1998).

31. Bak, T. H. & Chandran, S. What wires together dies together: Verbs, actions and neurodegeneration in motor neuron disease. *Cortex* **48**, 936–944 (2012).

32. Rascovsky, K. *et al.* Sensitivity of revised diagnostic criteria for the behavioural variant of frontotemporal dementia. *Brain* **134**, 2456–2477 (2011).

33. Strong, M. J. *et al. Amyotrophic lateral sclerosis - frontotemporal spectrum disorder (ALS-FTSD): Revised diagnostic criteria*. *Amyotrophic Lateral Sclerosis and Frontotemporal Degeneration* **18**, 153–174 (Taylor & Francis, 2017).

34. Okita, T. *et al.* Can Awaji ALS criteria provide earlier diagnosis than the revised El Escorial criteria? *J. Neurol. Sci.* **302**, 29–32 (2011).

35. Abrahams, S., Newton, J., Niven, E., Foley, J. & Bak, T. H. Screening for cognition and behaviour changes in ALS. *Amyotroph. Lateral Scler. Front. Degener.* **15**, 9–14 (2014).

36. The ALS CNTF Treatment Study (ACTS) Phase I-II Study Group *et al.* The Amyotrophic Lateral Sclerosis Functional Rating Scale: Assessment of Activities of Daily Living in Patients With Amyotrophic Lateral Sclerosis. *Archives of Neurology* **53**, 141 (1996).

37. Cedarbaum, J. M. *et al. The ALSFRS-R: a revised ALS functional rating scale that incorporates*

assessments of respiratory function. Journal of the Neurological Sciences **169**, 13–21 (Elsevier, 1999).

38. Gordon, P. H., Miller, R. G. & Moore, D. H. *ALSFRS-R. Amyotrophic Lateral Sclerosis and Other Motor Neuron Disorders* **5**, 90–93 (2004).

39. Volk, A. E. *et al.* Current knowledge and recent insights into the genetic basis of amyotrophic lateral sclerosis Introduction and clinical aspects. *medizinische Genet.* (2018). doi:10.1007/s11825-018-0185-3

40. Mathis, S., Goizet, C., Soulages, A., Vallat, J.-M. & Masson, G. Le. *Genetics of amyotrophic lateral sclerosis: A review. Journal of the Neurological Sciences* **399**, 217–226 (2019).

41. Zou, Z.-Y. *et al.* Genetic epidemiology of amyotrophic lateral sclerosis: a systematic review and meta-analysis. *J Neurol Neurosurg Psychiatry* **88**, 540–549 (2017).

42. Rosen, D. R. *et al.* Mutations in Cu/Zn superoxide dismutase gene are associated with familial amyotrophic lateral sclerosis. *Nature* **155**, 400–402 (1993).

43. DeJesus-Hernandez, M. *et al.* Expanded GGGGCC Hexanucleotide Repeat in Noncoding Region of C9ORF72 Causes Chromosome 9p-Linked FTD and ALS. *Neuron* **72**, 245–256 (2011).

44. Renton, A. E. *et al.* A Hexanucleotide Repeat Expansion in C9ORF72 Is the Cause of Chromosome 9p21-Linked ALS-FTD. *Neuron* **72**, 257–268 (2011).

45. Balendra, R. & Isaacs, A. M. C9orf72-mediated ALS and FTD: multiple pathways to disease. *Nat. Rev. Neurol.* **14**, 544–558 (2018).

46. Butti, Z. & Patten, S. A. RNA Dysregulation in Amyotrophic Lateral Sclerosis. (2019). doi:10.3389/fgene.2018.00712

47. Taylor, J. P., Brown, R. H. & Cleveland, D. W. Decoding ALS: from genes to mechanism. *Nature* **539**, 197–206 (2016).

48. Foxe, D. *et al.* Intrafamilial Phenotypic Variability in the C9orf72 Gene Expansion: 2 Case Studies. *Front. Psychol.* **9**, 1615 (2018).

49. Sreedharan, J. *et al.* TDP-43 Mutations in Familial and Sporadic Amyotrophic Lateral Sclerosis. *Science (80-.).* **319**, 1668–1672 (2008).

50. Kabashi, E. *et al.* Gain and loss of function of ALS-related mutations of TARDBP (TDP-43) cause motor deficits in vivo. *Hum. Mol. Genet.* **19**, 671–683 (2010).

51. Iguchi, Y. *et al.* Loss of TDP-43 causes age-dependent progressive motor neuron degeneration. *Brain* **136**, 1371–1382 (2013).

52. Yang, C. *et al.* Partial loss of TDP-43 function causes phenotypes of amyotrophic lateral sclerosis. *Proc. Natl. Acad. Sci. U. S. A.* **111**, E1121-9 (2014).

53. Vance, C. *et al.* Mutations in FUS, an RNA Processing Protein, Cause Familial Amyotrophic Lateral Sclerosis Type 6. *Science (80-.).* **323**, 1208–1211 (2009).

54. Kwiatkowski, T. J. *et al.* Mutations in the FUS/TLS gene on chromosome 16 cause familial amyotrophic lateral sclerosis. *Science* **323**, 1205–8 (2009).

55. Dormann, D. & Haass, C. TDP-43 and FUS: a nuclear affair. *Trends Neurosci.* **34**, 339–348 (2011).

56. Chen, H.-J. *et al.* Characterization of the properties of a novel mutation in VAPB in familial

amyotrophic lateral sclerosis. *J. Biol. Chem.* **285**, 40266–81 (2010).

57. Prosser, D. C., Tran, D., Gougeon, P.-Y., Verly, C. & Ngsee, J. K. FFAT rescues VAPA-mediated inhibition of ER-to-Golgi transport and VAPB-mediated ER aggregation. *J. Cell Sci.* **121**, 3052–61 (2008).

58. Ju, J. S. *et al.* Valosin-containing protein (VCP) is required for autophagy and is disrupted in VCP disease. *J. Cell Biol.* **187**, 875–888 (2009).

59. Greenway, M. J. *et al.* A novel candidate region for ALS on chromosome 14q11.2. *Neurology* **63**, 1936–1938 (2004).

60. Bennett, C. L. *et al.* Senataxin mutations elicit motor neuron degeneration phenotypes and yield TDP-43 mislocalization in ALS4 mice and human patients. *Acta Neuropathol.* **136**, 425–443 (2018).

61. Fecto, F. *et al. SQSTM1 Mutations in Familial and Sporadic Amyotrophic Lateral Sclerosis*. *Archives of Neurology* **68**, 1440 (American Medical Association, 2011).

62. Goutman, S. A., Chen, K. S., Paez-Colasante, X. & Feldman, E. L. Emerging understanding of the genotype–phenotype relationship in amyotrophic lateral sclerosis. *Handbook of Clinical Neurology* **148**, 603–623 (2018).

63. Mizuno, Y. *et al.* Immunoreactivities of p62, an ubiqutin-binding protein, in the spinal anterior horn cells of patients with amyotrophic lateral sclerosis. (2006). doi:10.1016/j.jns.2006.05.060

64. Yang, Y. *et al.* The gene encoding alsin , a protein with three guanine-nucleotide exchange factor domains , is mutated in a form of recessive amyotrophic lateral sclerosis. **29**, 160–165 (2001).

65. Toth, R. P. & Atkin, J. D. Dysfunction of Optineurin in Amyotrophic Lateral Sclerosis and Glaucoma. *Front. Immunol.* **9**, 1017 (2018).

66. Richter, B. *et al.* Phosphorylation of OPTN by TBK1 enhances its binding to Ub chains and promotes selective autophagy of damaged mitochondria. *Proc. Natl. Acad. Sci.* **113**, 4039–4044 (2016).

67. Teyssou, E. *et al.* Novel UBQLN2 mutations linked to amyotrophic lateral sclerosis and atypical hereditary spastic paraplegia phenotype through defective HSP70-mediated proteolysis. *Neurobiol. Aging* **58**, 239.e11-239.e20 (2017).

68. Williams, K. L. *et al.* UBQLN2/ubiquilin 2 mutation and pathology in familial amyotrophic lateral sclerosis. *Neurobiol. Aging* **33**, 2527.e3-2527.e10 (2012).

69. Boillée, S., Vande Velde, C. & Cleveland, D. W. ALS: a disease of motor neurons and their nonneuronal neighbors. *Neuron* **52**, 39–59 (2006).

70. Gupta, R. *et al.* The Proline/Arginine Dipeptide from Hexanucleotide Repeat Expanded C9ORF72 Inhibits the Proteasome. *eNeuro* **4**, ENEURO.0249-16.2017 (2017).

71. Mitsumoto, H. *et al. Oxidative stress biomarkers in sporadic ALS*. *Amyotrophic Lateral Sclerosis* **9**, 177–183 (Taylor & Francis, 2008).

72. Chang, Y. *et al.* Messenger RNA Oxidation Occurs Early in Disease Pathogenesis and Promotes Motor Neuron Degeneration in ALS. *PLoS One* **3**, e2849 (2008).

73. Laslo, P., Lipski, J., Nicholson, L. F. B., Miles, G. B. & Funk, G. D. GluR2 AMPA Receptor Subunit Expression in Motoneurons at Low and High Risk for Degeneration in Amyotrophic Lateral Sclerosis. *Exp. Neurol.* **169**, 461–471 (2001).

74. De Vos, K. J. *et al.* Familial amyotrophic lateral sclerosis-linked SOD1 mutants perturb fast axonal transport to reduce axonal mitochondria content Europe PMC Funders Group. *Hum Mol Genet* **16**, 2720–2728 (2007).

75. Williamson, T. L. & Cleveland, D. W. Slowing of axonal transport is a very early event in the toxicity of ALS–linked SOD1 mutants to motor neurons. *Nat. Neurosci.* **2**, 50–56 (1999).

76. Nishimura, A. L. *et al. A Mutation in the Vesicle-Trafficking Protein VAPB Causes Late-Onset Spinal Muscular Atrophy and Amyotrophic Lateral Sclerosis*. *Am. J. Hum. Genet* **75**, (2004).

77. Maruyama, H. *et al.* Mutations of optineurin in amyotrophic lateral sclerosis. *Nature* **465**, 223–226 (2010).

78. Lagier-Tourenne, C. *et al.* Divergent roles of ALS-linked proteins FUS/TLS and TDP-43 intersect in processing long pre-mRNAs. *Nat. Neurosci.* **15**, 1488–1497 (2012).

79. Herzog, J. J., Deshpande, M., Shapiro, L., Rodal, A. A. & Paradis, S. TDP-43 misexpression causes defects in dendritic growth. *Sci. Rep.* **7**, 15656 (2017).

80. Polymenidou, M. *et al.* Long pre-mRNA depletion and RNA missplicing contribute to neuronal vulnerability from loss of TDP-43. *Nat. Neurosci.* **14**, 459–468 (2011).

81. Haeusler, A. R., Donnelly, C. J. & Rothstein, J. D. The expanding biology of the C9orf72 nucleotide repeat expansion in neurodegenerative disease. *Nature Reviews Neuroscience* **17**, 383–395 (2016).

82. Taylor, J. P., Brown, R. H., Cleveland, D. W. & Cleveland, D. W. Decoding ALS: from genes to mechanism. *Nature* **539**, 197–206 (2016).

83. Webster, C. P. *et al.* The C9orf72 protein interacts with Rab1a and the ULK1 complex to regulate initiation of autophagy. *EMBO J.* **35**, 1656–76 (2016).

84. Leigh, P. N. *et al.* Ubiquitin-immunoreactive intraneuronal inclusions in amyotrophic lateral sclerosis. Morphology, distribution, and specificity. *Brain* **114 (Pt 2)**, 775–88 (1991).

85. Nishitoh, H. *et al.* ALS-linked mutant SOD1 induces ER stress- and ASK1-dependent motor neuron death by targeting Derlin-1. *Genes Dev.* **22**, 1451–1464 (2008).

86. Vance, C. *et al.* ALS mutant FUS disrupts nuclear localization and sequesters wild-type FUS within cytoplasmic stress granules. *Hum. Mol. Genet.* **22**, 2676–2688 (2013).

87. Meyer, H. H., Wang, Y. & Warren, G. Direct binding of ubiquitin conjugates by the mammalian p97 adaptor complexes, p47 and Ufd1-Npl4. *EMBO J.* **21**, 5645–52 (2002).

88. Zhang, Y.-J. *et al.* Aggregation-prone c9FTD/ALS poly(GA) RAN-translated proteins cause neurotoxicity by inducing ER stress. *Acta Neuropathol.* **128**, 505–524 (2014).

89. Katsuragi, Y., Ichimura, Y. & Komatsu, M. p62/SQSTM1 functions as a signaling hub and an autophagy adaptor. *FEBS J.* **282**, 4672–4678 (2015).

90. Türk, M. *et al. C9ORF72* -ALS: P62- and ubiquitin-aggregation pathology in skeletal muscle. *Muscle Nerve* **50**, 454–455 (2014).

91. Kabashi, E., Agar, J. N., Taylor, D. M., Minotti, S. & Durham, H. D. Focal dysfunction of the proteasome: a pathogenic factor in a mouse model of amyotrophic lateral sclerosis. *J. Neurochem.* **89**, 1325–1335 (2004).

92. Hjerpe, R. *et al.* UBQLN2 Mediates Autophagy-Independent Protein Aggregate Clearance by the Proteasome. *Cell* **166**, 935–949 (2016).

93. Barmada, S. J. *et al.* Autophagy induction enhances TDP43 turnover and survival in neuronal ALS models. *Nat. Chem. Biol.* **10**, 677–685 (2014).

94. Ryan, T. A. & Tumbarello, D. A. Optineurin: A Coordinator of Membrane-Associated Cargo Trafficking and Autophagy. *Front. Immunol.* **9**, 1024 (2018).

95. Oakes, J. A., Davies, M. C. & Collins, M. O. TBK1: a new player in ALS linking autophagy and neuroinflammation. *Mol. Brain* **10**, 5 (2017).

96. Goode, A. *et al.* Defective recognition of LC3B by mutant SQSTM1/p62 implicates impairment of autophagy as a pathogenic mechanism in ALS-FTLD. *Autophagy* **12**, 1094–1104 (2016).

97. Soo, K. Y. *et al.* ALS-associated mutant FUS inhibits macroautophagy which is restored by overexpression of Rab1. *Cell Death Discov.* **1**, 15030 (2015).

98. Parkinson, N. *et al.* ALS phenotypes with mutations in CHMP2B (charged multivesicular body protein 2B). *Neurology* **67**, 1074–7 (2006).

99. Sreedharan, J. *et al.* TDP-43 Mutations in Familial and Sporadic Amyotrophic Lateral Sclerosis. *Science (80-.).* **33**, (2008).

100. Neumann, M. *et al.* Ubiquitinated TDP-43 in Frontotemporal Lobar Degeneration and Amyotrophic Lateral Sclerosis. *Science (80-.).* **314**, 130–133 (2006).

101. Rosen, D. R. Mutations in Cu/Zn superoxide dismutase gene are associated with familial amyotrophic lateral sclerosis. *Nature* **364**, 362–362 (1993).

102. Neumann, M. *et al.* Ubiquitinated TDP-43 in frontotemporal lobar degeneration and amyotrophic lateral sclerosis. *Science* **314**, 130–3 (2006).

103. Shibata, N. *et al.* Cu/Zn superoxide dismutase-like immunoreactivity in Lewy body-like inclusions of sporadic amyotrophic lateral sclerosis. *Neurosci. Lett.* **179**, 149–52 (1994).

104. Wen, X. *et al.* Antisense proline-arginine RAN dipeptides linked to C9ORF72-ALS/FTD form toxic nuclear aggregates that initiate in vitro and in vivo neuronal death. *Neuron* **84**, 1213–25 (2014).

105. Ling, S.-C., Polymenidou, M. & Cleveland, D. W. Converging mechanisms in ALS and FTD: disrupted RNA and protein homeostasis. *Neuron* **79**, 416–38 (2013).

106. Godena, V. K. *et al.* TDP-43 Regulates Drosophila Neuromuscular Junctions Growth by Modulating Futsch/MAP1B Levels and Synaptic Microtubules Organization. *PLoS One* **6**, e17808 (2011).

107. Feiguin, F. *et al.* Depletion of TDP-43 affects *Drosophila motoneurons* terminal synapsis and locomotive behavior. *FEBS Lett.* **583**, 1586–1592 (2009).

108. Reber, S. *et al.* Minor intron splicing is regulated by FUS and affected by ALS-associated FUS mutants. *EMBO J.* **35**, 1504–21 (2016).

109. Mori, K. *et al.* hnRNP A3 binds to GGGGCC repeats and is a constituent of p62-positive/TDP43-negative inclusions in the hippocampus of patients with C9orf72 mutations. *Acta Neuropathol.* **125**, 413–423 (2013).

110. Khosravi, B. *et al.* Cytoplasmic poly-GA aggregates impair nuclear import of TDP-43 in C9orf72 ALS/FTLD. *Hum. Mol. Genet.* **26**, 790–800 (2017).

111. Schwartz, J. C. *et al.* FUS binds the CTD of RNA polymerase II and regulates its phosphorylation at Ser2. *Genes Dev.* **26**, 2690–5 (2012).

112. Kamelgarn, M. *et al.* Proteomic analysis of FUS interacting proteins provides insights into FUS function and its role in ALS. *Biochim. Biophys. Acta - Mol. Basis Dis.* **1862**, 2004–2014 (2016).

113. Yu, Y. *et al.* U1 snRNP is mislocalized in ALS patient fibroblasts bearing NLS mutations in FUS and is required for motor neuron outgrowth in zebrafish. *Nucleic Acids Res.* **43**, 3208–3218 (2015).

114. Rogelj, B. *et al.* Widespread binding of FUS along nascent RNA regulates alternative splicing in the brain. *Sci. Rep.* **2**, 603 (2012).

115. Orozco, D. *et al.* Loss of fused in sarcoma (FUS) promotes pathological Tau splicing. *EMBO Rep.* **13**, 759–764 (2012).

116. Moloney, E. B., de Winter, F. & Verhaagen, J. ALS as a distal axonopathy: molecular mechanisms affecting neuromuscular junction stability in the presymptomatic stages of the disease. *Front. Neurosci.* **8**, 252 (2014).

117. Kawahara, Y. & Mieda-Sato, A. TDP-43 promotes microRNA biogenesis as a component of the Drosha and Dicer complexes. *Proc. Natl. Acad. Sci. U. S. A.* **109**, 3347–52 (2012).

118. Morlando, M. *et al.* Coupling between snoRNP assembly and 3′ processing controls box C/D snoRNA biosynthesis in yeast. *EMBO J.* **23**, 2392–2401 (2004).

119. Porta, S., Kwong, L. K., Trojanowski, J. Q. & Lee, V. M.-Y. Drosha Inclusions Are New Components of Dipeptide-Repeat Protein Aggregates in FTLD-TDP and ALS *C9orf72* Expansion Cases. *J. Neuropathol. Exp. Neurol.* **74**, 380–387 (2015).

120. Sobue, G., Mcalary, L., Taylor, J. P. & Purice, M. D. Linking hnRNP Function to ALS and FTD Pathology. *Front. Neurosci.* | *www.frontiersin.org* **1**, 326 (2018).

121. Ranjith Sama, R. K. *et al.* FUS/TLS Assembles Into Stress Granules and Is a Prosurvival Factor During Hyperosmolar Stress. *J. Cell. Physiol* **228**, 2222–2231 (2013).

122. Zhang, K. *et al.* Stress Granule Assembly Disrupts Nucleocytoplasmic Transport. *Cell* **173**, 958-971.e17 (2018).

123. Higgins, C. M. J., Jung, C. & Xu, Z. ALS-associated mutant SOD1G93A causes mitochondrial vacuolation by expansion of the intermembrane space and by involvement of SOD1 aggregation and peroxisomes. *BMC Neurosci.* **4**, 16 (2003).

124. Pasinelli, P. *et al.* Amyotrophic Lateral Sclerosis-Associated SOD1 Mutant Proteins Bind and Aggregate with Bcl-2 in Spinal Cord Mitochondria. *Neuron* **43**, 19–30 (2004).

125. Wiedemann, F. R., Manfredi, G., Mawrin, C., Beal, M. F. & Schon, E. A. Mitochondrial DNA and respiratory chain function in spinal cords of ALS patients. *J. Neurochem.* **80**, 616–625 (2002).

126. Sathasivam, S., Grierson, A. J., Shaw, P. J. & Shaw, P. J. Characterization of the caspase cascade in a cell culture model of SOD1-related familial amyotrophic lateral sclerosis: expression, activation and therapeutic effects of inhibition. *Neuropathol. Appl. Neurobiol.* **31**, 467–685 (2005).

127. Damiano, M. *et al.* Neural mitochondrial Ca^{2+} capacity impairment precedes the onset of motor symptoms in G93A Cu/Zn-superoxide dismutase mutant mice. *J. Neurochem.* **96**, 1349–1361 (2006).

128. Hautbergue, G. M. *et al.* SRSF1-dependent nuclear export inhibition of C9ORF72 repeat transcripts prevents neurodegeneration and associated motor deficits. *Nat. Commun.* **8**, 16063 (2017).

129. Johnson, J. O. *et al.* Exome Sequencing Reveals VCP Mutations as a Cause of Familial ALS. *Neuron* **68**, 857–864 (2010).

130. Sutton, M. A. & Schuman, E. M. Dendritic Protein Synthesis, Synaptic Plasticity, and Memory. *Cell* **127**, 49–58 (2006).

131. Kiaei, M. *et al.* Matrix metalloproteinase-9 regulates TNF-α and FasL expression in neuronal, glial cells and its absence extends life in a transgenic mouse model of amyotrophic lateral sclerosis. *Exp. Neurol.* **205**, 74–81 (2007).

132. Ferraiuolo, L., Kirby, J., Grierson, A. J., Sendtner, M. & Shaw, P. J. Molecular pathways of motor neuron injury in amyotrophic lateral sclerosis. *Nat. Rev. Neurol.* **7**, 616–630 (2011).

133. Duan, W. *et al.* Mutant TAR DNA-binding protein-43 induces oxidative injury in motor neuron-like cell. *Neuroscience* **169**, 1621–1629 (2010).

134. Shibata, N. *et al.* Morphological evidence for lipid peroxidation and protein glycoxidation in spinal cords from sporadic amyotrophic lateral sclerosis patients. *Brain Res.* **917**, 97–104 (2001).

135. Zarei, S. *et al. A comprehensive review of amyotrophic lateral sclerosis*. *Surgical neurology international* **6**, 171 (Wolters Kluwer -- Medknow Publications, 2015).

136. Johnson, J. A. *et al.* The Nrf2-ARE Pathway. *Ann. N. Y. Acad. Sci.* **1147**, 61–69 (2008).

137. Kirby, J. *et al.* Mutant SOD1 alters the motor neuronal transcriptome: implications for familial ALS. *Brain* **128**, 1686–1706 (2005).

138. Stolz, A. & Wolf, D. H. Endoplasmic reticulum associated protein degradation: A chaperone assisted journey to hell. *Biochim. Biophys. Acta - Mol. Cell Res.* **1803**, 694–705 (2010).

139. Atkin, J. D. *et al.* Endoplasmic reticulum stress and induction of the unfolded protein response in human sporadic amyotrophic lateral sclerosis. *Neurobiol. Dis.* **30**, 400–407 (2008).

140. Vijayalakshmi, K. *et al.* Evidence of endoplasmic reticular stress in the spinal motor neurons exposed to CSF from sporadic amyotrophic lateral sclerosis patients. *Neurobiol. Dis.* **41**, 695–705 (2011).

141. Barber, S. C. & Shaw, P. J. Chapter 4 Molecular mechanisms of motor neuron degeneration in amyotrophic lateral sclerosis. *Handbook of Clinical Neurology* **82**, 57–87 (2007).

142. Liu, J. *et al.* Toxicity of familial ALS-linked SOD1 mutants from selective recruitment to spinal mitochondria. *Neuron* **43**, 5–17 (2004).

143. Shibata, N. *et al.* Morphological evidence for lipid peroxidation and protein glycoxidation in spinal cords from sporadic amyotrophic lateral sclerosis patients. *Brain Res.* **917**, 97–104 (2001).

144. Pardo, C. A. *et al.* Superoxide dismutase is an abundant component in cell bodies, dendrites, and axons of motor neurons and in a subset of other neurons. *Proc. Natl. Acad. Sci. U. S. A.* **92**, 954–8 (1995).

145. Williams, T. L., Day, N. C., Ince, P. G., Kamboj, R. K. & Shaw, P. J. Calcium-permeable alpha-amino-3-hydroxy-5-methyl-4-isoxazole propionic acid receptors: A molecular determinant of selective vulnerability in amyotrophic lateral sclerosis. *Ann. Neurol.* **42**, 200–207 (1997).

146. Bakhti, M. & Winter, C. Inhibition of Myelin Membrane Sheath Formation by Oligodendrocyte-derived Exosome-like Vesicles. *J. Biol. Chem.* (2011). doi:10.1074/jbc.M110.190009

147. Krämer-Albers, E.-M. *et al.* Oligodendrocytes secrete exosomes containing major myelin and stress-protective proteins: Trophic support for axons? *Proteomics. Clin. Appl.* **1**, 1446–61 (2007).

148. Raposo, G. *et al. B Lymphocytes Secrete Antigen-presentingVesicles*. (1996).

149. Valadi, H. *et al.* Exosome-mediated transfer of mRNAs and microRNAs is a novel mechanism of genetic exchange between cells. *Nat. Cell Biol.* **9**, 654–659 (2007).

150. Wiley, R. D. & Gummuluru, S. Immature dendritic cell-derived exosomes can mediate HIV-1 trans infection. *Proc. Natl. Acad. Sci. U. S. A.* **103**, 738 (2006).

151. Théry, C., Ostrowski, M. & Segura, E. Membrane vesicles as conveyors of immune responses. *Nat. Rev. Immunol.* **9**, 581–593 (2009).

152. Pan, B. T., Teng, K., Wu, C., Adam, M. & Johnstone, R. M. Electron microscopic evidence for externalization of the transferrin receptor in vesicular form in sheep reticulocytes. *J. Cell Biol.* **101**, 942–8 (1985).

153. Mathivanan, S., Ji, H. & Simpson, R. J. Exosomes: Extracellular organelles important in intercellular communication. *J. Proteomics* **73**, 1907–1920 (2010).

154. Le Bihan, M.-C. *et al.* In-depth analysis of the secretome identifies three major independent secretory pathways in differentiating human myoblasts. *J. Proteomics* **77**, 344–56 (2012).

155. Ristorcelli, E. *et al.* Human tumor nanoparticles induce apoptosis of pancreatic cancer cells. *The FASEB Journal* **22**, 3358–3369 (2008).

156. Fröhlich, D. *et al. Multifaceted effects of oligodendroglial exosomes on neurons: Impact on neuronal firing rate, signal transduction and gene regulation*. *Philosophical Transactions of the Royal Society B: Biological Sciences* **369**, (The Royal Society, 2014).

157. Frühbeis, C. *et al.* Neurotransmitter-Triggered Transfer of Exosomes Mediates Oligodendrocyte–Neuron Communication. *PLoS Biol.* **11**, e1001604 (2013).

158. Harding, C., Heuser, J. & Stahl, P. Receptor-mediated endocytosis of transferrin and recycling of the transferrin receptor in rat reticulocytes. *J. Cell Biol.* **97**, 329–339 (1983).

159. Pan, B. T. & Johnstone, R. M. Fate of the transferrin receptor during maturation of sheep reticulocytes in vitro: Selective externalization of the receptor. *Cell* **33**, 967–978 (1983).

160. Johnstone, R. M., Adam, M., Hammonds, J. R., Orro, L. & Turbide, C. *Vesicle Formation during Reticulocyte Maturation ASSOCIATION OF PLASMA MEMBRANE ACTIVITIES WITH RELEASED VESICLES (EXOSOMES)**. **262**, (1987).

161. Fauré, J. *et al.* Exosomes are released by cultured cortical neurones. *Mol. Cell. Neurosci.* **31**, 642–648 (2006).

162. Potolicchio, I. *et al.* Proteomic Analysis of Microglia-Derived Exosomes: Metabolic Role of the Aminopeptidase CD13 in Neuropeptide Catabolism. *J. Immunol.* **175**, 2237–2243 (2005).

163. Fevrier, B. *et al.* Cells release prions in association with exosomes. *Proc. Natl. Acad. Sci. U. S. A.* **101**, 9683–8 (2004).

164. Lopez-Verrilli, M. A., Picou, F. & Court, F. A. Schwann cell-derived exosomes enhance axonal regeneration in the peripheral nervous system. *Glia* **61**, 1795–1806 (2013).

165. Guescini, M., Genedani, S., Stocchi, V. & Agnati, L. F. Astrocytes and Glioblastoma cells release exosomes carrying mtDNA. *J. Neural Transm.* **117**, 1–4 (2010).

166. Lachenal, G. *et al.* Release of exosomes from differentiated neurons and its regulation by synaptic glutamatergic activity. *Mol. Cell. Neurosci.* **46**, 409–418 (2011).

167. Vrijsen, K. R. *et al.* Cardiomyocyte progenitor cell-derived exosomes stimulate migration of

endothelial cells. *J. Cell. Mol. Med.* **14**, 1064–70 (2010).

168. Le Bihan, M. C. *et al.* In-depth analysis of the secretome identifies three major independent secretory pathways in differentiating human myoblasts. *J. Proteomics* **77**, 344–356 (2012).

169. Kapustin, A. N. *et al.* Vascular Smooth Muscle Cell Calcification Is Mediated by Regulated Exosome Secretion. *Circ. Res.* **116**, 1312–1323 (2015).

170. Zitvogel L, Regnault A, Lozier A, Wolfers J, Flament C, Tenza D, Ricciardi-Castagnoli P, Raposo G, A. S. *et al.* Eradication of established murine tumors using a novel cell-free vaccine: dendritic cell-derived exosomes. *Nat. Med.* **4**, 594–600 (1998).

171. Skokos, D. *et al.* Mast Cell-Dependent B and T Lymphocyte Activation Is Mediated by the Secretion of Immunologically Active Exosomes. *J. Immunol.* **166**, 868–876 (2014).

172. Lugini, L. *et al.* Immune Surveillance Properties of Human NK Cell-Derived Exosomes. *J. Immunol.* **189**, 2833–2842 (2012).

173. Heijnen, H. F. *et al.* Multivesicular bodies are an intermediate stage in the formation of platelet alpha-granules. *Blood* **91**, 2313–25 (1998).

174. Blanchard, N. *et al.* TCR Activation of Human T Cells Induces the Production of Exosomes Bearing the TCR/CD3/ζ Complex. *J. Immunol.* **168**, 3235–3241 (2002).

175. Bruno, S. *et al. Mesenchymal stem cell-derived microvesicles protect against acute tubular injury*. *Journal of the American Society of Nephrology* **20**, A14–A14 (American Society of Nephrology, 2009).

176. Kang, D., Oh, S., Ahn, S.-M., Lee, B.-H. & Moon, M. H. Proteomic Analysis of Exosomes from Human Neural Stem Cells by Flow Field-Flow Fractionation and Nanoflow Liquid Chromatography−Tandem Mass Spectrometry. *J. Proteome Res.* **7**, 3475–3480 (2008).

177. Tűzesi, Á. *et al.* Pediatric brain tumor cells release exosomes with a miRNA repertoire that differs from exosomes secreted by normal cells. *Oncotarget* **8**, 90164–90175 (2017).

178. Van Niel, G. *et al.* Intestinal epithelial cells secrete exosome–like vesicles. *Gastroenterology* **121**, 337–349 (2001).

179. Riches, A., Campbell, E., Borger, E. & Powis, S. Regulation of exosome release from mammary epithelial and breast cancer cells – A new regulatory pathway. *Eur. J. Cancer* **50**, 1025–1034 (2014).

180. Kapsogeorgou, E. K., Abu-Helu, R. F., Moutsopoulos, H. M. & Manoussakis, M. N. Salivary gland epithelial cell exosomes: A source of autoantigenic ribonucleoproteins. *Arthritis Rheum.* **52**, 1517–1521 (2005).

181. Müller, G., Jung, C., Straub, J., Wied, S. & Kramer, W. Induced release of membrane vesicles from rat adipocytes containing glycosylphosphatidylinositol-anchored microdomain and lipid droplet signalling proteins. *Cellular Signalling* **21**, 324–338 (2009).

182. Zhang, Y.-Z. *et al.* Exosomes derived from human umbilical vein endothelial cells promote neural stem cell expansion while maintain their stemness in culture. *Biochem. Biophys. Res. Commun.* **495**, 892–898 (2018).

183. Saeed-Zidane, M. *et al.* Cellular and exosome mediated molecular defense mechanism in bovine granulosa cells exposed to oxidative stress. *PLoS One* **12**, e0187569 (2017).

184. Conde-Vancells, J. *et al.* Characterization and comprehensive proteome profiling of exosomes secreted by hepatocytes. *J. Proteome Res.* **7**, 5157–66 (2008).

185. Chavez-Muñoz, C., Morse, J., Kilani, R. & Ghahary, A. Primary human keratinocytes externalize stratifin protein via exosomes. *J. Cell. Biochem.* **104**, 2165–2173 (2008).

186. Nguyen, D. G., Booth, A., Gould, S. J. & Hildreth, J. E. K. Evidence that HIV budding in primary macrophages occurs through the exosome release pathway. *J. Biol. Chem.* **278**, 52347–54 (2003).

187. Haque, S. *et al.* Monocyte-derived exosomes upon exposure to cigarette smoke condensate alter their characteristics and show protective effect against cytotoxicity and HIV-1 replication. *Sci. Rep.* **7**, 16120 (2017).

188. Nazarenko, I. *et al.* Cell Surface Tetraspanin Tspan8 Contributes to Molecular Pathways of Exosome-Induced Endothelial Cell Activation. *Cancer Res.* **70**, 1668–1678 (2010).

189. Laulagnier, K. *et al.* PLD2 is enriched on exosomes and its activity is correlated to the release of exosomes. *FEBS Lett.* **572**, 11–14 (2004).

190. Welton, J. L. *et al.* Proteomics analysis of bladder cancer exosomes. *Mol. Cell. Proteomics* **9**, 1324–38 (2010).

191. Graner, M. W., Cumming, R. I. & Bigner, D. D. The Heat Shock Response and Chaperones/Heat Shock Proteins in Brain Tumors: Surface Expression, Release, and Possible Immune Consequences. *J. Neurosci.* **27**, 11214–11227 (2007).

192. Wolfers, J. *et al.* Tumor-derived exosomes are a source of shared tumor rejection antigens for CTL cross-priming. *Nat. Med.* **7**, 297–303 (2001).

193. Horibe, S., Tanahashi, T., Kawauchi, S., Murakami, Y. & Rikitake, Y. Mechanism of recipient cell-dependent differences in exosome uptake. *BMC Cancer* **18**, 47 (2018).

194. Zhang, S. *et al.* Exosomes promote cetuximab resistance via the PTEN/Akt pathway in colon cancer cells. *Brazilian J. Med. Biol. Res. = Rev. Bras. Pesqui. medicas e Biol.* **51**, e6472 (2017).

195. Christianson, H. C., Svensson, K. J., van Kuppevelt, T. H., Li, J.-P. & Belting, M. Cancer cell exosomes depend on cell-surface heparan sulfate proteoglycans for their internalization and functional activity. *Proc. Natl. Acad. Sci. U. S. A.* **110**, 17380–5 (2013).

196. Hazan-Halevy, I. *et al.* Cell-specific uptake of mantle cell lymphoma-derived exosomes by malignant and non-malignant B-lymphocytes. *Cancer Lett.* **364**, 59–69 (2015).

197. Purushothaman, A. *et al.* Fibronectin on the Surface of Myeloma Cell-derived Exosomes Mediates Exosome-Cell Interactions. *J. Biol. Chem.* **291**, 1652–63 (2016).

198. Klibi, J. *et al.* Blood diffusion and Th1-suppressive effects of galectin-9–containing exosomes released by Epstein-Barr virus–infected nasopharyngeal carcinoma cells. *Blood* **113**, 1957–1966 (2009).

199. Keller, S. *et al.* Systemic presence and tumor-growth promoting effect of ovarian carcinoma released exosomes. *Cancer Lett.* **278**, 73–81 (2009).

200. Rana, S., Claas, C., Kretz, C. C., Nazarenko, I. & Zoeller, M. Activation-induced internalization differs for the tetraspanins CD9 and Tspan8: Impact on tumor cell motility. *Int. J. Biochem. Cell Biol.* **43**, 106–119 (2011).

201. Llorente, A., de Marco, M. C. & Alonso, M. A. Caveolin-1 and MAL are located on prostasomes secreted by the prostate cancer PC-3 cell line. *J. Cell Sci.* **117**, 5343–5351 (2004).

202. Dixon, C. L. *et al.* Amniotic Fluid Exosome Proteomic Profile Exhibits Unique Pathways of Term and Preterm Labor. *Endocrinology* **159**, 2229–2240 (2018).

203. Kang, G.-Y. *et al.* Exosomal Proteins in the Aqueous Humor as Novel Biomarkers in Patients with Neovascular Age-related Macular Degeneration. *J. Proteome Res.* **13**, 581–595 (2014).

204. Admyre, C. *et al.* Exosomes with immune modulatory features are present in human breast milk. *J. Immunol.* **179**, 1969–78 (2007).

205. Admyre, C. *et al.* Exosomes with major histocompatibility complex class II and co-stimulatory molecules are present in human BAL fluid. *Eur. Respir. J.* **22**, 578–83 (2003).

206. Harrington, M. G. *et al.* The morphology and biochemistry of nanostructures provide evidence for synthesis and signaling functions in human cerebrospinal fluid. *Cerebrospinal Fluid Res.* **6**, 10 (2009).

207. da Silveira, J. C., Veeramachaneni, D. N. R., Winger, Q. A., Carnevale, E. M. & Bouma, G. J. Cell-Secreted Vesicles in Equine Ovarian Follicular Fluid Contain miRNAs and Proteins: A Possible New Form of Cell Communication Within the Ovarian Follicle1. *Biol. Reprod.* **86**, (2012).

208. Caby, M.-P., Lankar, D., Vincendeau-Scherrer, C., Raposo, G. & Bonnerot, C. Exosomal-like vesicles are present in human blood plasma. *Int. Immunol.* **17**, 879–887 (2005).

209. Ogawa, Y., Kanai-Azuma, M., Akimoto, Y., Kawakami, H. & Yanoshita, R. Exosome-like vesicles with dipeptidyl peptidase IV in human saliva. *Biol. Pharm. Bull.* **31**, 1059–62 (2008).

210. Poliakov, A., Spilman, M., Dokland, T., Amling, C. L. & Mobley, J. A. Structural heterogeneity and protein composition of exosome-like vesicles (prostasomes) in human semen. *Prostate* **69**, 159–67 (2009).

211. Skriner, K., Adolph, K., Jungblut, P. R. & Burmester, G. R. Association of citrullinated proteins with synovial exosomes. *Arthritis Rheum.* **54**, 3809–3814 (2006).

212. Pisitkun, T., Shen, R.-F. & Knepper, M. A. Identification and proteomic profiling of exosomes in human urine. *Proc. Natl. Acad. Sci. U. S. A.* **101**, 13368–73 (2004).

213. Théry, C., Amigorena, S., Raposo, G. & Clayton, A. Isolation and Characterization of Exosomes from Cell Culture Supernatants and Biological Fluids. in *Current Protocols in Cell Biology* **Chapter 3**, Unit 3.22 (John Wiley & Sons, Inc., 2006).

214. B Lymphocytes Secrete Antigen-presentingVesicles. **183**, (1996).

215. Théry, C. *et al.* Molecular characterization of dendritic cell-derived exosomes. Selective accumulation of the heat shock protein hsc73. *J. Cell Biol.* **147**, 599–610 (1999).

216. Guescini, M. *et al.* C2C12 myoblasts release micro-vesicles containing mtDNA and proteins involved in signal transduction. *Exp. Cell Res.* **316**, 1977–1984 (2010).

217. Baietti, M. F. *et al.* Syndecan–syntenin–ALIX regulates the biogenesis of exosomes. *Nat. Cell Biol.* **14**, 677–685 (2012).

218. Ghossoub, R. *et al.* Syntenin-ALIX exosome biogenesis and budding into multivesicular bodies are controlled by ARF6 and PLD2. *Nat. Commun.* **5**, 3477 (2014).

219. Colombo, M., Raposo, G. & Théry, C. Biogenesis, Secretion, and Intercellular Interactions of Exosomes and Other Extracellular Vesicles. *Annu. Rev. Cell Dev. Biol.* **30**, 255–289 (2014).

220. Hessvik, N. P. & Llorente, A. Current knowledge on exosome biogenesis and release. *Cell. Mol. Life Sci.* **75**, 193–208 (2018).

221. Rider, M. A., Hurwitz, S. N. & Meckes, D. G. ExtraPEG: A Polyethylene Glycol-Based Method for

Enrichment of Extracellular Vesicles. *Sci. Rep.* **6**, 23978 (2016).

222. Methods and compositions for exosome isolation. (2013).

223. Théry, C., Zitvogel, L. & Amigorena, S. Exosomes: composition, biogenesis and function. *Nat. Rev. Immunol.* **2**, 569–79 (2002).

224. Aalberts, M. *et al.* Identification of Distinct Populations of Prostasomes That Differentially Express Prostate Stem Cell Antigen, Annexin A1, and GLIPR2 in Humans1. *Biol. Reprod.* **86**, (2012).

225. Zabeo, D. *et al.* Exosomes purified from a single cell type have diverse morphology. *J. Extracell. Vesicles* **6**, 1329476 (2017).

226. Koning, R. I. & Koster, A. J. Cryo-electron tomography in biology and medicine. *Ann. Anat.* **191**, 427–445 (2009).

227. Bobrie, A., Colombo, M., Krumeich, S., Raposo, G. & Théry, C. Diverse subpopulations of vesicles secreted by different intracellular mechanisms are present in exosome preparations obtained by differential ultracentrifugation. *J. Extracell. Vesicles* **1**, 18397 (2012).

228. Willms, E. *et al.* Cells release subpopulations of exosomes with distinct molecular and biological properties OPEN. (2016). doi:10.1038/srep22519

229. Chevillet, J. R. *et al.* Quantitative and stoichiometric analysis of the microRNA content of exosomes. *Proc. Natl. Acad. Sci. U. S. A.* **111**, 14888–93 (2014).

230. Montecalvo, A. *et al. Mechanim of transfer of functional microRNAs between moouse dendritic cells via exosomes*. *Blood* **119**, 756–66 (The American Society of Hematology, 2012).

231. Smith, Z. J. *et al.* Single exosome study reveals subpopulations distributed among cell lines with variability related to membrane content. *J. Extracell. Vesicles* **4**, 28533 (2015).

232. Trajkovic, K. *et al.* Ceramide Triggers Budding of Exosome Vesicles into Multivesicular Endosomes. *Source Sci. New Ser.* **319**, 1244–1247 (2008).

233. Wubbolts, R. *et al.* Proteomic and biochemical analyses of human B cell-derived exosomes. Potential implications for their function and multivesicular body formation. *J. Biol. Chem.* **278**, 10963–72 (2003).

234. Miyanishi, M. *et al.* Identification of Tim4 as a phosphatidylserine receptor. *Nature* **450**, 435–439 (2007).

235. Kalra, H. *et al.* Focus on Extracellular Vesicles: Introducing the Next Small Big Thing. *Int. J. Mol. Sci.* **17**, 170 (2016).

236. van Niel, G., D'Angelo, G. & Raposo, G. Shedding light on the cell biology of extracellular vesicles. *Nat. Rev. Mol. Cell Biol.* **19**, 213–228 (2018).

237. Van Niel, G., Porto-Carreiro, I., Simoes, S. & Raposo, G. Exosomes: A common pathway for a specialized function. *J. Biochem.* **140**, 13–21 (2006).

238. Hoen, E. N. M. N.-'t *et al.* Deep sequencing of RNA from immune cell-derived vesicles uncovers the selective incorporation of small non-coding RNA biotypes with potential regulatory functions. *Nucleic Acids Res.* **40**, 9272 (2012).

239. Janas, T., Janas, M. M., Sapoń, K. & Janas, T. Mechanisms of RNA loading into exosomes. *FEBS Lett.* **589**, 1391–1398 (2015).

240. Baglio, S. R. *et al.* Human bone marrow- and adipose-mesenchymal stem cells secrete exosomes enriched in distinctive miRNA and tRNA species. *Stem Cell Res. Ther.* **6**, 127 (2015).

241. Anand, S., Samuel, M., Kumar, S. & Mathivanan, S. Ticket to a bubble ride: Cargo sorting into exosomes and extracellular vesicles. *Biochim. Biophys. Acta - Proteins Proteomics* (2019). doi:10.1016/J.BBAPAP.2019.02.005

242. Babst, M. A Protein's Final ESCRT. *Traffic* **6**, 2–9 (2005).

243. Villarroya-Beltri, C. *et al.* Sumoylated hnRNPA2B1 controls the sorting of miRNAs into exosomes through binding to specific motifs. *Nat. Commun.* **4**, 2980 (2013).

244. Keller, S., Sanderson, M. P., Stoeck, A. & Altevogt, P. Exosomes: From biogenesis and secretion to biological function. *Immunol. Lett.* **107**, 102–108 (2006).

245. de Gassart, A., Geminard, C., Fevrier, B., Raposo, G. & Vidal, M. Lipid raft-associated protein sorting in exosomes. *Blood* **102**, 4336–44 (2003).

246. Guduric-Fuchs, J. *et al.* Selective extracellular vesicle-mediated export of an overlapping set of microRNAs from multiple cell types. *BMC Genomics* **13**, 357 (2012).

247. McKenzie, A. J. *et al.* KRAS-MEK Signaling Controls Ago2 Sorting into Exosomes. *Cell Rep.* **15**, 978–987 (2016).

248. Shurtleff, M. J. *et al.* Broad role for YBX1 in defining the small noncoding RNA composition of exosomes. *Proc. Natl. Acad. Sci. U. S. A.* **114**, E8987–E8995 (2017).

249. Luga, V. *et al.* Exosomes mediate stromal mobilization of autocrine Wnt-PCP signaling in breast cancer cell migration. *Cell* **151**, 1542–56 (2012).

250. Théry, C. *et al.* Proteomic analysis of dendritic cell-derived exosomes: a secreted subcellular compartment distinct from apoptotic vesicles. *J. Immunol.* **166**, 7309–18 (2001).

251. Colombo, M. *et al.* Analysis of ESCRT functions in exosome biogenesis, composition and secretion highlights the heterogeneity of extracellular vesicles. *J. Cell Sci.* **126**, 5553–65 (2013).

252. Williams, R. L. & Urbé, S. The emerging shape of the ESCRT machinery. *Nat. Rev. Mol. Cell Biol.* **8**, 355–368 (2007).

253. Hanson2012-MVB morphogenesis.pdf.

254. Colombo, M., Raposo, G. & Théry, C. Biogenesis, Secretion, and Intercellular Interactions of Exosomes and Other Extracellular Vesicles. *Annu. Rev. Cell Dev. Biol* **30**, 255–289 (2014).

255. Stuffers, S., Sem Wegner, C., Stenmark, H. & Brech, A. Multivesicular Endosome Biogenesis in the Absence of ESCRTs. *Traffic* **10**, 925–937 (2009).

256. McMahon, H. T. & Boucrot, E. Membrane curvature at a glance. *Journal of cell science* **128**, 1065–70 (2015).

257. Charrin, S., Jouannet, S., Boucheix, C. & Rubinstein, E. Tetraspanins at a glance. *J. Cell Sci.* **127**, 3641–8 (2014).

258. Zimmerman, B. *et al.* Crystal Structure of a Full-Length Human Tetraspanin Reveals a Cholesterol-Binding Pocket. *Cell* **167**, 1041-1051.e11 (2016).

259. Charrin, S. *et al.* A physical and functional link between cholesterol and tetraspanins. *Eur. J. Immunol.* **33**, 2479–2489 (2003).

260. Termini, C. M. & Gillette, J. M. Tetraspanins Function as Regulators of Cellular Signaling. *Front. Cell Dev. Biol.* **5**, 34 (2017).

261. Raposo, G. & Stoorvogel, W. Extracellular vesicles: exosomes, microvesicles, and friends. *J. Cell Biol.* **200**, 373–83 (2013).

262. Bonifacino, J. S. & Glick, B. S. *Review The Mechanisms of Vesicle Budding and Fusion ganelles of the pathway. Such observations inspired the vesicular transport hypothesis, which states that the transfer of cargo molecules between organelles of the*. *Cell* **116**, (2004).

263. Palmulli, R. & van Niel, G. To be or not to be... secreted as exosomes, a balance finely tuned by the mechanisms of biogenesis. *Essays Biochem.* **62**, 177–191 (2018).

264. Ostrowski, M. *et al.* Rab27a and Rab27b control different steps of the exosome secretion pathway. *Nat. Cell Biol.* **12**, 19–30 (2010).

265. Hsu, C. *et al.* Regulation of exosome secretion by Rab35 and its GTPase-activating proteins TBC1D10A-C. *J. Cell Biol.* **189**, 223–32 (2010).

266. Gross, J. C., Chaudhary, V., Bartscherer, K. & Boutros, M. Active Wnt proteins are secreted on exosomes. *Nature Cell Biology* **14**, 1036–1045 (2012).

267. Alvarez-Erviti, L. *et al.* Delivery of siRNA to the mouse brain by systemic injection of targeted exosomes. *Nat. Biotechnol.* **29**, 341–345 (2011).

268. Le Bihan, M.-C. *et al.* In-depth analysis of the secretome identifies three major independent secretory pathways in differentiating human myoblasts. *J. Proteomics* **77**, 344–356 (2012).

269. Franzen, C. A. *et al.* Characterization of uptake and internalization of exosomes by bladder cancer cells. *Biomed Res. Int.* **2014**, 619829 (2014).

270. Peinado, H. *et al.* Melanoma exosomes educate bone marrow progenitor cells toward a pro-metastatic phenotype through MET. *Nat. Med.* **18**, 883–891 (2012).

271. Fitzner, D. *et al.* Selective transfer of exosomes from oligodendrocytes to microglia by macropinocytosis. *J. Cell Sci.* **124**, 447–58 (2011).

272. Hung, W.-T. *et al.* Stage-specific follicular extracellular vesicle uptake and regulation of bovine granulosa cell proliferation. *Biol. Reprod.* **97**, 644–655 (2017).

273. Svensson, K. J. *et al.* Exosome uptake depends on ERK1/2-heat shock protein 27 signaling and lipid Raft-mediated endocytosis negatively regulated by caveolin-1. *J. Biol. Chem.* **288**, 17713–24 (2013).

274. Zhao, H. *et al.* Tumor microenvironment derived exosomes pleiotropically modulate cancer cell metabolism. *Elife* **5**, e10250 (2016).

275. Morelli, A. E. *et al.* Endocytosis, intracellular sorting, and processing of exosomes by dendritic cells. *Blood* **104**, 3257–3266 (2004).

276. Koumangoye, R. B., Sakwe, A. M., Goodwin, J. S., Patel, T. & Ochieng, J. Detachment of breast tumor cells induces rapid secretion of exosomes which subsequently mediate cellular adhesion and spreading. *PLoS One* **6**, e24234 (2011).

277. Suetsugu, A., Honma, K., Saji, S., Moriwaki, H. & Hoffman, R. M. Imaging exosome transfer from breast cancer cells to stroma at metastatic sites in orthotopic nude-mouse models. *Adv. Drug Deliv. Rev.* **65**, 383–390 (2013).

278. Hakulinen, J., Junnikkala, S., Sorsa, T. & Meri, S. Complement inhibitor membrane cofactor protein (MCP; CD46) is constitutively shed from cancer cell membranes in vesicles and converted by a metalloproteinase to a functionally active soluble form. *Eur. J. Immunol.* **34**, 2620–2629 (2004).

279. Kamerkar, S. *et al.* Exosomes facilitate therapeutic targeting of oncogenic KRAS in pancreatic cancer. *Nature* **546**, 498–503 (2017).

280. Escrevente, C., Keller, S., Altevogt, P. & Costa, J. Interaction and uptake of exosomes by ovarian cancer cells. *BMC Cancer* **11**, 108 (2011).

281. Bretz, N. P. *et al.* Body fluid exosomes promote secretion of inflammatory cytokines in monocytic cells via Toll-like receptor signaling. *J. Biol. Chem.* **288**, 36691–702 (2013).

282. Wang, R. *et al.* Exosome Adherence and Internalization by Hepatic Stellate Cells Triggers Sphingosine 1-Phosphate-dependent Migration. *J. Biol. Chem.* **290**, 30684–96 (2015).

283. Segura, E., Guérin, C., Hogg, N., Amigorena, S. & Théry, C. CD8+ dendritic cells use LFA-1 to capture MHC-peptide complexes from exosomes in vivo. *J. Immunol.* **179**, 1489–96 (2007).

284. Nolte-'t Hoen, E. N. M., Buschow, S. I., Anderton, S. M., Stoorvogel, W. & Wauben, M. H. M. Activated T cells recruit exosomes secreted by dendritic cells via LFA-1. **113**, 1977–1981 (2009).

285. Segura, E. *et al.* ICAM-1 on exosomes from mature dendritic cells is critical for efficient naive T-cell priming. *Blood* **106**, 216–223 (2005).

286. Näslund, T. I. *et al.* Exosomes from breast milk inhibit HIV-1 infection of dendritic cells and subsequent viral transfer to CD4+ T cells. *AIDS* **28**, 171–180 (2014).

287. CLAYTON, A. *et al.* Adhesion and signaling by B cell-derived exosomes: the role of integrins. *FASEB J.* **18**, 977–979 (2004).

288. Rieu, S., Géminard, C., Rabesandratana, H., Sainte-Marie, J. & Vidal, M. Exosomes released during reticulocyte maturation bind to fibronectin via integrin α4β1. *Eur. J. Biochem.* **267**, 583–590 (2000).

289. Hanayama, R. *et al.* Identification of a factor that links apoptotic cells to phagocytes. *Nature* **417**, 182–187 (2002).

290. Kamerkar, S. *et al.* Exosomes facilitate therapeutic targeting of oncogenic KRAS in pancreatic cancer. *Nature* **546**, 498–503 (2017).

291. Hao, S. *et al.* Mature dendritic cells pulsed with exosomes stimulate efficient cytotoxic T-lymphocyte responses and antitumour immunity. *Immunology* **120**, 90–102 (2007).

292. Barrès, C. *et al.* Galectin-5 is bound onto the surface of rat reticulocyte exosomes and modulates vesicle uptake by macrophages. *Blood* **115**, 696–705 (2010).

293. Saunderson, S. C., Dunn, A. C., Crocker, P. R. & McLellan, A. D. CD169 mediates the capture of exosomes in spleen and lymph node. *Blood* **123**, 208–16 (2014).

294. Parolini, I. *et al.* Microenvironmental pH Is a Key Factor for Exosome Traffic in Tumor Cells. *J. Biol. Chem.* **284**, 34211–34222 (2009).

295. Lowy, R. J. *et al. Observation of single influenza virus-cell fusion and measurement by fluorescence video microscopy (membrane fusion/octadecylrhodamine)*. *Proc. Natl. Acad. Sci. USA* **87**, (1990).

296. Kirchhausen, T. Clathrin. *Annu. Rev. Biochem.* **69**, 699–727 (2000).

297. Mulcahy, L. A., Pink, R. C. & Carter, D. R. F. Routes and mechanisms of extracellular vesicle

uptake. *J. Extracell. vesicles* **3**, (2014).

298. Tian, T. *et al.* Exosome uptake through clathrin-mediated endocytosis and macropinocytosis and mediating miR-21 delivery. *J. Biol. Chem.* **289**, 22258–67 (2014).

299. Anderson, R. G. W. THE CAVEOLAE MEMBRANE SYSTEM. *Annu. Rev. Biochem.* **67**, 199–225 (1998).

300. Nanbo, A., Kawanishi, E., Yoshida, R. & Yoshiyama, H. Exosomes Derived from Epstein-Barr Virus-Infected Cells Are Internalized via Caveola-Dependent Endocytosis and Promote Phenotypic Modulation in Target Cells. (2013). doi:10.1128/JVI.01310-13

301. Kerr, M. C. & Teasdale, R. D. Defining Macropinocytosis. *Traffic* **10**, 364–371 (2009).

302. Feng, D. *et al.* Cellular Internalization of Exosomes Occurs Through Phagocytosis. *Traffic* **11**, 675–687 (2010).

303. Doherty, G. J. & McMahon, H. T. *Endocytosis mechnaisms - Doherty et al - 2009.pdf*. *Annual Review of Biochemistry* **78**, 857–902 (2009).

304. McKelvey, K. J., Powell, K. L., Ashton, A. W., Morris, J. M. & McCracken, S. A. Exosomes: Mechanisms of Uptake. *J. Circ. biomarkers* **4**, 7 (2015).

305. Mathieu, M., Martin-Jaular, L., Lavieu, G. & Théry, C. Specificities of secretion and uptake of exosomes and other extracellular vesicles for cell-to-cell communication. *Nat. Cell Biol.* **21**, 9–17 (2019).

306. Gruenberg, J. & van der Goot, F. G. Mechanisms of pathogen entry through the endosomal compartments. *Nat. Rev. Mol. Cell Biol.* **7**, 495–504 (2006).

307. Falguières, T. *et al.* In Vitro Budding of Intralumenal Vesicles into Late Endosomes Is Regulated by Alix and Tsg101. *Mol. Biol. Cell* **19**, 4942–4955 (2008).

308. Abrami, L., Lindsay, M., Parton, R. G., Leppla, S. H. & van der Goot, F. G. Membrane insertion of anthrax protective antigen and cytoplasmic delivery of lethal factor occur at different stages of the endocytic pathway. *J. Cell Biol.* **166**, 645–51 (2004).

309. Le Blanc, I. *et al.* No Title. **7**, (2005).

310. Abrami, L. *et al.* Hijacking multivesicular bodies enables long-term and exosome-mediated long-distance action of anthrax toxin. *Cell Rep.* **5**, 986–96 (2013).

311. Komiya, Y. & Habas, R. Wnt signal transduction pathways. *Organogenesis* **4**, 68–75 (2008).

312. Gross, J. C., Chaudhary, V., Bartscherer, K. & Boutros, M. Active Wnt proteins are secreted on exosomes. *Nat. Cell Biol.* **14**, 1036–1045 (2012).

313. Zhu W *et al.* Exosomes derived from human bone marrow mesenchymal stem cells promote tumor growth in vivo. *Cancer Letters* **315**, 28–37 (2012).

314. Taverna, S. *et al.* Role of exosomes released by chronic myelogenous leukemia cells in angiogenesis. *Int. J. Cancer* **130**, 2033–2043 (2012).

315. Fauré, J. *et al.* Exosomes are released by cultured cortical neurones. *Molecular and Cellular Neuroscience* **31**, 642–648 (2006).

316. Rajendran, L. *et al.* Alzheimer ' s disease [illegible] -amyloid peptides are released in association with

exosomes. (2006).

317. Emmanouilidou, E. *et al.* Neurobiology of Disease Cell-Produced-Synuclein Is Secreted in a Calcium-Dependent Manner by Exosomes and Impacts Neuronal Survival. (2010). doi:10.1523/JNEUROSCI.5699-09.2010

318. Hall, E. D., Oostveen, J. A. & Gurney, M. E. Relationship of microglial and astrocytic activation to disease onset and progression in a transgenic model of familial ALS. *Glia* **23**, 249–56 (1998).

319. Marcuzzo, S. *et al.* Hind limb muscle atrophy precedes cerebral neuronal degeneration in G93A-SOD1 mouse model of amyotrophic lateral sclerosis: A longitudinal MRI study. *Exp. Neurol.* **231**, 30–37 (2011).

320. Loeffler, J.-P., Picchiarelli, G., Dupuis, L. & Gonzalez De Aguilar, J.-L. The Role of Skeletal Muscle in Amyotrophic Lateral Sclerosis. *Brain Pathol.* (2016). doi:10.1111/bpa.12350

321. Pramatarova, A., Laganière, J., Roussel, J., Brisebois, K. & Rouleau, G. A. Neuron-specific expression of mutant superoxide dismutase 1 in transgenic mice does not lead to motor impairment. *J. Neurosci.* **21**, 3369–74 (2001).

322. Lino, M. M., Schneider, C. & Caroni, P. *Accumulation of SOD1 Mutants in Postnatal Motoneurons Does Not Cause Motoneuron Pathology or Motoneuron Disease*. (2002).

323. Jaarsma, D., Teuling, E., Haasdijk, E. D., De Zeeuw, C. I. & Hoogenraad, C. C. Neuron-specific expression of mutant superoxide dismutase is sufficient to induce amyotrophic lateral sclerosis in transgenic mice. *J. Neurosci.* **28**, 2075–88 (2008).

324. Clement, A. M. Wild-Type Nonneuronal Cells Extend Survival of SOD1 Mutant Motor Neurons in ALS Mice. *Science (80-.).* **302**, 113–117 (2003).

325. Thomsen, G. M. *et al.* Delayed disease onset and extended survival in the SOD1G93A rat model of amyotrophic lateral sclerosis after suppression of mutant SOD1 in the motor cortex. *J. Neurosci.* **34**, 15587–600 (2014).

326. Nagai, M. *et al.* Astrocytes expressing ALS-linked mutated SOD1 release factors selectively toxic to motor neurons. *Nat. Neurosci.* **10**, 615–622 (2007).

327. Di Giorgio, F. P., Carrasco, M. A., Siao, M. C., Maniatis, T. & Eggan, K. Non–cell autonomous effect of glia on motor neurons in an embryonic stem cell–based ALS model. *Nat. Neurosci.* **10**, 608–614 (2007).

328. Komine, O. & Yamanaka, K. Neuroinflammation in motor neuron disease. *Nagoya J. Med. Sci.* **77**, 537–49 (2015).

329. Liao, B., Zhao, W., Beers, D. R., Henkel, J. S. & Appel, S. H. Transformation from a neuroprotective to a neurotoxic microglial phenotype in a mouse model of ALS. *Exp. Neurol.* **237**, 147–152 (2012).

330. Harraz, M. M. *et al.* SOD1 mutations disrupt redox-sensitive Rac regulation of NADPH oxidase in a familial ALS model. *J. Clin. Invest.* **118**, 659–70 (2008).

331. Rizzo, F. *et al.* Cellular therapy to target neuroinflammation in amyotrophic lateral sclerosis. *Cell. Mol. Life Sci.* **71**, 999–1015 (2014).

332. Hensley, K. *et al.* Primary glia expressing the G93A-SOD1 mutation present a neuroinflammatory phenotype and provide a cellular system for studies of glial inflammation. *Oklahoma Med. Res. Found.* (2006). doi:10.1186/1742-2094-3-2

333. Corcia, P. *et al.* Molecular Imaging of Microglial Activation in Amyotrophic Lateral Sclerosis. *PLoS*

One **7**, e52941 (2012).

334. Mantovani, S. *et al.* Immune system alterations in sporadic amyotrophic lateral sclerosis patients suggest an ongoing neuroinflammatory process. *J. Neuroimmunol.* **210**, 73–79 (2009).

335. Kuhle, J. *et al.* Increased levels of inflammatory chemokines in amyotrophic lateral sclerosis. doi:10.1111/j.1468-1331.2009.02560.x

336. Lee, Y. *et al.* Oligodendroglia metabolically support axons and contribute to neurodegeneration. *Nature* **487**, 443–8 (2012).

337. Ferraiuolo, L. *et al.* Oligodendrocytes contribute to motor neuron death in ALS via SOD1-dependent mechanism. *Proc. Natl. Acad. Sci. U. S. A.* **113**, E6496–E6505 (2016).

338. Heckman, C. J. & Enoka, R. M. Motor Unit. in *Comprehensive Physiology* **2**, 2629–82 (John Wiley & Sons, Inc., 2012).

339. Slater, C. R. The Structure of Human Neuromuscular Junctions: Some Unanswered Molecular Questions. *Int. J. Mol. Sci.* **18**, (2017).

340. Liu, W. & Chakkalakal, J. V. *The Composition, Development, and Regeneration of Neuromuscular Junctions*. *Current Topics in Developmental Biology* **126**, 99–124 (Academic Press, 2018).

341. Fischer, L. R. *et al.* Amyotrophic lateral sclerosis is a distal axonopathy: evidence in mice and man. *Exp. Neurol.* **185**, 232–240 (2004).

342. Tallon, C., Russell, K. A., Sakhalkar, S., Andrapallayal, N. & Farah, M. H. Length-dependent axo-terminal degeneration at the neuromuscular synapses of type II muscle in SOD1 mice. *Neuroscience* **312**, 179–89 (2016).

343. Funakoshi, H. *et al.* Muscle-derived neurotrophin-4 as an activity-dependent trophic signal for adult motor neurons. *Science (80-.).* **268**, 1495–1499 (1995).

344. Kablar, B. & Rudnicki, M. A. Development in the Absence of Skeletal Muscle Results in the Sequential Ablation of Motor Neurons from the Spinal Cord to the Brain. *Dev. Biol.* **208**, 93–109 (1999).

345. Dupuis, L. *et al.* Muscle mitochondrial uncoupling dismantles neuromuscular junction and triggers distal degeneration of motor neurons. *PLoS One* **4**, e5390 (2009).

346. Taetzsch, T., Tenga, M. J. & Valdez, G. Muscle Fibers Secrete FGFBP1 to Slow Degeneration of Neuromuscular Synapses during Aging and Progression of ALS. *J. Neurosci.* **37**, 70–82 (2017).

347. Dobrowolny, G. *et al.* Skeletal Muscle Is a Primary Target of SOD1G93A-Mediated Toxicity. *Cell Metab.* **8**, 425–436 (2008).

348. Wong, M. & Martin, L. J. Skeletal muscle-restricted expression of human SOD1 causes motor neuron degeneration in transgenic mice. *Hum. Mol. Genet.* **19**, 2284 (2010).

349. Miller, T. M. *et al.* Gene transfer demonstrates that muscle is not a primary target for non-cell-autonomous toxicity in familial amyotrophic lateral sclerosis. *Proc. Natl. Acad. Sci. U. S. A.* **103**, 19546–51 (2006).

350. Towne, C., Raoul, C., Schneider, B. L. & Aebischer, P. Systemic AAV6 Delivery Mediating RNA Interference Against SOD1: Neuromuscular Transduction Does Not Alter Disease Progression in fALS Mice. *Mol. Ther.* **16**, 1018–1025 (2008).

351. Li, S. *et al.* Stable transduction of myogenic cells with lentiviral vectors expressing a

minidystrophin. *Gene Ther.* **12**, 1099–1108 (2005).

352. Gregorevic, P. *et al. Systemic delivery of genes to striated muscles using adeno-associated viral vectors*. *Nature Medicine* **10**, 828–834 (2004).

353. Frühbeis, C. *et al.* Neurotransmitter-Triggered Transfer of Exosomes Mediates Oligodendrocyte–Neuron Communication. *PLoS Biol.* **11**, e1001604 (2013).

354. Gomes, C., Keller, S., Altevogt, P. & Costa, J. Evidence for secretion of Cu,Zn superoxide dismutase via exosomes from a cell model of amyotrophic lateral sclerosis. *Neurosci. Lett.* **428**, 43–46 (2007).

355. Basso, M. *et al.* Mutant Copper-Zinc Superoxide Dismutase (SOD1) Induces Protein Secretion Pathway Alterations and Exosome Release in Astrocytes: IMPLICATIONS FOR DISEASE SPREADING AND MOTOR NEURON PATHOLOGY IN AMYOTROPHIC LATERAL SCLEROSIS*. *J. Biol. Chem.* **288**, 15699 (2013).

356. Kamelgarn, M. *et al.* Proteomic analysis of FUS interacting proteins provides insights into FUS function and its role in ALS. *Biochim. Biophys. Acta - Mol. Basis Dis.* **1862**, 2004–2014 (2016).

357. Nonaka, T. *et al.* Prion-like properties of pathological TDP-43 aggregates from diseased brains. *Cell Rep.* **4**, 124–34 (2013).

358. Ding, X. *et al.* Exposure to ALS-FTD-CSF generates TDP-43 aggregates in glioblastoma cells through exosomes and TNTs-like structure. *Oncotarget* **6**, 24178–24191 (2015).

359. Westergard, T. *et al.* Cell-to-Cell Transmission of Dipeptide Repeat Proteins Linked to C9orf72-ALS/FTD. *Cell Rep.* **17**, 645–652 (2016).

360. Grad, L. I. *et al.* Intercellular propagated misfolding of wild-type Cu/Zn superoxide dismutase occurs via exosome-dependent and -independent mechanisms. *Proc. Natl. Acad. Sci. U. S. A.* **111**, 3620–5 (2014).

361. Feiler, M. S. *et al.* TDP-43 is intercellularly transmitted across axon terminals. *J. Cell Biol.* **211**, 897–911 (2015).

362. Romagnoli, C., Pampaloni, B. & Brandi, M. L. Muscle endocrinology and its relation with nutrition. *Aging Clin. Exp. Res.* **31**, 783–792 (2019).

363. Duguez, S. *et al.* Dystrophin deficiency leads to disturbance of LAMP1-vesicle-associated protein secretion. *Cell. Mol. Life Sci.* **70**, 2159–2174 (2013).

364. Pan, B. T., Teng, K., Wu, C., Adam, M. & Johnstone, R. M. Electron microscopic evidence for externalization of the transferrin receptor in vesicular form in sheep reticulocytes. *J. Cell Biol.* **101**, 942–948 (1985).

365. Fauré, J. *et al.* Exosomes are released by cultured cortical neurones. *Molecular and Cellular Neuroscience* **31**, A14–A14 (2009).

366. Rajendran, L. *et al. Alzheimer's disease β-amyloid peptides are released in association with exosomes*. **103**, (2006).

367. Forterre, A. *et al.* Myotube-derived exosomal miRNAs downregulate Sirtuin1 in myoblasts during muscle cell differentiation. *Cell Cycle* **13**, 78–89 (2014).

368. Fischer, L. R. *et al.* Amyotrophic lateral sclerosis is a distal axonopathy: evidence in mice and man. *Exp. Neurol.* **185**, 232–240 (2004).

369. Al-Chalabi, A., van den Berg, L. H. & Veldink, J. Gene discovery in amyotrophic lateral sclerosis: implications for clinical management. *Nat. Rev. Neurol.* **13**, 96–104 (2017).

370. Zammit, P. S., Partridge, T. A. & Yablonka-Reuveni, Z. The Skeletal Muscle Satellite Cell: The Stem Cell That Came in From the Cold. *J Histochem Cytochem* **54**, 1177–1191 (2006).

371. Merrick, D., Chen, H.-C., Larner, D. & Smith, J. Adult and Embryonic Skeletal Muscle Microexplant Culture and Isolation of Skeletal Muscle Stem Cells. *J. Vis. Exp.* 1–11 (2010). doi:10.3791/2051

372. Walsh, F. ., Dickson, J. ., Moore, S. . & Barton, C. . Unmasking N-CAM. (1989).

373. Maury, Y. *et al.* Combinatorial analysis of developmental cues efficiently converts human pluripotent stem cells into multiple neuronal subtypes. *Nat. Biotechnol.* (2014). doi:10.1038/nbt.3049

374. Sigma-Aldrich. Technical bulletin. 1–4

375. Pradat, P.-F. *et al.* Muscle gene expression is a marker of amyotrophic lateral sclerosis severity. *Neurodegener. Dis.* **9**, 38–52 (2012).

376. Bakay, M. *et al.* Nuclear envelope dystrophies show a transcriptional fingerprint suggesting disruption of Rb-MyoD pathways in muscle regeneration. *Brain* **129**, 996–1013 (2006).

377. Kowal, J., Tkach, M. & Théry, C. Biogenesis and secretion of exosomes. *Curr. Opin. Cell Biol.* **29**, 116–125 (2014).

378. Campion, D. R. The Muscle Satellite Cell: A Review. *Int. Rev. Cytol.* **87**, 225–251 (1984).

379. Scaramozza, A. *et al.* Skeletal Muscle Satellite Cells in Amyotrophic Lateral Sclerosis. 1–8 (2014). doi:10.3109/01913123.2014.937842

380. Pradat, P.-F. *et al.* Abnormalities of satellite cells function in amyotrophic lateral sclerosis. *Amyotroph. Lateral Scler.* **12**, 264–271 (2011).

381. Turner, M. R. *et al.* Controversies and priorities in amyotrophic lateral sclerosis. *Lancet Neurol.* **12**, 310–322 (2013).

382. Turner, M. R. *et al.* Mechanisms, models and biomarkers in amyotrophic lateral sclerosis. *Amyotroph. Lateral Scler. Frontotemporal Degener.* **14 Suppl 1**, 19–32 (2013).

383. Gonzalez de Aguilar, J.-L. *et al.* Gene profiling of skeletal muscle in an amyotrophic lateral sclerosis mouse model. *Physiol. Genomics* **32**, 207–218 (2008).

384. Zeringer, E., Barta, T., Li, M. & Vlassov, A. V. Strategies for isolation of exosomes. *Cold Spring Harb. Protoc.* **2015**, 319–23 (2015).

385. Zhang, M. *et al.* Methods and Technologies for Exosome Isolation and Characterization. *Small Methods* **2**, 1800021 (2018).

386. Albertsson, P.-Å. Partition of Cell Particles and Macromolecules in Polymer Two-Phase Systems. *Adv. Protein Chem.* **24**, 309–341 (1970).

387. Yamamoto, K. R., Alberts, B. M., Benzinger, R., Lawhorne, L. & Treiber, G. Rapid bacteriophage sedimentation in the presence of polyethylene glycol and its application to large-scale virus purification. *Virology* **40**, 734–744 (1970).

388. Paolini, L. *et al.* Residual matrix from different separation techniques impacts exosome biological

activity. *Sci. Rep.* **6**, 23550 (2016).

389. Ludwig, A.-K. *et al.* Precipitation with polyethylene glycol followed by washing and pelleting by ultracentrifugation enriches extracellular vesicles from tissue culture supernatants in small and large scales. *J. Extracell. Vesicles* **7**, 1528109 (2018).

390. Théry, C. *et al.* Minimal information for studies of extracellular vesicles 2018 (MISEV2018): a position statement of the International Society for Extracellular Vesicles and update of the MISEV2014 guidelines. *J. Extracell. Vesicles* **7**, 1535750 (2018).

391. Buchthal, F. & Schmalbruch, H. *Motor Unit of Mammalian Muscle*. *PHYSIOLOGICAL REVIEWS* **60**, (1980).

392. Burke, R. E., Levine, D. N., Salcman, M. & Tsairis, P. Motor units in cat soleus muscle: physiological, histochemical and morphological characteristics. *J. Physiol.* **238**, 503–514 (1974).

393. Duddy, W. *et al.* Muscular dystrophy in the mdx mouse is a severe myopathy compounded by hypotrophy, hypertrophy and hyperplasia. *Skelet. Muscle* **5**, 16 (2015).

394. Duddy, W. J., Cohen, T., Duguez, S. & Partridge, T. A. The isolated muscle fibre as a model of disuse atrophy: characterization using PhAct, a method to quantify f-actin. *Exp. Cell Res.* **317**, 1979–93 (2011).

395. Herbert, A. D., Carr, A. M. & Hoffmann, E. FindFoci: A Focus Detection Algorithm with Automated Parameter Training That Closely Matches Human Assignments, Reduces Human Inconsistencies and Increases Speed of Analysis. *PLoS One* **9**, e114749 (2014).

396. Zhang, K. *et al.* The C9orf72 repeat expansion disrupts nucleocytoplasmic transport. *Nature* **525**, 56–61 (2015).

397. Zhou, J. *et al.* Hyperactive Intracellular Calcium Signaling Associated with Localized Mitochondrial Defects in Skeletal Muscle of an Animal Model of Amyotrophic Lateral Sclerosis * □ S. (2009). doi:10.1074/jbc.M109.041319

398. Savina, A., Furlán, M., Vidal, M. & Colombo, M. I. Exosome release is regulated by a calcium-dependent mechanism in K562 cells. *J. Biol. Chem.* **278**, 20083–90 (2003).

399. Sproviero, D. *et al.* Pathological Proteins Are Transported by Extracellular Vesicles of Sporadic Amyotrophic Lateral Sclerosis Patients. *Front. Neurosci.* **12**, 487 (2018).

400. Feneberg, E. *et al.* Limited role of free TDP-43 as a diagnostic tool in neurodegenerative diseases. *Amyotroph. Lateral Scler. Front. Degener.* **15**, 351–356 (2014).

401. Sandri, M. Signaling in muscle atrophy and hypertrophy. *Physiology (Bethesda).* **23**, 160–70 (2008).

402. Lai, R. C. *et al.* Proteolytic Potential of the MSC Exosome Proteome: Implications for an Exosome-Mediated Delivery of Therapeutic Proteasome. *Int. J. Proteomics* **2012**, 971907 (2012).

403. Chen, H. *et al.* Modeling ALS with iPSCs reveals that mutant SOD1 misregulates neurofilament balance in motor neurons. *Cell Stem Cell* **14**, 796–809 (2014).

404. Boeynaems, S., Bogaert, E., Van Damme, P. & Van Den Bosch, L. Inside out: the role of nucleocytoplasmic transport in ALS and FTLD. *Acta Neuropathol.* **132**, 159–173 (2016).

405. Kim, J.-E. *et al.* Altered nucleocytoplasmic proteome and transcriptome distributions in an in vitro model of amyotrophic lateral sclerosis. *PLoS One* **12**, e0176462 (2017).

406. Freibaum, B. D. *et al.* GGGGCC repeat expansion in C9orf72 compromises nucleocytoplasmic

transport. *Nature* **525**, 129–133 (2015).

407. Mitchell, J. C. *et al.* Overexpression of human wild-type FUS causes progressive motor neuron degeneration in an age- and dose-dependent fashion. *Acta Neuropathol.* **125**, 273–288 (2013).

408. Qiu, H. *et al.* ALS-associated mutation FUS-R521C causes DNA damage and RNA splicing defects. *J. Clin. Invest.* **124**, 981–999 (2014).

409. Wang, W.-Y. *et al.* Interaction of FUS and HDAC1 regulates DNA damage response and repair in neurons. *Nat. Neurosci.* **16**, 1383–1391 (2013).

410. Baechtold, H. *et al.* Human 75-kDa DNA-pairing protein is identical to the pro-oncoprotein TLS/FUS and is able to promote D-loop formation. *J. Biol. Chem.* **274**, 34337–42 (1999).

411. Guescini, M. *et al.* Muscle Releases Alpha-Sarcoglycan Positive Extracellular Vesicles Carrying miRNAs in the Bloodstream. *PLoS One* **10**, e0125094 (2015).

412. Morales-Prieto, D. M. *et al.* Peripheral blood exosomes pass blood-brain-barrier and induce glial cell activation. doi:10.1101/471409

413. Koyuncu, O. O., Hogue, I. B. & Enquist, L. W. Virus infections in the nervous system. *Cell Host Microbe* **13**, 379–93 (2013).

414. Gluska, S. *et al.* Rabies Virus Hijacks and Accelerates the p75NTR Retrograde Axonal Transport Machinery. *PLoS Pathog.* **10**, e1004348 (2014).

415. Lewis, P., Fu, Y. & Lentz, T. L. Rabies virus entry at the neuromuscular junction in nerve-muscle cocultures. *Muscle Nerve* **23**, 720–30 (2000).

416. SOUDAIS, C., LAPLACE-BUILHE, C., KISSA, K. & KREMER, E. J. Preferential transduction of neurons by canine adenovirus vectors and their efficient retrograde transport in vivo. *FASEB J.* **15**, 2283–2285 (2001).

417. Février, B. & Raposo, G. Exosomes: endosomal-derived vesicles shipping extracellular messages. *Curr. Opin. Cell Biol.* **16**, 415–421 (2004).